THE PRESS FORMING BEHAVIOUR OF AUSTENITIC AND METASTABLE STAINLESS STEELS

by

ALAN JAMES GRIFFITHS, B.Sc.(Aston), A.I.M.

A thesis for consideration for the degree of Doctor of Philosophy of the University of Aston in Birmingham

August, 1967.

SUMMARY

in 18/8 type nickel-chromium steels

The present state of knowledge of austenite stability, transformation of austenite to α' martensite, and the deformation and press formability of austenitic stainless steels has been reviewed.

Experimental work is described for a range of chromium-nickel stainless steels of different austenite stability used in press forming. The steels were processed to give a wide range of properties at the final gauge and the effects of prior deformation and of prior transformation on mechanical properties and press formability were assessed with respect to austenite stability. An analysis has also been made of the complex true stress-true strain relationships obtained with steels of this type for the three stress systems, uniaxial tension, biaxial tension, and plane strain compression, and the results related to press formability.

The results showed that transformation to α' martensite during deformation is beneficial to stretch formability and to those mechanical properties governed by strength, but only beneficial to deep drawing when its presence does not impair ductility. The presence of α' martensite was shown to resist localised necking. Unlike mild steel, the drawing capacity of stainless steel is not influenced markedly by the anisotropy ratio R.

The stress-strain curve for stainless steels does not obey the Ludwik relationship and an alternative function has been derived. α' martensite formation markedly affects the shape of this curve and this is reflected in the constants governing the derived function. However, the strain level at which a change in the slope of the stress-strain curve occurs, does not correspond to the strain level at which α' martensite is initiated and an alternative theory is offered.

Using the derived function, a theoretical prediction of stress-strain data, and various mechanical and press forming properties can be obtained from knowledge of the austenite stability of the steel.

CONTENTS

		Page
1.0.	INTRODUCTION	1.
2.0.	SURVEY OF THE LITERATURE	3.
2.1.	Introduction	3.
2.2.	Austenite Stability	4.
2.3.	The Effect of Austenite Stability on the Martensite Transformation	6.
2.4.	The Morphology of the Martensite Transformation	11.
2.5.	The Effect of Deformation on the Mechanical Properties of Stainless Steels	14.
2.6.	The Effect of Strain Rate Variations on the Mechanical Properties of Stainless Steels	16.
2.7.	The Mechanisms of Deformation and Work Hardening in Stainless Steels	17.
2.8.	The Press Forming of Sheet Metal	18.
2.9.	Assessment of the Press Forming Properties of Sheet Metal	20.
	2.9.1. The Theoretical Approach	20.
	2.9.2. The Use of Simulative Tests	22.
	2.9.2.1. Stretch Forming Tests	22.
	2.9.2.2. Deep Drawing Tests	24.
	2.9.2.3. Assessment of the Individual Rôles of Stretch Forming and Deep Drawing as a Measure of Drawability	26.
	2.9.3. The Use of Non-Simulative Tests	28.
	2.9.3.1. The Tensile Test	29.
	2.9.3.2. The Plane Strain Compression Test	31.
2.10.	The Correlation of Simulative and Non-Simulative Tests with Pressing Performance	32.
2.11.	The Rôle of Anisotropy in Sheet Metal Forming	33.

		Page
2.12.	The Relationship between the Limiting Drawing Ratio and Anisotropy	37.
2.13.	The Press Forming Properties of Stainless Steel	39.
2.14.	Engineering Press Forming Requirements	42.
2.15.	Summary to the Survey of the Literature	42.
3.0.	EXPERIMENTAL PROCEDURE	44.
3.1.	Materials	44.
3.2.	Material Processing	44.
3.3.	Assessment of Austenite Stability	45.
3.4.	Assessment of the Quantity of Transformation Products resulting from Deformation	47.
	3.4.1. Magnetic Measurement of the α' Martensite Content	47.
	3.4.1.1. Measurement of Coercive Force	47.
	3.4.1.2. Measurement of Magnetic Response	49.
	3.4.2. Determination of the Onset of α' Martensite Formation from the Tensile Test	50.
	3.4.3. X-ray Determination of the Volume Fraction of α' Martensite	50.
3.5.	Optical Microscopy	51.
3.6.	Electron Microscopy	51.
3.7.	Tensile Testing	52.
	3.7.1. Tensile Test Pieces	52.
	3.7.2. Tensile Test Procedure	52.
	3.7.3. Tensile Test Results	53.
	3.7.4. Effect of Volume Changes during Testing on the Accuracy of the Results	54.
	3.7.5. Determination of a Function to define the True Stress - True Strain Relationship	55.

		Page
3.8.	Plane Strain Compression Testing	55.
	3.8.1. Plane Strain Compression Test Pieces	56.
	3.8.2. Plane Strain Compression Test Procedure	56.
	3.8.3. Plane Strain Compression Test Results	56.
3.9.	Hydrostatic Bulge Testing	57.
	3.9.1. Hydrostatic Bulge Test Pieces	57.
	3.9.2. Hydrostatic Bulge Test Procedure	57.
	3.9.3. Hydrostatic Bulge Test Results	57.
	3.9.3.1. Calculation of Strain	57.
	3.9.3.2. Calculation of Stress	58.
3.10.	Hardness Tests	58.
3.11.	Press Forming	58.
	3.11.1. Calibration of Press Forming Equipment	59.
	3.11.2. The Erichsen Cupping Test	60.
	3.11.3. The Erichsen Cup Drawing Test	60.
3.12.	Earing Measurements	61.
3.13.	Measurement of the Areas beneath the Punch Load/ Travel Diagrams	62.
3.14.	Thickness Strain and Hardness Measurements on Sectioned Drawn Cups	62.
3.15.	Correlation Matrix	62.
4.0.	EXPERIMENTAL RESULTS	64.
4.1.	Introduction	64.
4.2.	The Effect of Deformation on the Formation of α' Martensite	64.
4.3.	Mechanical Test Results	66.
4.4.	Assessment of Work Done during Deformation	67.
4.5.	True Stress-True Strain Data obtained from the Tensile Test	67.

		Page
4.6.	True Stress-True Strain Data obtained from the Plane Strain Compression Test	69.
4.7.	True Stress-True Strain Data obtained from the Hydrostatic Bulge Test	70.
4.8.	Hardness and Strain Distribution in Drawn Cups	72.
4.9.	Performance Factors	72.
4.10.	Correlation Matrix	75.
5.0.	DISCUSSION	76.
5.1.	Introduction	76.
5.2.	The Effect of Austenite Stability on the Formation of α' Martensite	76.
5.3.	The Effect of Austenite Stability on the Mechanical Properties of Stainless Steels	77.
5.4.	The Relationship between Stretch Formability and Austenite Stability	78.
5.5.	The Relationship between Deep Drawability and Austenite Stability	79.
5.6.	The Effect of Prior Deformation on the Mechanical Properties of Stainless Steels	80.
5.7.	The Effect of Prior Deformation on the Stretch Formability of Stainless Steels	82.
5.8.	The Effect of Prior Deformation on the Deep Drawability of Stainless Steels	83.
5.9.	The Relationship between Plastic Anisotropy and Press Formability	84.
	5.9.1. Planar Anisotropy	84.
	5.9.2. Normal Anisotropy	86.
5.10.	Thickness Strain and Hardness Distribution in Drawn Cups	88.
5.11.	Correlation of Mechancial Properties and Press Formability of Stainless Steel	91.

		Page
	5.11.1. Stretch Forming	92.
	5.11.2. Deep Drawing	94.
5.12.	Evaluation of Certain Performance Functions for Stretch Forming and Deep Drawing	96.
	5.12.1. Stretch Forming	96.
	5.12.2. Deep Drawing	99.
5.13.	An Analysis of the True Stress-True Strain Data obtained in Uniaxial Tension	101.
5.14.	The Significance and Relationship of the Quadratic Function to existing Stress-Strain Formulae	106.
5.15.	An Analysis of the True Stress-True Strain Data obtained from Plane Strain Compression Tests	108.
5.16.	An Analysis of the True Stress-True Strain Data obtained from Hydrostatic Bulge Tests	110.
5.17.	The Effect of Austenite Stability and Prior Deformation on the Analysis of the Stress-Strain Data	111.
5.18.	The Relationship between the Analysis of the Stress-Strain Data and the Mechanical Properties of Stainless Steel	115.
5.19.	The Relationship between the Analysis of the Stress-Strain Data and the Press Formability of Stainless Steel	116.
	5.19.1. Stretch Forming	116.
	5.19.2. Deep Drawing	117.
5.20.	Information Derivable from the Analysis of the Stress-Strain Data	118.
6.0.	CONCLUDING SUMMARY	120.
7.0	CONCLUSIONS	123.
7.1.	Suggestions for Further Work	125.
8.0	ACKNOWLEDGMENTS	126.
9.0.	REFERENCES	127.
10.0.	APPENDIX	133.

1.0. INTRODUCTION

The first systematic attempt to make and study the properties of the now familiar iron-chromium-nickel steels was published in 1920 by Strauss and Maurer[1] and it was the result of this work that steels containing both chromium and nickel, were placed on the market. The steels were primarily developed to combat corrosion and were introduced to the public in the form of table cutlery.

It was soon realised that in addition to good corrosion resistance, the austenitic stainless steels, of which the 18 per cent chromium - 8 per cent nickel, is a typical example, also exhibited relatively high strength at both elevated and low temperatures, good formability and weldability, together with the important property of possessing a pleasing appearance. These attributes have therefore resulted in the steel being used for many architectural, domestic and industrial applications.[2]

The 18/8 type of alloy possesses a high rate of work hardening together with good ductility and as would be expected from such a combination of properties, the material is ideal for stretch forming applications. These properties are, to some degree, related to the ability of the steel to transform crystallographically as it is being deformed. The parent austenite phase is metastable at room temperature in that a given free energy change will initiate a shear transformation of the parent lattice. Such a change can be induced by deformation; the face centred cubic austenite changes to the body centred martensite phase. The stability of the austenite towards transformation is enhanced by raising the equivalent nickel content of the steel so that the influence of martensite on the mechanical and press forming properties of the steel is reduced.

This thesis will consider the present state of knowledge concerning the press formability of metastable and stable austenitic steels, the transformation of austenite to martensite and the effect of prior deformation on the mechanical properties of stainless steels. It will also describe experimental work which set out to quantitatively assess the effect of different modes of deformation, to

correlate basic physical properties with press forming behaviour, and to examine the complex true stress-true strain relationship that exists for steels of this type. Examination of these properties will be carried out on steels of different austenite stability for material in the annealed and cold worked conditions so that a better understanding of the factors affecting the formability of stainless steels may be obtained.

2.0. SURVEY OF THE LITERATURE

2.1. Introduction

Additions of nickel to a steel containing 17 to 18 per cent chromium not only increases the amount of austenite formed at high temperatures but also extends the range of temperatures to which the steel can be cooled without transformation to martensite. A minimum requirement of approximately 7.5% nickel renders the steel austenitic at room temperatures when it is rapidly cooled. With increased amounts of nickel, the fully austenitic condition is maintained even when the steels are cooled at relatively slow rates.

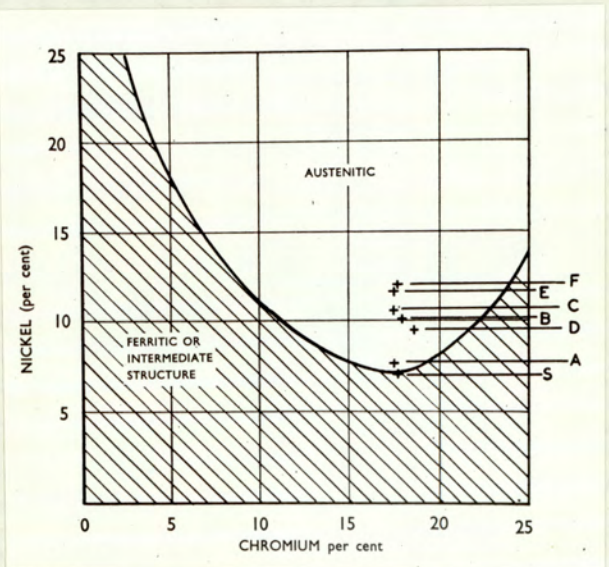

Fig.2.1. The Keating Diagram.[3]

Fig.2.1 shows the relationship between chromium and nickel for a carbon content of 0.1% for which the austenite phase can be retained at room temperature and the relative positions of the steels examined in this investigation. Steels whose compositions lie just within the upper zone of the Keating[3] diagram are metastable in that transformation to martensite can be induced by either deformation or cooling to below the Ms temperature. The degree of deformation required to initiate transformation is a measure of the stability of the steel.

Such steels are used extensively for deep drawing and press forming as they are readily formed, having ideal properties for these operations: high strength but still retaining adequate ductility together with a high . rate of work hardening, a factor which minimises the degree of thinning over the punch nose radius. From consideration of these basic properties their press forming behaviour should theoretically be superior to that of press forming quality mild steel sheet. The power requirements are however, greater and to avoid excessive die wear and scoring during pressing, excellent lubrication is required.

2.2. Austenite Stability

In pure iron the austenitic face centred cubic phase, is only stable at elevated temperatures between 910° C and 1400° C. Alloying elements added to the iron have a pronounced effect on the stability of the austenite. The effect of nickel is to progressively lower the temperature of transformation thereby making the austenite stable to lower temperatures. The austenite is not stable at room temperature however, until approximately 30% is added. Chromium on the other hand, forms an austenite loop so that alloys of greater than 13% cannot be austenitic.

Bain and Griffiths[4] showed that chromium and nickel present together in the steel tend to stabilise the austenite but that 5 - 10% of each was insufficient for complete stabilisation, i.e. the Ms temperature remained above room temperature and some martensite was produced on quenching. With higher alloy contents other workers noted that martensite was obtained after prolonged heating in the range 650° C to 800° C indicating that although the quenched product was austenite and therefore the Ms temperature is below room temperature, the equilibrium temperature for the austenite-martensite transformation is well above room temperature, and the austenite is therefore metastable. Aborn and Bain[5] confirmed the metastability of austenite in carbon bearing stainless alloys and demonstrated that the austenite could be transformed by

deformation at a temperature above that of the Ms. The upper temperature limit at which martensite is formed in this manner is called the Md temperature. They also stated that carbon and nitrogen stabilised the austenite opposing the breakdown to martensite. Mathieu[6] also confirmed the stabilising effect of carbon and nitrogen and further stated that the amount of martensite obtained increased with the degree of deformation but found that no martensite was obtained, irrespective of amount of cold work when the steel was deformed above 100° C.

At approximately the same time both Cina[7] and Angel[8] working separately carried out a systematic examination of the effect of deformation, temperature and composition on the formation of martensite in metastable austenitic steels. Cina was able to show the effect of increasing the chromium and nickel content in reducing the amount of martensite in compression. He examined both commercial alloys and super-pure alloys in order to establish the rôle of impurities in the steel, and found that the commercial material was markedly more stable than the steels produced from pure metals. He summarised that the impurity elements suppressed both the Ms and Md temperatures and that the relative order of effectiveness of added elements in suppressing both these temperatures was, Silicon, Manganese, Chromium, Nickel, Carbon and Nitrogen. Working on pure alloys, Cina first showed the presence of a third, close packed hexagonal phase when the steels were quenched. The phase was designated ε and had a c/a ratio of 1.585. Prior to this work it had always been assumed that the austenite transformed directly to martensite. Cina suggested that the new phase was intermediate, i.e. $\gamma \rightarrow \varepsilon \rightarrow \alpha^1$ but further contradicts himself when trying to justify the presence of this phase by saying that the ε phase could result from internal stresses "(probably compressive and shear)" set up in the austenite matrix by the formation of martensite. Thus he suggested that the ε phase was secondary to martensite and not an intermediate phase. The argument as to which phase

preceded which continued, however, for some time and the outcome of the argument will be discussed at a later stage when the morphology of the martensite reaction is considered.

2.3. The Effect of Austenite Stability on the Martensite Transformation

Although alloying elements fall into two main groups, namely ferrite and austenite stabilisers, they share with few exceptions the common effect of depressing the temperature at which austenite transforms to martensite. This transformation has been expressed thermodynamically by Kaufman and Cohen.[9]

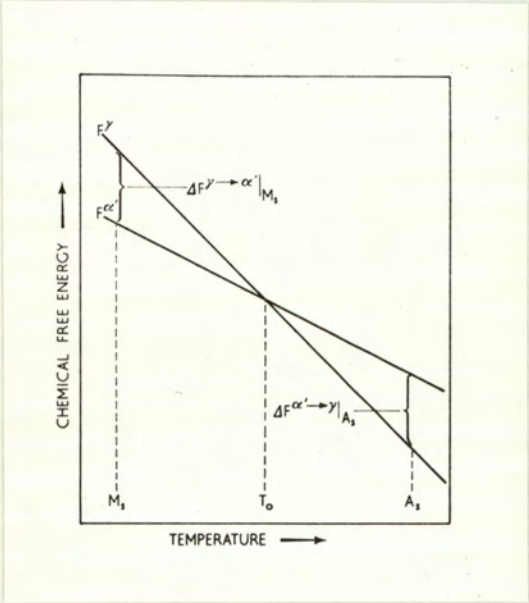

>To, austenite is thermodynamically stable

<To, martensite is the stable phase

and F_γ and F_α represent the free energies of austenite and martensite

Fig.2.2. The Relationship between chemical free energy and temperature for the two phases austenite and martensite.

On cooling an alloy from the austenitic range, transformation might be expected to occur at To, but this reaction does not, in fact, occur until a temperature corresponding to the Ms, which in iron based alloys can be as much as 200° C below To. At the Ms, the austenite has derived sufficient energy from undercooling to overcome the barriers of nucleation and interfacial strain which inhibit the growth of a b.c.c. nucleus in a f.c.c. matrix. In very stable steels, To is depressed and might not be reached even if cooled to absolute zero. For

less stable steels it is possible for To and Ms to be above room temperature and in such a case the austenite is said to be metastable.

When stress is applied to an alloy, the mechanical energy supplied interacts with the thermodynamics of the martensite reaction, as demonstrated by Patel and Cohen[10].

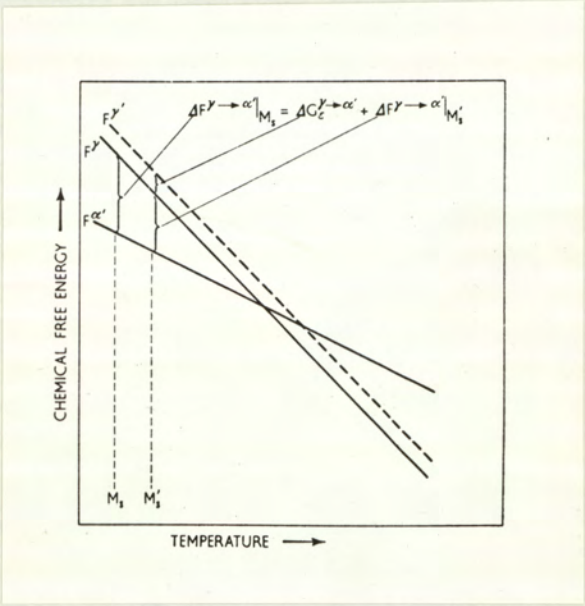

Fig.2.3. The Effect of Applied Stress on the Martensite reaction.

In the strained system F_γ is displaced by an amount $\Delta G_{\varepsilon}^{\gamma - \alpha^1}$, the mechanical energy due to the applied stress. The total free energy required for undercooling is therefore supplemented by mechanical energy so that cold working at temperatures above the Ms may result in the formation of martensite, i.e. to the Md temperature, and the response to such treatment will depend on the chemical analysis of the steel.

As a general rule, if the product of $\frac{\%\,Cr - 16\%\,C}{\%Ni}$ is less than 1.7 then the austenite is said to be stable with respect to deformation. This formula is an over-simplification and some form of quantitative assessment of austenite stability is required.

The first systematic attempt to quantitatively assess austenite stability, with respect to the Ms temperature, was carried out by Post and Eberly.[11] The authors examined the magnetic permeability variations with cold work and the effect of various alloy additions on austenite stability. As a measure of the point of transformation they evaluated a change of slope in the plot of permeability versus tensile strength for specimens previously cold rolled varying degrees. These data depend upon the temperature of the Md point relative to room temperature and are therefore the approximate relative effects of the alloying elements on the Ms temperature. The results were expressed as nickel equivalents and the difference between the summation of the nickel equivalent and the actual nickel content was used as a measure of the stability. This value was designated $\triangle$. Positive values indicated the presence of sufficient nickel to stabilise the alloy and negative ones, insufficient. The authors claimed that their method satisfied compositional variations of % Cr 14 - 25, % Ni 7.0 - 21.0, % Mo 0 - 3.0, % C 0.03 - 0.2 and % Mn 0.4 - 4.0. They did not, however, take into account the strong austenite stabilising effect of nitrogen and the significance of this will be discussed later.

At a later date, Eichelman and Hull[12] continued the work by examining the effect of composition on the Ms temperature using a dilatometric technique and expressing this temperature by a simple linear equation. The equation was deduced by carefully selecting melts whose basic composition remained unaltered but allowing significant variations in a given element and relating correction factors for each of the elements so varied, to the actual measured Ms temperatures. These workers took into account the strong austenite stabilisers carbon and nitrogen and presumably assumed that the ratio of To to Ms, given by Kaufman and Cohen,[9] to be constant. They deduced that the relative effectiveness of the additions, in their normal composition ranges, in lowering the Ms temperatures increased as follows:- silicon, manganese, chromium, nickel, carbon and nitrogen. The nickel equivalent for these additions are 0.45, 0.55, 0.68, 27

and 27, omitting nickel. These compare with the Post and Eberly values of 0.5, 1.0 and 35 for manganese, chromium and carbon. The main criticism of the work by Eichelman and Hull is that they did not study molybdenum bearing alloys. Even though the elements chromium and silicon are generally assumed to be ferrite-forming elements, they lower the Ms point as long as the chromium plus silicon content, expressed as chromium alone, does not exceed 20%. Using the $\triangle$ values obtained by Post and Eberly and plotting against their own temperature gives a good linear relationship whereas a similar plot using the results obtained by Eichelman and Hull does not produce equivalent results, presumably because their technique did not evaluate the effect of grain size, a decrease in which decreases the Ms temperature. For the purpose of this present work austenite stability has therefore been based on the Post and Eberly model.

A further measure of austenite stability is to calculate the Md_{30} temperature, a method proposed by Angel.[8] He used a multiple regression equation to calculate the temperature with respect to composition. The Md_{30} is the temperature in ^{o}C at which 50% of the structure is transformed on drawing a tapered tensile test bar after a true strain of 0.30 and is calculated from the formula:-

$$Md_{30}\ ^{o}C = 413 - 462\ (\%\ C + N) - 92\ (\%Si) - 8.1\ (\%\ Mn) - 13.7\ (\%\ Cr) - 9.5\ (\%\ Ni) - 18.5\ (\%\ Mo)$$

Unfortunately this formula only holds good for compositions of about 18/8.

Some ten years later, Barclay et al[13] studied the concept of alloy stability in relation to work hardening characteristics, strength and ductility by making known additions of nickel, manganese, and copper to basic 17% chromium steels. They too related the austenite stability to the Ms temperature, calculated using the empirical equation of Eichelman and Hull. They found that alloying elements suppressed martensite formation in proportion

to their ability to suppress the calculated Ms temperature, a conclusion previously arrived at by Post and Eberly. Although no quantitative assessment of alloying additions was given, it is worth noting the relative effects of these additions on the mechanical properties studied. Alloys with increasing copper content but constant chromium and nickel and manganese were found to exhibit a decrease in tensile and yield strength associated with an increase in elongation. They also found that small additions of manganese or nickel to an already stable alloy resulted in little change in the properties measured, but that the addition of copper to such a composition gave a measurable decrease in work hardening rate. They postulated that the influence of copper could be explained if it produced a greater increase in stacking fault energy than nickel, manganese or chromium. The larger copper atom could be expected to cause a slight increase in lattice parameter and decrease the elastic modulus, both of which effects would tend to produce narrower faults. With respect to compositional variations, Bressanelli and Moskowitz [14] supported the conclusions arrived at by Barclay and supplemented this work by further noting that as the characteristics of the steel changed from that of a stable austenite to one of a lower stability, elongation firstly increased, prior to a general decrease, as a result of the formation of martensite during plastic instability. This action minimised local necking.

The dependency of austenite stability on the stacking fault energy of stainless steels has not been widely studied although the first direct observation of stacking faults and the subsequent determination of its energy was on an austenitic steel. In general, the stability of the austenite increases with increase in stacking fault energy.

Dulieu and Nutting [15] measured increases in stacking fault energy with reference to a base 18/10 alloy and presented the results as a change per atomic percentage of solute added. The authors obtained energies by measuring dislocation node radii and also by measuring the number of twins present in the

material. The effect of the transition metal solutes appears to depend upon their position in the periodic table since the fault energy increment per atomic per cent, rises in the order cobalt - nickel - copper. The variations in stacking fault energy on a base value of 11 ergs cm^{-2} per atomic per cent solute were calculated to be + 0.5, + 1.4, - 3.4, - 0.55, + 3.6, + 3.2 and + 0.1 for the elements chromium, nickel, silicon, cobalt, copper, niobium and molybdenum respectively. The effect of the interstitial elements carbon and nitrogen was also measured and it was found that for all practical purposes their influence on the stacking fault energy could be neglected for the levels normally found in solution in commercial alloys. Although these two interstitial elements strongly affect austenite stability, from the results of Dulieu and Nutting it must be assumed that it is not directly as a result of increasing the stacking fault energy but merely as a physical factor in depressing in some way the Ms and Md temperatures.

2.4. The Morphology of the Martensite Transformation

Since the time when Edwards and Carpenter [16] considered that α' martensite was twinned austenite, a large amount of work has been done to study the transformation of austenite to martensite. Several workers proposed that α' martensite was heterogeneously nucleated at strain 'embryos' within the austenite. Knapp and Dehlinger [17] considered the embryo to be a thin oblate spheroid surrounded by a single dislocation loop lying in the habit plane. Since the discovery of an intermediate phase in the reaction by Cina, theories have been based on the rôle of stacking faults in the austenite. Several workers have now observed the presence of this intermediate phase, now redesignated ε, and it is now known that it occurs regardless of whether the martensite transformation is induced by cooling or deformation. Venables [18] found that the α' phase was always observed to be in contact with the ε phase, and that intersections of ε platelets on two different $\{111\}_\gamma$ planes were especially favourable sites for α' nucleation. In no case did he find a nucleus of α' phase not associated

with one or more ε platelets. He also assumed that since the ε phase appeared first on deformation that the α' phase was nucleated from the ε phase. During early stages in nucleation, α' martensite formed as needles along the $\langle 110 \rangle_\gamma$ direction. This coincided with the line of intersection of two ε platelets. At later stages, $\{225\}_\gamma$ was observed as the usual habit place though occasionally some plates were observed to have a $\{111\}_\gamma$ habit when formed from initially thick ε platelets. The orientation relationships arrived at by Venables were close to those previously proposed by Kurdjamov and Sachs[19] and Bergers[20], i.e. $(111)_\gamma // (0001)_\varepsilon // (011)\alpha'$ and $[10\bar{1}]\gamma // [11\bar{2}0] // [1\bar{1}1]\ \alpha'$ i.e. close packed planes and directions were parallel. The α' martensite habit plane was stated as $\{225\}_\gamma$. Reed[21] confirmed these results but further clarified the situation by saying that only half the traces measured corresponded to $[1\bar{1}0]\gamma$ and $(225)_\gamma$ habit planes and that this situation only occurred when the direction of the long section of the needle was parallel or nearly so to $\langle 1\bar{1}0 \rangle_\gamma$. If these sections were parallel to $\langle 110 \rangle_\gamma$ then the habit was not $\{225\}_\gamma$ and possible alternatives were offered. The $\{111\}_\gamma$ habit plane was also observed but only in specimens slowly cooled to - 196° C.

Other workers Gunter & Reed[22] using a difference method, viz. % ε martensite = 100 - (% α' + % γ), have shown that the amount of ε phase first increases with deformation then decreases while the amount of α' martensite increases continuously. This again suggests that the ε phase should be considered as a transition phase in the γ - α' transformation, but this idea was then questioned by Dash and Otte.[23] They disagreed with previous workers and stated that the phase was a consequence of induced stresses in the austenite that resulted from the formation of the α' martensite. The authors state that as a consequence of the low stacking fault energy of these alloys, it is relatively easy to dissociate dislocations and that formation of α' crystals above a certain size would be sufficient to induce extensive dissociation. This leads to the formation of bands containing the heavily faulted ε phase. Although they admit that in

certain cases α' martensite may be induced by stacking faults they maintain that the width and density of the bands seems to be a function of the relative size, shape and distance between the α' crystals. This theory is supported by Goldman, Robertson and Ross.[24]

The ε phase has been considered as "an ordered arrangement of stacking faults".[23] Lagneborg[25] using material deformed at room temperature has stated that both stacking faults and ε phase can be observed and that the habit plane for these conditions is $\{111\}_\gamma$ whilst on cooling is $\{225\}_\gamma$ or $\{259\}_\gamma$. He advances the theory by noting that α' martensite can also be formed by the interaction of active slip lines and the ε phase. He suggests a theory for formation of deformation martensite in which martensite volumes at partials form favourable transformation sites and by the aid of slip processes, these embryos are believed to grow to stable martensite crystals. The hypothesis that he proposes is consistent with the observation that deformation martensite forms preferably as needles with intersections between ε discs.

It is apparent that the situation is quite complicated, and that opposing theories as to which comes first, the α' or the ε , still exist. Each possibility has its supporters. Kelly[26] in reviewing this situation, concludes that if α' comes first, then any complementary strain of the austenite from α' formation, should be associated with ε bands. Examining the interaction between ε bands and surface scratches he found that ε formation was apparently inhomogeneous suggesting that if the complementary shear is accommodated by the austenite as a homogeneous shear leading to ε formation, then there is no need for lattice invariant shear. On the other hand if ε forms first and is inhomogeneous, then the ε band represents a region which has been subjected to both the complementary and lattice invariant shears. He suggests that only one invariant plane strain (plus a slight "shuffle" of atoms on adjacent $(0001)_\varepsilon$ planes) would then be necessary to convert ε to α'.

Both possibilities lead to the same result if ε formation is inhomogeneous.

Finally, it is unlikely that α' martensite is formed firstly in every case since it has been shown that α' can form in an existing ε band whether that band was induced by α' martensite or not.

2.5. The Effect of Deformation on the Mechanical Properties of Stainless Steels

In general it can be stated that the amount of α' martensite increases with degree of cold work and decreases with increasing austenite stability and increased working temperature; andthat above a certain temperature, Md, no amount of deformation induces transformation. From this statement it can therefore be deduced that the degree and rate of deformation and the strain rate, are important factors when considering the effect of α' formation on the mechanical properties of the steels.

Angel[8] showed the effect of temperature and strain.

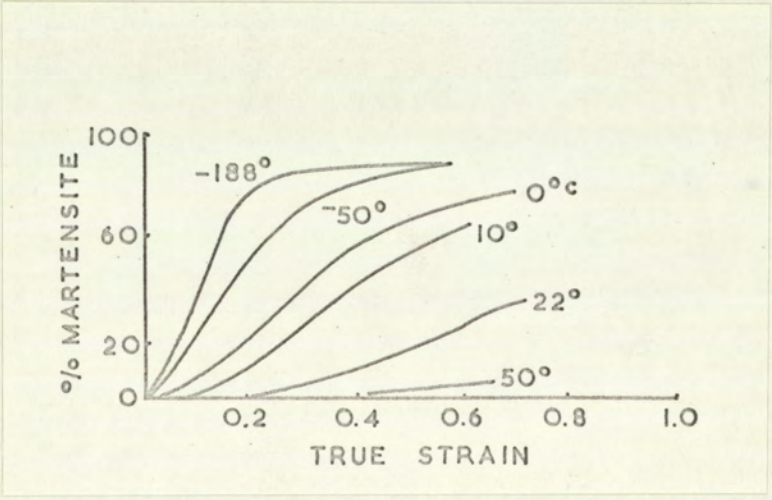

Fig.2.4. The effect of testing temperature on the amount of α' martensite produced.

He concluded from these tests that the amount of α' martensite decreased, for a given level of strain, with increase in temperature, so that above

the Md, this value becomes zero, that the amount of martensite formed never exceeds 90% and that the decreasing rate of its formation can be explained by the decreasing availability of austenite. He also showed that a given strain is necessary to initiate transformation and that this level of strain increases with both stability and temperature. He postulated that α' martensite formation is associated with a shear strain of 0.2 and that this value is unaffected by the temperature of testing although the amount of this phase produced at levels of strain greater than a shear strain of 0.2 is markedly affected by temperature. These points are illustrated in Fig.2.5.

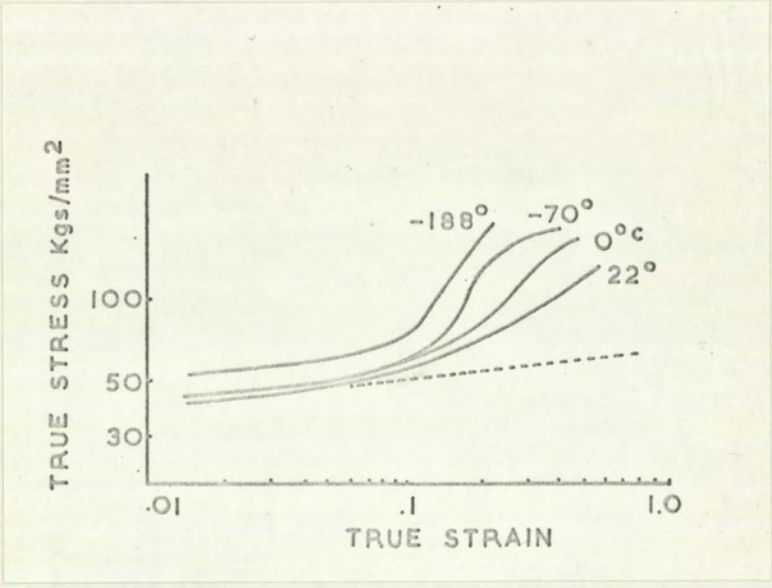

Fig.2.5. True stress-true strain relationships obtained at different testing temperatures. Angel.[8]

He interpreted the three stage curve as (a) initial slip of the austenite, (b) slip plus formation of α' martentire, and (c) deformation and strain hardening of the martensite itself. The martensite transformation can be regarded as a deformation process that competes with the usual slip process so that as the temperature is decreased the resistance to slip increases while the resistance to martensite

formation decreases.

Cina[7] in work carried out at approximately the same time showed a similar relation for % α' martensite against true strain for increasing austenite stability instead of increasing temperature. He was also able to show that more α' martensite was obtained in tension as opposed to compression: compression opposing the lattice expansion association with α' martensite formation.

It has been reported,[27] that the amount of α' martensite present in an individual grain depends on its orientation to the direction of deformation. Most of the α' martensite (this appears in sheets with traces approximately 60° to each other) is obtained when the tensile direction is approximately parallel to the $\langle 111 \rangle$. In grains that do not contain appreciable amounts of α' martensite the grain direction is parallel or almost so to the $\langle 100 \rangle$. In such grains α' martensite is observed in two directions lying almost perpendicular to each other. Bergers and Klosterman[27] quote values of active shear stresses for transformation by $\{111\}\langle 112\rangle_\gamma$ shears of a f.c.c. to one of b.c.c. lattice. These results show that for a given magnitude of applied stress, a tensile stress parallel to the $\langle 100 \rangle_\gamma$ is less favourable for a $\{111\}\langle 112\rangle_\gamma$ shear, than a tensile stress parallel to $\langle 111 \rangle_\gamma$. The fact that a reversal of stress direction does not correspond to a reversal of shear movement is said to account for the different orientation relationships that exist between the γ and α' phases and for the variation in amount of α' martensite for different stress systems.

2.6. The Effect of Strain Rate Variations on the Mechanical Properties of Stainless Steels

The effect of increasing tensile testing speed has often been shown to have a marked effect on the tensile properties of metastable austenitic stainless steels.[28-31] Several workers have shown that both the tensile strength and elongation decrease rapidly with increase in testing speed. Both of these effects have been attributed to the increase in specimen temperature resulting from the faster rates of deformation. The effect of increasing temperatures would be twofold: to increase

the tendency towards slip processes within the austenite and to reduce the possibility of α' martensite formation. Such reasoning readily explains the reductions in tensile strength values but not the decrease in elongation. Formation of α' martensite during straining has been shown not to be beneficial to elongation.[31 and 32] Bressanelli and Moskowitz [14] show, however, that the formation of a certain amount of martensite is beneficial to ductility. They believe that α' martensite increases the resistance of the steel to incipient necking at high strain levels. Non-transformable steels resist localised flow only through work hardening of the austenite. Such work hardening at low strains is sufficient to provide uniform elongation but at high strains this rate of work hardening is insufficient to provide the necessary strengthening to resist necking, and failure occurs. In metastable austenitic steels, martensite forms in the region of incipient necking and increases the strength of the necked portion so that it is no longer the weakest region, and deformation proceeds in adjacent regions.

At slow testing speeds (0.1 in. per min) sufficient time is available for the heat of deformation to be dissipated. Under such conditions Bressanelli and Moskowitz[14] found that the martensite content, at higher strain levels, increased almost linearly with strain. At high speeds, 20 in. per min, they recorded increases in temperature up to 200° F and found that the martensite content does not increase with increasing strain during the stage at which incipient necking occurs, failure occurring at a relatively low elongation. For these reasons only α' martensite formed during necking was deemed beneficial to elongation.

2.7. The Mechanisms of Deformation and Work Hardening in Stainless Steel

Using type A.I.S.I. 301 steel, Barclay[33] has studied the deformation mechanisms obtained during uniaxial tensile testing. For the material examined he found that α' formed at a strain level between 0.2 and 0.3. Initial straining resulted in the dislocation density of the austenite becoming very heavy.

Deformation twins were also present. At higher strain levels, α' martensite formed as plates containing a high dislocation density which appeared to be slightly less than that in the surrounding austenite. The increase in strain from 0.3 to 0.6 resulted in a greater quantity of martensite, more twinned austenite and a further increase in the dislocation density of the parent phase. Although not positively identified, Barclay suggests that beyond 0.6 strain the martensite itself was twinned. He also states that prior to martensite formation 'cell formation' and stacking faults are formed. The strain levels obtained by Barclay are high to those generally obtained with stainless steels.

2.8. The Press Forming of Sheet Metal

The pressing of metals is now known to involve two basic and fundamentally different processes: stretch forming and deep drawing. The latter process has been further equated to the summation of the two effects of stretch forming and pure drawing. In stretch forming the metal is clamped between a blankholder and a die and is restricted from drawing in. A punch is advanced and material is deformed by biaxial stretching over the punch profile. Failure in this operation occurs over the punch nose, its exact position being largely determined by the frictional conditions that exist between the punch and the metal. Since deformation is ideally that of stretching, % elongation in the tensile test is an almost direct measure of stretch formability. Ductility and work hardenability are therefore of paramount importance as controlling factors.

In deep drawing the blank is allowed to be drawn in as the punch is advanced and is typified by the process of forming a flat bottomed cup from a circular blank. The blank is held between the blankholder and the die with sufficient pressure to prevent wrinkling as metal is drawn in. This pressure is small compared with the pressure necessary to draw the blank into the die. As the draw is commenced, the sheet is bent under tension over the nose of the punch. Bending of material over the die entry radius and subsequent unbending as it enters the cup wall causes some thinning to take place depending on the severity of the

die entry radius. As the flange of the cup is drawn in, a compressive hoop stress is developed and if the blank holder pressure is insufficient, wrinkling occurs in an effort to reduce this stress. The compressive forces produced, cause thickening of the blank and unless an initial positive clearance between punch and die is used, metal in the cup flange will be ironed.

In the absence of ironing the total drawing load must be transmitted by the cup wall. The stress must be sufficient to draw in the blank, bend and unbend the material over the die entry radius and overcome the frictional forces between the blank and the tools. The stresses involved in deep drawing are more complex than stretch forming and include both biaxial tension and plane strain compression.

From the above considerations material for deep drawing should therefore have a high enough ductility for it to form initially over the punch nose. In order to transmit the high stresses needed to draw in the remainder of the blank, the cup walls must attain a high strength. A high work hardenability for this part of the drawing operation is therefore beneficial.

Failure occurs in the majority of deep drawing processes when the cup wall, at a position near to or at, the punch nose radius is no longer able to support the load necessary to draw in the remainder of the cup. The mechanism of failure in such a case, is stretching, in a similar manner to the failure obtained in stretch forming.

Drawing capacity can be improved by reducing the component of friction on the undrawn flange while keeping friction high over the punch nose as a means of reducing stretching. Improvement in drawing capacity can only occur, if the strength of the cup wall relative to the maximum drawing load can be increased. Overall strength increases alone merely increase the load required to draw in the cup flange.

2.9. Assessment of the Press Forming Properties of Sheet Metal

For many years an assessment of the pressing behaviour of sheet metal has been sought from both simulative and non-simulative techniques. A major programme made by Professor Swift[34] and his colleagues at Sheffield laid the foundation for much of this work. From a knowledge of basic stress-strain relations of the material and of plasticity theory, press and load requirements, together with drawing capacity have been calculated. Various simulative tests have also been developed which would indicate rapidly and reliably whether a given pressing would be satisfactory.

More recently, with the realisation of the complexity of deep drawing, a more systematic approach to the problem has been made. For instance, the behaviour of metal under individual stress systems such as biaxial tension, bending and plane strain compression have been studied. Unless a commercial pressing consists of either "pure" deep drawing or "pure" stretch forming, and this is most unlikely, it is hardly likely that a direct correlation with a simulative test would be obtained.

Considerable efforts have also been made to assess the relationships between various parameters, as determined in the tensile test, and the behaviour of sheet in the press. This approach has been largely due to Lankford, Snyder and Bauscher[35] who in 1950, showed that anisotropy, as measured by the R value in the tensile test, could be a means of increasing the drawing capacity of mild steel. Since that time, workers have tried to use the parameter and what is more difficult, to vary it independently of other mechanical properties, in order to improve press formability.

2.9.1. The Theoretical Approach

It has been shown[36] that in deep drawing three important stress systems will be imposed, either singly or in combination when a blank is deformed. The first stress system to become operative is that of biaxial tension in the plane of the sheet. This results from the force imposed by the punch against the restraining

effects of blank holder and die friction of the blank. Bending stresses in one or more planes are superimposed on the biaxial stress system causing a variation in stress through the thickness of the sheet. The bending stresses can be subdivided into the stress in the direction of bending, the thickness stress and the circumferential stress. Finally, if it is assumed that no thickening occurs, then compression normal to the plane of the sheet will result in the flange of the cup. Plane strain conditions exist in the cup wall if no change in radial strain occurs due to the restraining influence of the punch.

Attempts have been made to apply stress-strain relationships and yield criteria to these basic systems. Chung and Swift[34] used this approach and found good agreement between the theoretical and experimental curves of maximum punch load, total punch work and in the shape of the punch load/travel diagrams even to the extent of predicting the effect of ironing. Remarkably good agreement, for non-ferrous metal, was also obtained between predicted and actual strain distributions. This theory can, also be applied with confidence in predicting punch loads, power requirements and punch strokes, i.e. strength ratings for deep drawing presses. Unfortunately, the effects of anisotropy were not investigated, and mild steel, which exhibits a marked earing effect, did not completely comply with the theoretical predictions made of strain distribution. This work has been reviewed by Alexander.[36]

Theoretical analyses of deep drawing, at this stage, must be confined to relatively simple pressings such as flat bottomed cylindrical cups. Even so, the results of such examinations have been quite complex although in many cases simplifications have been made. Following the observation of Lankford et al, users of sheet metal have been increasingly concerned with the use of normally anisotropic material to improve drawability and this can only complicate the theoretical approach.

2.9.2. The Use of Simulative Tests

A large number of small scale simulative tests have been designed and related to performance under industrial pressing conditions. The advantage of such a test is that it is quick, reproducible and can give a sufficiently good correlation with industrial conditions if the test is representative of the actual pressing operation. The difficulty arises when the pressing operation involves an indefinite ratio of deep drawing and stretch forming since simulative tests tend to be one or the other. As yet no test is available that can precisely control the relative amounts of these two deformation processes. The whole field of testing sheet material has been reviewed by Wright.[37]

Simulative tests include simple bending, hole expanding, the formation of conical cups and wedge drawing, only a small number of which are used widely.

2.9.2.1. Stretch Forming Tests

These tests, which in principle are similar, include the Erichsen, Olsen and Jovignot tests, the essentials of which have been described by Jevons.[2] The most widely used test is the Erichsen cupping test. This test has now been adopted by the European Iron and Steel Community: their specification being Euronorm 14-58. The reliability of this test, with respect to specimen width, thickness, flatness, surface condition, holder pressure, tool dimensions, lubrication, drawing speed, machine rigidity and end point, has been adequately defined in the literature. It is important in this test to prevent drawing in of material and although not yet adopted as a standard procedure, Kaftanoglu and Alexander[38] have shown that this can only be effectively done by using serrated blank holder and die faces in order to grip the sheet.

The depth of punch penetration is taken as a measure of stretch formability of the metal and is expressed in millimetres. Regard must be paid, however, to the thickness of sheet tested. The appearance of the failed specimens give rise to additional information. Surface roughness is an indication of a large grain

size. The type and position of the fracture is also indicative of planar anisotropy or lack of it, and the frictional conditions between the punch and metal. Kaftanoglu and Alexander have carried out a detailed investigation of the Erichsen cupping test.[38]

In a recent paper, Pearce[39] stretch formed a variety of sheet metals with average strain ratios varying from 0.2 to 10.0 using a bulge test. As a measure of the degree of success of the test, values of fracture strain were measured.

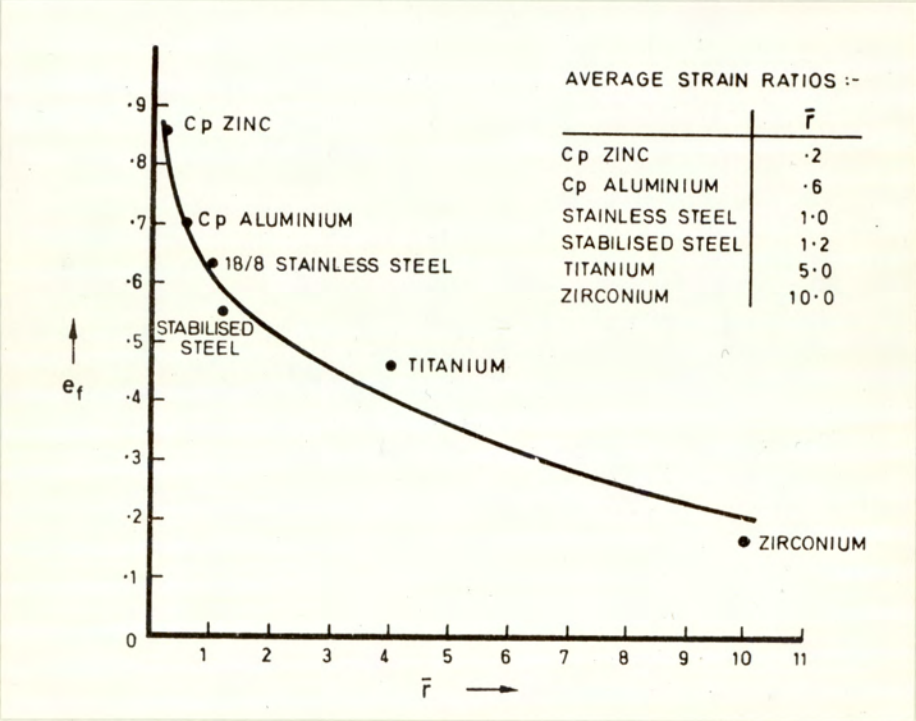

Fig.2.6. The relationship between fracture strain and $\bar{R}$ value for various materials.

The results showed, as one would expect, that as the R value was increased so the fracture strain decreased. Fracture strain, $ef = \frac{to - t_1}{to}$ measured as

the degree of thinning adjacent to the fracture which is suggested as being an alternative measure of the R value. Pearce, however, disregards the effect of $\bar{R}$ variations on bulge height which would have been a better measure of drawability. His results on cold worked aluminium show, over a limited range of $\bar{R}$, that there is an increase in bulge height with increase in $\bar{R}$ value.

2.9.2.2. Deep Drawing tests

Deep drawing is assessed, on a laboratory scale, by the forming of a flat bottomed cup and the results obtained, quoted as a measure of drawability The maximum blank diameter which can successfully be drawn into a cup is determined and the results are expressed in terms of the limiting drawing ratio: namely the blank diameter/punch diameter.

Swift[34] has shown that for pure radial drawing, the applied stress at any stage of drawing is given by the formula:-

$$\sigma r = K \left(\tfrac{1}{2}\right)^n \int_{ro}^{rp} \left[\ln \left(Ro^2 - ro^2/r^2 + 1\right) \right]^n dr/r$$

where Ro is the initial blank radius
ro is the radius of the outer edge of the undrawn flange
rp is the punch radius
r is a radius between ro and rp
and n is the strain hardening component

Due to opposing tendencies, strain hardening and diminishing reduction as the draw progresses, σr passes through a maximum for any ratio of blank to cup diameter. Using a series of integrations of the above equation, each for a different ro between Ro and rp, a limit (L.D.R.) is reached when the maximum drawing load becomes equal to the load for pure tensile instability at the unworked bottom of the cup wall. This material is unworked and therefore unstrengthened by work. For such a case involving pure radial drawing, the theoretical L.D.R. for isotropic material is 2.72, the natural base of logarithms and this relationship between drawability and 'n' as shown by Keeler and Backofen[40] is given in Fig.2.7.

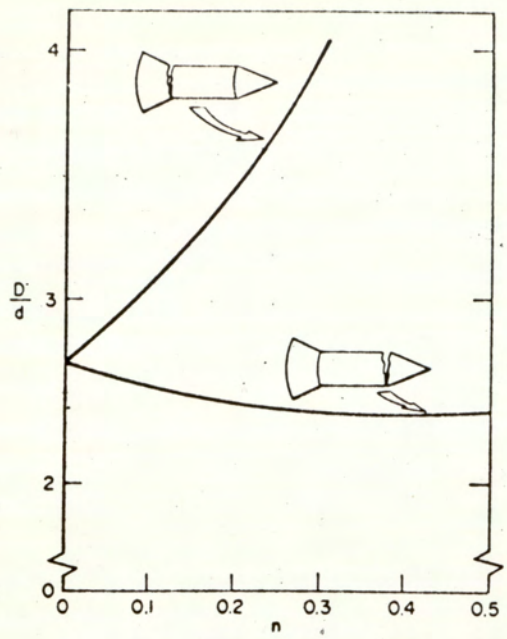

Dependence of LDR on n *from* $\sigma = K\varepsilon^{n}$. *The limit has been calculated for pure radial drawing with failure occurring at either of the two places*

Fig. 2.7. The relationship between 'n' and L.D.R.

Since the value of 2.72 isthe limit of drawability for isotropic materials, for flat bottomed cylindrical cups, practical results depict how this limit is modified by friction, anisotropy, work hardening and bending. The main factor that can be altered to increase this theoretical limit would appear to be $\bar{R}$, the anisotropy ratio so long as an increase does not also increase the value of σ r. This is now the widely accepted view.

The two most widely used cup drawing tests are the Erichsen and Swift.

The basic differences are those of tool geometry, the latter test employing a more liberal die entry radius than the former. It is important that direct comparisons of L.D.R., obtained from different tests, should be clarified as to tooling geometry and lubrication as minor variations can markedly affect the results.[41]

Cup drawing tests can also be used to provide a semi-quantitative assessment of planar anisotropy from the measurement of ear heights. Adequate punch/die clearance is necessary, however, for ironing of the flange, in the latter stages of the test, reduces the size of ears formed. Finally it must not be forgotten that cup drawing tests are used to evaluate process variables.

2.9.2.3. Assessment of the individual roles of stretch forming and deep drawing as a measure of drawability

It has been proposed[42] that a measure of fracture loads and drawing loads could provide an alternative criterion of drawing performance to that of the limiting drawing ratio. It is argued that since most sheet metal pressing operations involve both stretch forming and deep drawing and that these two modes of deformation are confined to the centre and outer regions of the blank, respectively, that both components contribute to the final depth of the pressing. Assuming that failure normally develops in the material stretched over the punch nose, particularly for hemispherically shaped punches then deformation in this region is limited by the inability of the material to resist necking under conditions of biaxial tension and/or bending. Using standardised conditions, it is considered that the maximum depth of draw is obtained when the stretch forming contribution is also a maximum, (Fig.2.8).

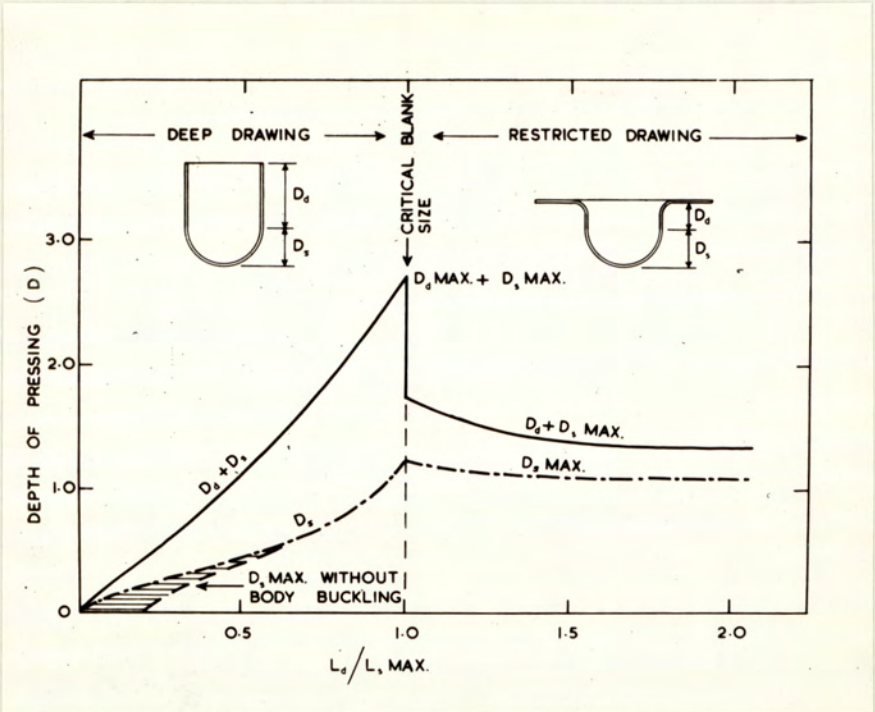

Fig.2.8. A schematic representation of the influence of the load ratio Ld/Ls on the limits of the deep drawing process. (42)

In the above figure the authors have designated the contribution made by stretch forming Ds, and its associated load Ls and that of the drawing component Dd and its load DLd.

The maximum possible depth of the drawing component is achieved when Ld = Ls max, (Ld increases with increase in blank diameter). This corresponds to the critical blank diameter of the material. For blanks of larger diameter Ls max $>$ Ld and fracture occurs within the stretch formed region of the blank. As the authors point out, for successful pressings, punch travel must be stopped

before the drawing load exceeds Ls max. Evaluation of drawability then consists of establishing Ls max; using a hemispherical punch which is forced through the sheet previously locked by serrated die and blank holder plates, it should be possible to draw two cups of an arbitrary size below that of the C.B.D. and extrapolate using a curve of blank diameter/load, to a value corresponding to Lsmax. Similarly, since the maximum attainable depth of pressing is largely determined by the magnitude of Ds max, study of Ls max would seem an ideal parameter for material evaluation studies. This approach has been used by Harper and Whiteley.[43] They state that any variable that increases the maximum load required to draw a blank increases the forming ratio Ld/Ls, and their work was aimed at providing a quantitative measure of the effect of these variables for mild steel samples. They examined materials in which there were $\bar{R}$ and 'n' differences, all other properties being kept constant, and process variables such as tooling geometry and blank sizes. The quantitative results confirm those postulated in an earlier paper.[42]

2.9.3. The Use of Non-Simulative Tests

As with simulative tests, numerous attempts have been made to correlate formability with various mechanical and physical sheet properties. Since such properties as yield strength, work hardenability and the anisotropy ratio, as determined in the tensile test, have been shown to markedly affect the performance of metal under the press, it is only natural that users have attempted to control drawability by use of some metallurgical parameter. The tensile test has the advantage that it is reproducible, unaffected by process variables and that it gives rise to a great deal of relevant information. Unfortunately, tensile testing represents deformation in the relatively simple case of uniaxial tension and the degree to which results, obtained under such conditions, can be related to deformation in press forming, has itself been the subject of much research. Evaluation of mechanical test data also seems

to be related more often to simulative test results rather than conditions existing within industry.

2.9.3.1. The Tensite Test

This test has been used more extensively in deep drawing research than any other test. The results obtained from this test must, however, be treated with caution. The ultimate tensile strength for instance, in reality has very little fundamental significance with regard to the strength of the metal unless the original cross sectional area of the test specimen is specified. For ductile metals this value can be regarded as a measure of the maximum load which a metal can withstand under the rarely found industrial condition of uniaxial loading. The relevance of the U.T.S. increases as the material becomes more brittle. A more rational approach, now being used more frequently, is to measure yield strength. Similarly, elongation figures are also markedly influenced by the geometry of this test specimen, particularly with respect to gauge length.

Two further factors, important in assessing press formability, can be obtained from the tensile test. These are R and 'n' values. 'R' is the ratio of width to thickness strain. This value, however, varies both with degree of strain and with the angle of testing to a reference direction, normally the rolling direction. This second variable can be minimised by testing samples at 0°, $22\frac{1}{2}^{\circ}$, 45°, $67\frac{1}{2}^{\circ}$ and 90° to the rolling direction and taking their average, but their value taken with respect to strain depends largely on the material being tested. For mild steel, for example, very little change in R with strain occurs so that for such cases it is general to quote figures that correspond to either 15 or 20% strain. (Values less than 10% are insufficiently accurate as such small dimensional changes are difficult to measure).
For materials that exhibit large changes in R value with respect to strain, it would seem more justifiable to average this value over a large range for as many readings as possible, i.e. one every 5% increase in strain from above

10% strain to approximately the strain level corresponding to the onset of instability.

If the cross sectional areas, corresponding to each load, are measured then the data obtained from the tensile test can be used to derive a true stress/true strain relationship. Accurate area measurements are only possible up to instability which, in the case of stainless steels, normally corresponds to natural strains of between 0.3 and 0.45. Beyond the limit of uniform elongation the validity of results is questionable as the basic stress mechanism deviates from that of uniaxial tension.

From the slope of the true stress-true strain relationship, plotted on logarithmic scales, a parameter, generally designeted 'n' and called the work or strain hardening coefficient, can be obtained. This parameter has received wide attention in the press forming field. The most commonly used function to describe the relationship between stress and strain is that proposed by Ludwik:-

$$\bar{\sigma} = K\delta^n$$

where $\bar{\sigma}$ = true stress
δ = true strain
K = constant
n = work hardening coefficient

If this relationship is obeyed then the physical significance of 'n' is that of the true strain corresponding to the point of instability. For metals that do not obey such a relationship this value may be obtained by Hill's or Considère's method.[44]

Grumbach and Pomey[45] have examined the accuracy of measurement of 'n', and the influence of factors such as the rate of work hardening, test piece dimensions, different materials, anisotropy and the measuring bases which may introduce systematic deviations. Not surprisingly, they found that the main source of variation in this parameter occurred in measurement of gauge length, i.e. $\pm$ 3%. They did not, however, examine accuracy with respect to test pieces of different gauge lengths.

Many objections have been made to the Ludwik relationship, the most fervent ones coming from Halstead, McCaughley and Markus[46] and Voce.[47] The main objections that Voce expresses are that the Ludwik relationship is purely empirical and that it suggests that all materials become infinitely strong after severe deformation, a fact easily demonstrated to be wrong from examination of pure aluminium. Voce offers an exponential function -

$$S = S_\infty - (S_\infty - S_o) \exp(-\eta/\eta_c)$$

where So is the threshold stress at which plastic deformation begins, S_∞ is the asymptotic stress attained after severe deformation, and η_c is the characteristic strain which determines the shape of the curve. A double logarithmic plot of this exponential function forms a curve of the correct shape in that it represents the true three stage shape of the curve and not merely the central portion, which is the part of the full curve described by the Ludwik equation.

2.9.3.2. The plane strain compression test

The main advantages of this test in relation to press formability are that the stress system employed simulates conditions which exist in deep drawing and that natural strains approaching 2.3 are permissible. This higher level of strain permits study of the third stage within the stress-strain relationship. The test is, however, time consuming, subject to friction and must be carried out at slow strain rates. It is also difficult to obtain reliable R value determinations. A method has been suggested by Hosford and Backofen[48] which entails making laminated specimens formed by cutting narrow strips from the sheet, stacking and glueing with epoxy resin and finally milling the composites to form new strips with the original width now the through thickness. The first part of this procedure, measurement of width strain, simply involves deformation of strips in the plane of the sheet, Fig.2.9. It is debatable whether the technique would be suitable for stainless steel since the accuracy would depend on the rigidity of the composite.

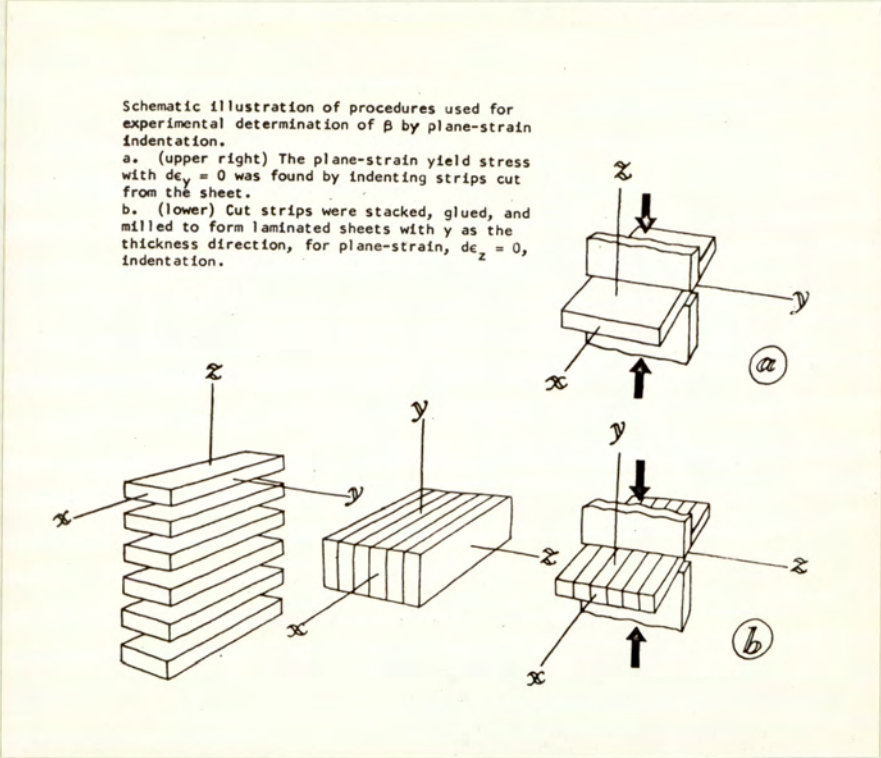

Fig. 2.9. A method for R value determination by plane strain compression.

2.10. Correlation of Simulative and Non-Simulative Tests with Pressing Performance

Unfortunately, very little information is available which correlates the use of both of these types of test with industrial performance and that which has been issued deals almost entirely with mild steel. A survey of the information available for stainless steel will be discussed in a later section. In the main, correlations have been made between simulative and non-simulative tests. The best, and most investigated correlation is that between R value and L.D.R. for mild steel using conditions of restricted stretch forming. No correlation

equal to that for mild steel, has been shown for other materials although Whiteley[49] has shown that a relationship exists between the L.D.R. of various metals and their $\bar{R}$ values. This is tantamount to categorising materials in order of their abillity to resist localised necking. Apart from correlations with the strain ratio it is probably true to say that tensile test results are more useful in predicting stretch formability than deep drawing. In deep drawing uniform elongation is a measure of only one of the material requirements, whereas in stretch forming processes, it is a major factor. Stretch formability should also be improved for materials exhibiting a high work hardening coefficient and indeed for materials obeying the Ludwik equation, this is really saying that they exhibit good uniform elongation.

Although simulative tests have been used for a considerable time it seems unlikely that they will ever adequately predict performance for more than a narrow range of pressings. Their value lies in their ability to investigate process variables in the pressing operation and in the metallurgy of the material being pressed.

2.11. The Rôle of Anisotropy in Sheet Metal Forming

There are two forms of anisotropy in sheet metal. First, the mechanical properties of an anisotropic sheet will vary with respect to the orientation of the test piece to that of the rolling direction: planar anisotropy. An obvious consequence of this "defect" is the formation of ears on the rim of a deep drawn component. Second, the properties through the thickness of the sheet can be different from those in the plane of the sheet: normal anisotropy. This latter type of anisotropy is considered to be desirable if in excess of unity, as certain materials are more formable as a result of its presence. Anisotropy may be caused by many factors but the most important cause in sheet metal forming is that of preferred crystallographic orientation.

Hill[44] proposed a method for measuring anisotropy normal to the

plane of the sheet which did not entail a measurement of through-thickness properties. He showed that the ratio of strain in the width and thickness directions of a uniaxial tensile test were dependent only on the direction of test and the anisotropy of the sheet. This strain ratio is defined as:-

$$R = \frac{\ln Wo/W}{\ln to/t}$$

where Wo and to are the initial width and thickness of the specimen.

The degree of both planar and normal anisotropy is indicated by the relative values of $R\,0^{\circ}$, $R\,45^{\circ}$, $R\,90^{\circ}$: test results at different angles to the rolling direction. The material is only completely isotropic when $R0^{\circ} = R\,45^{\circ} = R\,90^{\circ} = 1$. Equality of the strain ratios alone only indicates planar isotropy. These values are usually not equal to one another or to unity. The component of normal anisotropy can be defined as:-

$$R = \tfrac{1}{4}\,(R\,0^{\circ} + 2\,R\,45^{\circ} + R\,90\quad)$$

but that of planar anisotropy is not so clear. However, the value (44)

$$\triangle R = \tfrac{1}{2}\,(Ro - 2\,R\,45 + R\,90\,)$$

and more recently (42)

$$\triangle R = \frac{(R\,0,\ 90 - R\,45)}{Ra}$$

where Ra is the average R coefficient in the plane, have been used to show good agreement with earing in some metals.

The accuracy of R value measurement can be increased if instead of thickness, length changes are used and the thickness derived assuming that the volume of the gauge length remains constant. Then

$$R = \frac{\ln Wo/Wx}{\ln \frac{lx \times Wx}{lo \times Wo}}$$

where lo is the original gauge length.

Other strain ratios have been used, including a factor designated β by Hosford and Backofen.(48) β is the ratio of the plane strain tensile strength of the cup wall to the plane strain strength in compression in the flange

$$\beta = \frac{\sigma x \text{ (wall, } d\varepsilon\ y = 0)}{\sigma y \text{ (flange, } d\varepsilon\ z = 0)}$$

where x, y and z are the directions indicated in Fig.2.10

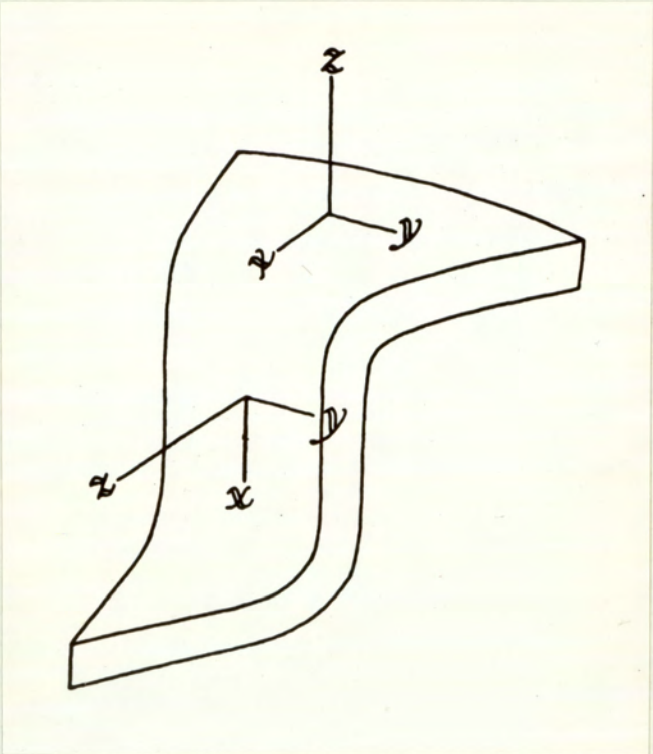

Fig.2.10. X, Y and Z Directions.

Since yielding within the cup wall can only occur by sheet thinning, maximum drawability is obtained when β is high: the wall strength should be as high as possible relative to that of the flange. Differential property control between wall and flange can be achieved by texture control.

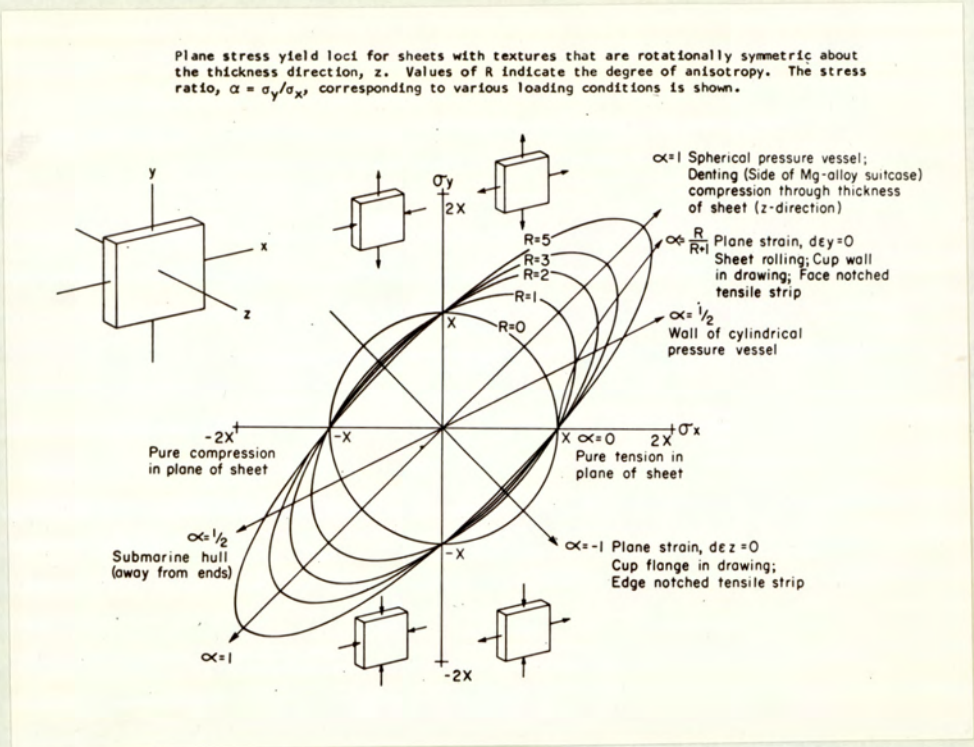

Fig.2.11. Anisotropic Yield Loci.

Examination of Fig.2.11, the anisotropic yield loci given by Hosford and Backofen,[48] indicates that the strength in the wall increases with R while that in the flange decreases. The drawing limit must therefore be strongly related to the factor β. In the special case of planar isotropy R and β are related thus:-

$$\beta = \sqrt{\frac{R+1}{2}}$$

or where there is planar anisotropy, the direction of measurement must be specified, i.e.

$$\beta = \sqrt{\frac{R_{rd}\ (R_{td}+1)}{R_{rd}+R_{td}}}$$

where R.rd and Rtd are the R values identified with the rolling direction or the transverse direction.

The factor β is obviously more relevant to deep drawing than is the R value but it is far simpler to measure the latter from a tensile test than β from two more difficult plane strain compression tests. The calculation of β would, however, be useful for materials of limited ductility in tension, where higher strains can be obtained by compression testing.

2.12. The Relationship between the Limiting Drawing Ratio and Anisotropy

The first attempt to relate normal anisotropy to drawability was made by Whiteley who showed that a positive correlation with L.D.R. existed for a number of materials. Stainless steel results now reported do not support this view.

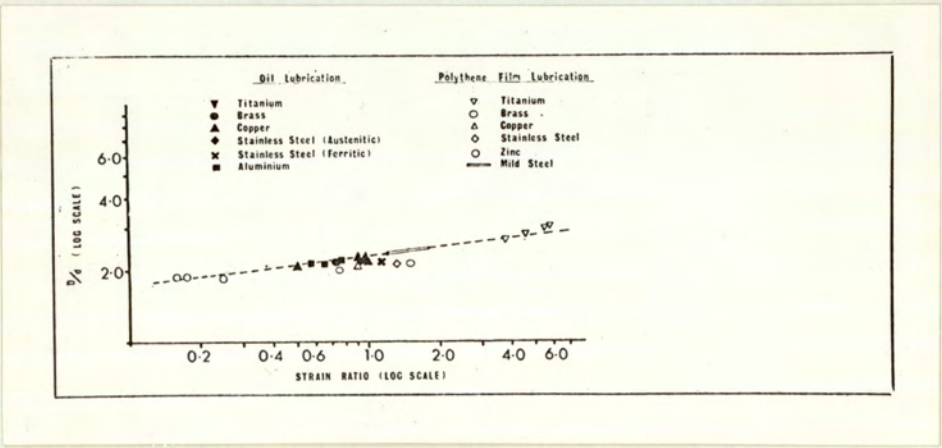

Fig.2.12. The Relationship between L.D.R. and R value.

In the appendix to Whiteley's [49] paper, the author derived the following expression for drawability:-

$$\ln D/d = \frac{1}{1+n}\sqrt{\frac{\bar{R}+1}{2}}$$

where D/d is the limiting drawing ratio, $\bar{R}$ the average strain ratio, and n a friction parameter with a value between 0.2 and 0.3.

This expression was based on Hill's anisotropic plasticity theory, with an analysis by Hu. This clearly shows the dependence of L.D.R. on $\bar{R}$. The analysis applies only to pure radial drawing with no bending and unbending round the tool radii and it also neglects the effect of work hardening. This latter point has been shown by Holcomb and Backofen[50] not to be too serious.

Hosford and Backofen[48] further calculated β values for rotationally symetrical textures with sheet normalson the boundaries of the basic stereographic triangle. (Fig.2.13).

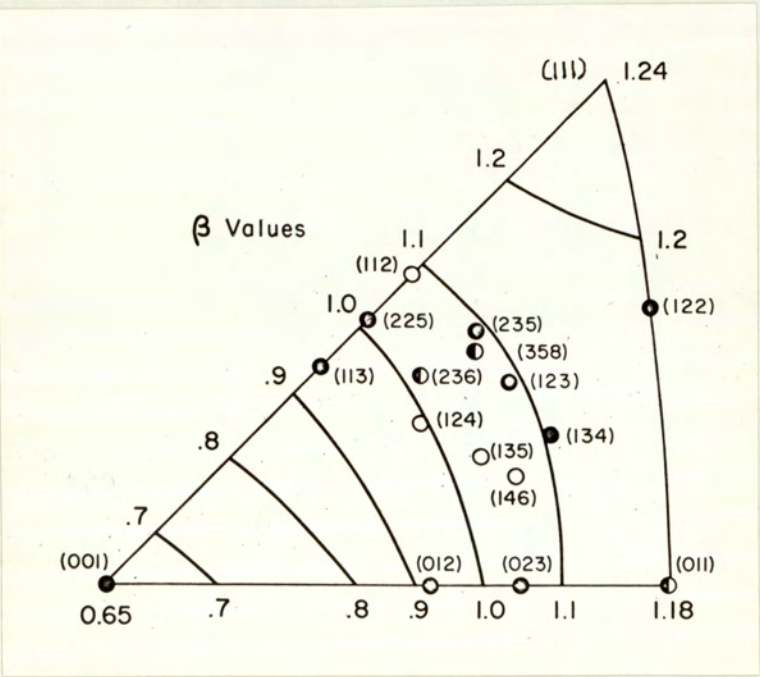

Fig.2.13. β Values for different textures.

Sheet normals near [111] are desirable for high drawability (β = 1.24) while those near [100] are undesirable. Using β max of 1.24 for a pure (111) texture, they calculated that the highest drawing limit for frictionless conditions

would be 3.46 which if a friction component of $\frac{1}{1+n} = .78$ is used, is reduced to 2.63. This value is approxi mately 20% greater than for isotropic material.

In a later paper by Holcomb and Backofen,[50] the equivalence of R and β was investigated. For mild steel and 70/30 brass, they found that, within the limits of experimental error, the results corresponded. Titanium, however, failed to give comparable results and this they postulated, resulted from the formation of shear cracks, in much the same way as occurs with magnesium. This they say explains the presence of failure sites in the cup flange for titanium drawn at room temperature. Lloyd,[51] on the other hand, reports a L.D.R. of 2.75 from tests on a titanium sheet of $\bar{R} = 3.8$.

Two further factors, in addition to anisotropy, appear to control the relationship between drawingload and cup wall strength. These are tool geometry and friction. This latter parameter has not received much attention. Atkinson[52] states that the true effect of normal anisotropic plasticity in cup drawing, may be masked by friction and that when it can be reduced, R values may be predictable from L.D.R. measurements, with an accuracy comparable with that of direct measurement. Again correlation between these two values only holds for mild steel. However, it is suggested by Atkinson,[52] that the general relationship between L.D.R. and $\bar{R}$ corresponds to $8 \log (\frac{D}{d}) = \text{Log } \bar{R} + 3$ which is equivalent to $(D/d)^8 = 1000\,\bar{R}$. Although it is suggested that this relationship can have little physical meaning, it shows that L.D.R. is only changed by relatively large changes in $\bar{R}$. This relationship also fits observed results better than does the Whiteley-Hu relationship.

2.13. The Press Forming Properties of Stainless Steel

In addition to good corrosion resistance to a wide variety of media and good formability, stainless steel can be supplied in many different attractive finishes.. These attributes are increasingly resulting in its use for many architectural, domestic and industrial applications. The steels are

used extensively for various formed and drawn parts. Within recent years, however, there has been a trend towards increased complexity of component, and in an attempt to reduce costs, fabricators are attempting to decrease the number of pressings and thereby minimising the number of intermediate annealing operations. The result has been an increased demand for improved formability and for a better understanding of the factors affecting it.

Ludwigson and Brickner[53] have made a survey of the factors affecting the formability of type 301 stainless steel. In making a comparison with mild steel they quote three press requirements; stronger and more rigid forming equipment; greater blank holder pressures to avoid wrinkling and greater attention to design so as to minimise problems of springback, stress cracking and distortion in severely formed parts. To this can be added improved lubrication.

With respect to an industrial application, that of a wheel disc, Divers[30] correlated the pressing performance of type 301 stainless to a somewhat dubious measure of work hardening,omega. He found that for the particular application studied, choice of material with omega values between 0.55 and 0.70, (high work hardening coefficients) gave considerably reduced failure rates and a decrease in the amount of waste material from 40% to less than 6%. Unfortunately, he also states that pressed material with omega values in excess of 0.52, which is less than his omega value for optimum pressing conditions, resulted in failure due to stress corrosion cracking in a subsequent plating operation. Divers, using multiple regression analysis, also related values of omega to composition but confined the range studied to that of the specification for type 301. The application studied by Divers was one of almost pure stretch forming for which a high rate of work hardening is beneficial.

For a similar application, Black and Lherbier[54] examined formability with respect to the true stress-true strain data, "springback" and composition,

namely nitrogen content. The authors offer a formula, originally proposed by Paulson et al (Boeing Co.), for the calculation of formability:-

$$f = \frac{\ln \left[\sigma m \, (1 - Eu) \right]}{A}$$

where σm is the stress at maximum load, Eu is the maximum uniform strain and A^{Eu} the deformation work area, i.e. the area under the stress strain curve to a point corresponding to σm. Low values indicate improved press formability. Analysis of this factor shows that of the three properties evaluated, uniform strain is by far the most important, and to achieve a low factor, stress at maximum load should be low while the other two factors should be as high as possible. However, a low stress at maximum load and a high uniform strain are opposing factors, and the latter must be maintained even at the expense of other factors in the equation.

Fabricators of metals are also aware of the power requirements necessary for permanent deformation and to this end generally prefer low yield stress material. Fortunately, a low yield stress indirectly improves the formability factor in that it increases uniform strain and the deformation work area but has little influence on the stress at maximum load. This therefore seemed an obvious way of improving formability and was achieved by Black and Lherbier by decreasing the nitrogen content of the steel.

Ancillary to the pressing operation, it is desirable to restrict die wear to a minimum and secondly to avoid "springback" or distortion in the final pressing. The authors show that a decrease in rate of work hardening causes a decrease on all of the factors given in the formability formula, resulting in a net decrease in formability. Particularly for stretch forming applications, high work hardening rates are desirable although in antithesis to power requirements, die wear and "springback". This latter defect can be offset by a decrease in yield strength.

As a method of quality control the formability factor must be extremely

useful so long as individual limits are fixed for characteristic operations.

2.14. Engineering Press Forming Requirements

In press forming operations the shape of the final product is determined at the design stage and therefore the metallurgist or engineer has only a limited number of variables from which he can obtain optimum conditions for any given pressing.

There are, however, several generalisations that can be made. Punch and die radii should, if possible, be between four to ten times that of the sheet thickness. Again depending on the operation, clearance between punch and die should be sufficient to eliminate ironing, although in some cases, ironing may be considered beneficial in reducing earing and in giving a more uniform wall thickness. Tool finish is also of great importance. Three further variables are available, drawing speed, temperature and lubrication, the individual effects of which are difficult to separate. Jevons[2] has expressed the view that decreased speed increases drawability particularly with respect to complex pressings. Nevertheless, there are many exceptions to this maxim. Mild steel, for instance, appears to favour high drawing speeds since the associated temperature increase results both in better lubrication and a decrease in the flow stress of the material. The evaluation and appreciation of these variables obviously constitute a large part to the art of press forming.

2.15. Summary to the Survey of the Literature

From a review of the above survey it seemed apparent that additional information could be gained from a more critical analysis of the rôle of non-simulative tests with respect to the press formability of stainless steel. To this end it was considered desirable to examine in greater depth, the complex stress-strain relationship that exists for metals of this type and to attempt to relate the results of this analysis to press formability. Using this approach it was also considered that useful information could be gained concerning the effect of prior deformation on both the mechanical properties and press formability.

It was also hoped that the relationship between austenite stability and composition could be strengthened from an assessment of the rôle of copper additions.

The above points will be discussed in a later section.

3.0. EXPERIMENTAL

3.1. Materials

The materials used for the experimental work are listed in Table 3.1.

Table 3.1.

Steel	Composition						
	% C	% Si	% Mn	% Cr	% Ni	% Mo	% N
A	0.09	0.52	1.26	17.47	7.73	-	0.036
B	0.035	0.66	0.82	18.19	10.06	-	0.035
C	0.03	0.49	0.75	17.86	10.90	-	0.030
F	0.055	0.43	1.71	17.85	11.94	2.75	0.041
S	0.08	0.50	0.62	17.65	7.06	-	0.025
D	0.045	0.40	1.03	18.74	9.69	-	0.035
E	0.051	0.51	1.67	17.70	11.73	2.72	0.040

The above steels were supplied as commercial products, A, B, C and F at 0.036" and S, D and E at approximately 1/8" thick. The first four steels had been annealed at 1050° C for ½ hour, cooled by an air blast and given a 2% stretch straightening operation. This material was used primarily for a number of preliminary and exploratory tests to investigate the range of pressing and mechanical properties available for annealed material. Where appropriate, results from these four steels have been used to substantiate the results from steels S , D and E.

The main bulk of the work has been carried out on steels S, D and E which were used to investigate the effects of prior cold working on both the mechanical properties and press formability of the material.

3.2. Material Processing

An outline of the processing of the steels S, D and E, including its rolling reductions, times and temperatures of intermediate and final anneals, is

given in diagrammatic form in Fig.3.1.

The material was rolled to a final thickness of 0.036" so that results from the deformed material could be compared with those obtained in the exploratory tests and because this gauge is a common one used in commercial practice. Strip rolling was performed on a 200 ton, 4 high experimental Fenn mill operated at the slowest speed. Care was taken during this operation, by use of slow rolling speeds, small and infrequent passes and oil lubrication, to minimise associated temperature rises in the metal which could have resulted in effective, warm working of the material. The final gauge of the material varied by less than ± 0.001" both across the width and along the length of the strip.

Intermediate and final annealing treatments were carried out in the same electrically heated furnace. Although the degree of temperature control varied by ± 10° C at 1050° C the heating zone was approximately twice that of the lengths of strips annealed so as to minimise temperature variations along the strip. All strips were water quenched after annealing to ensure a completely austenitic product. All rolled products were descaled in a solution of 25% HNo_3, 5% HF and 70% Water. Finally, the annealed material from steels S, D and E was roller levelled by "sandwiching" between pieces of soft copper.

3.3. Assessment of Austenite Stability

As has been described in the survey of the literature, several methods are available for the assessment of the strain level and degree to which austenite decomposes as a result of deformation (austenite stability or instability). For the purpose of this work it was decided that the empirical relationship given by Post and Eberly [11] would be most suitable. The relationship equates the actual nickel content with a theoretical content based on the summation of nickel equivalents, the equivalents varying in magnitude depending on their ability or inability to act as austenite stabilisers, i.e.

$$\%\,Ni_{(theoretical)} = \frac{(Cr\% + 1.5\,Mo\% - 20)^2}{12} - 0.5\,Mn\% - 35\,C\% + 15$$

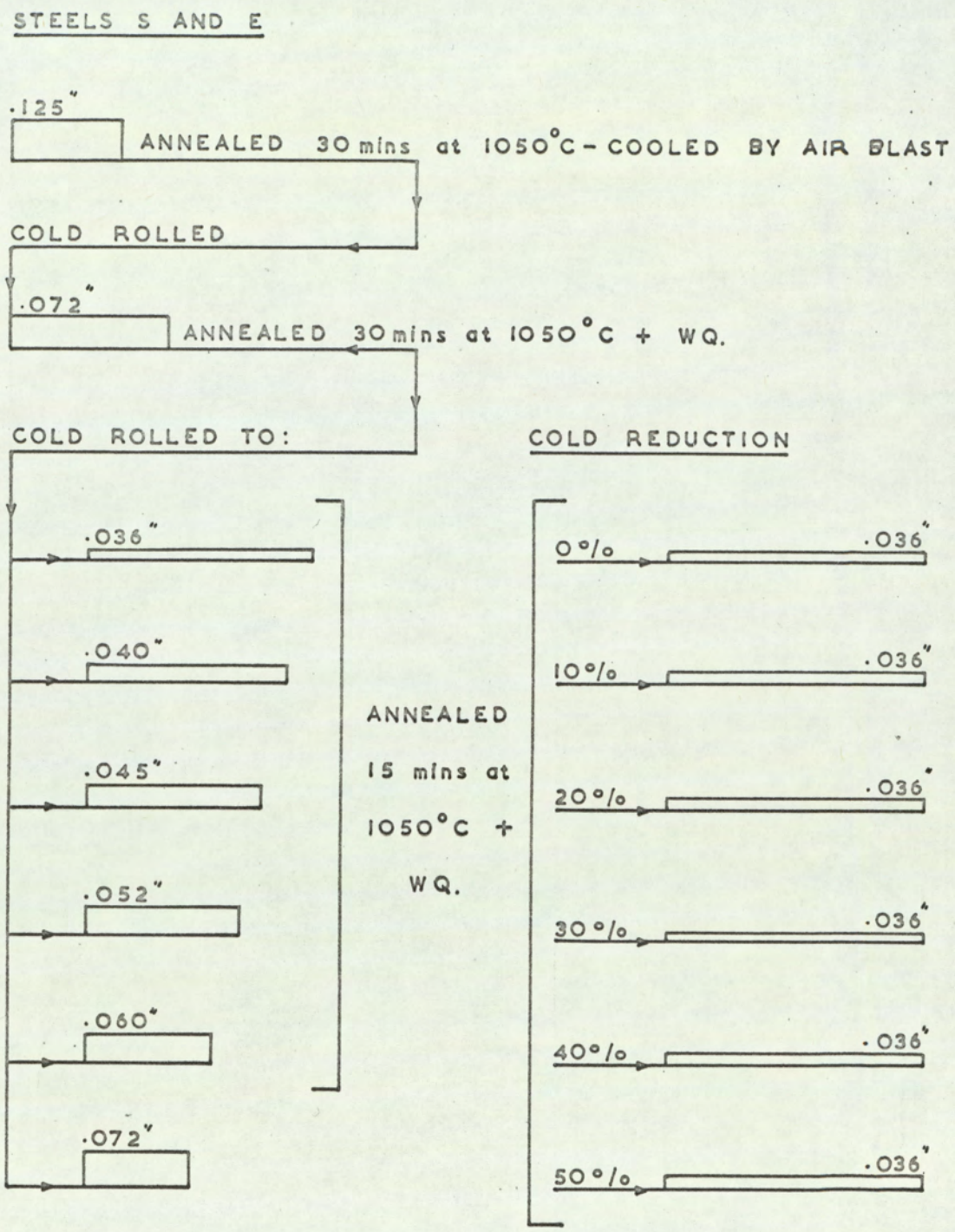

Fig. 3.1. The Processing Schedule for Steels S, D and E.

This equation expresses quantitatively the stability of the austenite in terms of a value Δ where

$$\Delta = \%\,Ni_{(analysed)} - \%\,Ni_{(theoretical)}$$

Positive values indicate that the alloy contains more nickel than is necessary to make the austenite phase stable at room temperature while negative values indicate insufficient nickel. Post and Eberly have indicated the following strain levels at which martensite is initiated by deformation:-

Table 3.2.

Δ	Degree of strain necessary to form α' martensite
- 4.0 - -2.0	1 - 10 % Cold Work
0	30 - 40 % " "
>+ 1.0	70 - 80% " "

The above equation does not take into account the strong stabilising effects of nitorgen and it would seem therefore that the calculated Δ values, for the steels examined, would be too negative. The magnitude of this effect was, however, minimised by using steels of similar nitrogen contents. An appendix to this thesis will suggest values for both the effect of nitrogen and of copper on the value of Δ .

The calculated Δ values for the steels examined are listed in order of increasing austenite stability in Table 3.3.

Table 3.3.

Steel	Post & Eberly Δ
S	- 5.29
A	- 4.12
B	- 3.57
D	- 3.34
C	- 3.05
E	- 0.9
F	- 0.6

3.4. Assessment of the Quantity of Transformation Products resulting from Deformation

As has been described, deformation of austenite results in the formation of three products-:

1. Deformed austenite
2. ε martensite
3. α' martensite

Evidence has been offered that states that both austenite and ε martensite are paramagnetic whilst α' martensite is ferromagnetic. There also exist differences between the three crystallographic structures since austenite is face centred, ε martensite close packed and α' martensite body centred. Associated with the differences in crystallographic structure are unit cell size differences and differences in electrode potential between the phases, particularly austenite and α' martensite. Finally there exists a metallographic difference between the three phases. These are some of the characteristics that have been examined in order to assess the amount of α' martensite obtained upon deformation.

3.4.1. Magnetic Measurement of the α' Martensite Content

Two magnetic techniques were examined, one using a Precision Coercive Force Meter Type 1.094 marketed by the Institut Dr. Förster of Reutlingen in W. Germany. The second technique utilised a simple magnetic method for measuring the magnetic response of the material.

3.4.1.1. Measurement of Coercive Force

Coercive force and permeability are physical characteristics of ferromagnetic materials which, for different material conditions, may vary greatly. When making permeability measurements, the physical shape of the test sample is of extreme importance, while coercive force represents a physical characteristic which can be measured almost independently of the physical shape of the sample.

Coercive force is the opposing field strength Hc required to bring the magnetization intensity J (JHc) or the induction B (BHc) to zero in a material following previous saturation magnetization. (Fig.3.2.)

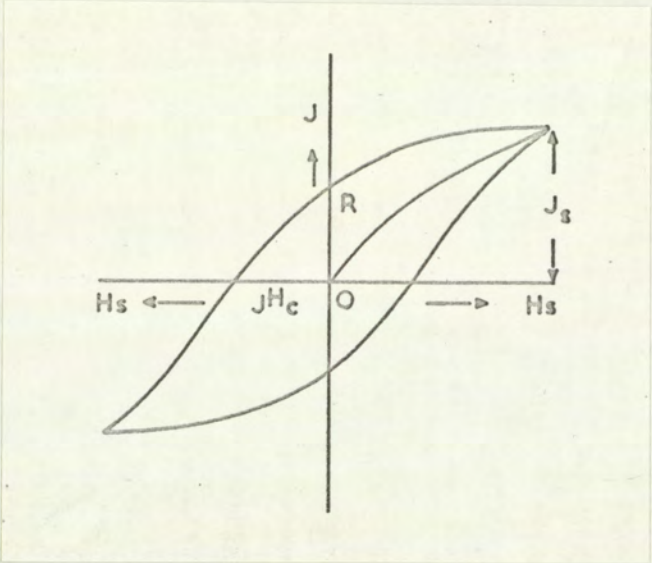

J = Magnetization Intensity
Js = Saturation Magnetization
R = Remanence Point
S = Saturation Point
H_s = Saturation Field Strength
JHC = Opposing Field Strength (J = 0) (Coercive Field Strength)

Fig.3.2. The relationship between magnetisation intensity and saturation field strength.

Initial trials indicated that the technique would be ideally suited for measuring small changes in magnetization and therefore α' martensite. Examination of Fig.3.3. shows that for Steel S, in which considerable amounts of α' martensite are produced by deformation, the coercive field strength decreases with the volume of α' martensite produced (i.e. strain). It also shows that the coercive field strength obtained from samples deformed in compression is higher than for tension, indicating that a tensional stressing system initiates more α' martensite. Thirdly, for material that undergoes no transformation in the strain range examined, Steel E, a fairly constant "background" level of force is obtained which indicates that the technique is not strain dependent. Unfortunately examination of the results for Steel D which has an austenite stability intermediate between S and E, shows a reverse tendency. The author does not offer an explanation for the anomalous behaviour of this latter steel and it was considered that the time required to

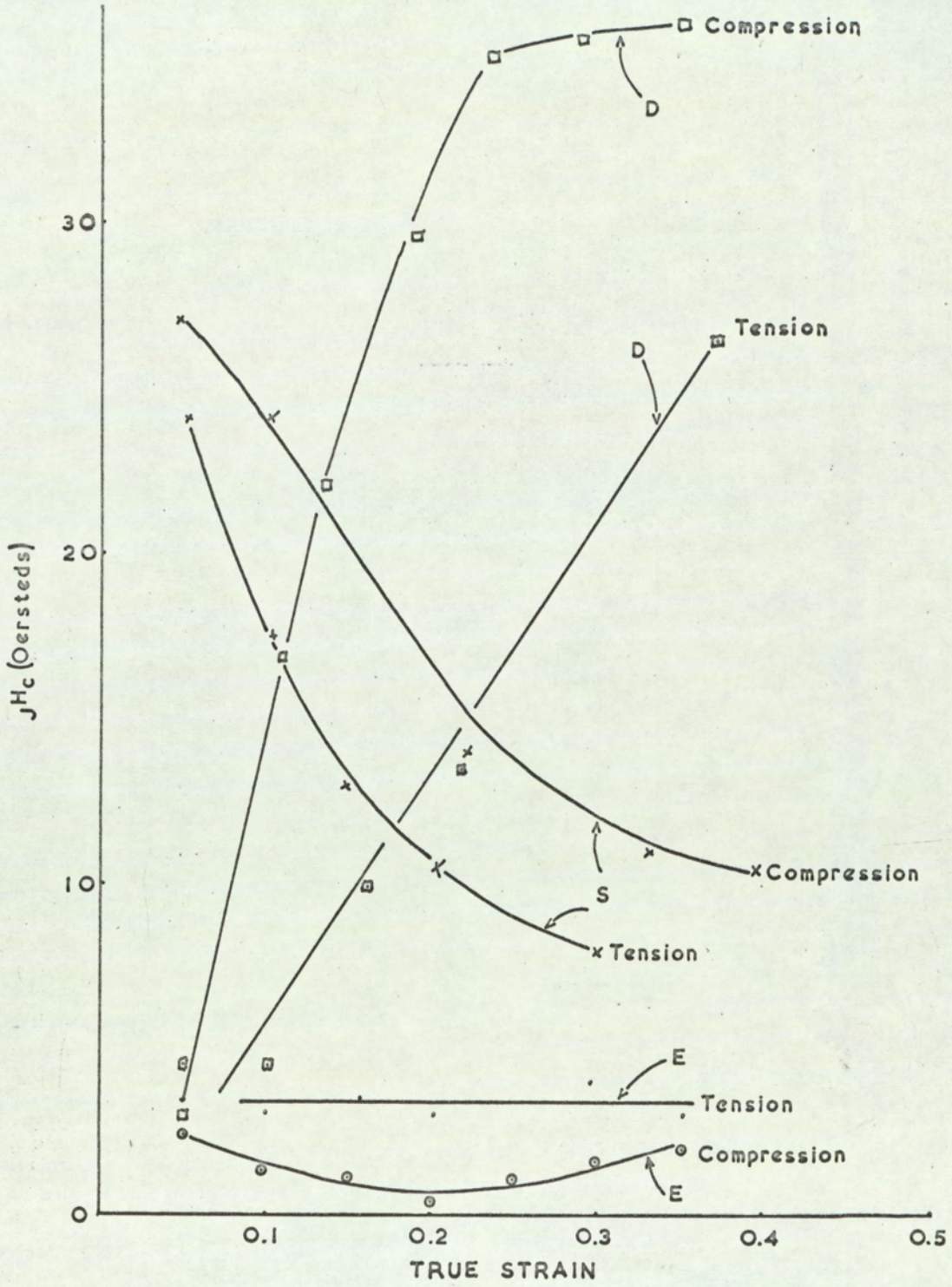

Fig. 3.3. The Relationship between Coercive Force and True Strain.

fully investigate this effect would have been unjustified for a technique that was only ancillary to the main theme of the project.

3.4.1.2. Measurement of Magnetic Response

In a D.E.W. Technical Report Dietrich[55] has evaluated the well known methods of destructive and non-destructive methods available for α' martensite determination. He found that the most reliable among the absolute methods was the use of saturation magnetization but the limitations of this process have already been detailed. The current non-destructive methods, of ferrite and α' martensite determination are more or less all based on the measurement of some magnetic property, in general the constant or alternating field permeability at medium field intensities. Both magnitudes, however, depend on shape and order of the magnetic particles in the austenitic matrix. A simple reproducible test was therefore devised to measure the magnetic response of the material and not any particular phase content. This response was found by measuring the force required to detach a permanent magnet from an electropolished $\frac{1}{2}$" diameter circle on the surface of the material. The $\frac{1}{2}$" x 1" bar magnet was firmly fixed into a 6" aluminium tube and the whole arrangement attached by a freely moving chain to the arm of a non-magnetic weight balance. The magnet and tube were placed vertically in contact with the surface to be tested and the weight in grams applied to the other side of the balance, which was just sufficient to detach the magnet from the metal surface, was recorded. Each test was repeated three times and the maximum reading taken as the most accurate measurement of magnetic response. Care was taken to ensure that the magnet rested perpendicularly on the metal surface. This method was quick, easy, reproducible and applicable to small areas, and gave the strain corresponding to the onset of α' martensite formation together with the magnetic response at higher strain levels.

3.4.2. Determination of the Onset of α' Martensite Formation from the Tensile Test

Since the formation of α' martensite is associated with an expansion of the lattice, then a decrease in the rate of narrowing and thinning for a constant rate of lengthening during the tensile test, should be an indication of the point at which α' martensite begins to form. A change in these rates was in fact observed for the steels that transformed. The rate of lengthening was measured from the rate of cross head travel of the tensile test machine which in turn was measured by a cathetometer.

3.4.3. X-ray Determination of Volume Fraction of α' Martensite

An X-ray diffraction method is often employed for determining the amounts of two or more phases in a material. The details of the method have been widely publicised. (56 and 57) In short the method is based upon the fact that the integrated intensity of a reflection is directly proportional to the volume fraction of the phase considered. In principle, the method only requires the measurement of the intensity of one reflection for each phase. The methods most severe shortcoming is that it disregards influences from preferred orientation. In a diffractometer where this type of analysis is carried out the geometry is such that the diffracting planes for a given Bragg peak are parallel to the specimen surface. The occurrence of diffracting planes parallel to the surface must therefore be as frequent as for any oriented physical plane of the sample. Such a condition will only be fulfilled for texture free material. Unfortunately, in this present work strong textures developed as a result of deformation. The problem was two fold in that not only did the degree of preferred orientation increase with deformation but the volume fraction of the second phase also increased. An attempt was made to isolate the effect of preferred orientation in a two phase material by studying an α - β brass. Initial trials again suggested that the amount of work necessary to solve this problem would be unjustified. Gullberg and Lagneborg[58] have since offered a method for the

X-ray determination of phases in a textured material but they point out that cold worked 18/8 type steels did not fit their results. Obviously the two effects of deformation and transformation interact to form a complex situation.

Several additional techniques for the determination of the volume fraction of α' martensite were examined but unfortunately none proved satisfactory.

After consideration of the above techniques it was decided to use the simple magnetic technique to measure the magnetic response of the material.

3.5. Optical Microscopy

Optical microscopy was used to measure the grain sizes of material in the annealed condition.

Samples were micropolished in the normal way and finally electropolished for five minutes in a solution of 185 parts perchloric acid (d = 1.60), 765 parts acetic acid and 50 parts of water at a current density of 0.04 - 0.06 and at a temperature of less than 30° C.

3.6. Electron Microscopy

A replica technique for the examination of deformed structures was used to confirm the strain levels at which α' martensite was initially formed. The formation of this phase induces surface discontinuities and thereby lends itself well to this technique.

Samples were electropolished and lightly etched in a solution of 3 parts Hcl, 1 part HNO_3 and 2 parts glycerol. They were then coated with a $2\frac{1}{2}$ - 3% solution of nitro-cellulose in amyl-acetate, dried and the coating removed with cellotape. A shadowed carbon replica was then made from the coating using a technique described by Kay.[59] Replicas were examined at 80 Kv in a Phillips E.M 200 microscope.

3.7. Tensile Testing

3.7.1. Tensile Test Pieces

Duplicate strips 6" long by 1" wide were sheared for each test at 0°, 45° and 90° to the rolling direction. Each strip was then machined to the British Standard design for strip tensile test pieces. These dimensions are indicated in Fig.3.4.

Care was taken during the machining of the above specimens to avoid transformation to α' martensite that could have resulted from deformation of the test piece edges.

3.7.2. Tensile Test Procedure

The average thickness of the strip was determined from four equally spaced micrometer readings taken within the 2" gauge length (micrometer readings to 0.0001"). One side of the gauge length was then thinly coated with engineers' blue and gauge marks were made with a template, every $\frac{1}{4}$" between the shoulders of the specimen. The additional markings within the 2" gauge length were made so that after testing, an estimation of uniform elongation could be made. The test piece was then mounted into the tensile machine and prior to testing, the width was measured at four equally spaced points within the gauge length with a micrometer and the gauge length measured with a cathotometer. The test procedure for the determination of both anisotropy ratios and tensile test data has been previously described.[60]

An electrically driven Hounsfield Tensometer was used for all the tests. The speed of cross head travel was kept constant at a rate of 0.062 in/min. (1.6 mm/min). Although this means that the true strain rate changed progressively during the test, the slowest average strain rate (0.00021/sec) was considered sufficient to minimise the effects of heat generated within the specimen and still be comparable to the slowest deep drawing average strain rate.

The load/extension diagram plotted semi-automatically with the

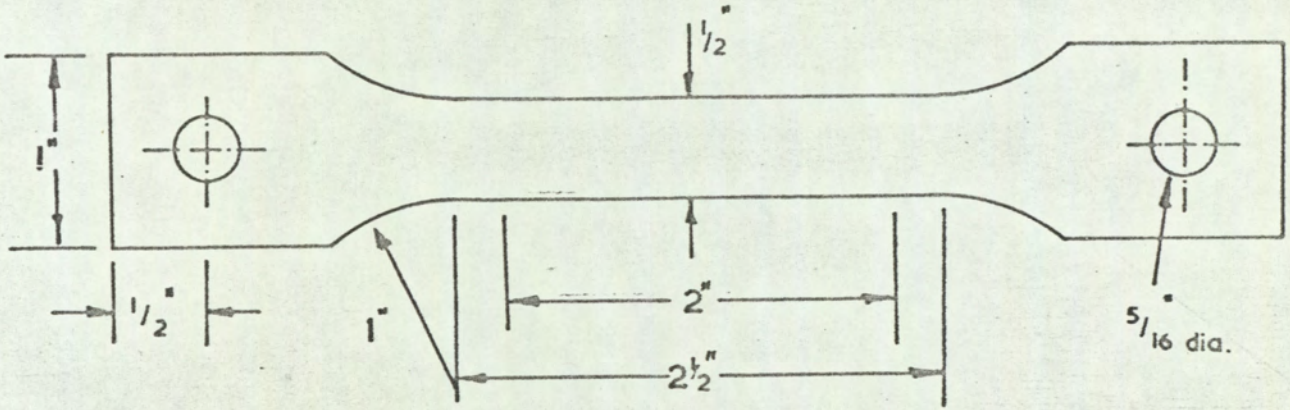

Fig. 3.4. Tensile Test Piece Dimensions.

Hounsfield tensometer does not give a true interpretation of specimen extension since the elongation of the entire test piece together with beam and machine deflections is also included. Values of uniform elongation were therefore calculated from measurements taken from the fractured test piece. Strain measurements, both before and during the test, were derived from direct measurements of the nominal 2" gauge length, with a cathetometer. The load/extension diagrams were used primarily for the calculation of stress data. The Hounsfield tensometer and cathetometer used is illustrated in Fig.3.5.

3.7.3. Tensile Test Results

The following parameters were obtained from each test:-

(a) Ultimate tensile strength.

(b) True stress corresponding to ultimate tensile strength.

(c) 0.5% proof stress. This was the minimum value of proof stress that was considered could accurately be determined from the load/extension curves since stainless steel does not show a well defined yield point.

(d) Elongation to fracture on a 2" gauge length.

(e) The uniform elongation from length measurements before and after the test.

(f) The ratio of 0.5% proof stress to ultimate tensile strength.

(g) R, the anisotropy ratio.

(h) The area beneath the load/extension curve. This value will be used as a relative measure of work required to deform the test piece.

(j) A measure of the work hardening capacity of the material.

Since stainless steels, in general, do not obey the Ludwik[61] relationship, $\sigma = K\delta^n$ a direct comparison with the conventional work hardening index, n, is difficult.

In addition to the above tests, considerable information concerning true stress/true strain data was also obtained from the load/extension curves. True stress and true strain were calculated from the following formulae:-

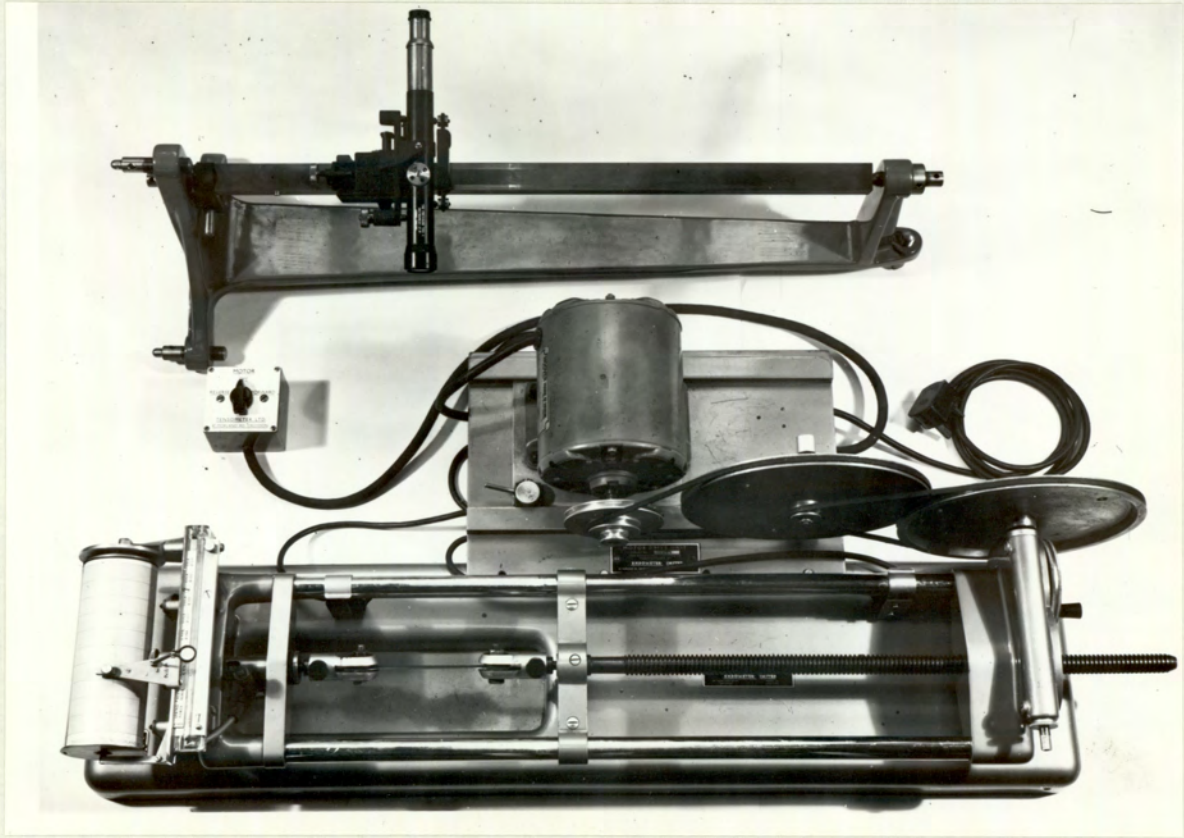

Fig. 3.5. The Layout of the Hounsfield Tensometer and Cathetometer.

$$\sigma = \frac{P(1+\varepsilon)}{Ao} \qquad \ldots\ldots 1.$$

$$\delta = \ln(1+\varepsilon) \qquad \ldots\ldots 2.$$

where σ = true stress
P = Load
ε = Arithmetic strain
Ao = Original area of specimen
δ = true strain

3.7.4. The Effect of Volume Change during Testing on the Accuracy of the Results

Angel[8] in work that has already been described, used an expression for the calculation of true strain which took into account the increase in total volume due to transformation:-

$$\varepsilon = 1/3 \left(\ln {}^{Ao}/_{A} + 2 \left(\ln {}^{l}/_{l_o}\right)\right.$$

He found that the difference between the value of strain obtained using this formula and $\varepsilon = \ln {}^{l}/_{l_o}$ to be negligible and therefore, for convenience, used the latter.

In order to substantiate these results it was decided to investigate this effect more fully. From test piece measurements it was found that the gauge length at the end of a test was approximately 3% less than it would have been had transformation not occurred, thickness was approximately 3 % larger and width approximately 6% larger; an overall volume increase of 6%.

From the two formulae, given in the previous section, which were used to calculate true stress and strain, it is obvious that the only maasurement that affects the accuracy of their calculation is length. If it is assumed that 100% transformation occurs during testing then the value of strain obtained should be smaller than it actually was, if transformation had occurred. Theoretical strains have therefore been calculated using the formula

$$\varepsilon_t = \ln \frac{(l \times {}^{3}/_{100})}{l_o}$$

and compared with actual strain values.

At maximum strain levels, assuming 100% transformation, there was a strain difference of 0.041 and a stress difference of 2.3 tons. In practice, actual differences in these values would be less for in no case is 100% transformation to α'martensite obtained. The actual and theoretical stress-strain curves showed little difference in shape and were within the limits of spread obtained from duplicate tests. It was therefore assumed that Angel's results had been substantiated.

3.7.5. Determination of a Function to define the True Stress-True strain Relationship

From the onset of plastic deformation to about 0.035 strain the true stress/true strain plot on a log/log basis is a straight line and by definition obeys the Ludwik relationship ($\sigma = K\delta^{n}$). This relationship does not hold for the second part of the curve. To determine a relationship for this second part, the true stress/true strain data were analysed by an Elliot 803 B computer. A modified Autocode library programme fitted a polynomial to a set of values of a function of one variable, using a method of orthogonal polynomials. Given pairs of values (xj, yj) $j = 1, 2 \ldots\ldots, M$, $M \leq 200$, the programme was able to compute a series of polynomials P1(x), P2(x), etc. where

P1(x) is in the form $Co + C1x$

and P2(x) is in the form $Co + C1x + C2x^{2}$ and so on up to P20(x).

Each of these polynomials Pi(x) was such that if $Yij = Pi(xj)$ then the sum of the squares of the deviations $\sum j(Yj - Yij)^{2}$ was a minimum. The sum of the squares of the deviations was a measure of the degree of fit.

3.8. Plane Strain Compression Testing

Plane strain and biaxial stress systems have a considerable influence on metal deformation in both deep drawing and stretch forming and it was considered necessary to investigate the rôle of each. An attempt has been made to relate the results to those obtained in tension and press forming. The method used is basically that developed by Ford [62] and described in detail by Watts & Ford. [63]

3.8.1. Plane Strain Compression Test Pieces

The test piece was in the form of a rectangular sectioned plate approximately $1\frac{1}{2}$" wide by .125" thick. Various relationships between tool and test piece geometry must be maintained during the test. These are described in detail in the paper by Watts and Ford, but the most important are:-

i. the ratio of strip width to thickness must be greater than 6, and

ii. the ratio of die breadth to strip thickness must lie between 2 and 4.

3.8.2. Plane Strain Compression Test Procedure

The test strip is indented incrementally between smooth dies and the indentation and load causing the indentation recorded. The lubricant used was a molybdenum disulphide grease (Castrolease MS3) and the tests were carried out on a 50 ton Dennison tensile machine. The test procedure of incremental loading was continued until a reduction in thickness of about 90% was achieved.

3.8.3. Plane Strain Compression Test Results

The plane strain was calculated from the formula:-

$$\varepsilon_p = \log_e \frac{to}{tx}$$ (where to is the initial thickness and tx the thickness after deformation)

The plane stress was calculated from:-

$$\varepsilon_p = \frac{\text{Load}}{\text{Die Breadth x strip width at indentation}}$$

These results were then converted to their tensile equivalents as follows:-

$$\varepsilon = \varepsilon_p \times \frac{2}{\sqrt{3}} \quad \text{and} \quad \sigma = \sigma_p \times \frac{\sqrt{3}}{2}.$$

An illustration of "failed" test specimens for the plane strain compression, hydrostatic bulge and tensile tests is given in fig.3.6, and the equipment used to obtain plane strain compression results is shown in Fig.3.7.

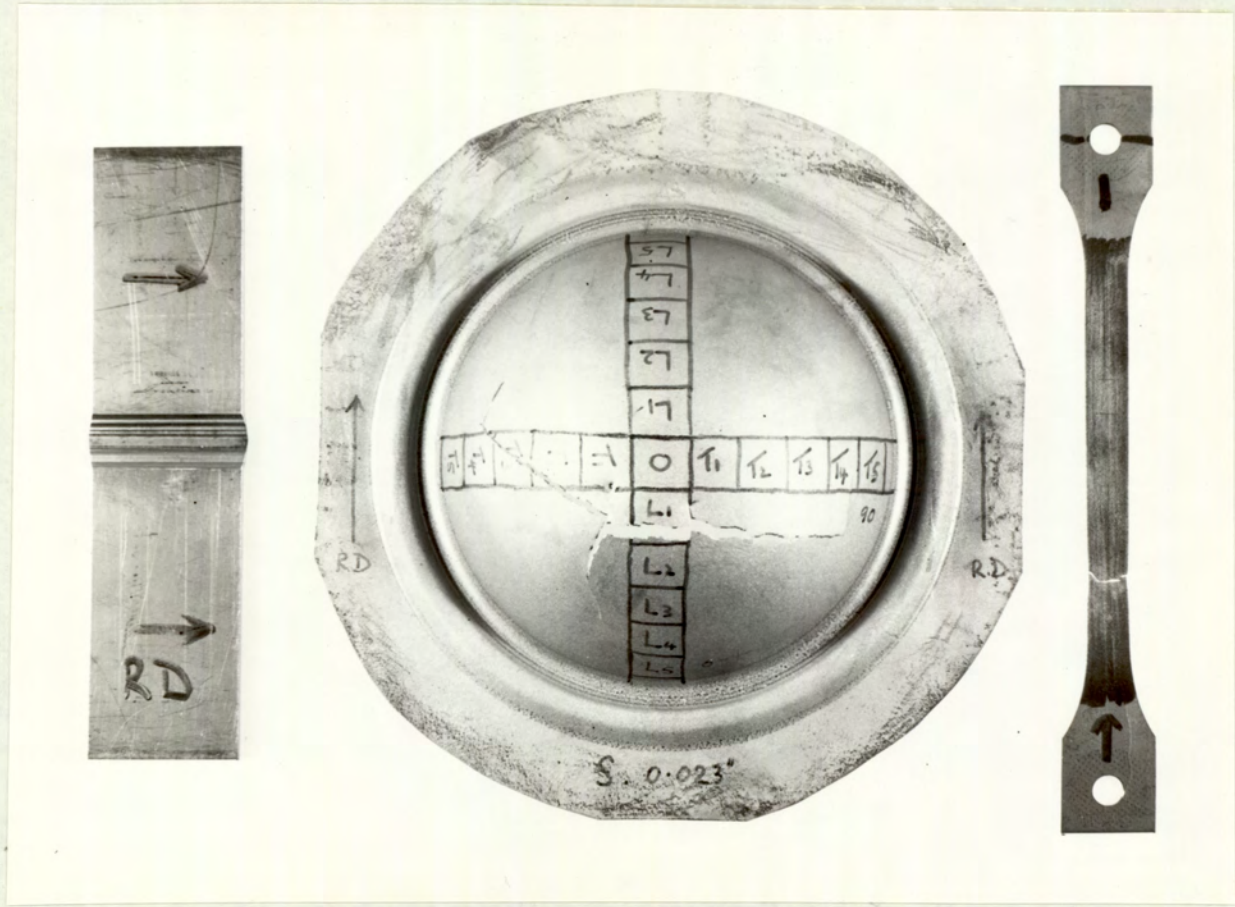

Fig. 3.6. An Illustration of Failed Test Pieces for the Three Tests examined – Tensile, Hydrostatic Bulge and Plane Strain Compression.

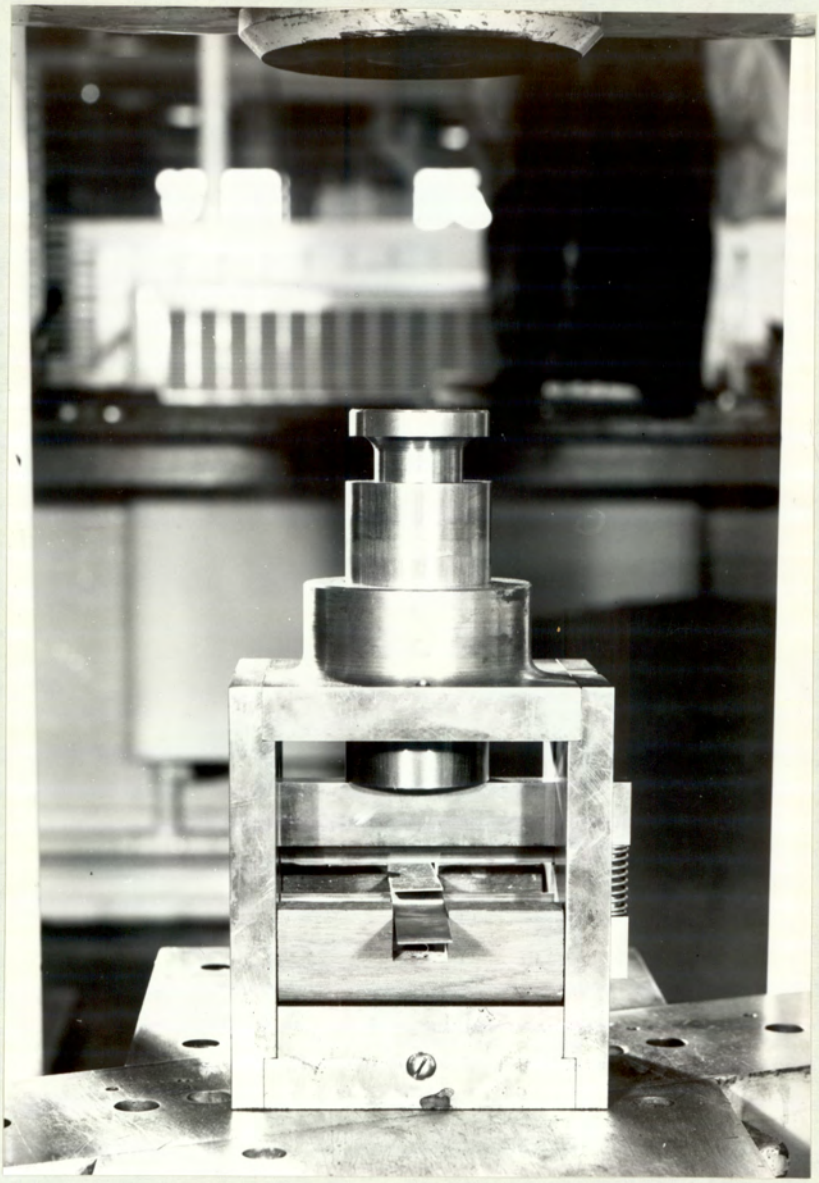

Fig. 3.7. The Plane Strain Compression Testing Equipment.

3.9. Hydrostatic Bulge Testing

The biaxial test extensometer measures extension and curvature at the centre of a circular diaphram which has been deformed by hydrostatic pressure. The deformation of such a diaphram has been extensively investigated by Mellor.[64] The true stress-strain curve for the diaphram can be computed from the extensometer readings. A method for deriving the relationship from the forming process is fully described by Johnson and Mellor.[65] The equipment used for the tests is shown in Fig.3.8.

3.9.1. Hydrostatic Bulge Test Pieces

No special techniques are required to prepare the $7\frac{1}{2}$" diameter disc test piece. As the specimen is clamped at the periphery the method used to cut the specimen does not influence the test i.e. care need not be exercised to ensure that specimen edges are not work hardened.

3.9.2. Hydrostatic Bulge Test Procedure

Five thickness measurements were made on the circular diaphram, one in the centre and at four other positions. The specimen was placed in the die and clamped. Pressure was then applied with a hand pump and incremental readings taken from the extensometer. The extensometer consists of a spherometer, for measuring the radius of curvature of the diaphram and an extension indicator combined in one unit as shown in Figs. 3.9 and 3.10. It rests on the surface of the diaphram and is allowed to rise freely as the specimen deforms.

3.9.3. Hydrostatic Bulge Test Results

3.9.3.1. Calculation of Strain

From examination of Figs. 3.9 and 3.10 it can be seen that the two probes rest on the flat specimen, initially at a distance Do apart. As the test proceeds, these move to a distance D1. The logarithmic circumferential strain around a circle of initial diameter Do then becomes $\text{Log}_e(\pi D1/\pi Do)$. It is assumed that the strains in this region are uniform so that the membrane

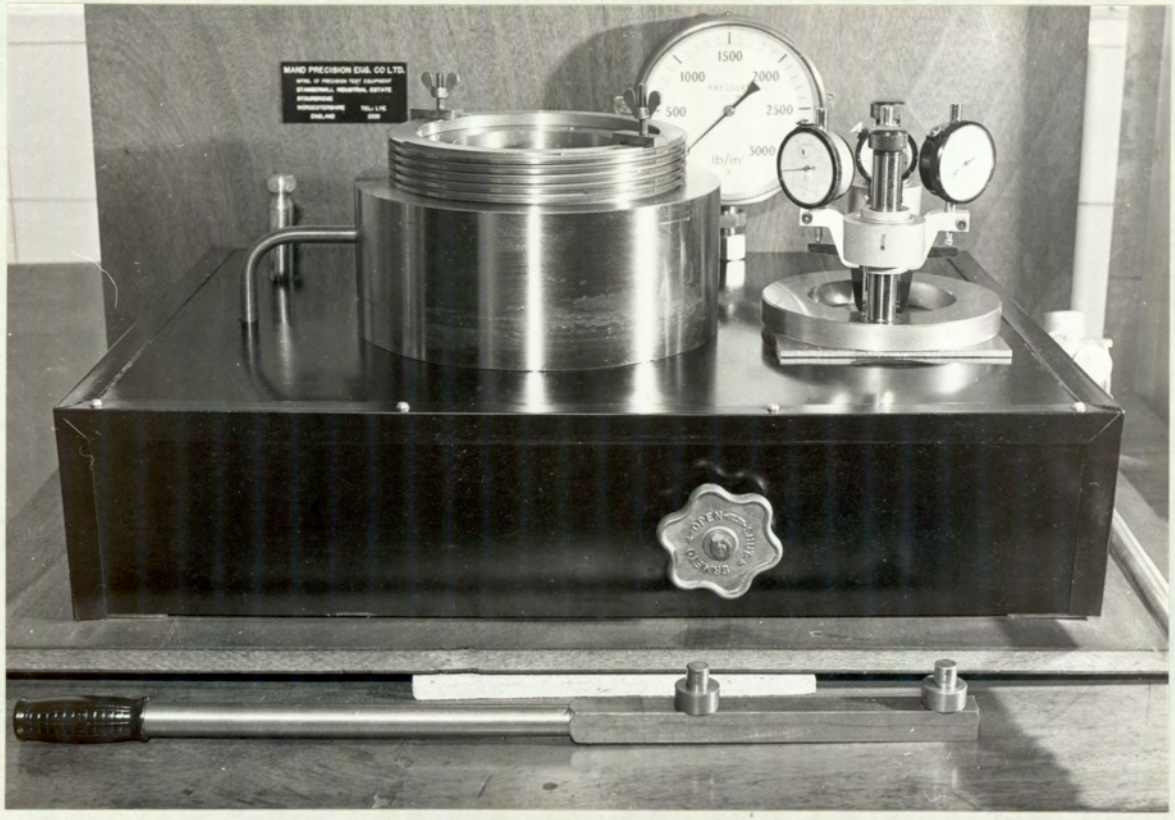

Fig. 3.8. The Hydrostatic Bulge Testing Equipment.

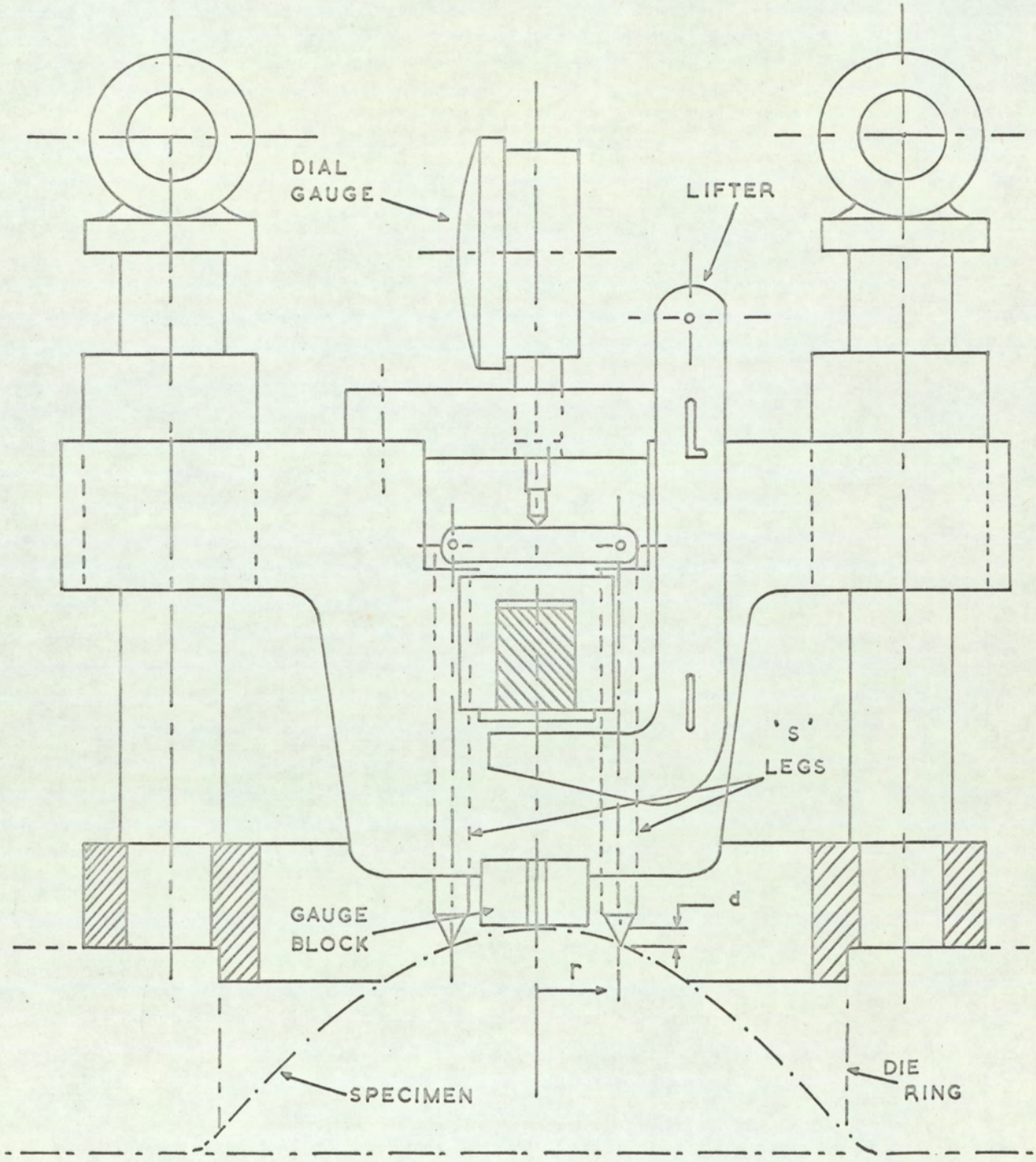

Fig. 3.9. The Extensometer Unit used in the Hydrostatic Bulge Tests.

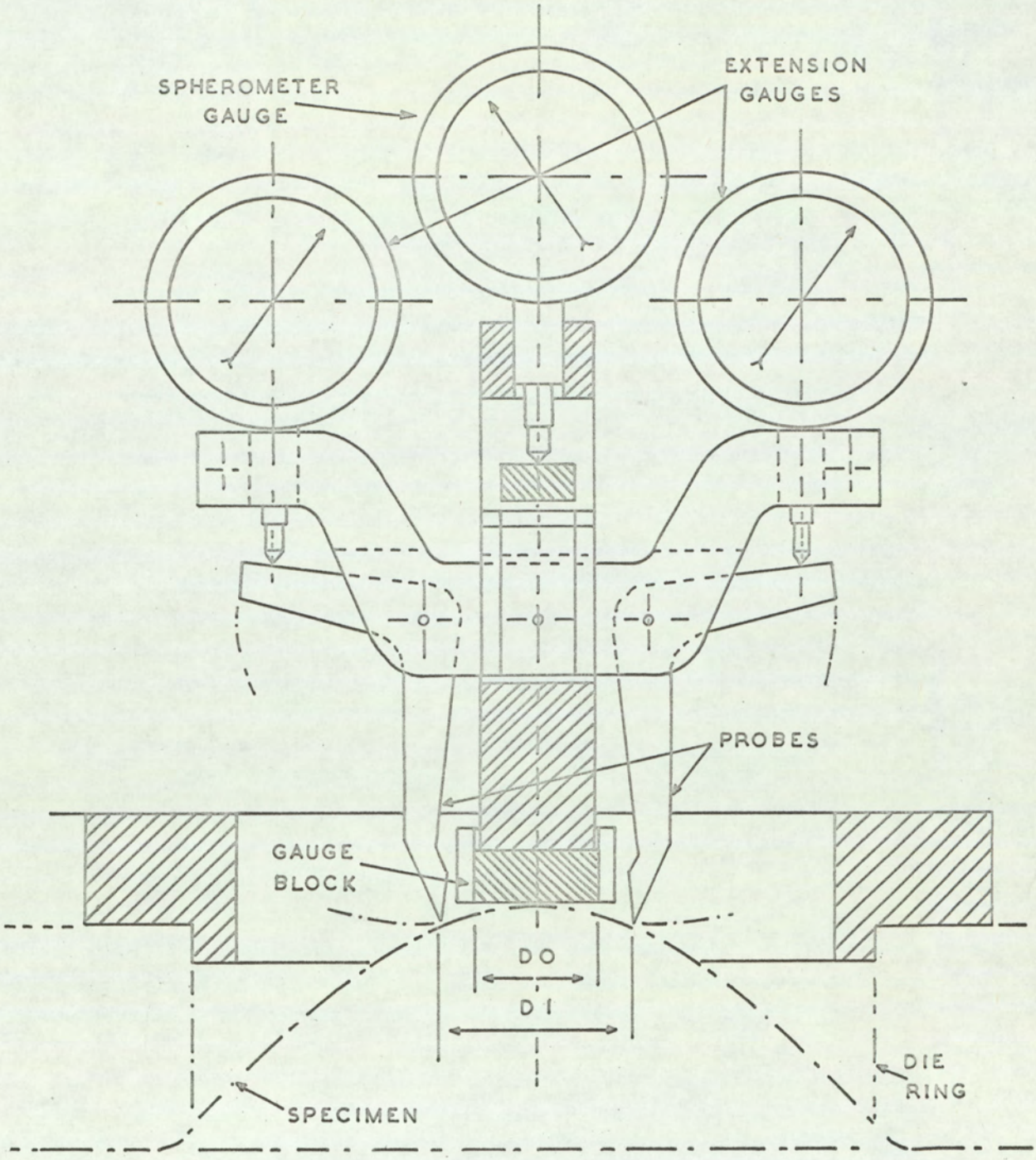

Fig. 3.10. The Extensometer Unit used in the Hydrostatic Bulge Tests.

strain in all directions at the pole is $\varepsilon = \log_e (\frac{D1}{Do})$. This strain, in terms of the two outer dial gauge readings a1 and a2 and the magnification of the lever system, K, is $\varepsilon = \log_e \left[1 + \frac{K(a1 + a2)}{Do} \right]$

3.9.3.2. Calculation of Stress

To obtain the representative stress it is necessary to derive the current thickness at the pole. The ratio of original, to, to current thickness, t, is

$$\frac{to}{t} = \log_e{}^{-1}(-\varepsilon t) = \log_e{}^{-1}(2\varepsilon) \quad \text{which is equal to} \quad \left[1 + \frac{K(a1 + a2)}{Do} \right]^2$$

The representative stress is then given by $\sigma = \frac{P}{2to} \cdot R. \frac{to}{t}$ where P is the load and R the radius of curvature. This latter value is derived from the centre dial gauge reading, d, thus $R = (r^2 + d^2)/2d$ where r is the radius of each spherometer leg. Since K, Do and r are constants for the instrument used, charts were available giving $\bar{\varepsilon}$, R and to/t in terms of dial gauge readings.

3.10. Hardness Tests

Hardness measurements using a Vickers hardness testing machine and a diamond pyramid indentor were made on every test strip and on selective samples deformed to different degrees in both tension and compression. The tests were made on selected electropolished surfaces.

Vickers hardness measurements were also made on various cup sections.

3.11. Press Forming

Press forming tests were carried out on a modified Erichsen Model 123 Electro-hydraulic sheet metal testing machine, Fig.3.11. The machine was modified by incorporating a load cell in the punch stem. This gave a continuous and more accurate record of load with punch travel as the test progressed and allowed an assessment to be made of the work required to form the material.

The modification to the 33 mm punch is shown in Fig.3.12. The load cell was made from EN.24, quenched and tempered to give a minimum U.T.S.

Fig. 3.11. The Erichsen Model 123 Electro-Hydraulic Press with Recording Equipment.

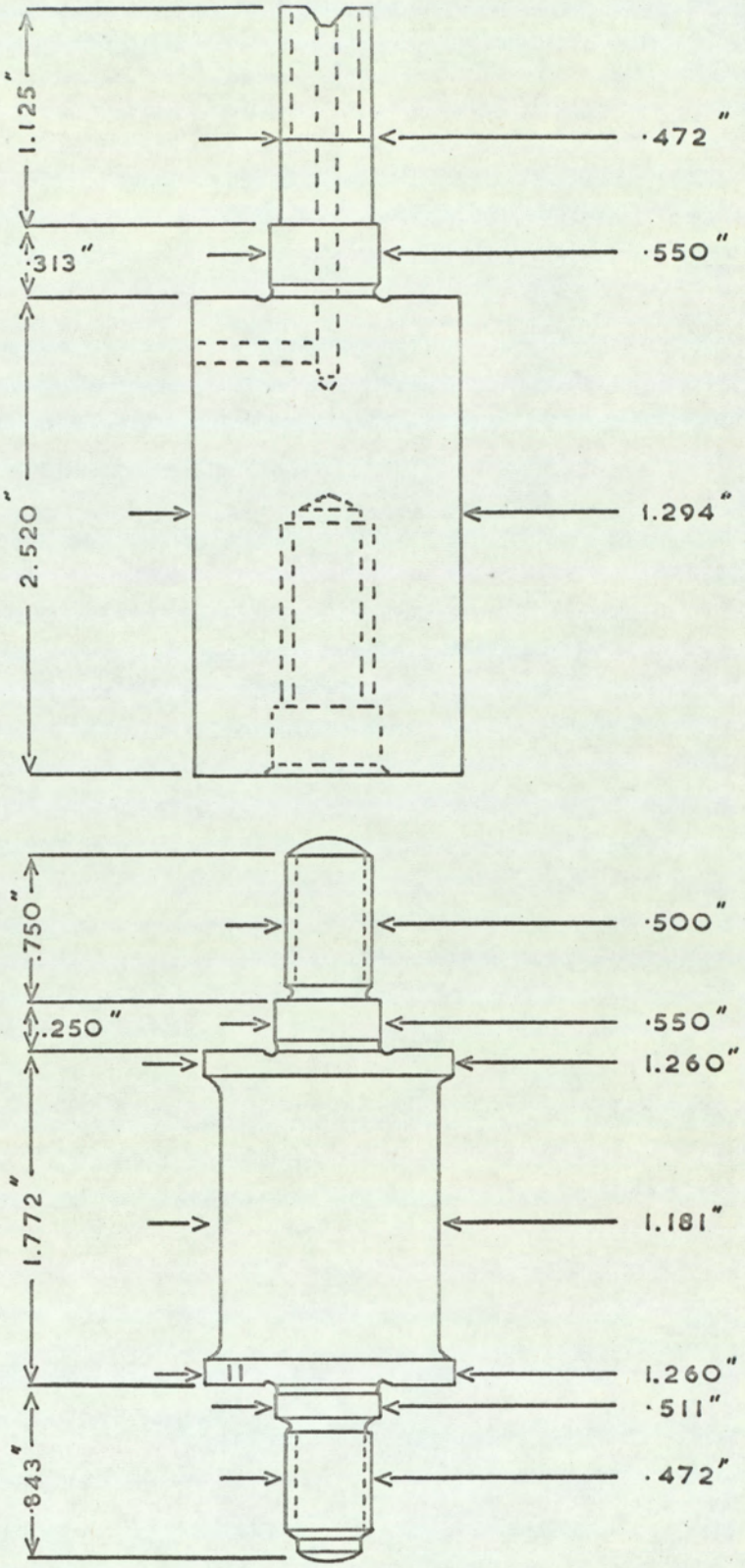

Fig. 3.12. The Modified Erichsen Punch and Load Cell.

of 100 tons s.i. and a yield strength of approximately 80 t.s.i. This was done to ensure that operating service loads gave a linear output from the strain gauges. From preliminary tests it was found that the maximum load requirement was unlikely to exceed 15,000 Kgs or 14.73 tons. This value is well within the elastic limit of the steel.

Eight Saunders-Roe 120 foil gauges were used in the cell. Dummy gauges were used in series to compensate for temperature variations. The electrical circuit together with the strain gauge arrangement used in shown in Fig.3.13.

Initial balancing of the cell was made with a variable resistance across gauges 6 amd 8. A further resistance of 84 ohms was used to modify the stabilised 6 volt input so that at maximum load full scale deflection on a Honeywell recorder was obtained.

3.11.1. Calibration of Press Forming Equipment

The cell was calibrated by incremental compressive loading in units of 1000 Kgs, in a 50 ton Dennison tensile machine. Full scale deflection using a 6 volt input gave a maximum loading of 10,000 Kgs. By reducing the input voltage to 3 volts it is possible to obtain recorded loads of approximately 19,000 Kgs: although the input voltage is halved, because of the inclusion of the 84 ohm resistance in the power supply circuit the recorder scale deflection is not exactly half of that obtained with a 6 volt input. Using a 3 volt input a linear deflection was obtained up to 19,000 Kgs thereby justifying the earlier assumptions.

It was also necessary to automate punch travel measurement. This was obtained simply by using the existing dial gauge to activate a transducer across which a voltage was applied and from which the output operated the recorder chart drive. The transducer circuit was modified so that 1" of chart corresponded to 1 mm of punch travel. Again the relationship between punch and chart travel was made linear. The two circuits were then synchronised and

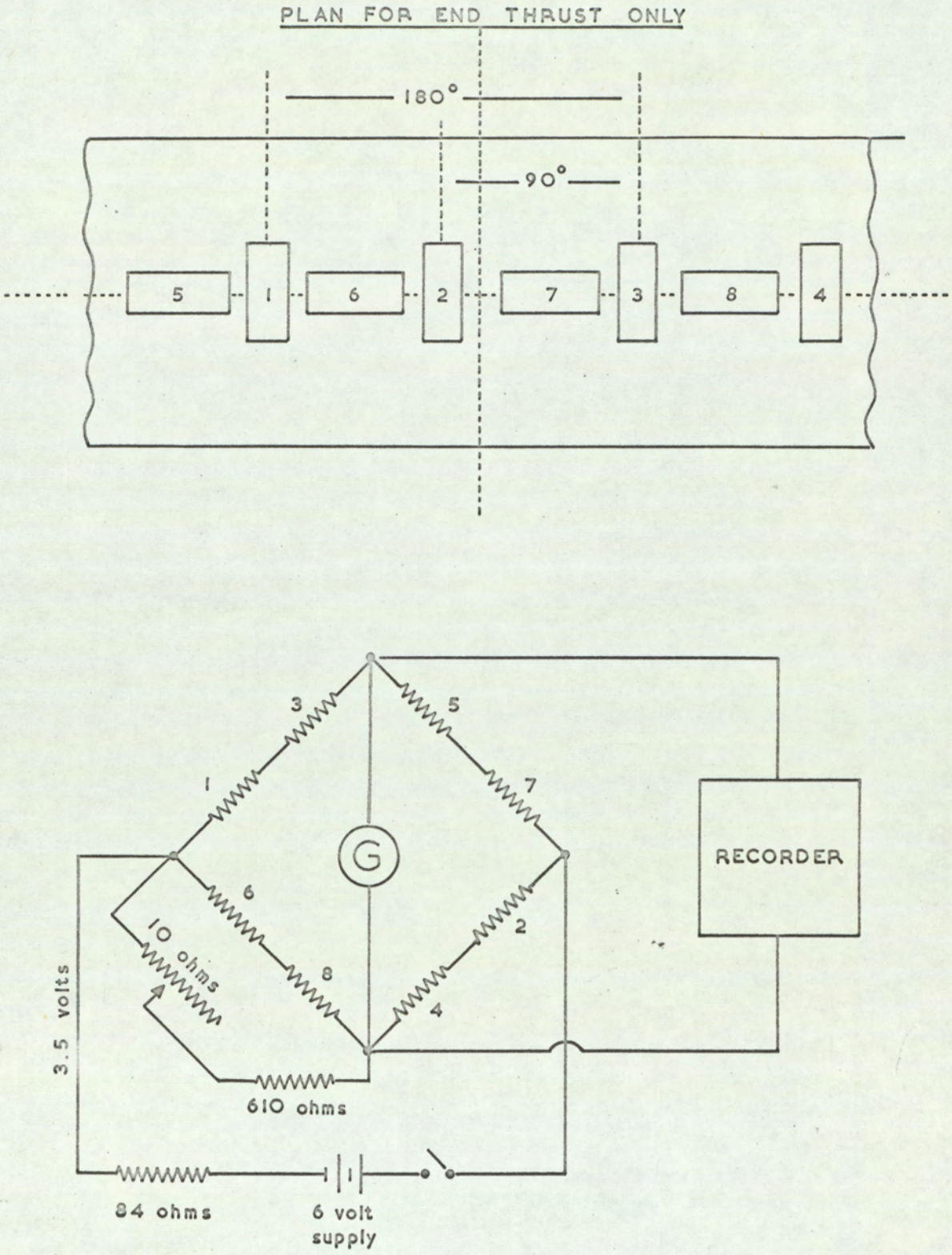

Fig. 3.13. Strain Gauge Arrangement and Electrical Circuit for the Load Cell.

simultaneous outputs fed into the recorder.

3.11.2. The Erichsen Cupping Test

Stretch forming results were obtained using the Euronorm Specification 14-58 of the Euronorm Iron and Steel Community but with modified lubrication. Polythene sheet was used as the lubricant over the punch nose. Although polythene gives a greater depth to failure it also gives a more consistent pattern of results. The effect of polythene as a lubricant compared with graphite grease will be demonstrated in a later section. It is assumed that the improved lubrication with polythene reduces surface effects. Since the research undertaken in this study was concerned primarily with material properties it was decided to use polythene in order to reduce to a minimum, operational variables. For example, in all press forming tests a constant punch travel speed was maintained at a rate of 10 mm/min. This corresponds to an approximate average strain rate of 0.0023/sec.; somewhat faster than that employed in tensile testing but since the drawn product was in contact with relatively large masses of metal it was decided that the associated temperature effects arising from metal deformation could be ignored. Tests were carried out in duplicate and maximum punch loads, punch/travel diagrams and their areas were also recorded. Tool dimensions are shown in Fig.3.14.

3.11.3. The Erichsen Cup Drawing Test

The normal version of the Erichsen cup drawing test forms a circular blank into a flat bottomed cup with an internal diameter of 33 mms. The die diameter for .036" thick material is 34.7 mm and the die entry radius 3 mm. Exploratory trials indicated that stainless steel was prone to severe radial cracking in the wall of the cup. This resulted from severity of bending and unbending over the die entry radius and from poor lubrication.

Fig.3.15 shows the effect on maximum punch load with:-

(a) decrease in the severity of die entry radius,
(b) increased surface lubrication: polythene, as opposed to a graphitic grease.

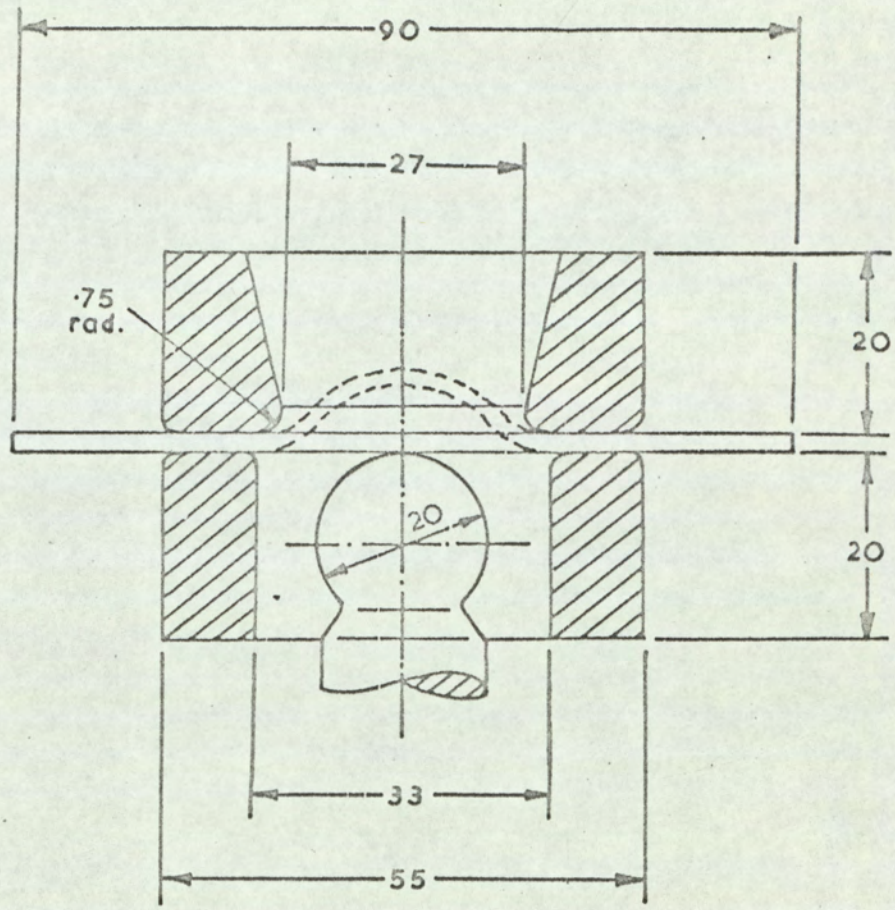

Fig. 3.14. The Erichsen Stretch Forming Tools.

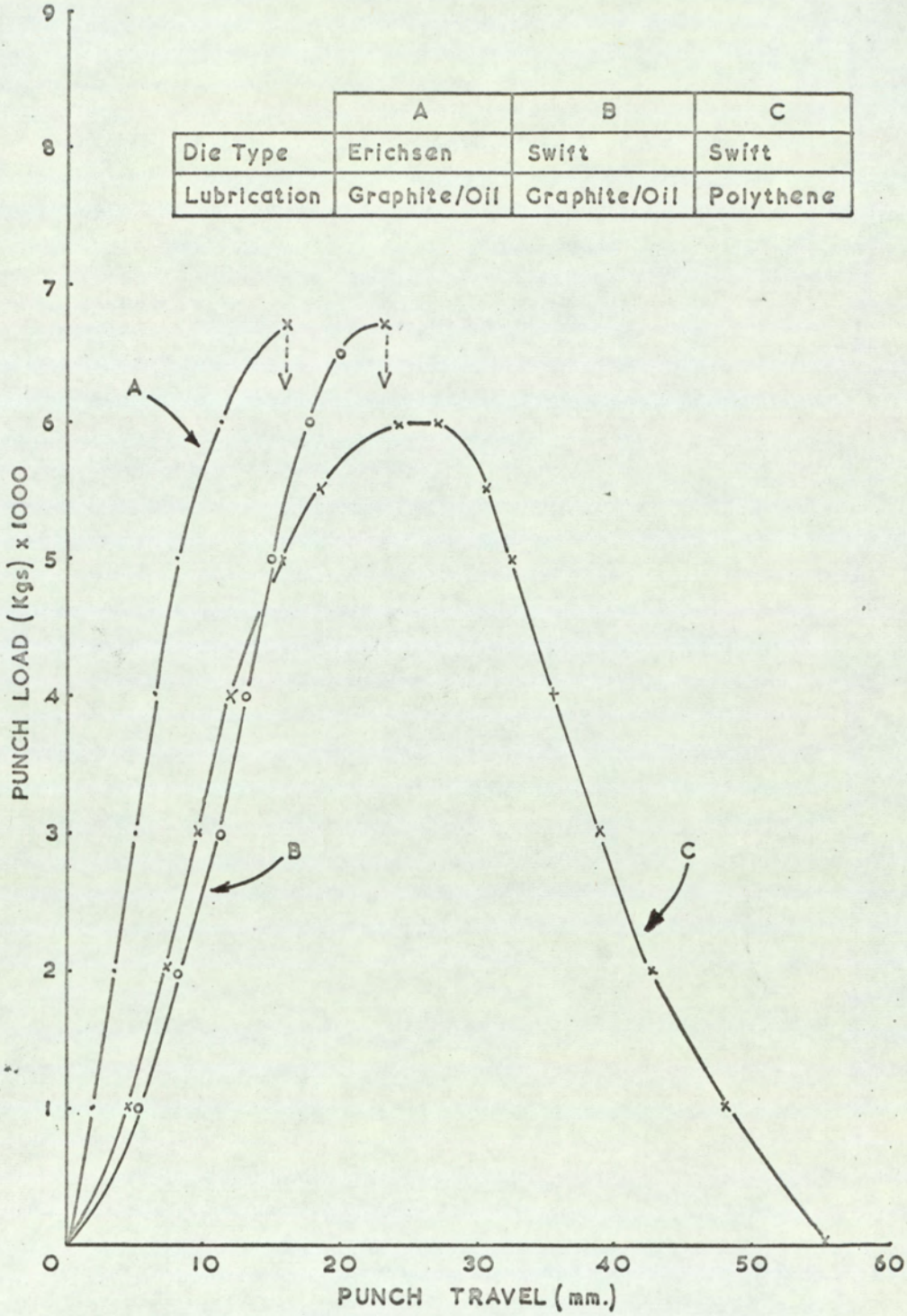

Fig. 3.15. The Effect of Increased Lubrication and Die Entry Radius on the Drawing Capacity of 75 mm. dia. Blanks.

For these reasons polythene was used as the lubrication for both stretch forming and deep drawing and a Swift die with a die entry radius of 12.4 mm, together with a 33 mm Erichsen punch used for the drawing tests. It was decided to use the Erichsen and not a Swift punch in order that the percentage clearance between punch and die, using 0.036"thick material would be just sufficient to eliminate ironing. The clearance obtained with these tools was 36.8%. Tool dimensions for this test are shown in Fig.3.16.

Each strip was tested to determine the largest blank that could successfully be drawn. This diameter is then described as either the critical blank diameter or expressed in terms of the limiting drawing ratio. Test blanks were cut with a range of diameters in increments of 1 mm using the blanking press built into the Erichsen machine. Critical blank diameters are therefore expressed as an exact size in millimetres.

Prior to the application of a blank holder load a clearance of 1 mm was left between the blank and the die. This was done to ensure that an excessive rise in blank holder pressure resulting from blank thickening during drawing did not cause premature cup failure.

For the actual determination of C.B.D.s., the blank holder load was that, that was just sufficient to eliminate wrinkling of the blank. This was determined to be 3000 Kgs. For each test blank, the diameter, success or failure, maximum punch load, punch travel to failure, and load/punch travel diagram were determined. The C.B.D. recorded was that blank size at which at least three blanks formed complete cups whilst at a size 1 mm greater three cups failed.

3.12. Earing Measurements

Special cups all at 67 mm were drawn for the assessment of earing tendency. The percentage earing has been calculated from average ear and average trough height, i.e.

$$\text{Percentage Earing} = \frac{\text{Average ear height} - \text{average trough height}}{\text{Average trough height}} \times 100$$

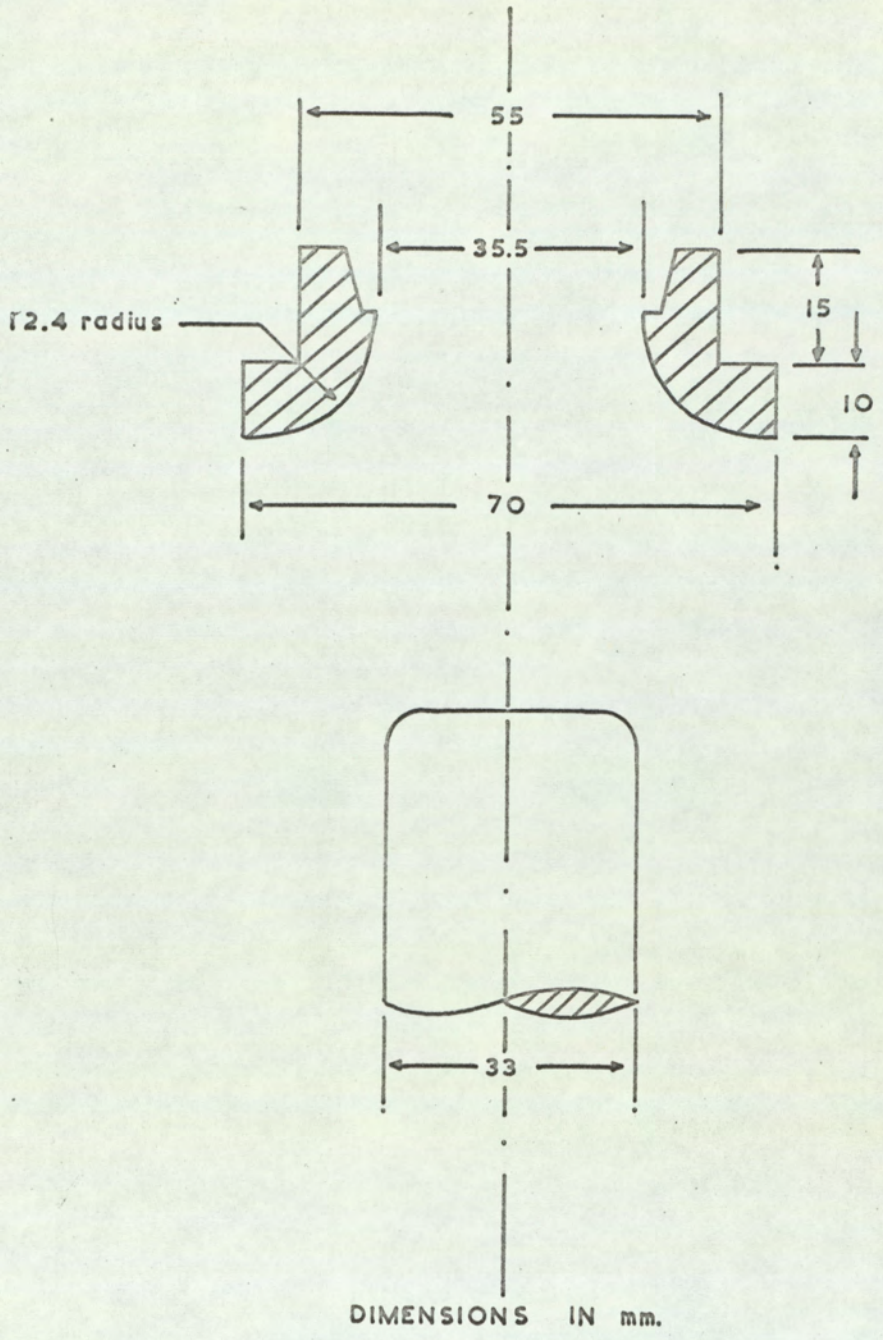

Fig. 3.16. The Cup Drawing Test Tools.

The methods and significance of the press formability tests mentioned have been described in detail elsewhere.[37]

3.13. Measurement of Areas beneath the Punch Load/Travel Diagrams

The areas under punch load/punch travel diagrams in stretch forming and deep drawing tests and beneath the load/extension curves in tensile tests were measured to assess the relative work required to deform materials in different conditions. Measurement was made using an OTT-Planimeter type 17. Duplicate measurements were made on duplicate tests so that values quoted are the average of four readings.

3.14. Thickness Strain and Hardness Measurements on Sectioned Drawn Cups

Thickness strain and hardness distribution were assessed on several selected drawn cup sections. The drawn cups were sectioned in all cases at positions corresponding to positions of ear formation irrespective of whether this position coincided with the rolling direction of the material. Thickness measurements were made in increments of 1/8" from the pole to the cup flange using a ball ended micrometer (to .0001"). The cups were then mounted in cold setting plastic, lightly ground on top and bottom faces and polished. Hardness measurements were made using a normal Vickers hardness machine and a load of 20 Kgs. In order to obtain accurate distances from the cup pole indentation distances were measured using a travelling microscope.

3.15. Correlation Matrix

As will be evident from the results section, the initial computer programme evaluated the stress-strain curves in terms of certain important parameters. A second computer programme was used to relate these parameters to the mechanical and physical properties of the steels examined. In making this correlation, the computer also examined direct relationships between all of the classes of test results and data derived from them. This also gave a good assessment of any lack of correlation between properties and the properties and coefficients. The correlation matrix obtained is given in

a later section in this thesis and shows the correlation between the variables denoted by the numbers heading the column and those ending the row. The coefficients lie between - 1.0 and + 1.0. The negative sign indicates a negative slope to the relationship and the positive sign, the reverse. Values in excess of 0.9 have significance levels better than 0.1%.

4.0. EXPERIMENTAL RESULTS

4.1. Introduction

The basic intention of this work was to obtain a wide variation in the mechanical properties of the material examined by varying amounts of prior cold work and to assess the effect of this cold work on mechanical properties and on press formability. Both of these groups of properties will be examined in the light of austenite stability and the degree of associated transformation to α' martensite. It is also intended that variations between several of the mechanical properties will be discussed together with obvious relationships between mechanical and press forming properties. Most of the results describe an analysis of the complex stress-strain relationships obtained with stainless steels of this type and this analysis will also be related to press formability.

4.2. Effect of Deformation on the Formation of α' Martensite

It is general knowledge that deformation of stainless steels of the 18/8 type may result in the formation of α' martensite particularly at high strains and in metastable steels, and that the strain level at which the phase is initiated increases with austenite stability i.e. solute additions such as manganese, nickel, nitrogen and carbon, etc. An initial investigation was therefore undertaken to assess these levels, and to determine the amounts of α' martensite formed at higher strain levels. As has previously been explained, it was not considered necessary to actually determine the percentage α' martensite formed but merely to assess the magnetic response of the material. Fig.4.1 shows how the magnetic response, for the seven steels examined, varies with strain level to which the material was deformed: in this case by cold rolling. After initiation of martensite, its rate of formation becomes constant over the range of strain examined. However, at higher levels of strain, particularly with steels of low austenite stability, it is expected that the rate of formation would decrease in its later stages so that complete transformation would be represented in fig.4.1, by an 'S' type of curve.

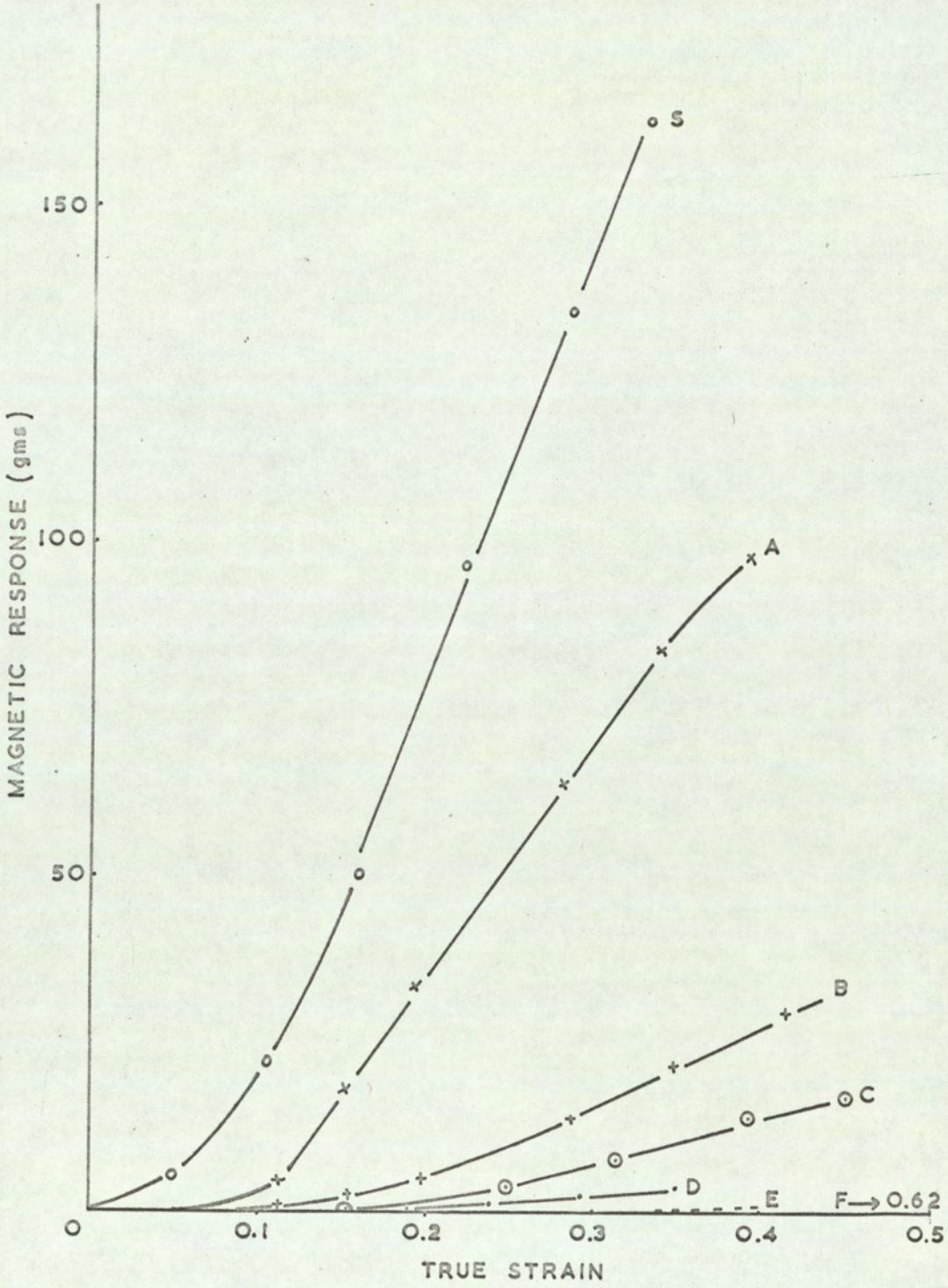

Fig. 4.1. The Magnetic Response of the Seven Steels examined after Deformation by Cold Rolling.

It may be possible that at a given stage, the amount of α' martensite formed would be balanced by deformation of the martensite itself and as this latter type of deformation increased so would the formation of martensite decrease. As a measure of the relative rates of martensite formation, the slopes of the linear portion of the curves given in Fig.4.1, together with a value of magnetic response for a strain level of 0.3, have been plotted against austenite stability in Fig.4.2. Both curves are complementary in that they show how the rate of formation of martensite decreases with increase in austenite stability. Using Δ values calculated from the Post and Eberly formula it can be seen that large amounts of α' martensite are not formed for values of Δ more positive than - 3.5 and that above this value, to approximately - 5.0 to - 6.0, the rate of formation increases almost tenfold. Thus, there appears to be a threshold level at this point of increase, at which the stacking fault energy of the material is just insufficient to inhibit transformation of the material to martensite. This point will be discussed more fully at a later stage of the thesis. Not only does the amount of α' martensite decrease with increase in austenite stability but examination of Fig.4.3, shows that the strain level at which the onset of martensite was recorded, also increases. The plot shows that the threshold strain levels for initiation of martensite in tension were higher than for those obtained by the magnetic response method, both in tension and compression. Obviously, these values should be similar and it is assumed that a much larger volume fraction needs to be present in the tensile method before it can be detected. There appears, however, to be a legitimate difference between tension and compression in that martensite is initiated at lower strain levels in tension than in compression. This latter point was examined in more detail and Figs. 4.4 and 4.5 show curves for both hardness and magnetic response obtained on steels S, D and E deformed in tension and in plane strain compression. It is apparent that at higher strain levels,

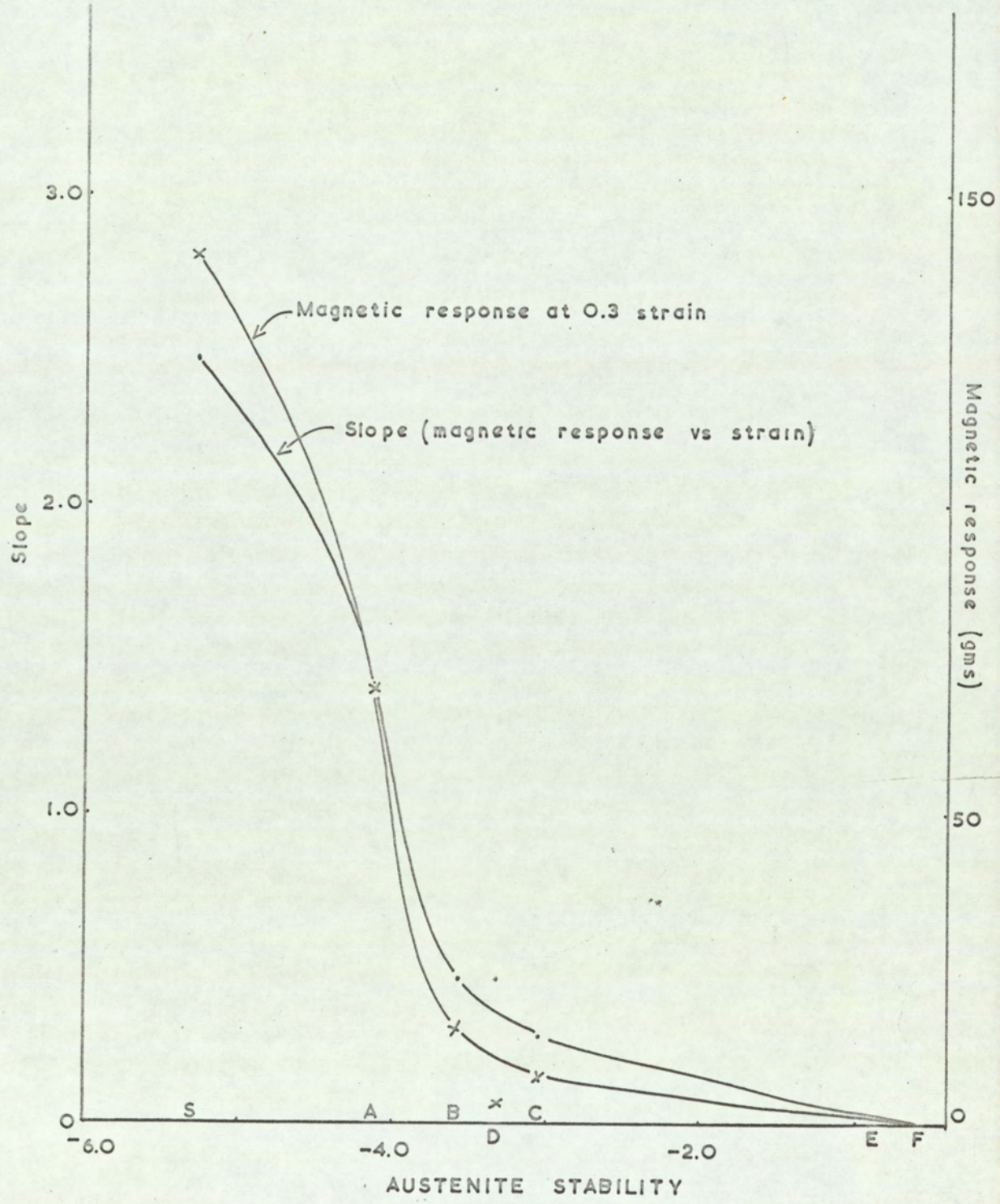

Fig. 4.2. Magnetic Response (0.3 Strain) and Slope (previous Fig.) versus Austenite Stability.

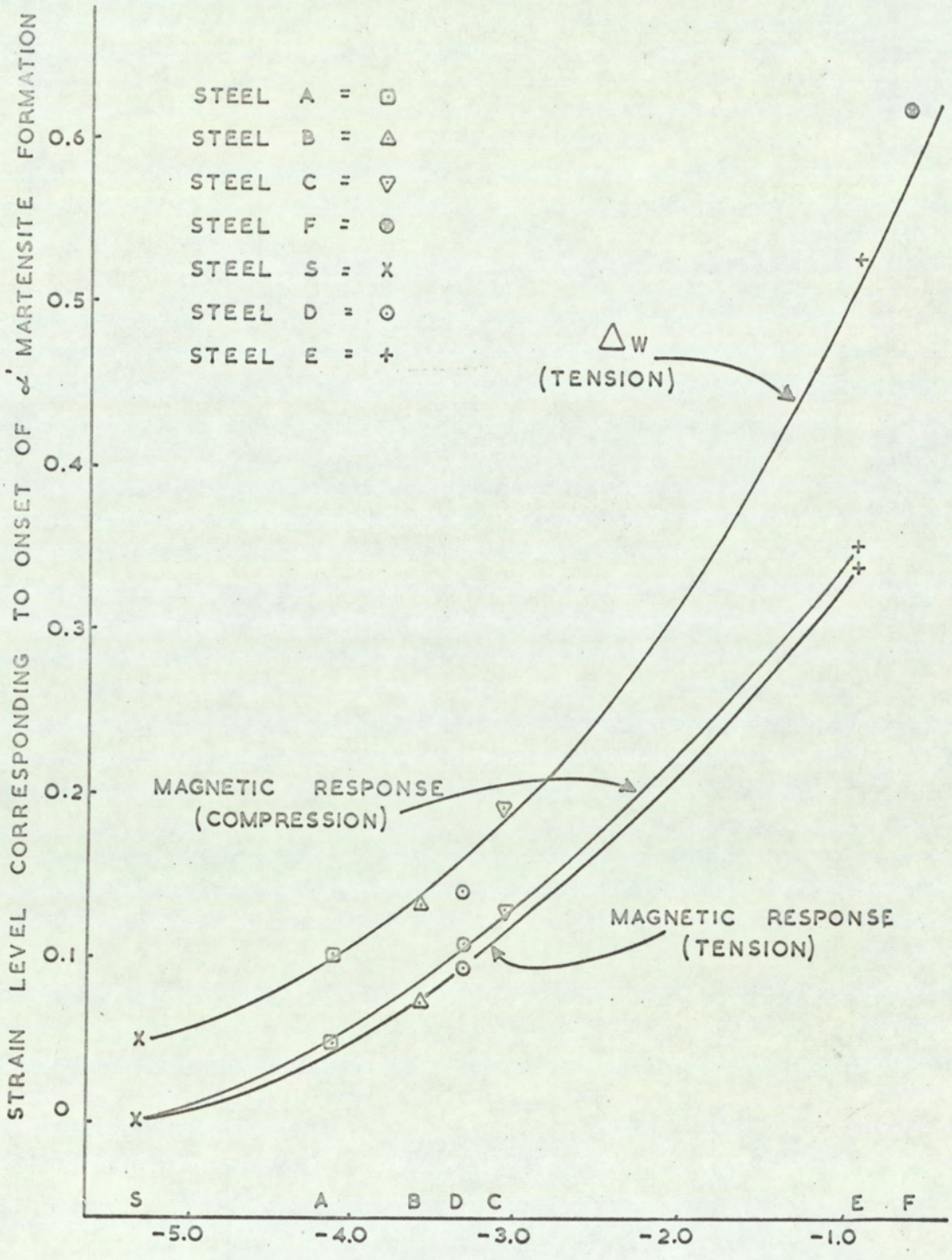

Fig. 4.3. The Strain Level at which α' Martensite was recorded for Different Tests.

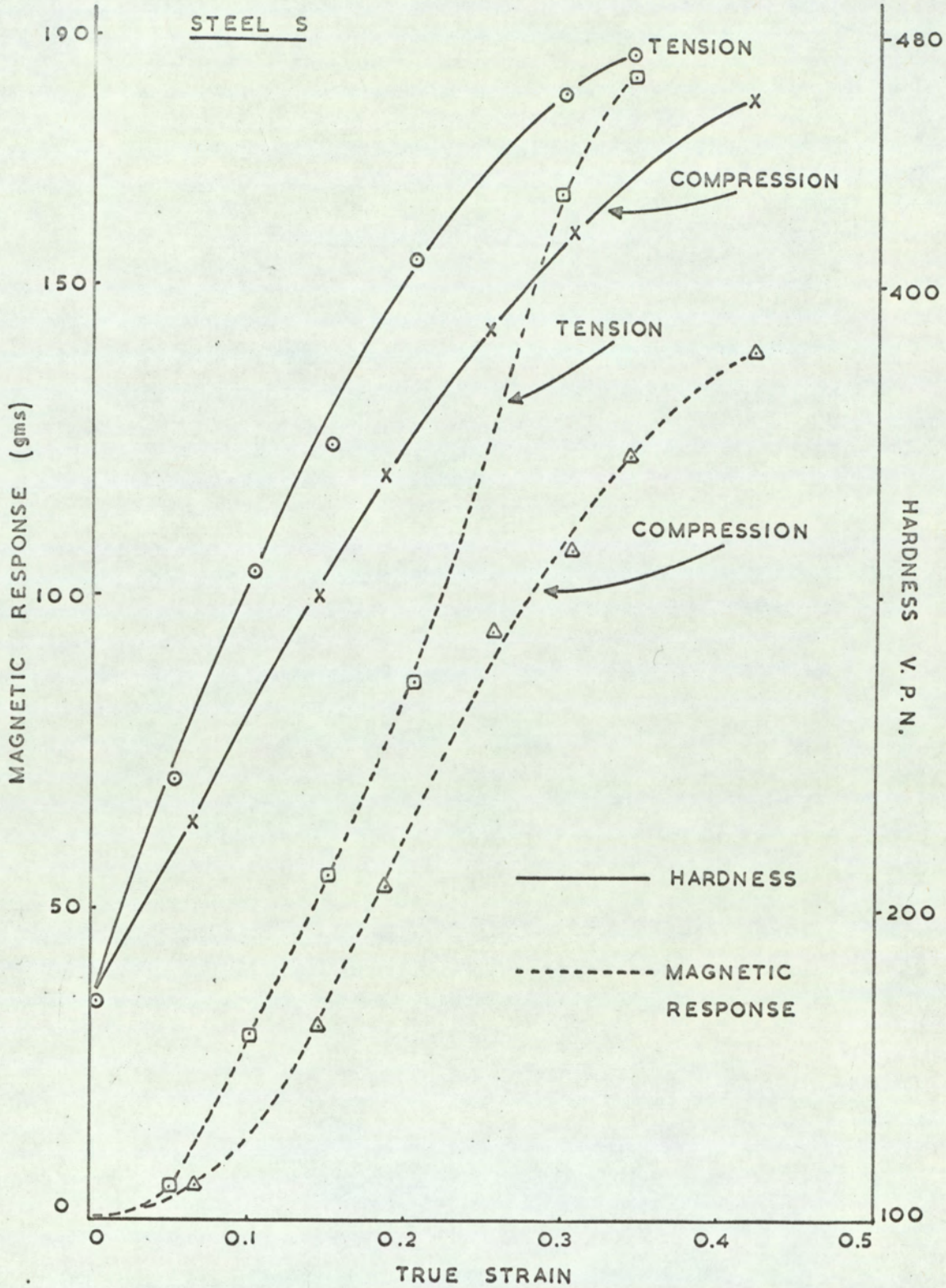

Fig. 4.4. The Effect of α' Martensite Formation on Hardness and Magnetic Response for Compression and Tension.

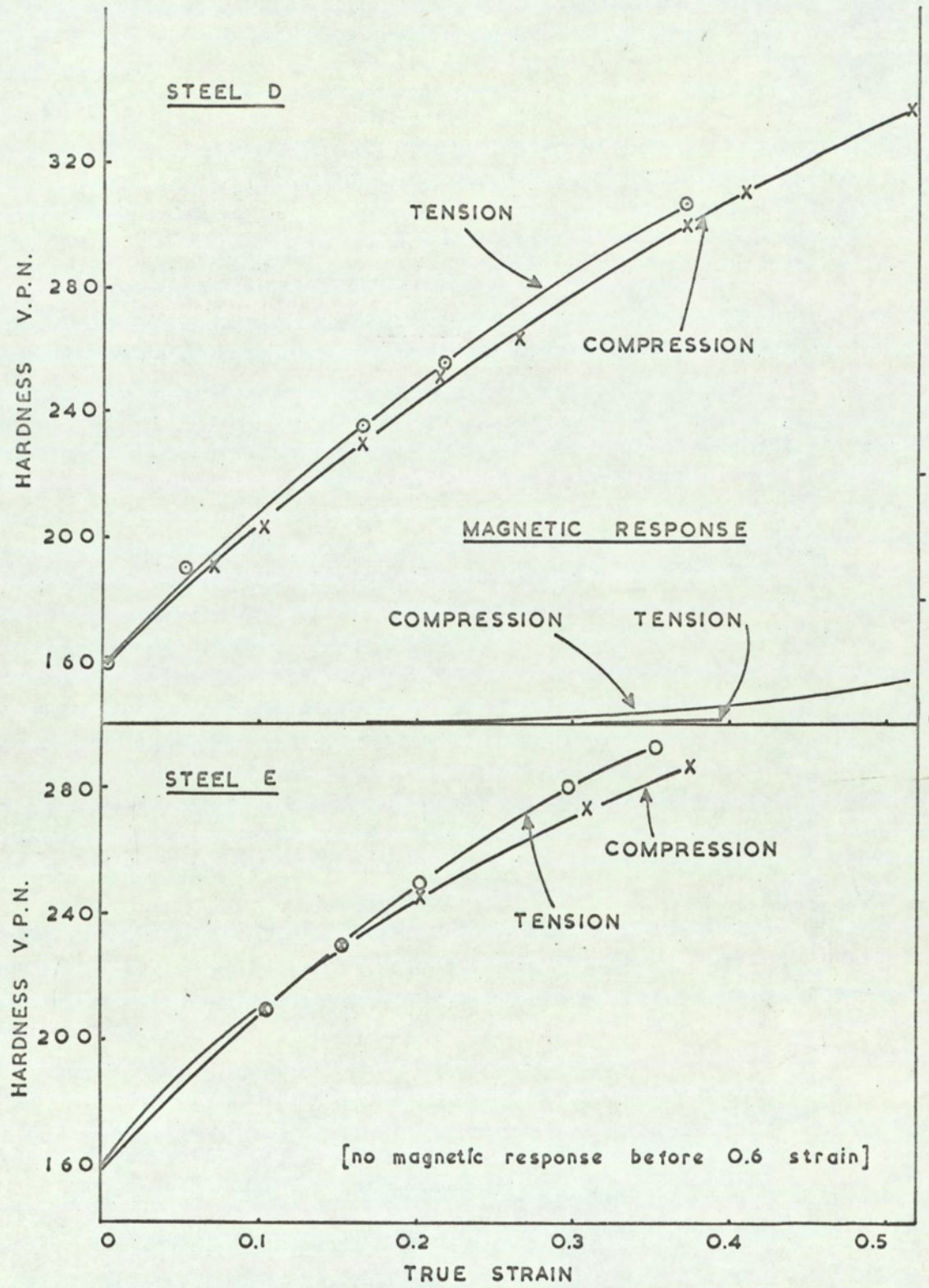

Fig. 4.5. The Effect of α Martensite Formation on Hardness and Magnetic Response for Compression and Tension.

more α' martensite is produced in tension than in compression and this fact is reflected in the resulting hardness values.

To illustrate the relationship between hardness and magnetic response, Fig.4.6 was plotted for a convenient degree of cold work, namely 48%, obtained by cold rolling. It shows that as the magnetic response increases with decreasing austenite stability, the rate of hardening of the material slightly decreases from linearity, which is presumably a reflection of the ease with which α' martensite is formed in the lower stacking fault energy materials, i.e. metastable austenites.

4.3. Mechanical Test Results

The initial results of mechanical properties of steels S, D and E examined in different degrees of cold work and at different angles to the rolling direction are summarised in Table 4.1. Each value recorded is the average of duplicate tests. These results are further summarised together with the results from the pressing tests in Table 4.2. In this and all subsequent tables unless otherwise stated, the average of tests at 0°, 45° and 90° to the rolling direction have been averaged using the formula:-

$$\text{Average} = \frac{\text{Value at } 0^{\circ} + \text{Value at } 90^{\circ} + 2\,(\text{Value at } 45^{\circ})}{4}$$

It was known that the material used for the exploratory trials, Steels A, B, C and F had been stretch straightened "some 2%" after annealing. Detailed examination of the true stress/true strain relationships showed that the stretch straightening operation had a pronounced effect for certain steels on some of the mechanical properties. To investigate this effect, samples of these four steels were re-annealed and retested. These summarised results together with those from the original tests are shown in Table 4.3.

Following the conclusions arrived at by Grimes[60] the true stress values corresponding to the ultimate tensile strength in the tensile test have been calculated and are reported in Table 4.4. The earing characteristics

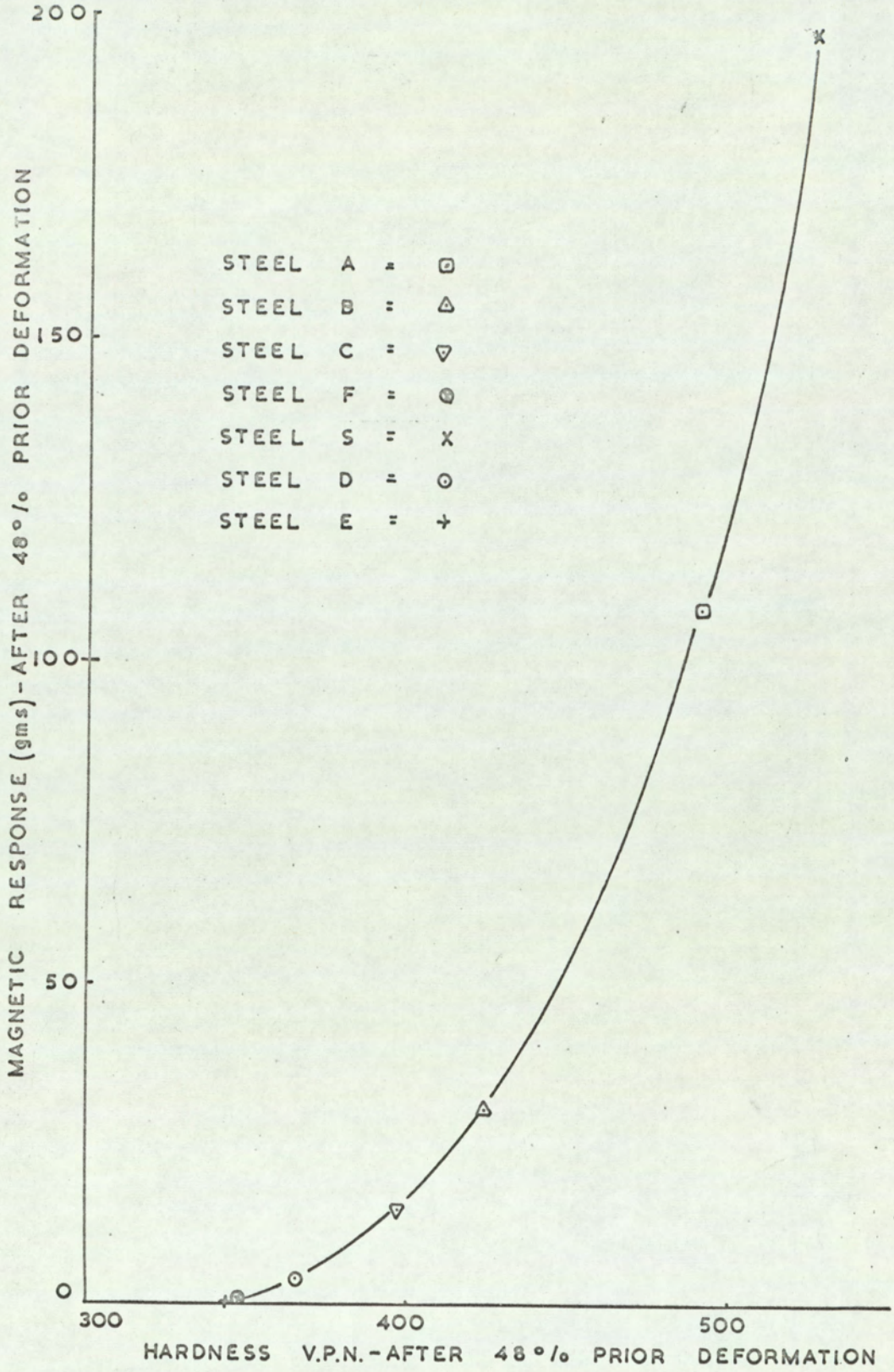

Fig. 4.6. TheRelationship between Hardness and Magnetic Response after 48% Prior Deformation.

TABLE 4.1. RESULTS OF TENSILE TESTS ON STEELS S, D and E at 0°, 45° and 90° TO THE ROLLING DIRECTION

STEEL	CONDITION	0.5% P.S. (t.s.i.)			U.T.S. (t.s.i.)			PS/UTS			TOTAL ELONGATION			UNIFORM ELONGATION			R		
		0°	45°	90°	0°	45°	90°	0°	45°	90°	0°	45°	90°	0°	45°	90°	0°	45°	90°
S 0	ANNEALED	17.7	19.6	19.4	60.7	61.0	60.5	.29	.32	.32	52.4	62.0	57.9	46.7	55.2	53.6	.87	.90	.92
S 10	10% COLD WORK	33.8	38.3	37.0	72.4	71.0	73.4	.47	.54	.51	37.0	35.3	34.6	33.0	30.4	30.2	.67	.63	.94
S 20	20% " "	53.2	53.7	52.1	79.0	79.0	78.0	.67	.68	.66	25.6	24.6	20.5	21.8	21.1	17.5	.65	.67	.82
S 30	30% " "	85.9	87.9	88.5	91.4	92.7	95.2	.94	.95	.93	11.5	15.7	11.8	5.5	11.7	6.6	.53	.64	.80
S 40	40% " "	98.5	99.1	101.8	99.0	100.4	104.0	.99	.99	.98	9.6	4.4	5.0	5.8	0.9	2.6	-	-	-
S 50	50% " "	-	-	-	110.5	107.8	112.7	1.0	1.0	1.0	2.6	3.1	2.4	<1.0	<1.0	<1.0	-	-	-
D 0	ANNEALED	17.3	17.3	16.8	39.4	37.1	38.8	.44	.46	.43	64.1	71.2	76.8	55.9	62.6	69.5	.67	1.07	.88
D 10	10% COLD WORK	36.3	35.5	37.0	48.0	44.7	47.1	.76	.80	.78	47.8	47.1	51.7	39.4	37.5	44.0	.75	1.26	1.40
D.20	20% " "	46.4	46.3	45.9	53.1	51.9	53.3	.87	.89	.86	34.5	28.7	34.3	26.8	18.0	25.2	.72	1.12	1.47
D.30	30% " "	52.1	53.5	52.9	58.1	58.7	59.4	.90	.91	.89	22.5	14.3	15.4	15.2	5.2	6.4	.67	1.06	1.86
D 40	40% " "	58.0	57.6	58.8	64.0	66.3	68.0	.91	.87	.87	15.4	11.5	10.5	10.2	3.7	1.8	.67	1.16	2.20
D 50	50% " "	72.7	73.5	75.5	75.1	78.0	79.9	.97	.94	.95	5.4	4.7	8.5	1.2	1.5	1.8	.51	.89	1.90
E 0	ANNEALED	18.7	19.7	19.6	36.0	37.9	38.6	.52	.52	.51	58.7	62.6	66.7	51.9	54.5	58.4	.45	.94	1.48
E 10	10% COLD WORK	30.8	32.3	34.1	40.4	42.0	43.4	.76	.77	.79	46.7	51.7	52.7	38.4	42.3	44.3	.45	.92	1.66
E 20	20% " "	41.7	42.9	42.2	42.2	47.5	48.6	.90	.90	.87	32.3	37.1	35.5	25.2	29.9	26.5	.49	.99	2.04
E 30	30% " "	48.6	50.0	49.5	51.3	54.2	55.5	.95	.92	.89	21.7	22.9	23.8	14.0	13.1	13.2	.47	1.05	2.19
E 40	40% " "	54.2	56.7	55.3	59.2	62.6	63.4	.92	.91	.87	12.7	11.1	14.9	6.8	3.2	9.6	.52	1.06	2.21
E 50	50% " "	60.8	55.8	52.5	68.0	71.1	72.5	.89	.79	.72	7.3	7.0	10.1	4.6	2.5	2.8	.64	1.07	2.24

TABLE 4.2. THE SUMMARISED PRESSING AND MECHANICAL TEST RESULTS ON STEELS S, D and E.

STEEL	CONDITION	C.B.D. (mm)	ERICHSEN VALUE (mm)	Hd* (20 Kg)	0.5% PS (t.s.i.)	U.T.S. (t.s.i.)	PS/ U.T.S.	TOTAL ELONGATION	UNIFORM ELONGATION	$\bar{R}$	% EARING (67 mm) BLANKS
S 0	ANNEALED	76	15.7	170	19.1	60.8	.31	58.6	52.7	.90	1.6
S 10	10% COLD WORK	76	10.4	272	36.9	71.9	.51	35.6	30.9	.72	6.3
S 20	20% " "	75	8.0	377	53.2	79.0	.67	23.8	20.4	.70	4.2
S 30	30% " "	70	6.7	461	87.5	93.0	.94	13.7	8.9	.65	-
S 40	40% " "	-	4.9	484	99.6	101.0	.99	5.9	2.5	-	-
S 50	50% " "	-	3.6	523	-	109.7	1.0	2.8	<1.0	-	-
D 0	ANNEALED	77	13.9	152	17.2	38.1	.45	70.8	62.7	.92	11.0
D 10	10% COLD WORK	75 (+)	10.4	218	36.1	46.1	.78	48.4	39.6	1.17	12.2
D 20	20% " "	74	8.6	267	46.2	52.5	.88	31.6	22.0	1.11	9.8
D 30	30% " "	72	6.9	296	53.0	58.8	.90	16.6	8.0	1.16	6.1
D 40	40% " "	70	6.3	324	58.1	66.2	.88	12.2	4.9	1.30	5.2
D 50	50% " "	67	6.1	366	73.9	77.7	.95	5.8	1.5	1.05	4.9
E 0	ANNEALED	78	13.5	147	19.4	37.6	.52	62.7	54.8	.95	1.3
E 10	10% COLD WORK	76	10.9	208	32.2	42.0	.77	50.7	41.8	.99	3.3
E 20	20% " "	74	8.6	247	42.4	47.4	.90	35.5	27.8	1.13	3.8
E 30	30% " "	70	7.2	291	49.5	53.8	.92	22.8	13.3	1.19	0.9
E 40	40% " "	69	6.4	315	54.5	61.9	.90	12.5	4.5	1.21	3.4
E 50	50% " "	67	5.8	344	56.2	70.7	.80	7.8	3.1	1.25	1.91

* Material tested in 'as Rolled' condition

TABLE 4.3. THE SUMMARISED PRESSING AND MECHANICAL TEST RESULTS ON STEELS A, B, C and F.

STEEL	CONDITION	C.B.D. (mm)	ERICHSEN VALUE (mm)	Hd (20 Kg)	0.5% P.S (t.s.i.)	U.T.S. (t.s.i.)	PS/ U.T.S.	TOTAL ELONGATION	UNIFORM ELONGATION	$\bar{R}$
A	ANNEALED AND STRAIGHTENED	76	15.3	164	16.0	46.6	.34	48.0	46.2	.96
B	" " "	76	14.5	157	17.3	41.2	.42	69.8	61.1	.95
C	" " "	76	13.8	152	17.3	40.0	.43	61.4	53.1	.87
F	" " "	76	13.9	164	18.7	39.9	.47	66.0	56.6	.88
A	ANNEALED ONLY	-	14.7	157	15.4	49.3	.31	75.1	68.6	.94
B	" "	-	13.8	140	15.0	36.1	.42	69.8	59.7	.92
C	" "	-	13.8	119	13.0	35.7	.36	72.4	63.3	.96
F	" "	-	13.3	153	15.7	35.4	.44	64.5	55.7	.91

TABLE 4.4. TRUE STRESSES CORRESPONDING TO ULTIMATE TENSILE STRENGTHS FOR STEELS S, D and E IN DIFFERENT CONDITIONS

STEEL	CONDITION	TRUE STRESS (t.s.i.)			
		0°	45°	90°	Av.
S 0	ANNEALED	89.1	94.7	92.9	92.9
S 10	10% COLD WORK	96.0	91.5	95.5	94.1
S 20	20% " "	96.2	95.8	92.6	95.0
S 30	30% " "	96.4	104.0	101.5	101.3
S 40	40% " "	104.3	101.3	106.8	103.4
S 50	50% " "	111.1	108.3	113.3	110.3
D 0	ANNEALED	61.3	60.4	65.7	62.0
D 10	10% COLD WORK	66.8	61.4	67.9	64.4
D 20	20% " "	67.3	61.2	66.7	64.1
D 30	30% " "	66.9	62.1	62.7	63.5
D 40	40% " "	70.5	68.8	69.2	69.3
D 50	50% " "	76.0	79.2	81.3	78.9
E 0	ANNEALED	54.7	58.6	61.1	58.3
E 10	10% COLD WORK	55.0	59.7	62.7	59.5
E 20	20% " "	57.8	61.6	61.4	60.6
E 30	30% " "	58.4	61.3	62.9	61.0
E 40	40% " "	63.2	64.5	66.3	64.6
E 50	50% " "	71.2	72.9	74.6	72.9

of the materials have also been examined to see if the formation of α' martensite enhances or retards their formation. These results are also detailed in Table 4.2. Measurements were taken on cups drawn from 67 mm diameter blanks.

4.4. Assessment of Work Done during Deformation

For reasons that have previously been mentioned (Section 3.13), the areas beneath the load/extension diagrams from the tensile test and punch load/punch travel diagrams from the press forming tests have been measured, and are given, together with values of maximum punch loads for different tests in Table 4.5. Also included in this table is the product of stress at maximum load and the strain at instability, a function which will be shown to be related to deformation work area.

4.5. True Stress-True Strain Data obtained from the Tensile Test

True Stress/true strain data were calculated from the load/extension curves using the formulae given in section 3.7.3. The results were then plotted on a log-log basis. Such data for conventional non-transforming materials often obeys the Ludwik relationship and when plotted on a log-log basis gives a straight line. The slope of this line is normally designated 'n'; the strain or work hardening coefficient. An extrapolation of this line to the intersection with the stress axis, corresponding to $\delta = 1$, gives a measure of the strength coefficient K. Characteristic curves obtained from the present results are shown in Fig.4.7. It is quite apparent that this shape of curve does not obey the Ludwik relationship and it was therefore necessary to obtain a function that adequately described this type of curve.

From the results of the computer programme mentioned in section 3.7.5. an evaluation of the degree of fit for different curves was made. This degree of fit was assessed from the sum of the squares of the deviations for different degree polynomials and it was found that the higher the degree of polynomial used, the better was the fit. Since the degree of accuracy obtained from the actual tests was limited by the accuracy to which measurements could be made,

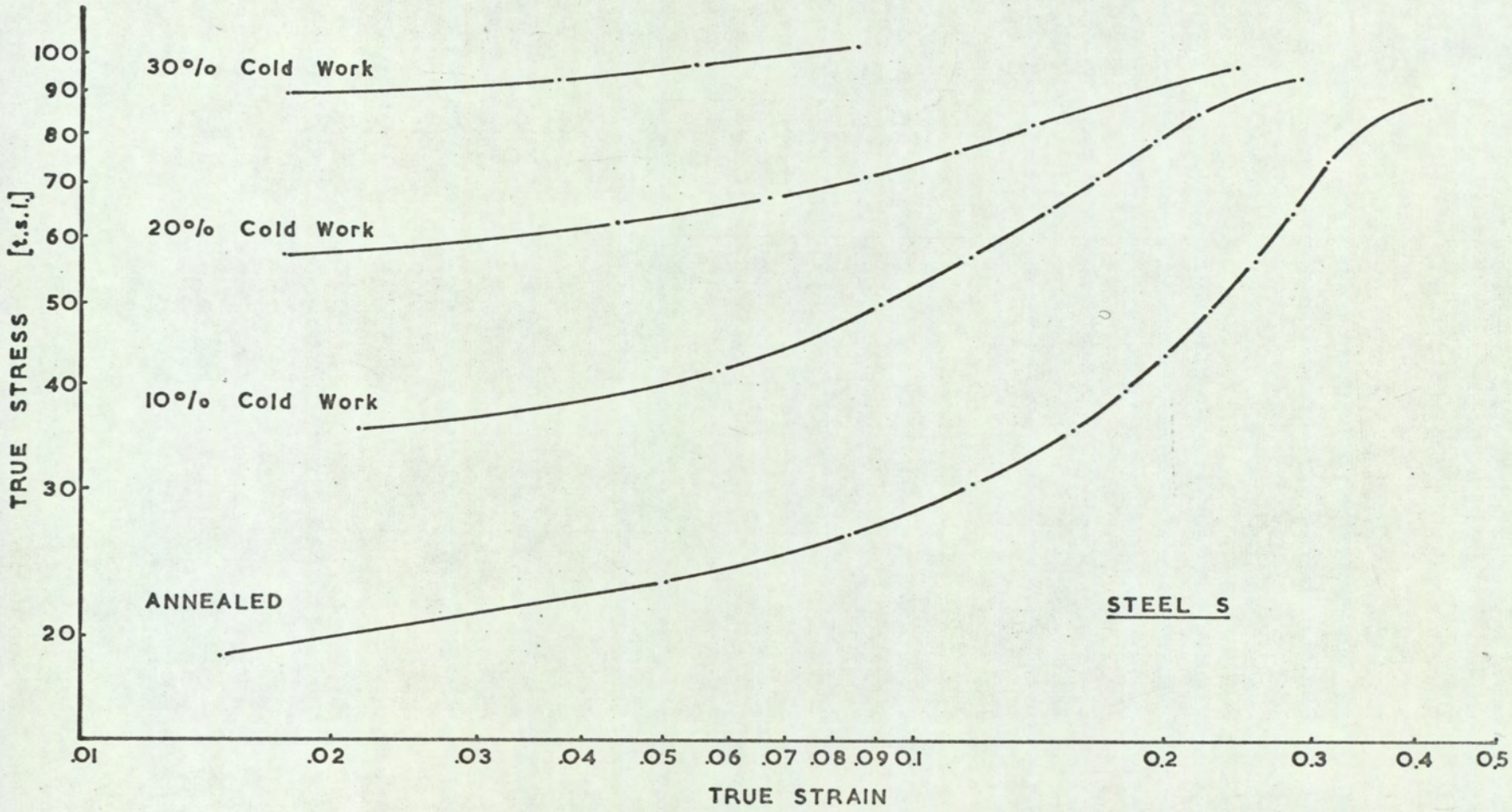

Fig. 4.7.a. Characteristic True Stress - True Strain Curves - Steel S.

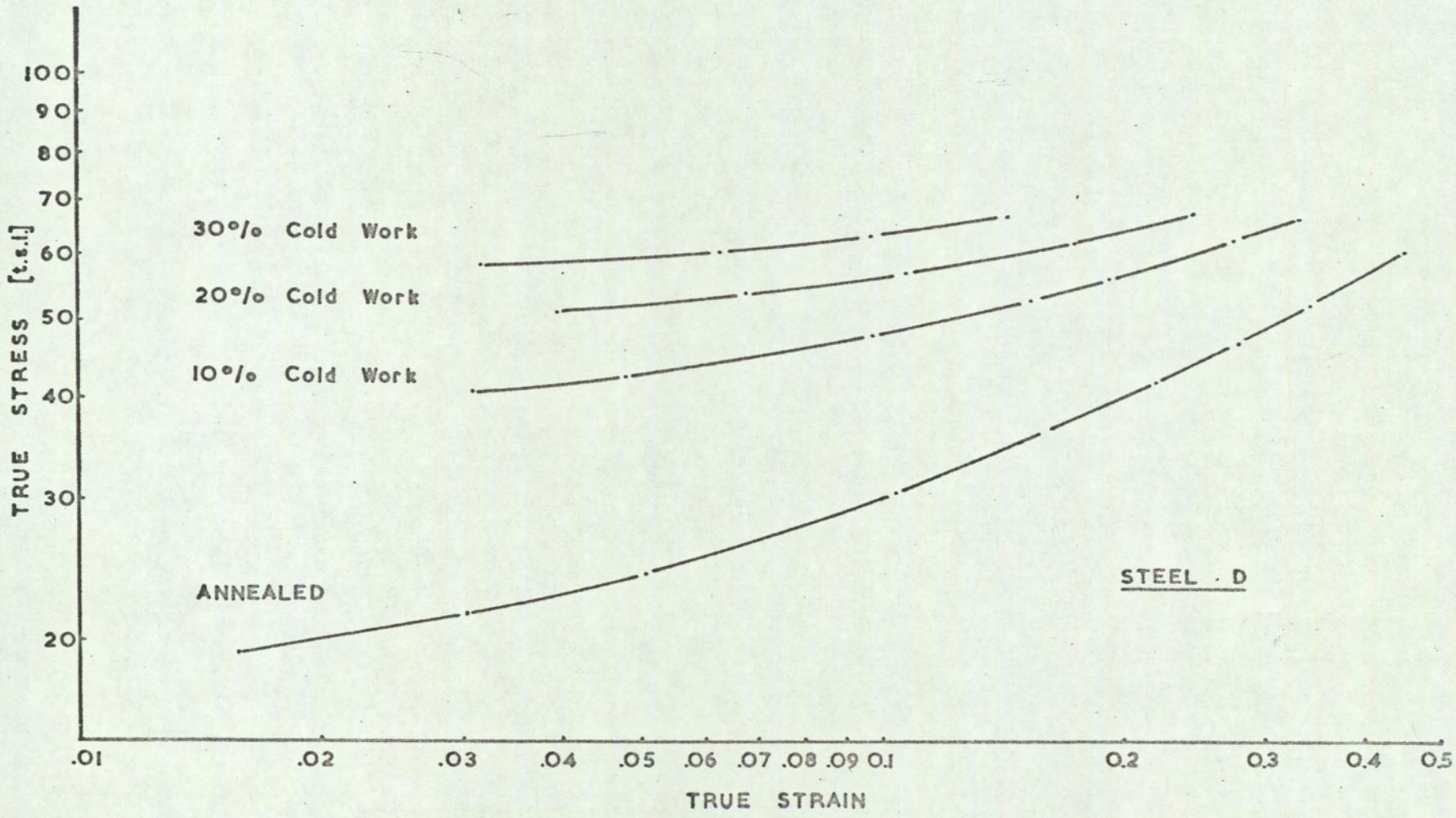

Fig. 4.7.b. Characteristic True Stress - True Strain Curves - Steel D.

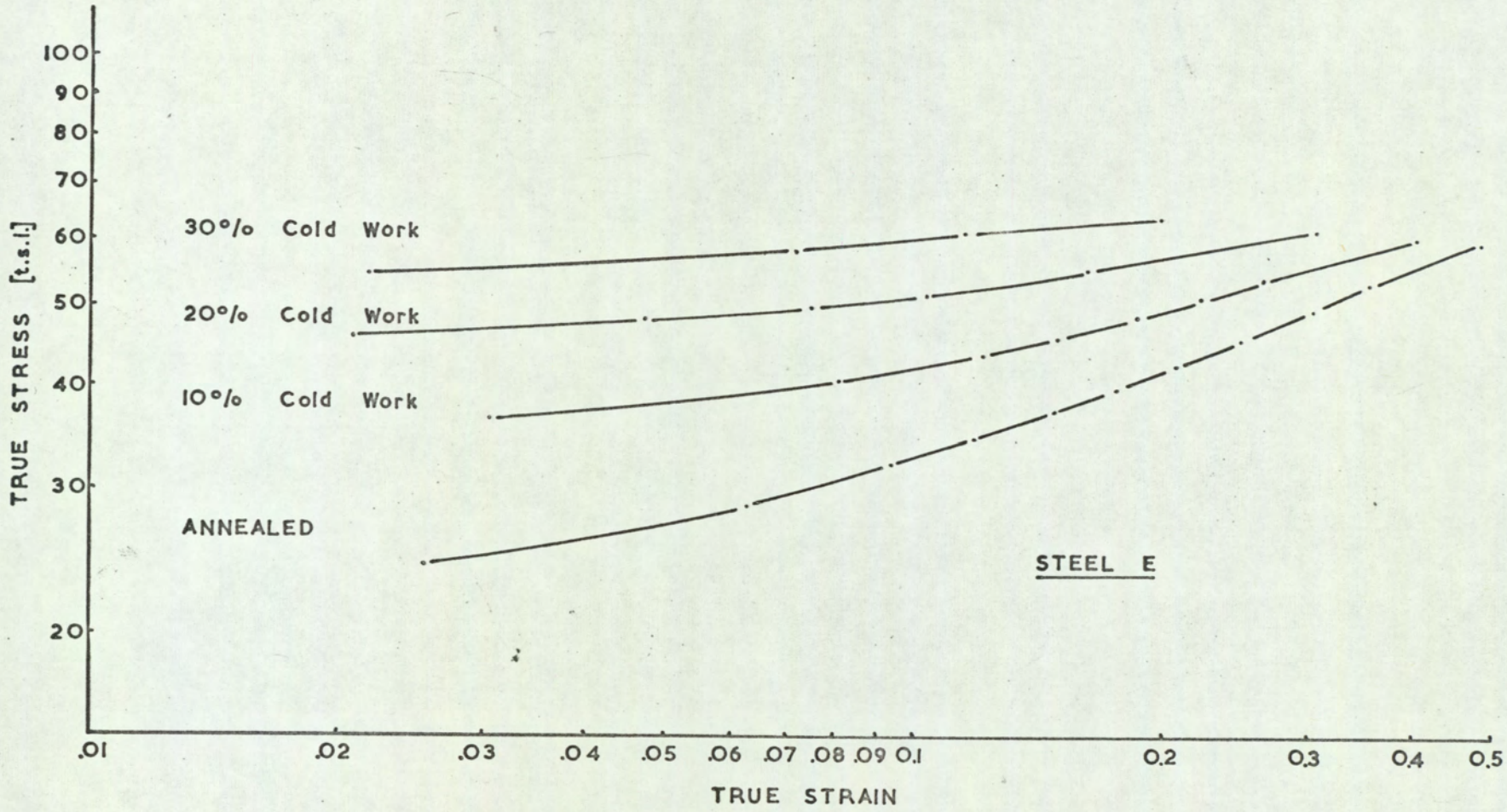

Fig. 4.7.c. Characteristic True Stress - True Strain Curves - Steel E.

TABLE 4.5. THE DEFORMATION WORK AREAS AND MAXIMUM PUNCH LOADS FOR STEELS S, D anJ E IN DIFFERENT CONDITIONS

STEEL	CONDITION	DEFORMATION WORK AREA (Sq ins)				MAXIMUM PUNCH LOADS (Kgs)			$\bar{\sigma}_m \times \delta_{ue}$ (TENSILE TEST)
		TENSILE TEST	STRETCH FORMING	DEEP DRAWING C.B.D.	DEEP DRAWING (67 mm BLANKS)	STRETCH FORMING	C.B.D.	67 mm dia. BLANKS	
S 0	ANNEALED	22.0	4.3	32.5	15.8	5075	8950	6620	39.3
S 10	10% COLD WORK	16.7	2.3	37.1	18.7	4350	10,500	7870	25.3
S 20	20% " "	12.3	1.5	44.5	21.0	3800	12,800	9100	17.6
S 30	30% " "	2.3	1.0	34.5	-	2950	12,400	-	8.7
S 40	40% " "	1.42	0.8	-	-	1800	-	-	2.5
S 50	50% " "	-	0.5	-	-	1075	-	-	1.0
D 0	ANNEALED	16.0	2.6	26.6	10.4	3200	6300	4110	30.2
D 10	10% COLD WORK	13.4	1.6	27.2	14.2	3050	7510	5590	21.5
D 20	20% " "	9.3	1.2	26.5	16.3	2750	8100	6200	12.8
D 30	30% " "	5.5	1.0	24.7	17.3	2320	8420	6770	4.9
D 40	40% " "	4.4	0.9	23.1	18.3	2050	8270	7150	3.3
D 50	50% " "	2.9	0.7	18.5	18.5	1900	7230	7230	1.2
E 0	ANNEALED	14.5	2.3	24.2	9.8	3050	6240	3850	25.5
E 10	10% COLD WORK	13.4	1.7	24.6	12.5	2800	6800	4900	20.8
E 20	20% " "	9.7	1.1	22.9	14.1	2525	7240	5420	14.9
E 30	30% " "	6.8	1.0	20.3	15.5	2075	6730	6520	7.6
E 40	40% " "	4.1	0.7	20.4	17.6	2000	7006	6780	2.8
E 50	50% " "	3.9	0.7	19.7	19.7	1850	7500	7500	2.2

only polynomials up to five terms were considered. The relationship obtained for a five degree polynomial was:-

$$\text{Log}\sigma = \frac{c}{e} + m \log \delta + n.e (\log \delta)^2 + p.e^2 (\log \delta)^3 + qe^3 (\log \delta)^4 + r.e^4 (\log \delta)^5 \quad \ldots\ldots 1$$

where σ = true stress
δ = true strain
e = 2.303
c, m, n, p, q and r are constants

Examination of the sum of the squares of the deviations, Table 4.6, showed that nothing significant could be gained by using relationships more complex than a quadratic for the purpose of representing the experimental data which had accuracies no better than 1%. It was therefore decided that a quadratic function was sufficiently accurate to describe the second part of the curve, i.e.

$$\log \sigma = \frac{c}{e} + m \log \delta + n.e. (\log \delta)^2 \quad \ldots\ldots 2$$

The constants for equation 2, for steels S, D and E in different degrees of cold work together with those for steels A, B, C and F in both the stretch straightened and re-annealed conditions are given in Table 4.7.

The curves from which the above constants have been calculated for steels S, D, and E, have been shown in Fig.4.7. With increase in prior deformation the slopes of the true stress/true strain curves decrease and this is accompanied by a substantial decrease in the m and n. e constants given in Table 4.7.

It can be seen that the rate of strain hardening, the slope of the true stress/ true strain curve, varies with increase in strain. This value has been designated n_δ. An appraisal of the change in n_δ with respect to strain, has been obtained by differentiation of equation 2:-

$$\frac{d (\log \sigma)}{d (\log \delta)} = m + 2ne (\log \delta) \quad \ldots\ldots 3$$

Values of n_δ have been obtained graphically and are presented together with those obtained from equation 3, in Table 4.8.

TABLE 4.6. THE SUM OF THE SQUARES OF THE DEVIATIONS FOR THE STRESS-STRAIN CURVES OF STEELS S, D and E.

STEEL	FUNCTION	ANGLE TO ROLLING DIRECTION					
		0°		45°		90°	
		Σ	Δ%	Σ	Δ%	Σ	Δ%
S 0	STRAIGHT LINE	.3616	0	.1163	0	.0727	0
	QUADRATIC	.0241	93.3	.0018	98.5	.0019	97.4
	CUBIC	.0029	99.2	.0005	99.6	.0006	99.2
S 10	STRAIGHT LINE	.0480	0	.0217	0	.0125	0
	QUADRATIC	.0008	98.3	.0002	99.1	.0002	98.4
	CUBIC	.0004	99.2	.0001	99.5	.0002	98.4
S 20	STRAIGHT LINE	.0031	0	.0011	0	.0004	0
	QUADRATIC	.0001	96.8	.00001	99.1	.00008	80.0
	CUBIC	.00002	99.4	.00001	99.1	.00005	87.5
D 0	STRAIGHT LINE	.0082	0	.0089	0	.0167	0
	QUADRATIC	.0001	98.8	.00005	99.4	.00006	99.6
	CUBIC	.00004	99.5	.00003	99.7	.00006	99.6
D 10	STRAIGHT LINE	.0044	0	.0029	0	.0030	0
	QUADRATIC	.00001	99.8	.000001	100	.00005	98.3
	CUBIC	.000001	100	.000001	100	.00001	99.7
D 20	STRAIGHT LINE	.0023	0	.0029	0	.0007	0
	QUADRATIC	.00013	94.3	3×10^{14}	100	.00003	95.7
	CUBIC	.00006	97.4	-	-	7×10^{-14}	100
E 0	STRAIGHT LINE	.0088	0	.0126	0	.0092	0
	QUADRATIC	.00028	96.8	.00009	99.3	.00003	99.7
	CUBIC	.0001	98.9	.00001	99.9	.00002	99.8
E 10	STRAIGHT LINE	.0026	0	.0058	0	.0055	0
	QUADRATIC	.000002	99.9	.00002	99.7	.00002	99.6
	CUBIC	.000001	99.9	.000005	99.9	3×10^{-6}	100
E 20	STRAIGHT LINE	.00038	0	.00026	0	.0012	0
	QUADRATIC	.000005	98.7	.000002	99.2	.00001	99.2
	CUBIC	1×10^{13}	100	8×10^{-12}	100	.000003	99.8

Σ = the sum of the squares of the deviations, i.e. $\Sigma i\ (yi - yij)^2$

Δ % = per cent difference between Σ for a straight line and the function examined,

i.e. Δ% quadratic $= \frac{\Sigma SL - \Sigma Quad}{\Sigma SL} \times 100$

TABLE 4.7. THE MEAN VALUES OF THE CONSTANTS FOR THE QUADRATIC FUNCTION

STEEL	CONDITION	CONSTANTS		
		$c/_e$ *	m	n.e. *
S 0	ANNEALED AND LEVELLED	2.498	1.573	0.549
S 10	10% COLD WORK	2.395	0.865	0.240
S 20	20% " "	2.217	0.401	0.090
D 0	ANNEALED AND LEVELLED	2.010	0.745	0.196
D 10	10% COLD WORK	2.013	0.507	0.158
D 20	20% " "	1.990	0.338	0.102
E 0	ANNEALED AND LEVELLED	1.964	0.597	0.141
E 10	10% COLD WORK	1.976	0.517	0.158
E 20	20% " "	1.925	0.301	0.085
A	ANNEALED AND STRAIGHTENED	2.150	0.866	0.243
B	" " "	2.030	0.700	0.182
C	" " "	2.000	0.615	0.129
F	" " "	1.980	0.557	0.120
A	ANNEALED ONLY	2.207	1.128	0.349
B	" "	1.988	0.738	0.172
C	" "	1.976	0.717	0.148
F	" "	1.948	0.627	0.129
S 0	" "	2.866	2.215	0.793

* e = 2.303

TABLE 4.8. SLOPE STRESS-STRAIN CURVE (n_s) AT DIFFERENT LEVELS OF STRAIN

STEEL	CONDITION	METHOD OF CALCULATION	TRUE STRAIN LEVEL							
			0.05	0.1	0.15	0.2	0.25	0.3	0.35	0.4
S 0	ANNEALED and LEVELLED	MEASURED GRAPHICALLY	.213	.378	.598	.839	1.01	1.09	-	-
"	" " "	QUADRATIC FUNCTION	.145	.475	.669	.806	.912	.999	1.073	1.136
S 10	10% COLD WORK	MEASURED GRAPHICALLY	.216	.404	.481	.512	-	-	-	-
"	" "	QUADRATIC FUNCTION	.241	.386	.470	.530	.576	-	-	-
S 20	20% COLD WORK	MEASURED GRAPHICALLY	.168	.242	.266	-	-	-	-	-
"	" "	QUADRATIC FUNCTION	.166	.221	.253	-	-	-	-	-
D 0	ANNEALED and LEVELLED	MEASURED GRAPHICALLY	.262	.350	.419	.485	.510	.545	.569	-
"	" "	QUADRATIC FUNCTION	.234	.353	.422	.471	.509	.540	.566	.589
D 10	10% COLD WORK	MEASURED GRAPHICALLY	.119	.193	.246	.301	.345	.360	-	-
"	" "	QUADRATIC FUNCTION	.096	.191	.247	.286	.317	.342	-	-
D 20	20% COLD WORK	MEASURED GRAPHICALLY	.073	.133	.198	.251	-	-	-	-
"	" "	QUADRATIC FUNCTION	.073	.135	.170	-	-	-	-	-
E 0	ANNEALED and LEVELLED	MEASURED GRAPHICALLY	.228	.325	.377	.411	.433	.452	-	-
"	" "	QUADRATIC FUNCTION	.230	.315	.364	.400	.427	.450	.469	.485
E 10	10% COLD WORK	MEASURED GRAPHICALLY	.123	.196	.260	.302	.365	-	-	-
"	" "	QUADRATIC FUNCTION	.106	.202	.257	.297	.327	.352	-	-
E 20	20% COLD WORK	MEASURED GRAPHICALLY	.075	.130	.185	-	-	-	-	-
"	" "	QUADRATIC FUNCTION	.079	.130	.160	.182	-	-	-	-
A	ANNEALED and STRAIGHTENED	MEASURED GRAPHICALLY	-	.381	-	.535	-	.666	-	.727
"	" " "	QUADRATIC FUNCTION	.234	.380	.466	.526	.573	.612	.644	.673
B	" " "	MEASURED GRAPHICALLY	-	.337	-	.468	-	.531	-	.551
"	" " "	QUADRATIC FUNCTION	.226	.336	.400	.445	.481	.510	.534	.555
C	" " "	MEASURED GRAPHICALLY	-	.384	-	.451	-	.490	-	-
"	" " "	QUADRATIC FUNCTION	.279	.358	.403	.435	.460	.480	.497	.512
F	" " "	MEASURED GRAPHICALLY	-	.321	-	.397	-	.466	-	-
"	" " "	QUADRATIC FUNCTION	.245	.317	.359	.389	.412	.432	.448	.462
A	ANNEALED ONLY	QUADRATIC FUNCTION	.220	.430	.553	.640	.708	.763	.810	.850
B	" "	QUADRATIC FUNCTION	.291	.394	.455	.498	.531	.558	.581	.601
C	" "	QUADRATIC FUNCTION	.333	.422	.474	.511	.538	.563	.582	.600
F	" "	QUADRATIC FUNCTION	.291	.369	.414	.447	.472	.492	.509	.524

4.6. True Stress-True Strain Data obtained from the Plane Strain Compression Tests

True stress-true strain data have also been obtained from plane strain compression and biaxial tension tests for steels S, D and E in the annealed condition only. Typical curves for these tests are shown in Fig.4.8. It can be seen that the stresses required to deform the material in plane strain are greater than for either biaxial tension or pure tension and that this difference in stress is less between steels D and E than it is between S and D.

Using a formula quoted by Hosford and Backofen[48] it can be deduced that the ratio of stress obtained in the plane strain compression test to that for uniaxial tension testing should be $\sqrt{\frac{2(R+1)}{2R+1}}$ where R is a measure of $\hat{R}_{normal}$ anisotropy. For isotropic materials the ratio should be 1.154. Using the relationship and the $\bar{R}$ values obtained in tension, the actual ratios of compression and tension at different levels of strain are compared in Table 4.9.

TABLE 4.9. THE RATIOS OF STRESS IN COMPRESSION : STRESS IN TENSION AT DIFFERENT LEVELS OF TRUE STRAIN

STEEL	RATIO OF $\frac{\text{STRESS IN COMPRESSION}}{\text{STRESS IN TENSION}}$ $\frac{\sigma_c}{\sigma_t}$				
	0.05	0.10	0.15	0.20	0.25
S	1.27	1.44	1.64	1.79	1.71
D	1.35	1.36	1.42	1.45	1.45
E	1.27	1.26	1.23	1.21	1.19

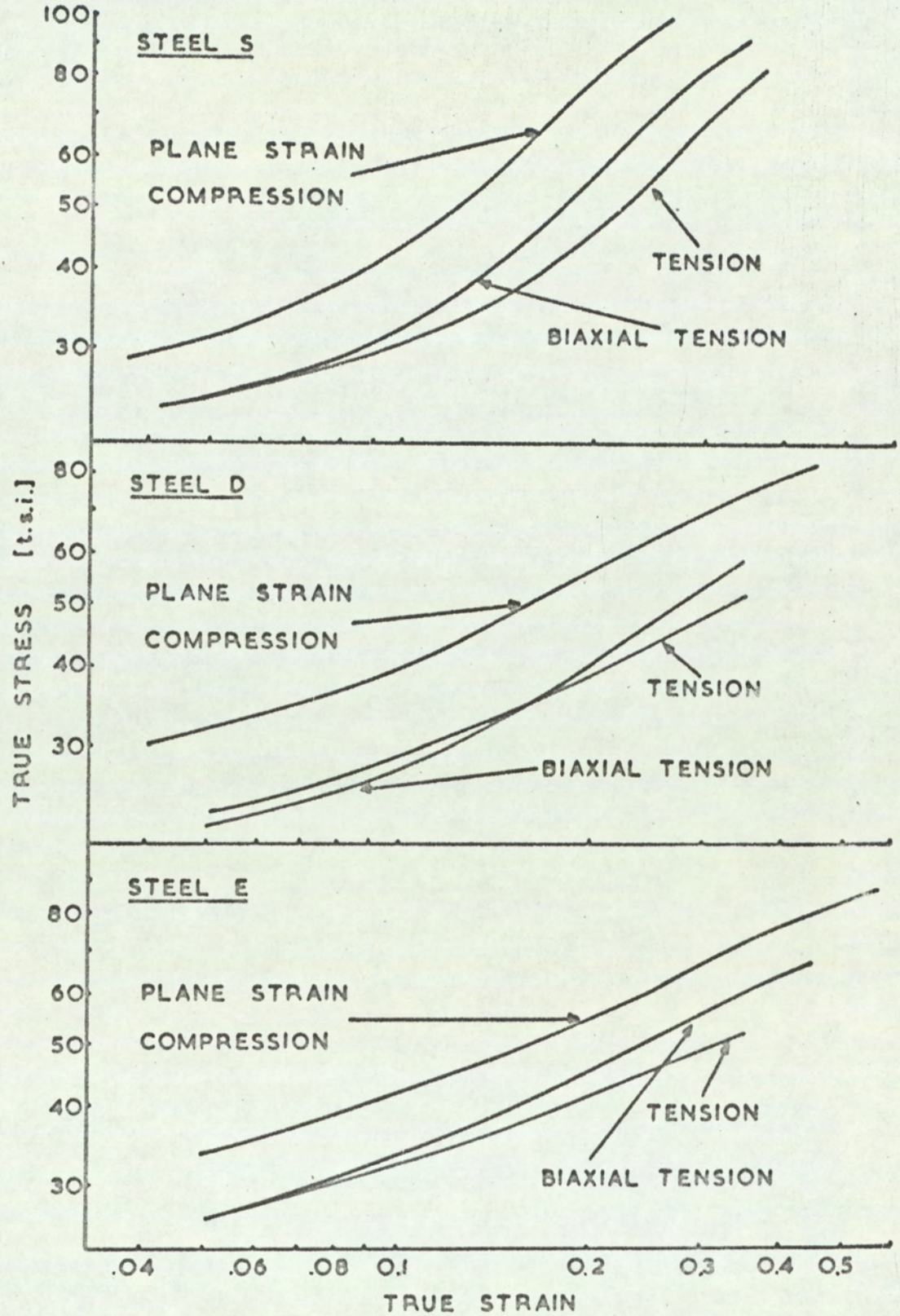

FIG. 4.8. TRUE STRESS - TRUE STRAIN CURVES OBTAINED FROM PLANE STRAIN COMPRESSION, HYDROSTATIC BULGE AND TENSILE TESTS.

4.7. True Stress-True Strain Data obtained from Hydrostatic Bulge Tests

Similar results have been obtained from the biaxial tension test; typical stress-strain curves have already been reported in Fig.4.8. Derived data from these curves is given in Table 4.10.

TABLE 4.10. THE RATIOS OF STRESS IN BIAXIAL TENSION : STRESS IN UNIAXIAL TENSION AT DIFFERENT LEVELS OF TRUE STRAIN

STEEL	RATIO OF STRESS IN BIAXIAL TENSION $\frac{\sigma_B}{\sigma_t}$ STRESS IN UNIAXIAL TENSION				
	0.05	0.10	0.15	0.20	0.25
S	1.02	1.08	1.17	1.23	1.26
D	0.95	0.95	0.99	1.05	1.08
E	1.00	1.04	1.07	1.09	1.12

It is apparent that the variation between the two stress systems becomes greater, with increase in strain. The actual ratios of the stress values, measured at similar levels of strain, for the two stress systems here examined can be predicted from the formula $\sqrt{\frac{R+1}{2}}$ i.e. for isotropic materials the two stress values should be equal. The values for steels D and E give good agreement within the limits of experimental error.

As with the tensile test data, the true stress-strain curves for both plane strain compression and biaxial tension, have been analysed by the computer for degree of fit. These curves obey a similar function to that obtained in tensile testing and the constants describing the curves are given in Table 4.11. The slopes of these curves with respect to strain, n_δ, have also been analysed and are included in this table, together with similar values that have been obtained by converting the plane strain compression results to a tensile equivalent.

For reasons that will be discussed in the next section, it was considered that the ultimate slope of the stress-strain curve; the slopes corresponding to the

TABLE 4.11. THE QUADRATIC CONSTANTS AND SLOPES OF THE STRESS-STRAIN CURVES (n_δ), FOR THE PLANE STRAIN COMPRESSION AND HYDROSTATIC BULGE TESTS.

STEEL	TEST	CONSTANTS			(n_δ) SLOPE AT DIFFERENT TRUE STRAIN LEVELS							
		$c/_e$	m	n.e	0.05	0.10	0.15	0.20	0.25	0.30	0.35	0.40
S	PLANE STRAIN COMPRESSION	2.960	1.955	0.635	.302	.684	.908	1.067	1.190	1.290	1.376	1.449
D	" " "	2.228	0.861	0.235	.250	.391	.474	.533	.578	.615	.647	.674
E	" " "	2.125	0.668	0.163	.243	.341	.399	.440	.471	.497	.519	.538
S	PLANE STRAIN COMPRESSION	2.779	1.876	0.635	.223	.605	.829	.988	1.111	1.211	1.279	1.370
D	(TENSILE EQUIVALENT)	2.113	0.832	0.235	.220	.362	.445	.503	.549	.586	.617	.645
E	" "	2.023	0.648	0.164	.223	.321	.379	.420	.451	.477	.499	.518
S	BIAXIAL TENSION	2.584	1.532	0.477	.290	.577	.745	.865	.957	1.033	1.097	1.152
D	" "	2.212	1.130	0.360	.192	.409	.536	.626	.696	.753	.801	.843
E	" "	2.089	0.755	0.189	.263	.377	.443	.491	.527	.557	.582	.604

limits of uniform and total elongation, should also be calculated. This has been done and the results for the tensile tests are given in Table 4.12.

TABLE 4.12. THE SLOPES OF THE STRESS-STRAIN CURVES AT THE LIMITS OF UNIFORM AND TOTAL ELONGATION

STEEL	CONDITION	SLOPE (n_s) AT STRAIN LEVEL CORRESPONDING TO:-	
		UNIFORM ELONGATION	TOTAL ELONGATION
S 0	ANNEALED & LEVELLED	1.163	1.204
S 10	10% COLD WORK	0.592	0.617
S 20	20% " "	0.267	0.280
D 0	ANNEALED & LEVELLED	0.622	0.639
D 10	10% COLD WORK	0.356	0.379
D 20	20% " "	0.195	0.224
E 0	ANNEALED & LEVELLED	0.496	0.509
E 10	10% COLD WORK	0.373	0.395
E 20	20% " "	0.197	0.213
A	ANNEALED & STRAIGHTENED	0.660	0.668
B	" " "	0.580	0.646
C	" " "	0.515	0.532
F	" " "	0.476	0.486
A	ANNEALED ONLY	0.931	0.952
B	" "	0.625	0.643
C	" "	0.626	0.639
F	" "	0.536	0.549

4.8. Hardness and Strain Distribution in Drawn Cups

With increasing prior cold work, the C.B.D. of Steels D and E decreased as the ductility of the material diminished. The C.B.D. of steel S, however, remained constant between 0 and 10% cold work, fell slightly after 20% and rapidly after 30%. Beyond this point the steel became undrawable using the tooling described because of the inability of the material to be bent over the punch nose radius.

In order to investigate why the drawability of steel S had not been impaired by the 10% prior deformation and to assess in general, the effect of prior cold work on a range of steels, hardness and thickness strain distribution measurements were made on sectioned cups. The results are shown in Fig.4.9. Since it is difficult to draw conclusions from hardness and thickness strain distributions for cups drawn from different blank diameters, comparison is also made with cups drawn from blank diameters of 67 mm. Also included are results from cups drawn with a hemispherically shaped punch to show the effect of increased stretch formability over the punch nose radius.

4.9. Performance Factors

Since the materials examined gave a wide range of mechanical properties but a relatively narrow range of deep drawability and materials of widely differing strength properties gave similar C.B.D. values, simple relationships between strength properties or hardness and deep drawability cannot be expected. Although there was a relationship between elongation and C.B.D. this was not as strong as the relationship between elongation and the Erichsen stretch forming value. It was therefore decided to examine some of the performance functions that have been proposed, to predict press formability, to comment on their significance for stainless steels and to compare them with relationships obtained from the present work.

Several relationships, particularly for mild steel have been obtained between deep drawability and the normal anisotropy ratio $\bar{R}$. The theoretical

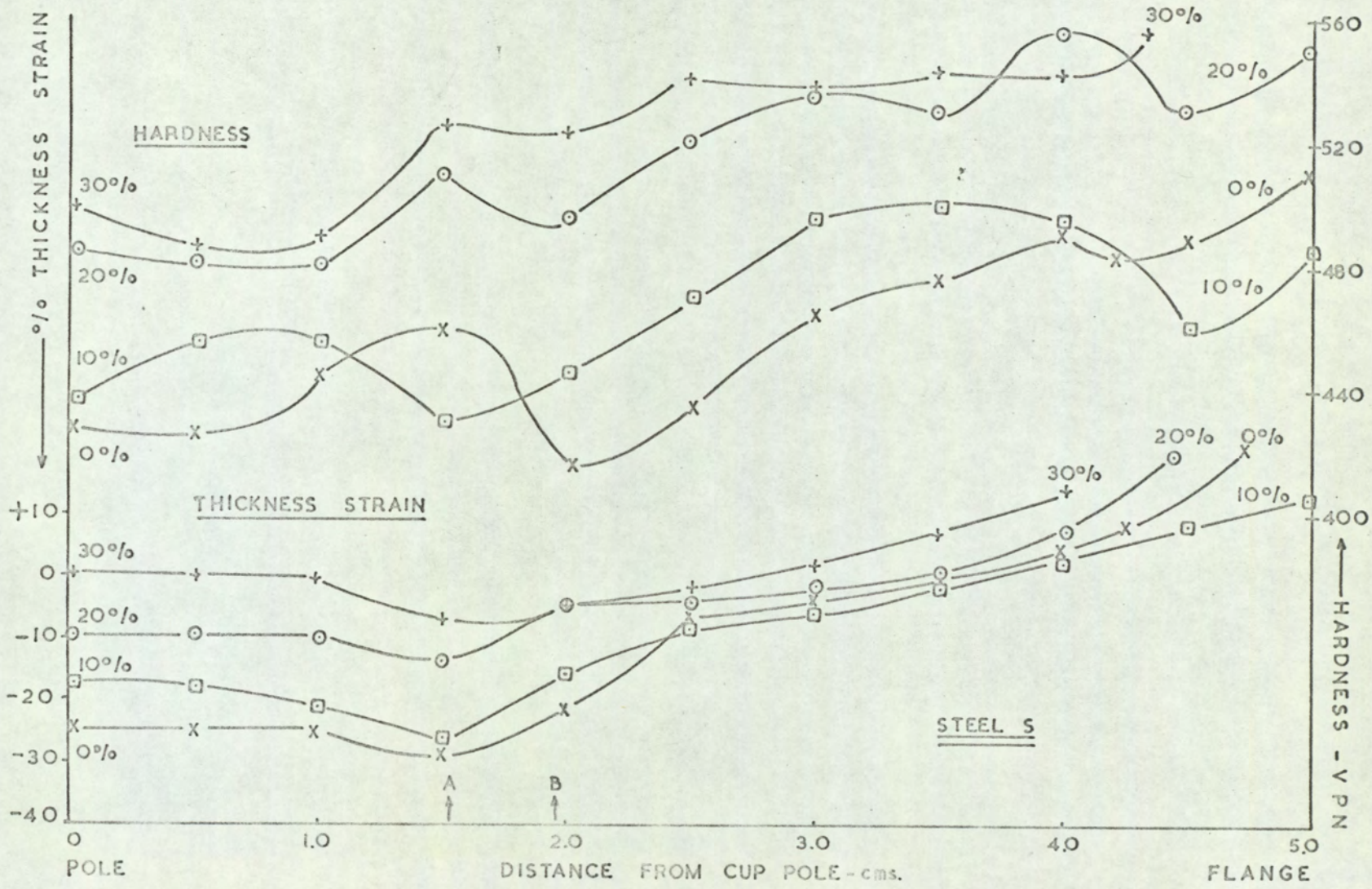

Fig. 4.9.a. Hardness and Thickness Strain Distribution Curves - Steel S. - C.B.D. Cups.

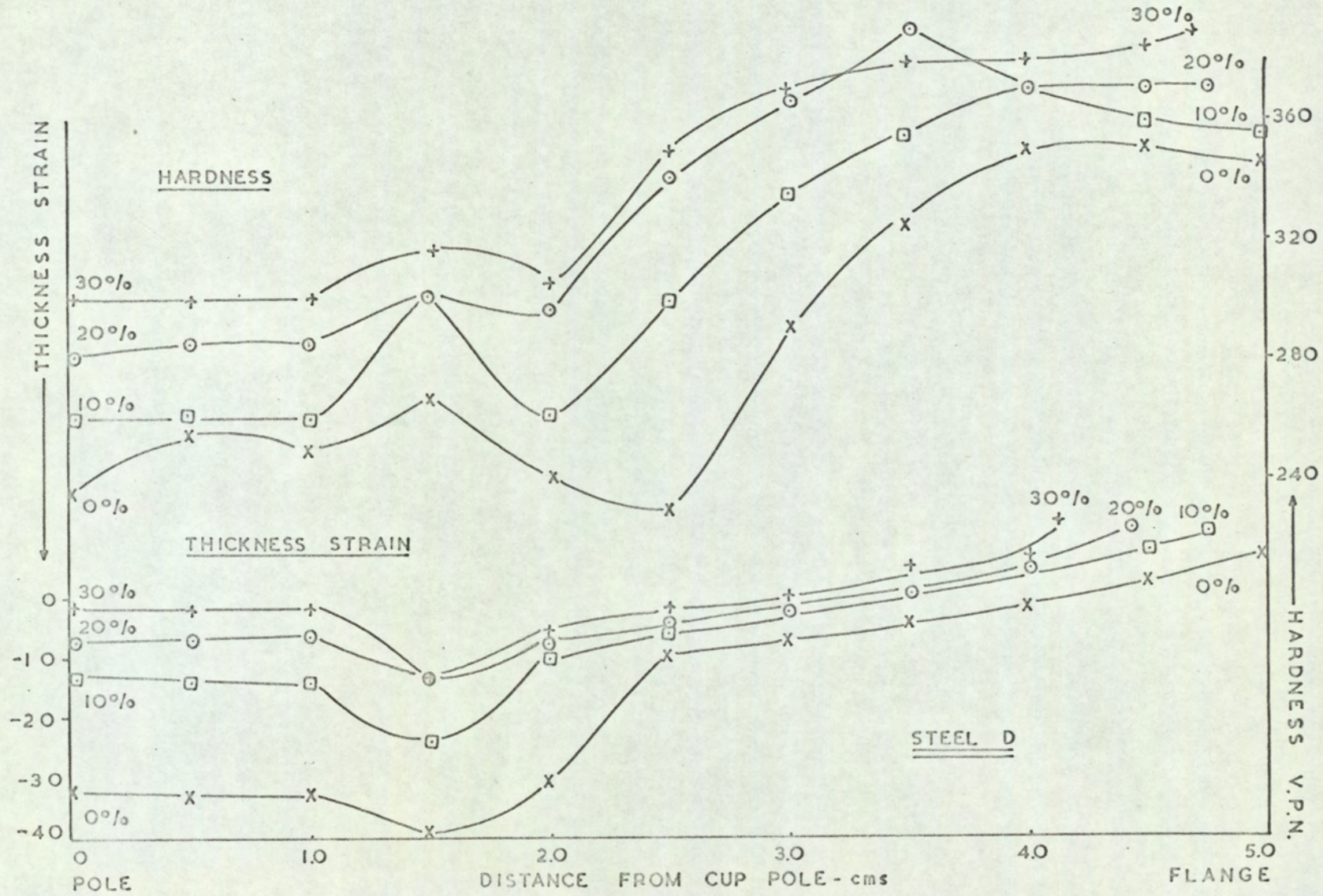

Fig. 4.9.a. Hardness and Thickness Strain Distribution Curves - Steel D - C.B.D. Cups.

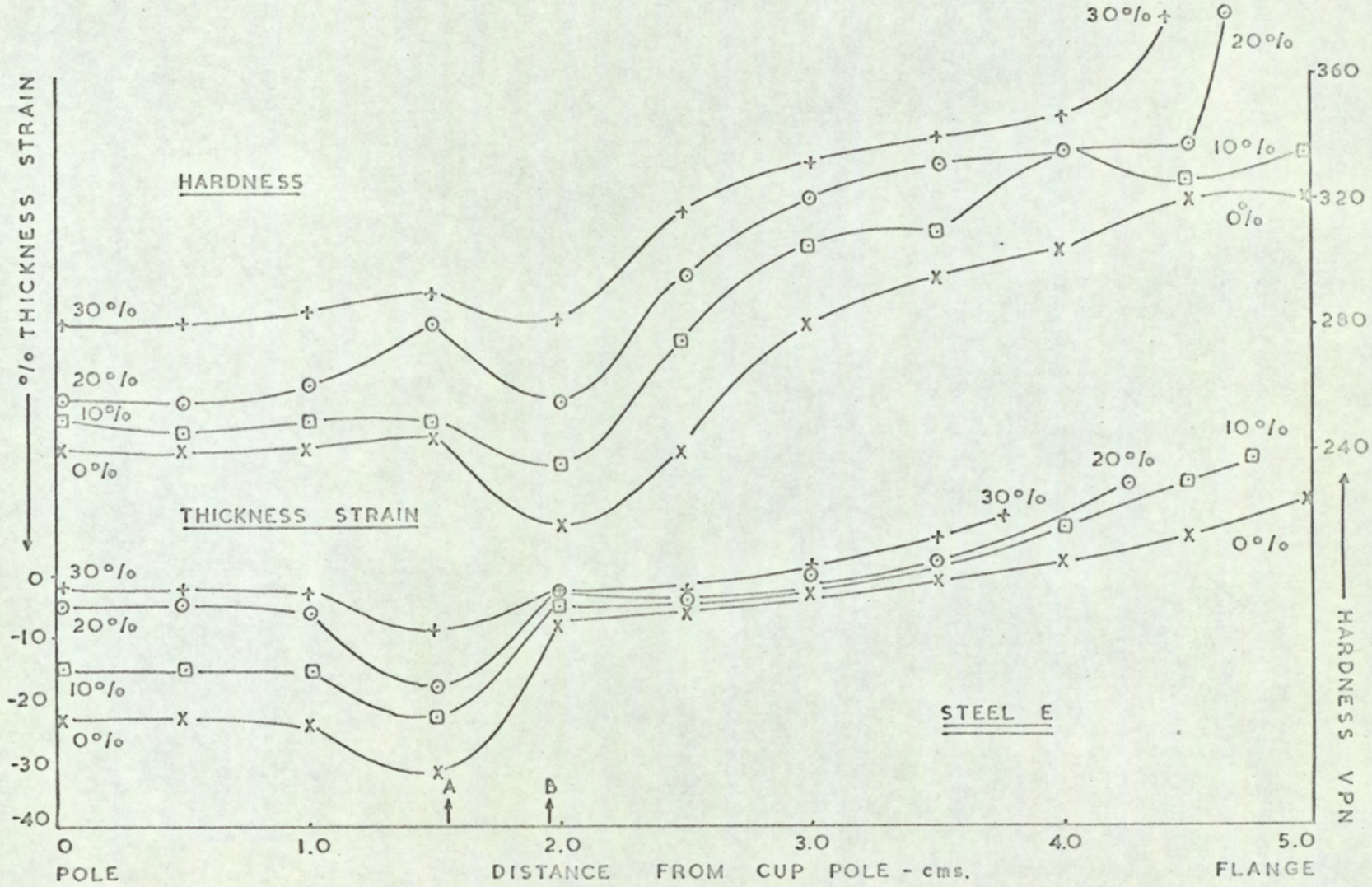

Fig. 4.9.a. Hardness and Thickness Strain Distribution Curves-Steel E - C.B.D. Cups.

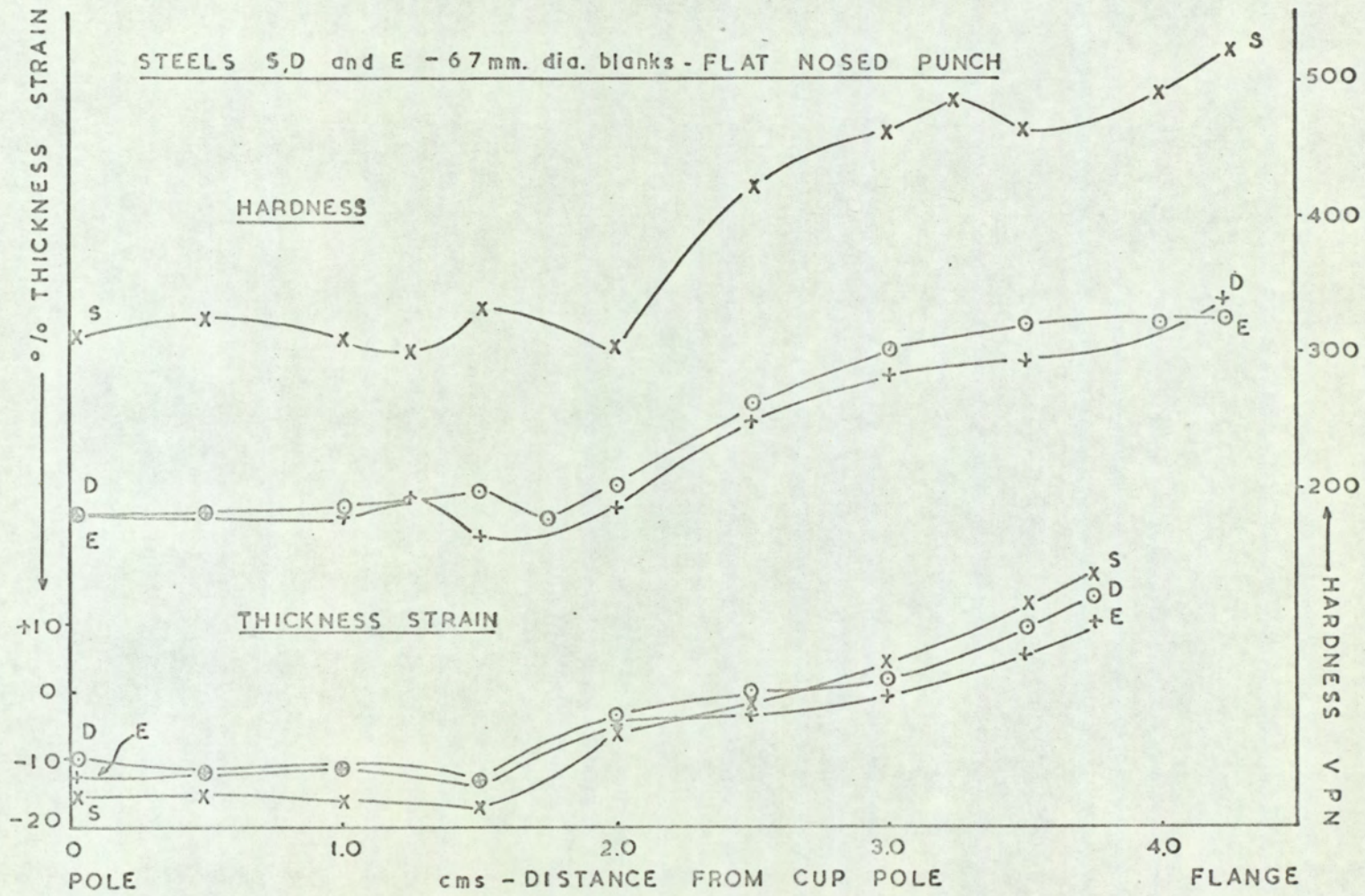

Fig. 4.9.b. Hardness and Thickness Strain Distribution Curves - 67 mm. dia Cups. - FNP.

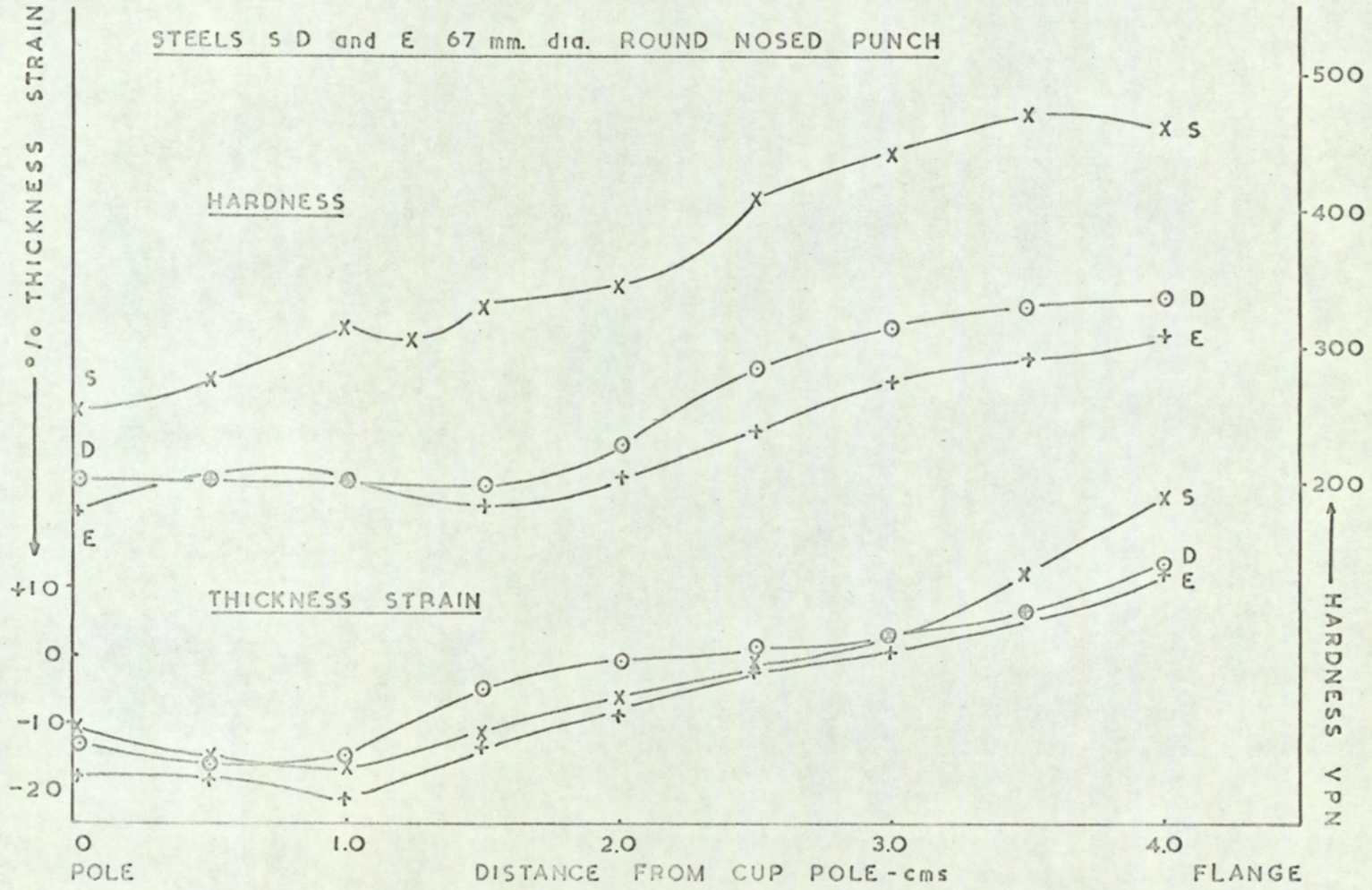

Fig. 4.9.c. Hardness and Thickness Strain Distribution Curves -67 mm. dia Cups - RNP.

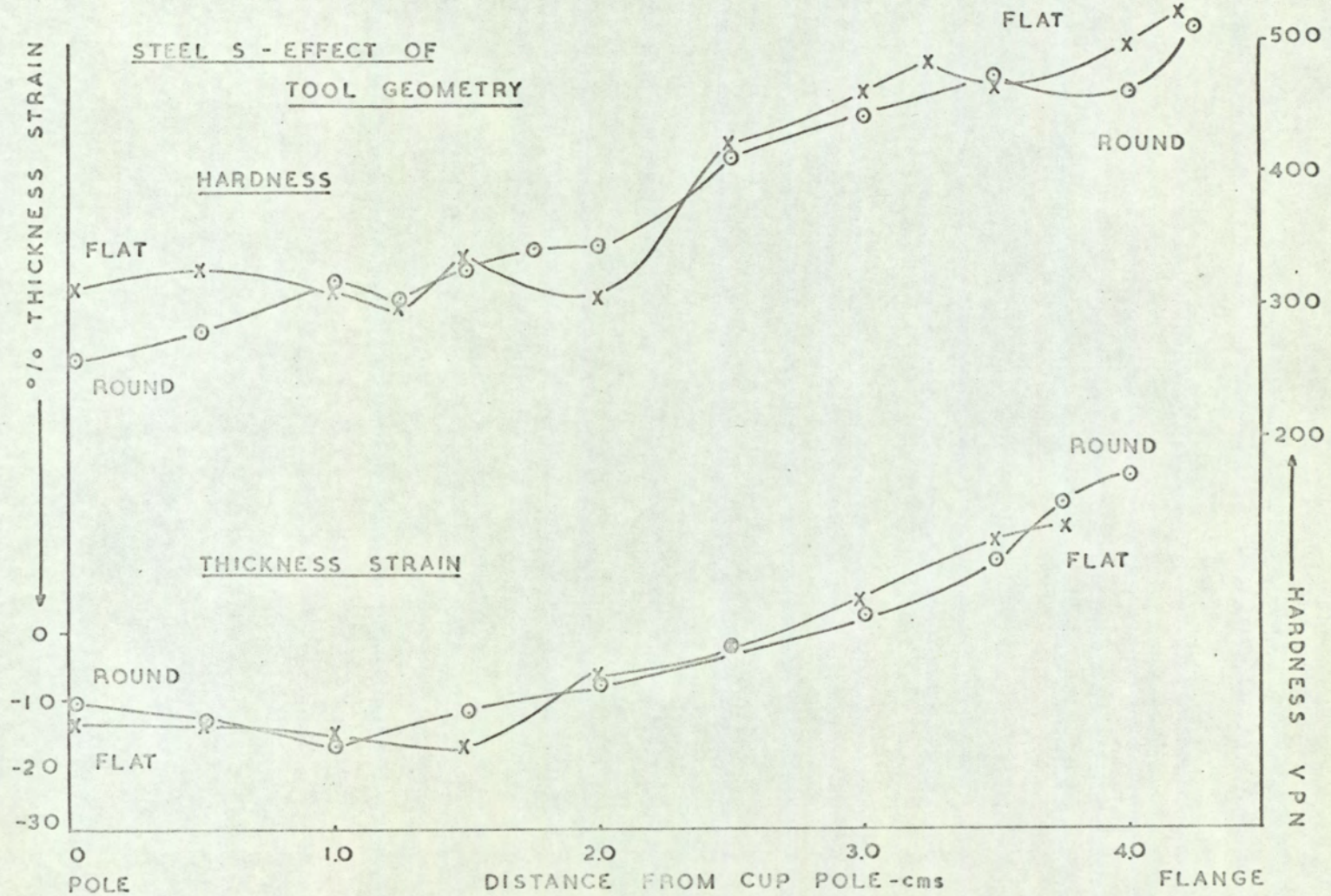

Fig. 4.9.d. The Effect of Punch Geometry on the Distribution of Hardness and Thickness Strain.

reasons for this relationship have been considered by Whiteley.[49] Starting from an analysis by Hu of the plastic deformation of a hollow cylinder, he derived the expression:-

$$\ln D/_d = \frac{1}{1+n}\sqrt{\frac{\bar{R}+1}{2}}$$ where $D/_d$ is the L.D.R. and n a frictional parameter. The analysis was really for plane radial drawing neglecting the effects of bending and unbending under tension over punch and die profiles and of work hardening. For the purpose of this work the die entry radius was increased to minimise the severity of bending and unbending but for the materials considered, the work hardening component was very high. For this latter reason poor agreement is obtained, (Table 4.13) between the predicted and actual C.B.Ds.

TABLE 4.13. COMPARISON OF ACTUAL AND PREDICTED VALUES OF C.B.D. FOR THE STEELS S, D and E IN DIFFERENT CONDITIONS

STEEL	CONDITION	ACTUAL $\ln D/_d$	PREDICTED $\ln D/_d$		
			n = .15	n = .20	n = .25
S 0	ANNEALED & LEVELLED	0.83	0.83	0.79	0.76
S 10	10% COLD WORK	0.83	0.81	0.78	0.75
S 20	20% " "	0.82	0.80	0.77	0.74
D 0	ANNEALED & LEVELLED	0.85	0.87	0.83	0.80
D 10	10% COLD WORK	0.83	0.90	0.86	0.82
D 20	20% " "	0.81	0.90	0.87	0.83
E 0	ANNEALED & LEVELLED	0.86	0.87	0.83	0.80
E 10	10% COLD WORK	0.83	0.88	0.84	0.81
E 20	20% " "	0.81	0.90	0.87	0.83

There is fair agreement when only the annealed material is considered, particularly if n, the frictional parameter is considered to be about 0.15. This was considered

justified in view of the fact that polythene sheet lubricant was used which would decrease the coefficient of friction.

The second function considered was one proposed by Paulson et al and quoted in a paper by Black and Lherbier.[54] They derived a function from examination of true stress/true strain tensile date for stainless steels. They contend that maximum uniform strain is the most important factor in press formability but that other parameters must also be considered. The function of which low values indicate improved formability, is:-

$$f = \frac{\ln\left[\sigma m\ (1 - Eu)\right]}{A^{Eu}}$$

where σm is the stress at maximum load, Eu is the maximum uniform strain and A^{Eu} the deformation work area. The function has been derived particularly for stainless steels and the properties required for highest formability are low stress at maximum load, high uniform strain coupled with a high deformation work area. Table 4.14. details the results obtained using this function.

TABLE 4.14. VALUES OF TWO FORMABILITY FACTORS FOR DIFFERENT MATERIAL CONDITIONS

STEEL	CONDITION	FORMABILITY FACTOR (BLACK AND LHERBIER	'F' FUNCTION (BUTLER)
S 0	ANNEALED AND LEVELLED	0.17	207.0
S 10	10% COLD WORK	0.25	96.6
S 20	20% " "	0.35	50.4
D 0	ANNEALED AND LEVELLED	0.20	171.0
D 10	10% COLD WORK	0.27	53.2
D 20	20% " "	0.42	32.6
E 0	ANNEALED AND LEVELLED	0.23	129.9
E 10	10% COLD WORK	0.26	66.4
E 20	20% " "	0.39	35.1

Finally a third function, initially derived by Butler [66] and modified by Grimes, [60] has been investigated. This function was primarily predicted to evaluate stretch formability using four mechanical properties, i.e.:-

$$F = \frac{\text{UTS} \times \text{Uniform Elongation}}{\text{Flow stress} \times \bar{R}\,\text{av.}}$$

Values for F have been calculated and are also presented in Table 4.14.

4.10. Correlation Matrix

The results of the correlation computer programme described in section 3.15 are presented in matrix form in Table 4.15. Values of the correlation coefficient, which are significant when tested at a 99.9% significance level, have been underlined.

TABLE 4.15. CORRELATION MATRIX

1. QUADRATIC CONSTANT c/e
2. QUADRATIC CONSTANT m
3. QUADRATIC CONSTANT n.e.
4. STRESS AT 0.15 STRAIN
5. SLOPE STRESS-STRAIN CURVE AT 0.15 STRAIN
6. SLOPE n_ε vs STRAIN CURVE
7. HARDNESS
8. $\bar{R}$ VALUE
9. ULTIMATE TENSILE STRENGTH
10. % UNIFORM ELONGATION
11. % TOTAL ELONGATION
12. ERICHSEN VALUE
13. AUSTENITE STABILITY
14. DEFORMATION WORK AREA - TENSION
15. DEFORMATION WORK AREA - STRETCH FORMING
16. DEFORMATION WORK AREA-DEEP DRAWING (67 mm)
17. 0.5% PROOF STRESS
18. PROOF STRESS/ULTIMATE TENSILE STRENGTH
19. STRESS AT MAXIMUM LOAD
20. % EARING
21. CRITICAL BLANK DIAMETER
22. MAXIMUM PUNCH LOAD - C.B.D.
23. DEFORMATION WORK AREA - C.B.D.
24. MAXIMUM PUNCH LOAD - STRETCH FORMING
25. MAXIMUM PUNCH LOAD - DEEP DRAWING (67 mm)
26. MAGNETIC RESPONSE - TENSION
27. MAGNETIC RESPONSE - COMPRESSION
28. n_ε AT FRACTURE STRAIN
29. n_ε AT INSTABILITY STRAIN
30. % PRIOR DEFORMATION

1																													
.80	2																												
.78	.99	3																											
.23	-.40	-.40	4																										
.79	.97	.91	-.37	5																									
.77	.99	1.0	-.41	.91	6																								
.17	-.43	-.41	.98	-.44	-.42	7																							
-.67	-.35	-.24	-.46	-.50	-.23	-.36	8																						
.73	.19	.18	.83	.20	.17	.79	-.69	9																					
0	.54	.48	-.87	.60	.48	-.90	.03	-.61	10																				
-.10	.48	.43	-.91	.52	.43	-.94	.14	-.70	.99	11																			
.31	.79	.74	-.79	.82	.74	-.83	-.12	-.37	.94	.91	12																		
.83	.51	.48	.46	.52	.48	.42	-.61	.80	-.19	-.27	.05	13																	
.76	.96	.92	-.40	.98	.92	-.46	-.45	.15	.64	.57	.84	.48	14																
.72	.95	.89	-.43	.99	.89	-.49	-.46	.12	.69	.61	.87	.50	.98	15															
.60	.02	.04	.88	-.01	.04	.88	-.50	.96	-.77	-.83	-.56	.74	-.05	-.09	16														
-.10	-.63	-.58	.89	-.69	-.58	.93	-.02	.57	-.98	-.97	-.97	.17	.70	-.74	.74	17													
-.67	-.86	-.76	.35	-.95	-.76	.45	.59	-.14	-.69	-.60	-.84	-.47	-.92	-.96	.11	.73	18												
.92	.53	.50	.56	.55	.50	.51	-.77	.93	-.28	-.39	0	.89	.51	.48	.82	.22	-.48	19											
-.28	-.30	-.29	.03	-.29	-.29	.04	.35	-.17	-.06	-.01	-.20	.19	-.27	-.20	-.03	.15	.28	-.25	20									
.07	.40	.28	-.54	.56	.28	-.66	-.32	-.37	-.83	.79	.77	-.12	.59	.59	-.58	-.81	-.71	-.10	-.21	21								
.65	.09	.08	.87	.11	.07	.84	-.70	.98	-.01	-.70	-.41	.77	.08	.05	.95	.61	-.10	.89	-.14	-.34	22								
.71	.22	.17	.76	.28	.16	.70	-.82	.93	-.40	-.50	-.21	.83	.26	.24	.85	.41	-.31	.91	-.11	-.11	.96	23							
.98	.87	.84	.08	.88	.84	.02	-.65	.62	.18	.08	.47	.82	.86	.84	.46	-.26	-.79	.87	-.24	.21	.55	.65	24						
.66	.09	.10	.87	.07	.09	.85	-.60	.99	-.69	-.77	-.48	.77	.05	0	.99	.67	0	.87	-.09	-.47	.98	.91	.53	25					
.48	-.05	-.11	.85	.03	-.12	.81	-.79	.87	-.51	-.60	-.39	.63	.01	-.01	.81	.55	-.11	.77	-.18	-.16	.94	.95	.40	.36	26				
.50	-.04	-.10	.86	.05	-.11	.81	-.81	.89	-.51	-.61	-.39	.64	.02	.01	.82	.55	-.12	.78	-.17	-.15	.94	.95	.42	.87	1.0	27			
.73	.99	.96	-.48	.98	.96	-.52	-.34	.09	.65	.58	.86	.44	.98	.97	-.09	-.72	-.90	.46	-.29	.50	.01	.16	.83	-.10	-.01	-.10	28		
.74	.99	.97	-.48	.98	.97	-.52	-.33	.10	.64	.57	.86	.45	.97	.97	-.08	-.72	-.89	.46	-.29	.48	.01	.16	.83	-.01	-.11	-.10	1.0	29	
-.23	-.69	-.61	.76	-.77	-.62	.84	.15	.41	-.95	-.92	-.97	0	-.79	-.81	.61	.97	.82	.06	.14	-.89	.44	.21	-.40	.52	.38	.37	-.77	-.77	30

CORRELATION COEFFICIENTS WITH SIGNIFICANCE LEVELS BETTER THAN 0.1% HAVE BEEN UNDERLINED

5.0. DISCUSSION

5.1. Introduction

For the purposes of convenience this section is subdivided into two main parts: that concerned with examination of mechanical properties and their relationship to press formability and a further section in which an analysis of the stress-strain data together with its relationship to press formability is considered.

5.2. The Effect of Austenite Stability on the Formation of α' Martensite

When comparing relative mechanical properties obtained from steels of different austenite stability, it is essential to know what degree of deformation is necessary to initiate the formation of α' martensite since its presence would obviously be expected to alter these properties. The strain levels at which its formation was initially detected by magnetic measurements are shown with respect to austenite stability in Fig.5.1. α' martensite is formed immediately deformation begins for a steel with an austenite stability of about - 5.3 and presumably steels with values more negative than this, with similar heat treatment histories, would contain this phase in the as quenched product, although it can still be retarded by numerous means including the use of high austenitising temperatures and faster rates of cooling. Not only does the α' martensite phase form at higher strain levels with increasing austenite stability, but from the results given in Section 4.2, the amount of martensite formed with continued deformation, decreases with increasing austenite stability. Solute additions affect the formation of martensite in two ways. They alter the inherent properties of the steel by their very presence and alter the austenite stability of the steel. Separation of these two effects is obviously extremely difficult but the overall effect can be studied from examination of properties with respect to austenite stability.

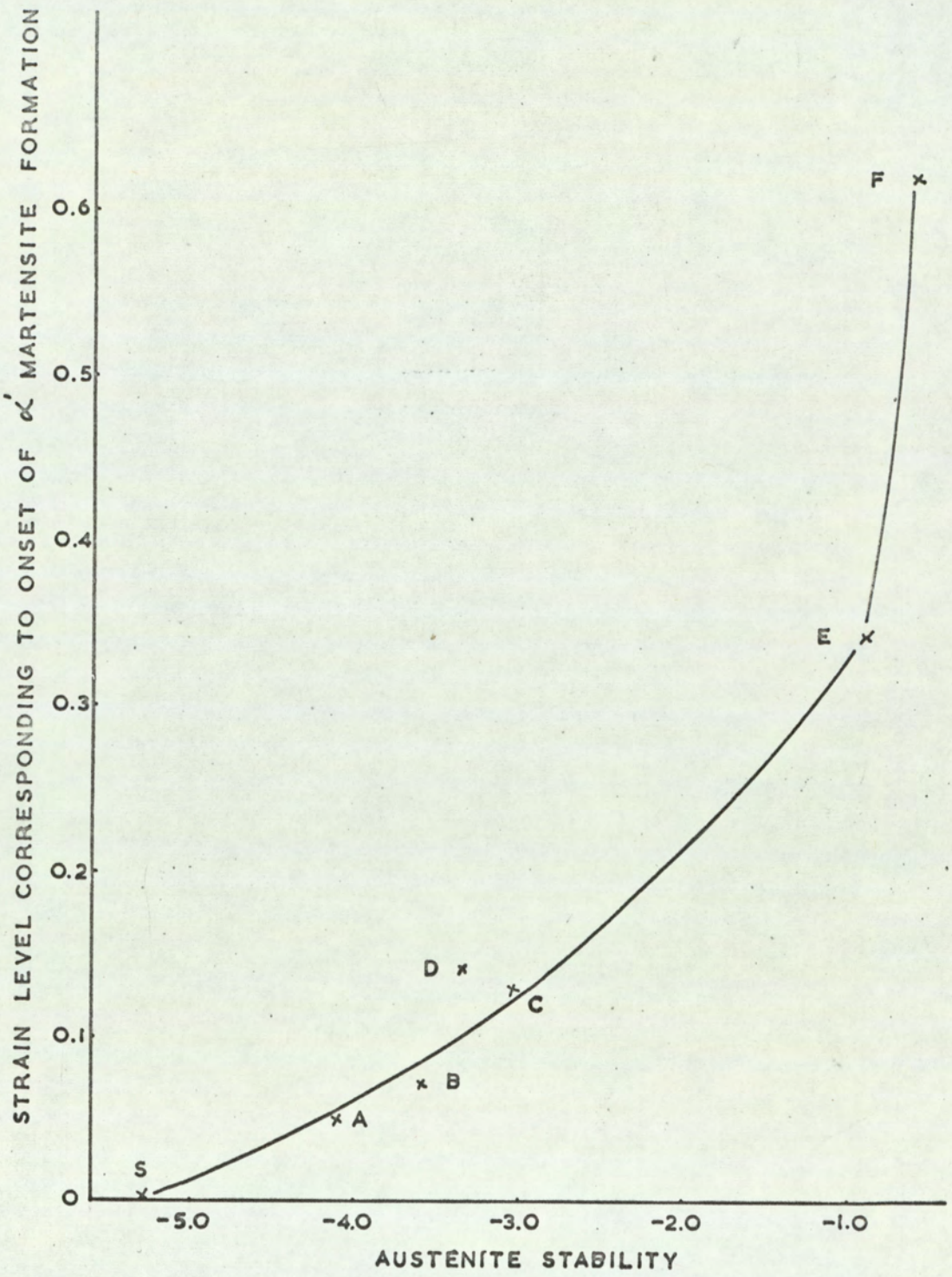

Fig. 5.1. The Strain Level Corresponding to Onset of α' Martensite Formation for the Seven Steels examined.

5.3. The Effect of Austenite Stability on the Mechanical Properties of Stainless Steels

The amount of α' martensite formed by deformation, is reflected in the mechanical properties obtained and the summarised results are shown in Fig.5.2.

Stainless steels do not show a well defined yield point and in order to accurately assess the point corresponding to the initiation of plastic deformation from a Hounsfield tensometer graph, values of 0.5% proof stress were measured. Reference to Fig.5.2 shows that this property varies only to a small degree over a large range of austenite stability. As an approximate measure of the onset of plastic deformation, the 0.5% proof stress would not be expected to show any marked dependence on α' martensite since only a very small volume of this phase would have been nucleated. The graph, however, shows that a minimum value of P.S was obtained for a stability of - 3.0. At lower stabilities, increase in proof stress results from the small amount of α' martensite formed, while at high stabilities an increase in this value, and therefore yield stress, arises as a direct result of solute hardening additions.

For the mechanical properties dependent on large deformations, the formation of α' martensite has an increased effect. Again Fig.5.2. shows that a decrease in the austenite stability from 0 to - 3.0 results in only a marginal increase in the U.T.S. of the material but beyond this point, the U.T.S. increases almost linearly at a rate corresponding to approximately ten tons per square inch per unit change in stability. At austenite stabilities more negative than - 6.0 it would be expected that the quenched product would contain increasing amounts of α' martensite. This rate of increase in strength would then diminish. In a similar manner the U.T.S. of the fully austenitic steels remains fairly constant.

Further evidence that reflects these changes is given in the plot of

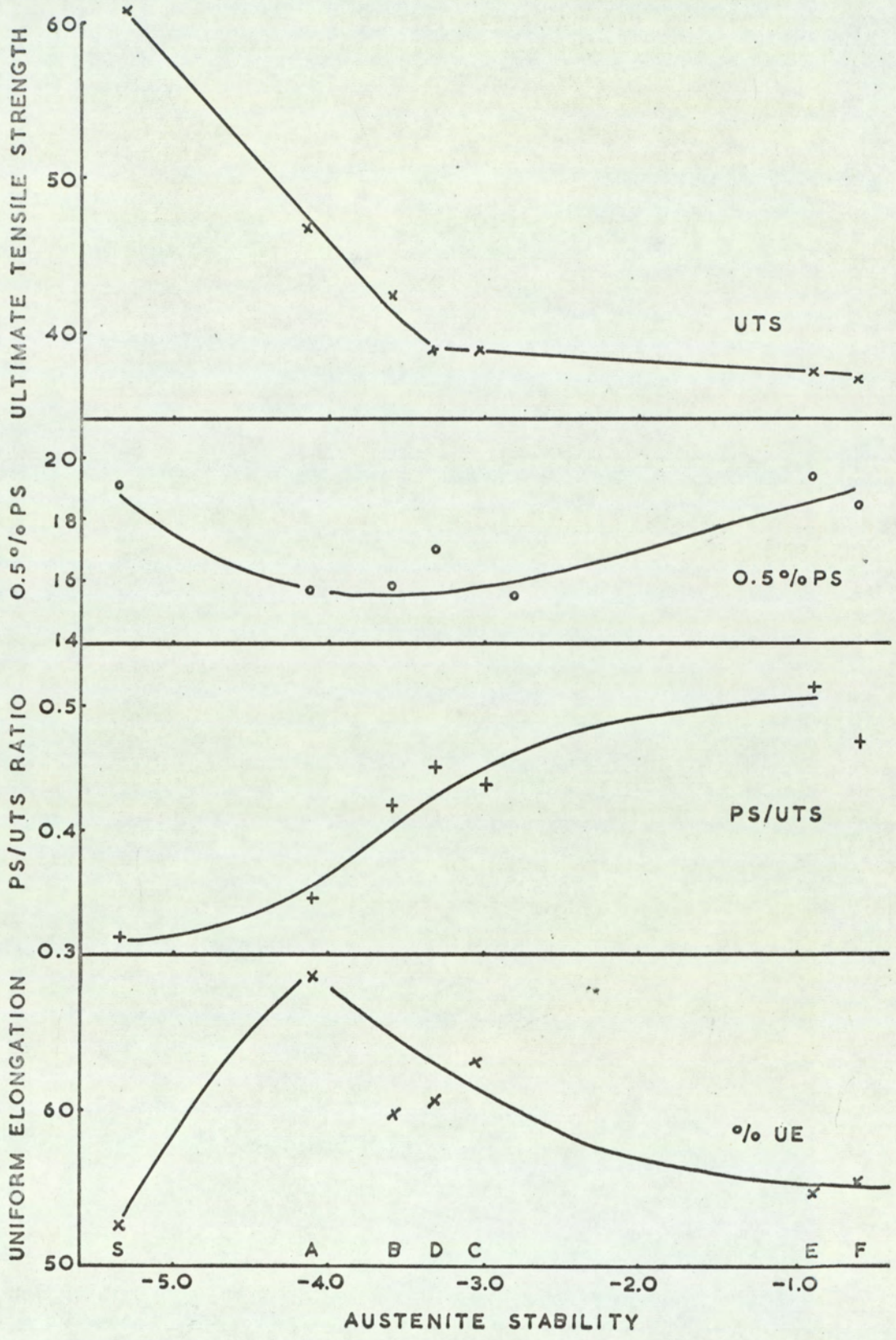

Fig. 5.2. The Summarised Tensile Test Results.

of 0.5% proof stress/U.T.S. ratio against austenite stability. There is a general increase in this ratio with increase in austenite stability. At low stabilities the U.T.S. is increased at a faster rate than is the proof stress value and the ratio of these two properties therefore stays correspondingly low. At the other end of the stability scale, the proof stress value is increased, with deformation, nearer to the U.T.S. value so that their ratio approaches unity.

Bressanelli and Moskowitz[14] have shown that, over the limited range studied in their investigation, that α' martensite formation was beneficial to elongation and that it was most effective for steels of intermediate stability. The reasons offered were that its formation was only beneficial during the final stages of necking and that its presence greatly reduced localised necking. Massive transformation to martensite at strain levels prior to the onset of instability resulted in a decrease in elongation. They also demonstrated the effect of testing speed. For testing speeds employed in this investigation the relationship between elongation and austenite stability is also given in Fig.5.2. The results now reported for a greater range of compositions, confirm those obtained by Bressanelli and Moskowitz but further directly relate this peak in uniform elongation to austenite stability and thereby composition. An almost identical curve to that for uniform elongation was obtained for total elongation. The two curves diverged to a greater degree with increase in austenite stability indicating more local necking in the stable material.

Finally, it is interesting to note that for stainless steels, original hardness prior to testing, corresponded better with proof stress than U.T.S. their respective correlations being 0.93 and 0.79.

5.4. The Relationship between Stretch Formability and Austenite Stability

Stretch formability, as measured by the Erichsen cupping test, can be seen, Fig.5.3(a) to increase almost linearly with decrease in austenite stability. Although stretch formability for most materials is strongly related

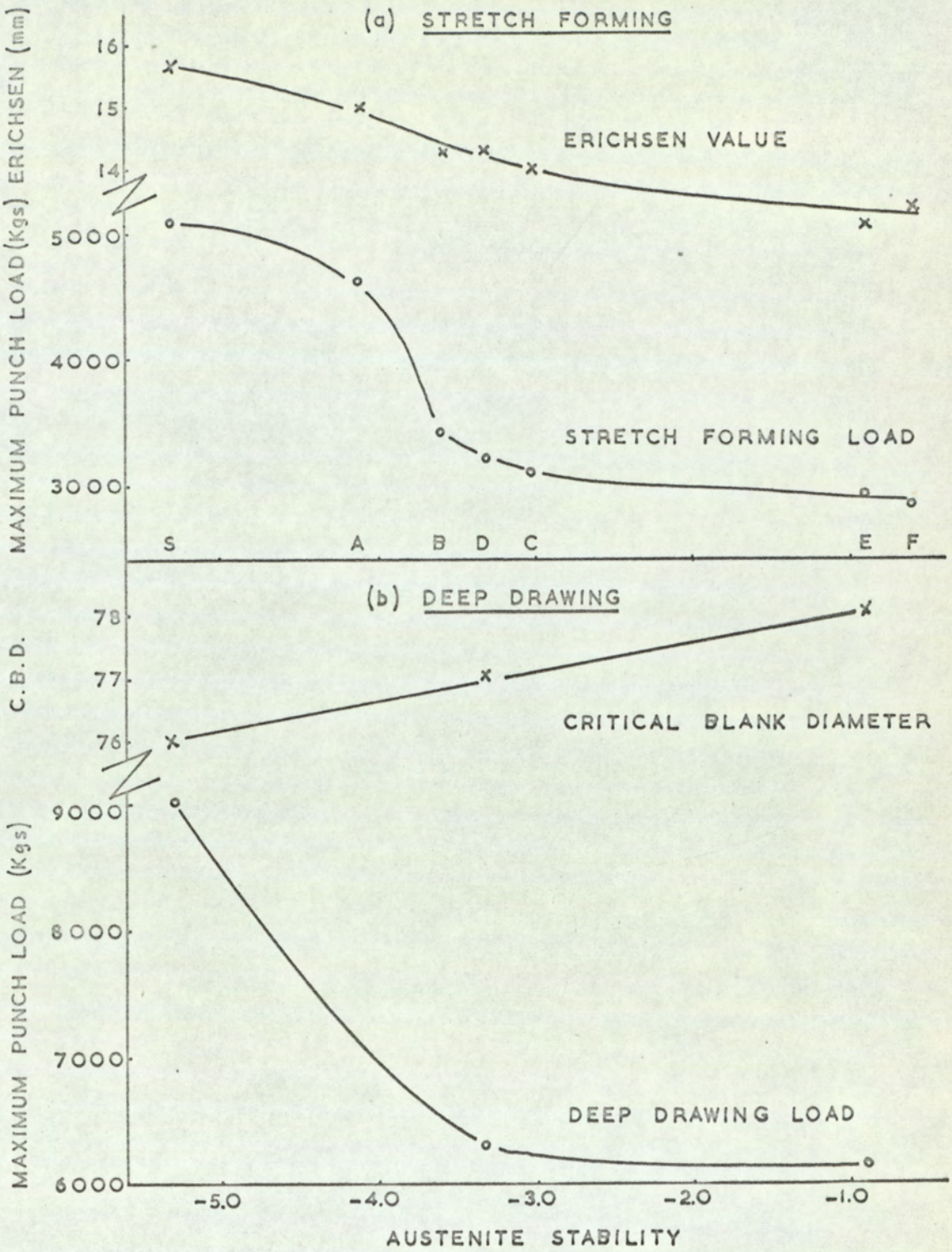

Fig. 5.3. The Summarised Press Forming Results.

to values of uniform elongation, and it is not expected that stainless steels are very different, it is obvious from comparison of Figures 5.2 and 5.3(a) that other factors must also affect this property. The elongation of steel S is inferior to that of steel A and yet its stretch formability is slightly higher. Under conditions of biaxial stress, as exist in this operation, the formation of α' martensite must play a greater part in minimising the effect of localised necking. Although the formation of α' martensite is not directly reflected in the Erichsen values obtained, its effect is apparent when the maximum punch loads are considered. (Fig.5.3(a). Maximum punch loads increase with decrease in austenite stability. The relationship obtained consists of a two stage curve that can be considered to be joined at a level of stability corresponding to the point of transition between transformable and non-transformable steels. At this point, corresponding to a Δ value of approximately -3.0, a rapid increase in maximum punch load is achieved. A similar relationship to that of punch load, for the area beneath the punch load/travel curves, obtained in stretch forming, and austenite stability was also obtained. Area measurements were taken in order to assess the power requirements necessary to form the material. The values of areas quoted in Section 4.4 can be expressed as work done in units of Kgmm, by multiplying by the factor 8264.

By expressing the above stretch forming results with respect to austenite stability, it should be possible to obtain some degree of material and production control from material composition.

5.5. The Relationship between Deep Drawability and Austenite Stability

Material properties for improved drawability are in opposition to those required for stretch forming. Examination of Fig.5.3(b) shows that, although improvement is only slight, there is a definite increase in critical blank diameter with increase in austenite stability. Again, as with stretch forming, uniform elongation is not the controlling factor since elongation

decreased in the order D, E and S. For mild steel normal anisotropy has been found to be strongly related to the L.D.R. The values of normal anisotropy obtained for steels S, D and E varied only from 0.9 to 0.95 and it is considered that such a small variation would not completely account for an increase in critical blank diameter from 76 mm to 78 mm. This point will be discussed more fully in a later section. Exploratory deep drawing trials suggested, however, that austenites of low stability resisted bending and unbending round a sharp die entry radius and that the effect was manifest in increasing the drawing load, Fig.5.3(b). This increase in drawing load is associated with lower values of uniform elongation in metastable steels. The combination of these two properties would therefore be expected to yield cups of a smaller critical size by increasing :- (a) the degree of thinning over the punch nose and (b) the degree of localised necking that occurs in the unsupported material between the punch nose radius and the cup wall.

5.6. The Effect of Prior Deformation on the Mechanical Properties of Stainless Steel

Deformation of metastable austenites is known to increase strength properties by deformation of the parent matrix and also as a result of the formation of α' martensite. An attempt has therefore been made, by studying a range of steels of varying austenite stabilities, to isolate these two effects. The effect of prior deformation on ultimate tensile strength and 0.5% proof stress is shown in Fig.5.4. If these curves are analysed it can be seen that up to values of 40% prior deformation the value of U.T.S. increases almost linearly and that for steel S, the rate of strength increase in units of tons per sq.in. per cent prior deformation is approximately 1.15 and that for steels D and E the rate is 0.7 and 0.63 respectively. The differences in these rates between steel S and the two virtually non-transformable steels must therefore be equivalent to the effect of the formation of α' martensite. The two differences are 0.45 and 0.52 respectively. The rate of increase in strength

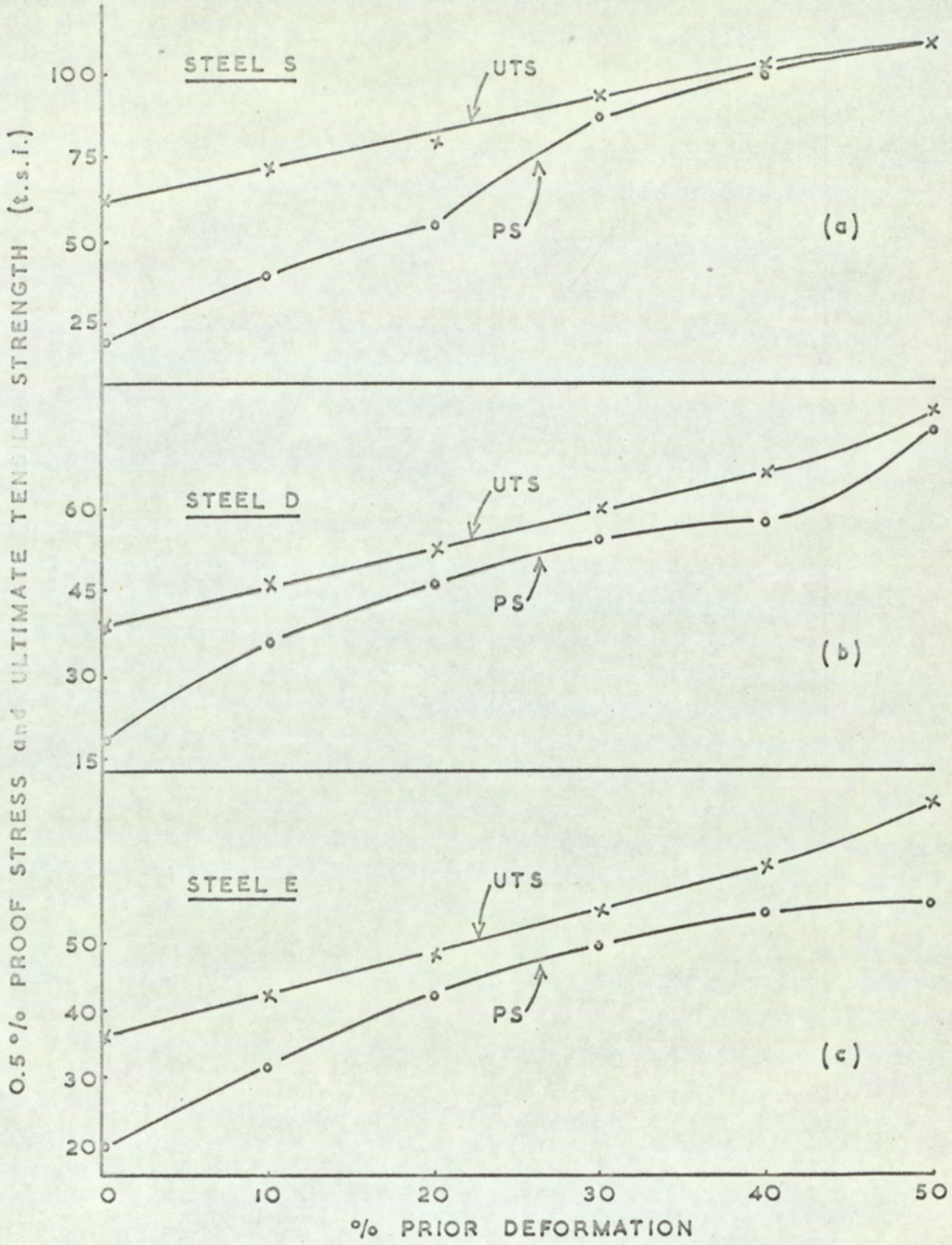

Fig. 5.4. The Effect of Prior Deformation on the Values of Proof Stress and Ultimate Tensile Strength.

decreases for steel S between 40 and 50% prior deformation and it is suggested that this is due to the lack of remaining austenite for transformation. A value of 40% corresponds to the strain level at which a decrease in the rate of magnetic response was recorded for this steel, (Section 4.2). On the other hand, results from the same section indicate that steels D and E do not transform with deformations less than 40%. Figs.5.4(b) and 5.4(c) show an increase in the rate of strengthening for steels D and E, only after prior deformations of 40%. The U.T.S. of steel D after 50% prior cold work is 5 tons greater than it would have been if strengthening had continued at the rate that existed over the initial level of prior deformation, and that for steel E is 4 tons greater.

With increased amounts of prior cold work, the proof stress approaches the value of the U.T.S. and is an obvious consequence of diminished ductility. The onset of α' martensite formation is again evident in these curves. Steel D shows an additional increase in both U.T.S. and proof stress after 40% prior cold work and steel E a similar increase for U.T.S. The strain levels corresponding to α' martensite formation for steel E must therefore be only just in excess of 40%. Measurement of proof stress could therefore be made prior to its formation but continued straining would result in α' martensite forming during testing and its presence would therefore be reflected in the value of U.T.S.

The ratio of proof stress to ultimate tensile strength has been used by industry as a parameter for quality control in press forming of sheet. Knight[67] suggests that for certain mild steels, good press runs were associated with values of this ratio of between 0.6 and 0.65. For the cold worked material reported here, both stretch formability and deep drawability decreased with increase in this ratio so that for any given steel it would be correct to say that press formability was at a maximum when this ratio was a minimum. In fact, stretch formability and the ratio of PS/UTS gave a negative correlation of - 0.84

and for deep drawability one of - 0.71. Considering the annealed conditions only, stretch formability and deep drawability required different values of this ratio in that a maximum value of the former was associated with a minimum PS/UTS ratio and that maximum deep drawability was obtained in the steel exhibiting the largest value of proof stress/UTS ratio. It is obvious that such a ratio would be unsuitable as a means of production control for stainless steel.

The effect of prior deformation on the property of uniform elongation (total elongation to fracture values followed a similar trend) is shown in Fig.5.5. An initial decrease in this value appears to be almost linear, the rate of decrease being less for steel E than for either D or S. There is, however, a marked arrest in the rate of decrease for steel S at approximately 10% prior deformation. This arrest shows the beneficial behaviour in α' martensite in increasing the effective value of elongation.

5.7. The Effect of Prior Deformation on the Stretch Formability of Stainless Steel

The effect of prior deformation on both the Erichsen values and the maximum punch loads obtained in deriving these values, has been combined in Fig.5.6. If the materials in their annealed condition are considered, the low stability steel shows better values of stretch formability, but this tendency is reversed with only 10% prior cold work. Beyond this point, the stretch formability of steel E became progressively better than the steels of lower stability. In contrast the power requirements, as measured by the maximum stretch forming loads, increase with austenite stability. This has already been demonstrated. It is interesting to note that the ratio of maximum punch load for steel S to a mean value of maximum punch load for steels D and E does not vary greatly either with (a) depth of penetration or (b) prior deformation up to 30%. For any given depth of penetration this ratio is fairly constant for approximately 1.5. It can therefore be assumed that 30% of the total load requirement, for steel S, is necessary to overcome the

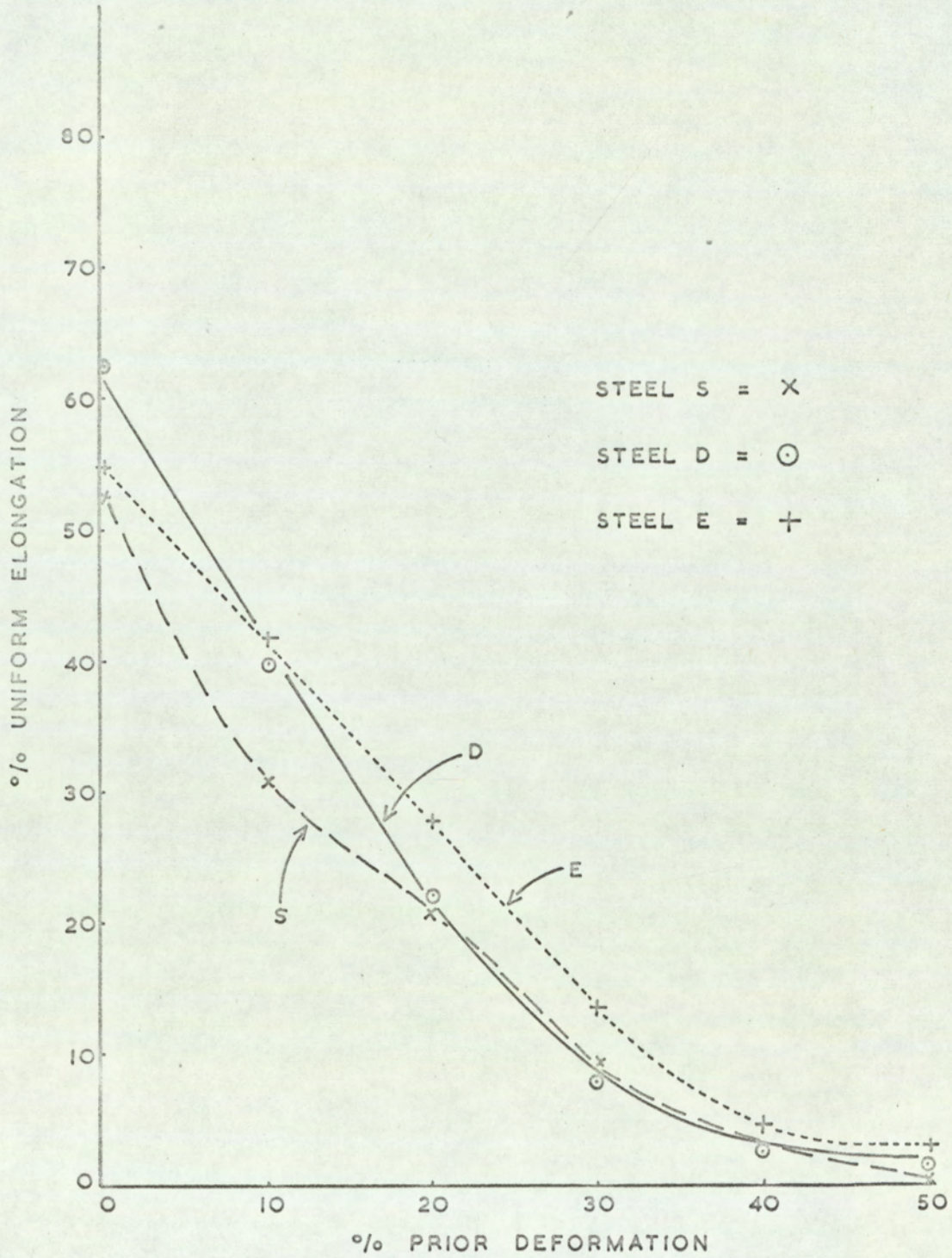

Fig. 5.5. The Effect of Prior Deformation on the Value of Uniform Elongation.

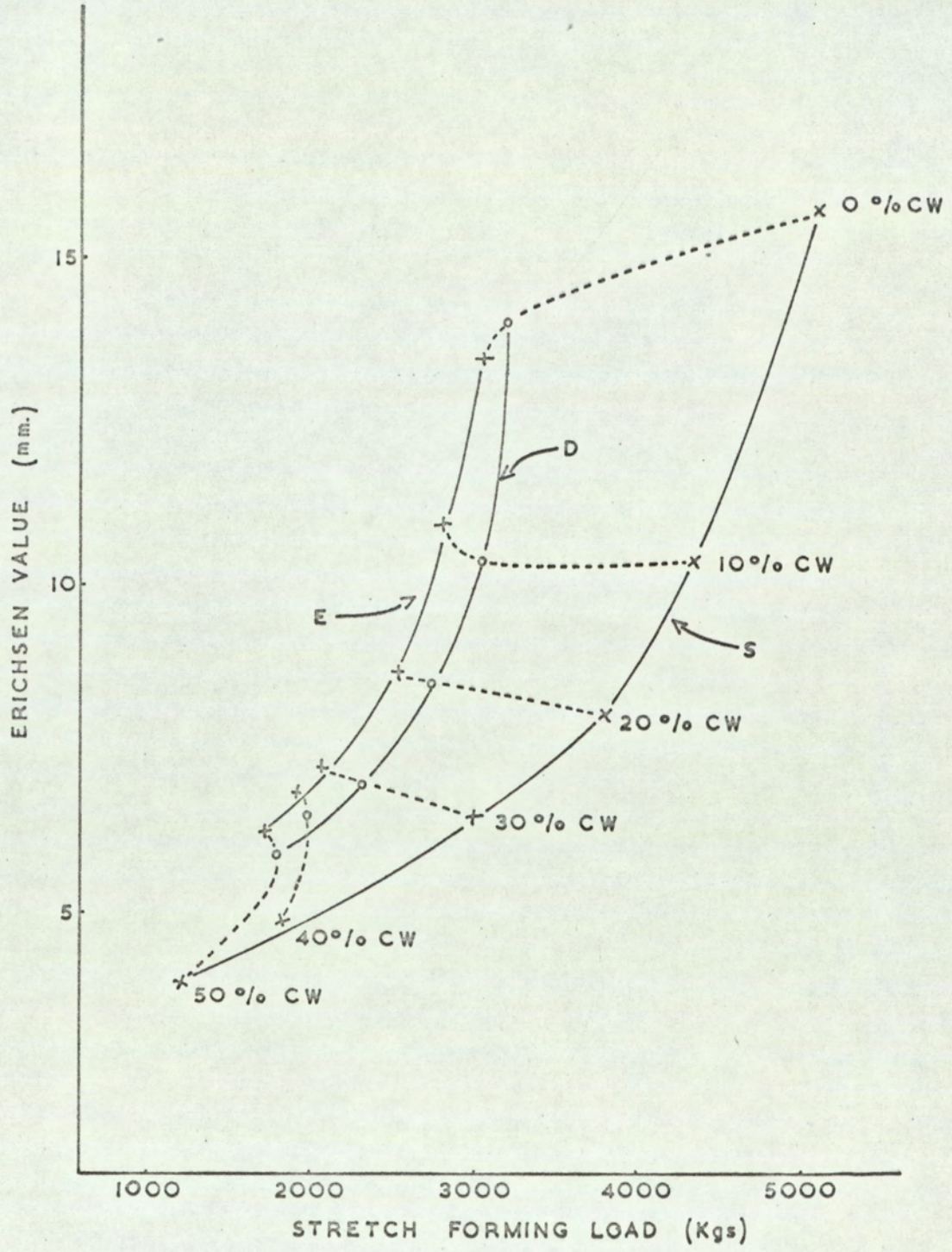

Fig. 5.6. The Effect of Prior Deformation on Stretch Formability.

formation and presence of α' martensite.

5.8. The Effect of Prior Deformation on the Deep Drawability of Stainless Steel

As with stretch formability, the deep drawing results have been related to both prior deformation and maximum drawing load, Fig.5.7. With one minor exception, the deep drawing behaviour of the steels studied was detrimentally affected by increasing cold work. The exception, was that steel S exhibited the same critical blank diameter after 10% cold work as that obtained in the annealed condition. The maximum punch load was, however, some 18% larger. It is again suggested that martensite formation was beneficial in reducing the amount of thinning strain within the cup wall. This fact will be substantiated when the distribution of strain within the cup is discussed in a later section. Similarly after reductions of 20%, the critical blank diameter for steel S was greater than that of the two other steels and although values of uniform elongation were less for the steel in this condition, the presence of α' martensite was still beneficial in resisting the onset of plastic instability. Reference to Fig.5.5, indicates that for further cold reductions the available ductility decreased to less than 10% and as a result, together with the large drawing loads required, drawability is greatly reduced, so much so that it was found impossible to obtain deep drawn cups for steel S after prior cold rolling reductions greater than 40%. Fig.5.8 shows the results of attempting to draw cups in such a condition. After 30% reduction it would seem that steel D begins to benefit from the formation of α' martensite (this occurs with steel D at approximately 40%: 30% of which would have been induced by prior deformation and the remaining deformation necessary would be obtained actually whilst drawing). Even after 50% prior cold work, steels D and E, which only had uniform elongations of between 3 and 4% in this condition, were still capable of being deep drawn into cups of 67 mm.

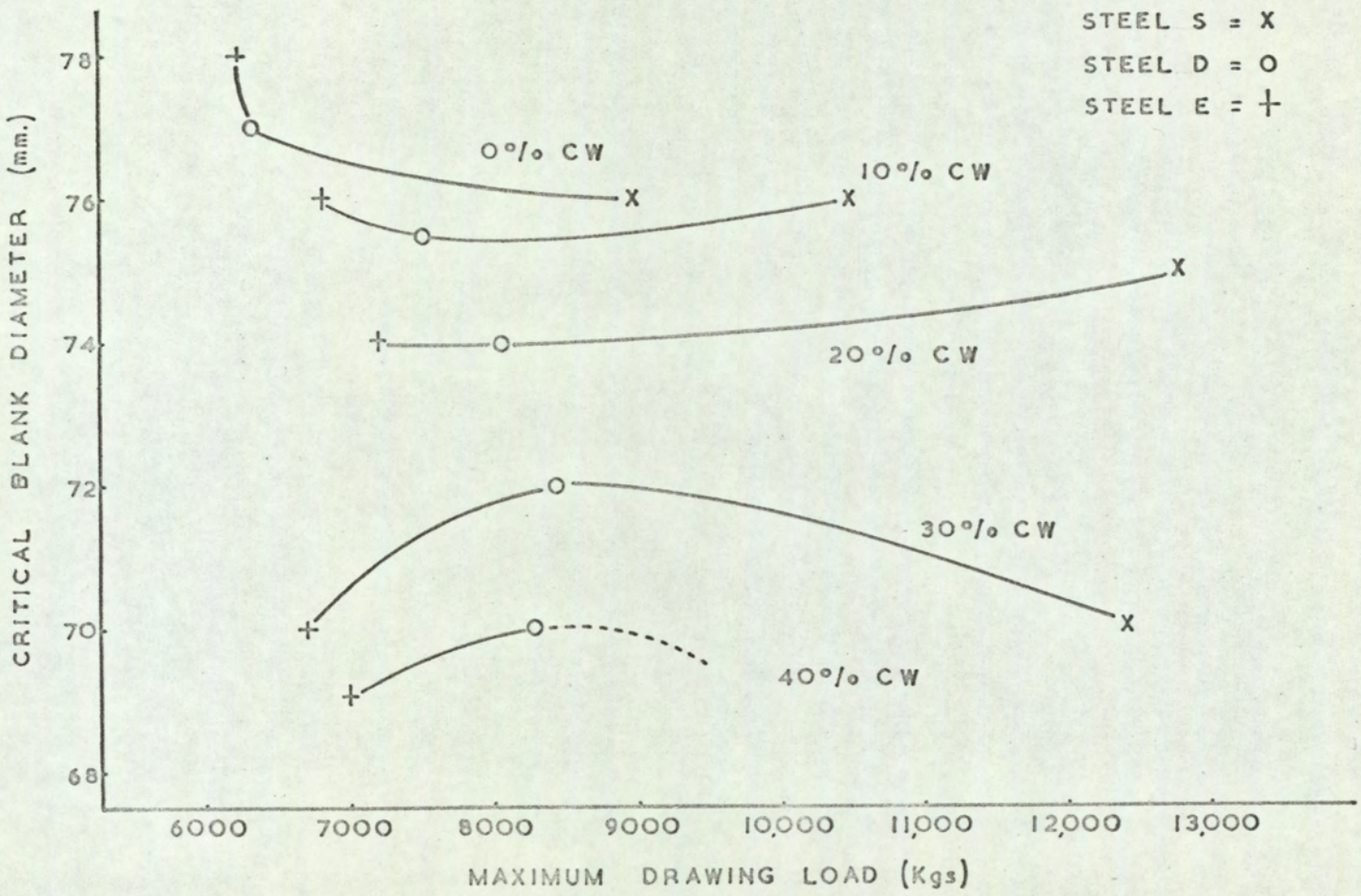

Fig. 5.7. The Effect of Prior Deformation on Deep Drawability.

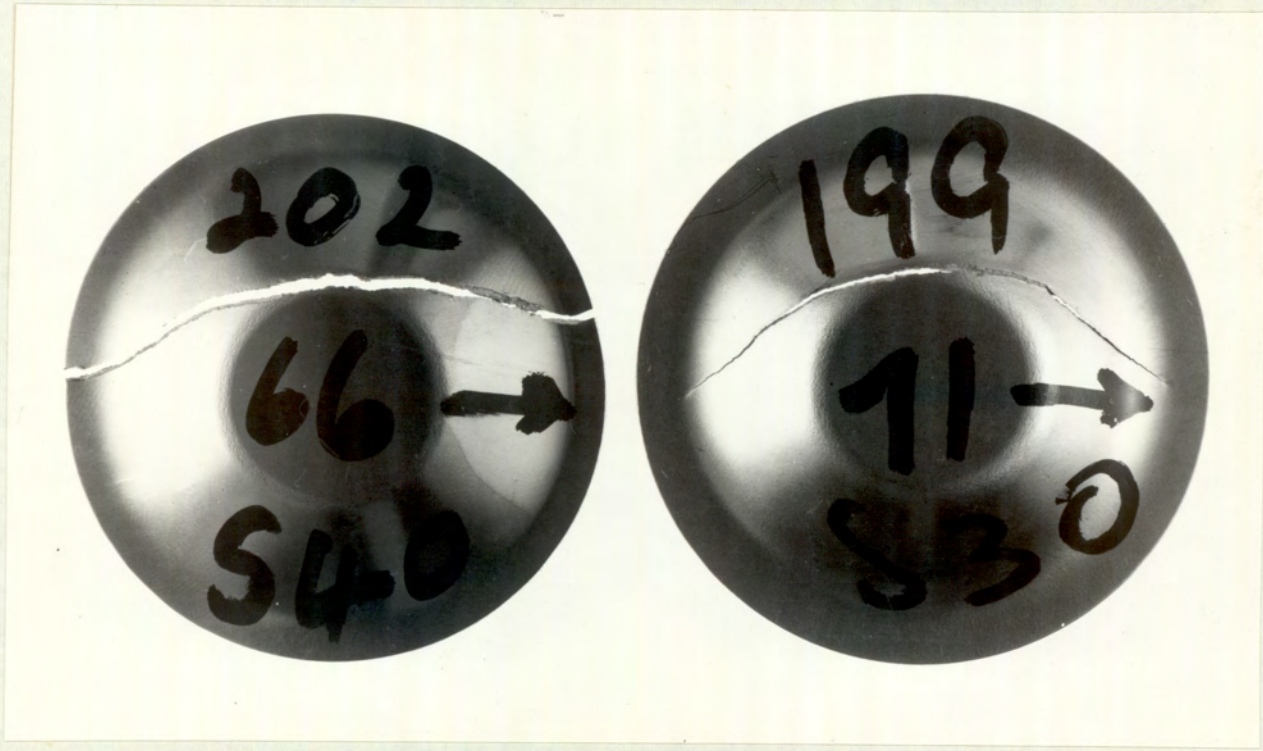

Fig. 5.8. The Results of Attempting to Draw Steel S after 30 and 40% Prior Cold Work.

5.9. The Relationship between Plastic Anisotropy and Press Formability

5.9.1. Planar Anisotropy

In the annealed conditions, the alloys studied showed that planar anisotropy increased with austenite stability. Since the original texture in sheet material, ex-works, would be extremely difficult to explain, even if an accurate knowledge of its history were available, it is intended to comment only on the effects of prior deformation and the resultant effect on the earing characteristics obtained.

The progressive development of rolling texture in f.c.c. metals, starting with a random slab, has been considered in detail by Dillamore and Roberts.[68] For stable austenitic materials it would be expected that a "Rolling-type texture" would be developed and as a result, earing in drawn cups would predominate at 45° to the rolling direction. Examination of Fig.5.9. shows that for steels D and E for the cold work conditions, earing occurs at 45° to the rolling direction. For steel S (it was only possible to obtain cups at 67 mm from material deformed up to 20%), earing occured at 0° and 90° to the rolling direction.

Deformation of steel S, produces the body centred structure, α' martensite, so that in opposition to the development of the f.c.c. rolling texture, a texture resultant from the formation of α' martensite would also form. Fig.5.10 shows the textures obtained for both $\{111\}_\gamma$ and $\{110\}_{\alpha'}$ pole figures for steel A. Although earing measurements were not carried out on this steel, the results are included to demonstrate the effect of the austenite-martensite transformation on the type of texture developed. Even after low deformations the $\{111\}_\gamma$ pole figure texture is of the "pure metal type" and quite strongly developed. Increased deformation results, however, in the intensity of this reflection becoming diminished. If on the other hand the $\{110\}_{\alpha'}$ pole figure intensities are considered it can be seen that these values increase with deformation. Referring again to steel S, it

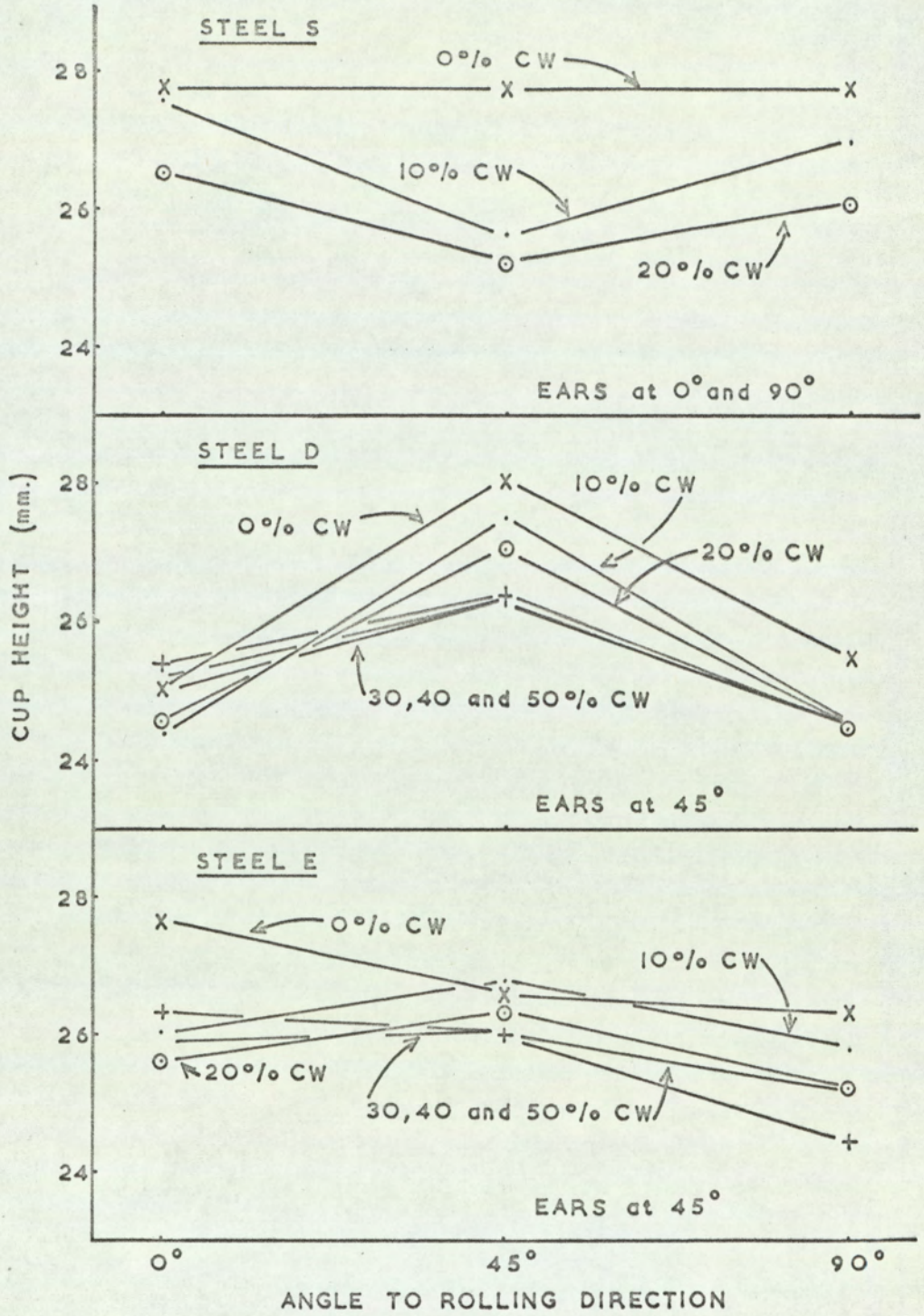

Fig. 5.9. R Value Variations at Different Angles to the Rolling Direction.

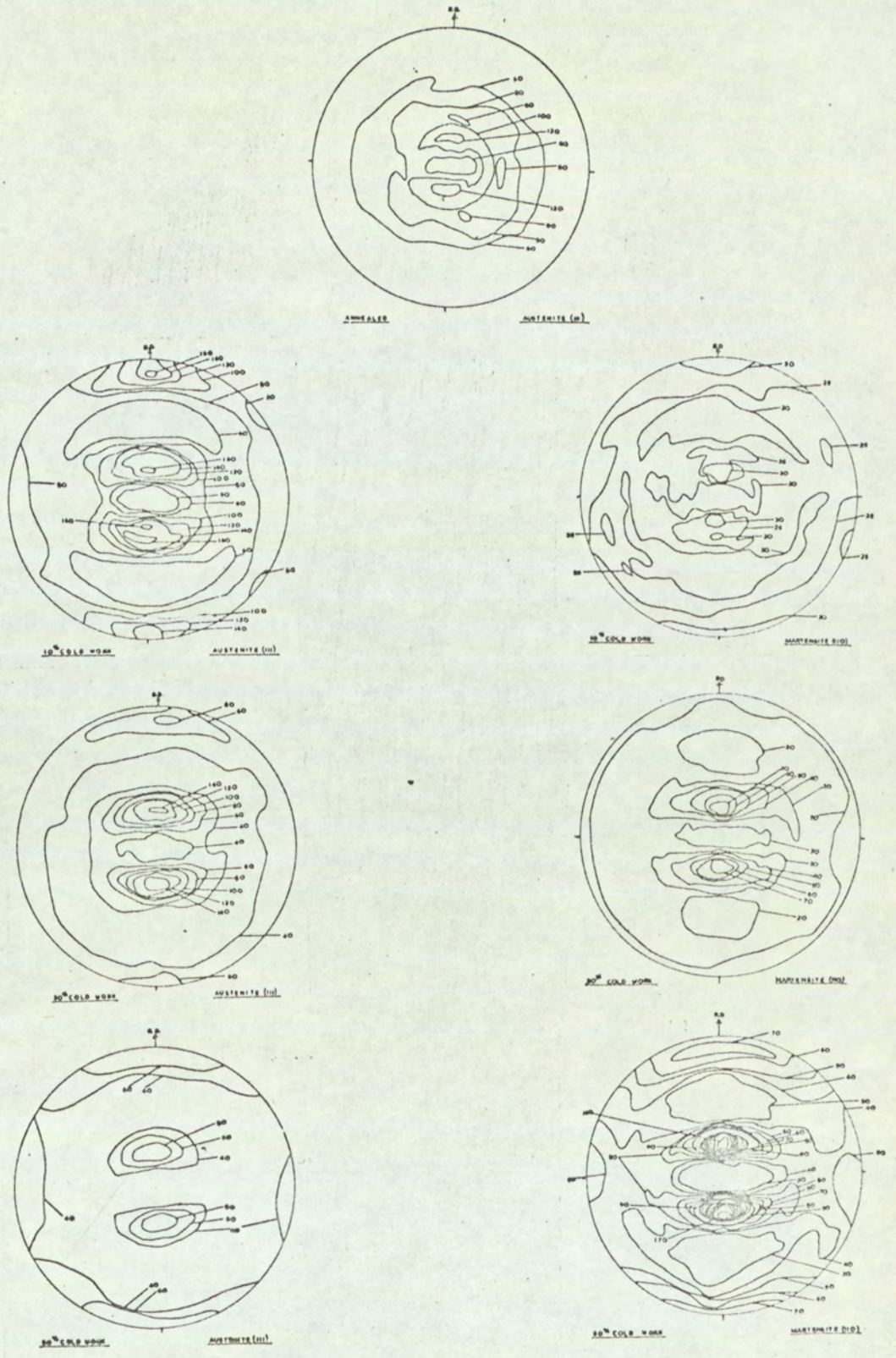

Fig. 5.10. {111} and {110} Pole Figures on Steel A in Different Degrees of Prior Deformation.

is probable that for deformations of up to 20%, a mixture of the two types of texture would be obtained. These results have been confirmed by Dixon[69] who shows a similar effect with a pure 18/10 type alloy which by comparison to a commercial alloy would be equivalent to the common 18/8 type, of which steel A is an example.

At low values of prior deformation (20%), it is difficult to state that earing in the case of steel S, is texture dependent but obviously the formation of α' martensite must considerably influence its development. It is also not known to what extent earing response is affected by prior deformation or by deformation that occurs during the drawing operation. It is likely however, that prior deformation is the more important factor since earing is evident at an early stage in the drawing operation. Possibly the technique of inverse pole figure determination would lead to a better understanding of the situation, particularly for weakly defined textures.

If it is assumed that, for standardised drawing conditions, including that of blank diameter, there should be little variation in percentage earing for stainless steels, then the results obtained for steel E are satisfactory. For steel D, per cent earing is fairly constant up to 30% prior deformation, which together with the deformation associated with the drawing operation, would initiate α' martensite. This, as has been pointed out would reduce the magnitude of earing. The general level of earing is higher for steel D than either S or E and could be explained by a higher level of retained "rolling texture" in the annealed sheet. This is implied from earing measurements. For steel S the onset of α' martensite formation and the subsequent formation of a "duplex texture" is manifest at much lower strain levels.

In general, no satisfactory relationship has yet been devised to assess earing behaviour from studies of preferred orientation in commercial polycrystalline sheets. The problem is particularly difficult for ill-defined textures such as exists with normal commercial material. As an alternative

method, attempts have been made to relate earing with R value variations in the plane of the sheet. Baldwin, Howald and Ross[70] working with copper, noted that ears formed in the radial direction of maximum R value and that the ear height was approximately proportional to (R 0, 90 - R 45). Wilson and Butler[42] have subsequently shown that ears formed in the tangential direction of maximum R value. For two of the three steels examined in this investigation neither of these conditions applied although for steel S, the transformable steel, ears coincided with the tangential or circumferential direction of maximum R value. Wilson and Butler further showed that by substituting the proportionate variation in R value, $\frac{(R\,0,\ 90 - R\,45)}{\bar{R}}$, the relationship with percentage ear height could be extended to include steel and aluminium in addition to that of copper. Using this relationship values have been calculated for stainless steels in different conditions of cold work and the results plotted in Fig.5.11. The results are not very encouraging when all the data are plotted together but for the annealed conditions only, a reasonable straight line relationship exists. It is interesting to note that for steel S, in which the tangential model applies the results give a better fit using the formula proposed by Baldwin et al and that with radial conditions, steels D and E, the relationship is marginally better satisfied with the formula by Wilson and Butler.

5.9.2. Normal Anisotropy

There is now a considerable amount of published data quantitatively relating the drawing performance of a flat bottomed cup to normal plastic anisotropy. A graph derived by Whitely and Lloyd has already been shown in Section 2.12. Stainless steels with $\bar{R}$ values of approximately 1.0, in general agree with the relationship given by Whiteley. It would be expected, however, that transformation would affect actual measurement of this parameter.

The values of $\bar{R}$ obtained in this investigation were 0.95, 0.92 and

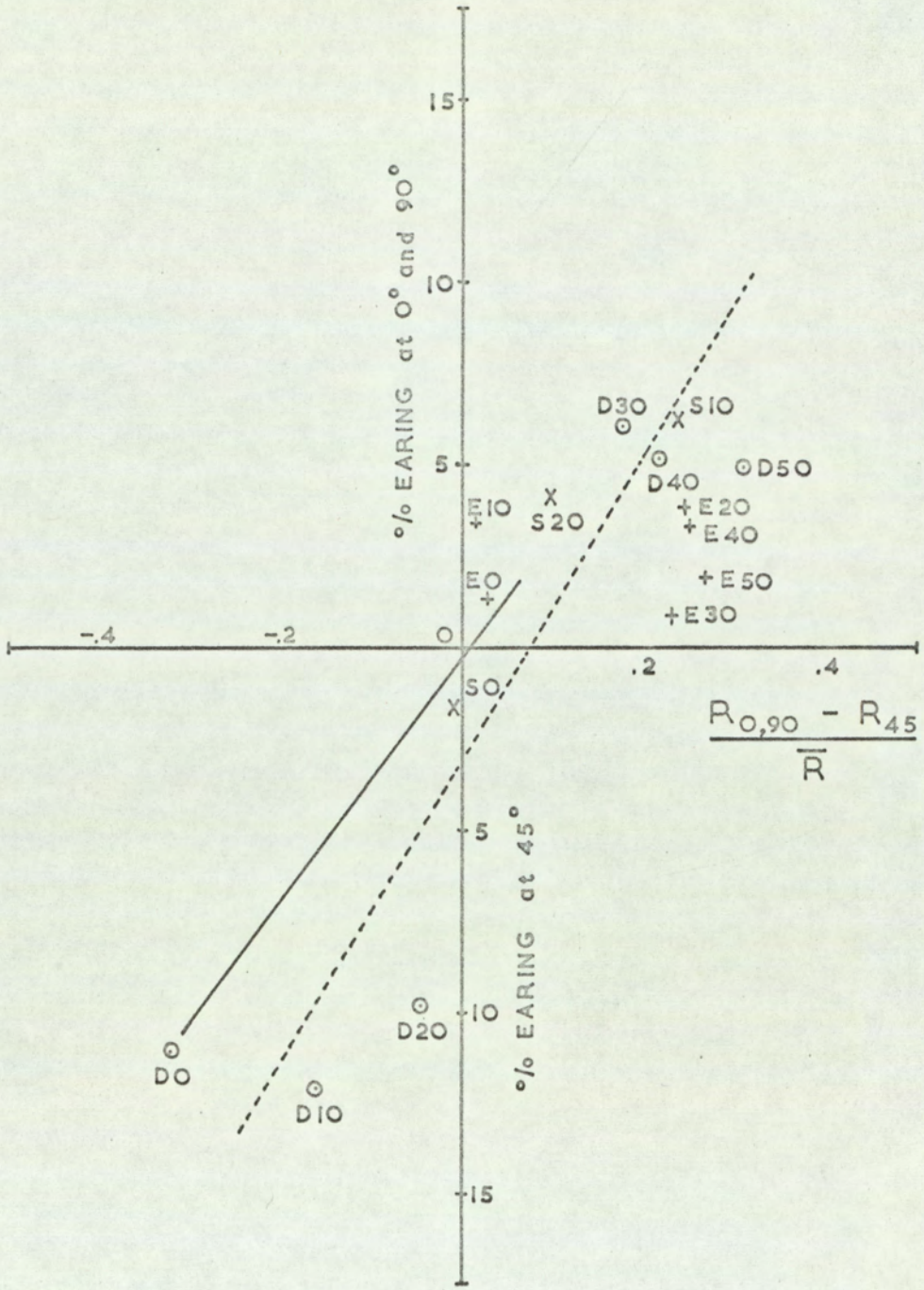

Fig. 5.11. Proportionate Variation in R Value versus Percentage Earing for Steels S, D and E in all Conditions of Cold Work.

0.9 for steels E, D and S respectively, in the annealed condition. During tensile testing it was found that α' martensite, depending on the amount formed, affected the individual measurements of length, width and thickness in different ways. Length measurements were approximately 3.0% less than they would have been had transformation not occured, width approximately 6% greater and thickness measurements also greater by about 3%. If these volume expansions and contractions which result from the production of α' martensite during tensile testing are taken into account, it is interesting to see to what extent they affect calculation of $\bar{R}$ values. Using actual values obtained with steel E after 20% strain it was found that if a similar degree of transformation had occurred to that of steel S, then a reduction in $\bar{R}$ value of between 0.05 and 0.07 would result. Although the effect is only small, it is nevertheless the magnitude of difference that exists between the values obtained for steel E and steel S.

Increase in prior deformation resulted, apart from the one exception already mentioned, in a general decrease in L.D.R. although steel D up to 40% prior deformation and steel E in all conditions gave increased values of $\bar{R}$. Steel S showed a progressive decrease in $\bar{R}$ value with cold work. It would seem apparent therefore that α' martensite formation affects the $\bar{R}$ value (steel S in all conditions and steel D at deformations in excess of 40%). For all the steels examined, it must therefore be concluded that the strong relationship that exists between L.D.R. and $\bar{R}$ value does not similarly exist for stainless steels.

Atkinson[52] has modified the Whiteley relationship between L.D.R. and $\bar{R}$ value by plotting these values on a log-log basis. The L.D.R. values obtained in the present work lie above the curve given by Atkinson and the use of polythene sheet as a lubricant and a Swift die with the increased die entry radius probably account for this improved drawability.

Pearce,[39] in considering the effect of $\bar{R}$ value on stretch formability

states that increasing the $\bar{R}$ value produces decreasing values of e_f or fracture strain ($e_f = \frac{to - tx}{to}$) where tx was the thickness of material at fracture. As has already been mentioned, it is considered that this value is another way of expressing $\bar{R}$ and therefore the results obtained by Pearce would have been predictable. Other workers,[71] however, encourage the view that a high $\bar{R}$ value will tend to increase the deformation by biaxial stretching, provided that other properties remain unchanged. It is likely that work hardening behaviour would influence this condition of stretching to a greater degree than the R value and evidence will be offered to support this view.

In general, it is not surprising that for both stretch forming and deep drawing of the cold worked materials the correlations obtained with $\bar{R}$ were not significant, i.e. - 0.12 and - 0.32 respectively.

5.10. Thickness Strain and Hardness Distribution in Drawn Cups

In a further attempt to clarify why the drawability of steel S had not been impaired by 10% prior deformation and to assess general hardness and strain distribution around the wall of deep drawn cups, these properties were measured on sectioned cups. The results are reported in Section 4.8.

Comparison of the thickness strains for the cups drawn from critical diameter blanks, (Fig.4.9(a)) shows that the degree of localised necking increases with austenite stability. With steels D and E, local necking, which can be seen to decrease with increasing prior cold work, is evident at the point of initial bending over the punch nose radius. With steel S, the degree of necking is less pronounced. It is proposed that during the drawing operation, the formation of α' martensite, inhibits continued deformation in regions that are already highly strained. Deformation therefore proceeds to areas that have received less strain, i.e. to a point further from the pole of the cup. Assuming that failure does not occur, the process is likely to continue until the wall of the cup is drawn into the die, at which time thickening occurs, and the process no longer becomes important.

Thinning over the punch and its radius, while it continues to be uniform, contributes considerably to the maximum size of cup for any given blank diameter. This point is illustrated in Fig. 5.12 in which the mean cup height for cups drawn from 67 mm blanks is plotted against % thinning over the punch nose. As thinning decreases towards zero, the drawn cups, irrespective of composition, approach a common mean cup height of approximately 25.6 mm. It is considered that the inability of steel S, particularly after 30% prior cold work, to form a cup, results from the increased resistance to bending that the steel offers in this condition. It was also considered necessary to examine cups drawn from similar size blanks. The results, (Fig.4.9(b)) show that steel S exhibits greater thinning both at the cup pole and over the punch nose radius. This steel also shows a greater degree of thickening in the cup flange than the less transformable steels. The drawing loads necessary for a steel of this type have been shown to be in excess of those necessary for stable austenite materials and as such the magnitude of the compressive hoop stress must also be assumed to be relatively higher. It has also been demonstrated that transformation to α' martensite is less pronounced in compression, i.e. conditions that exist for flange drawing. It is proposed that the presence of these two conditions would result in a greater amount of thickening within the material of the flange. Furthermore, the stresses necessary to deform material in the flange of the cup increase with decrease in $\bar{R}$ value. This additional fact further suggests that the compressive hoop stress should be larger for steel S than the two other steels. As the $\bar{R}$ value decreases with prior cold work in steel S, so the percentage flange thickness strain should also increase. This is the case.

The hardness (VPN) of the drawn material over the punch nose also reflects considerable transformation to α' martensite. Although the thickness strains only vary between 10 and 16% for the three steels in this region, steels D and E have gained some 25 - 30 hardness points while the hardness of steel S

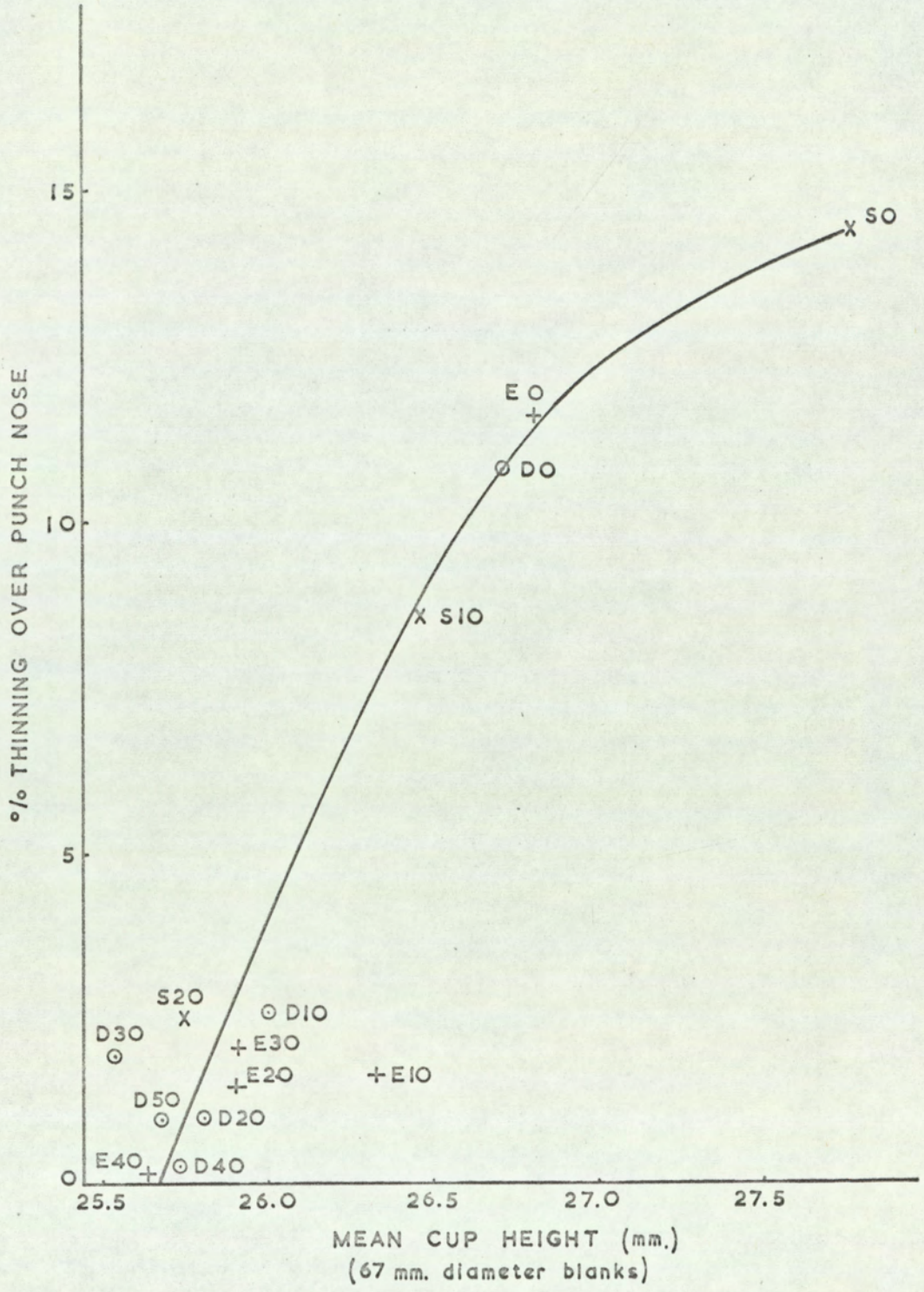

Fig. 5.12. The Relationship between % Thinning over Punch Nose and Mean Cup Height.

has increased by about 140 points. This is reflected in the loads required to draw the different materials. The general shape of these curves has been discussed in the literature[34] but it is interesting to note that the hardness peaks associated with initial bending under conditions of biaxial tension decrease with increasing austenite stability and similarly, the extent of the hardness 'troughs' resulting from the material that originally occupied a position in the press above the punch/die gap also increases. The hardness in the cup flange also decreases with increasing austenite stability.

It has already been shown that stretch formability is highest with unstable austenitic steels. The reason for this can be seen from examination of the thickness strain distribution curves obtained for cups drawn from 67 mm diameter blanks, with the hemispherically nosed punch, (Fig.4.9(c)). In this case steel S exhibits less thinning at the cup pole, there is no region of localised necking and thinning is fairly uniform over a large part of the punch nose radius. Maximum thinning at the cup pole was again obtained with the least transformable steel (E). Steels D and E both show slight decreases in hardness at a position some 15 mm from the cup pole: this position corresponds to an annulus of material that was initially positioned over the punch/die gap. This decrease in hardness does not appear with steel S, the hardness of which increases almost linearly from the position of the cup pole to the outer flange. With the increased drawing loads necessary for this steel, even slight material thinning would initiate α' martensite formation with the associated effect of increasing the hardness.

The influence of tool geometry has also been studied for steel S. Comparison of the curves obtained (Fig.4.9(d)) shows that there is very little difference in the amount of thinning that occurs over the punch nose. They differ only in the fact that thinning, at an almost constant level of 17%, is extended to a greater distance from the cup pole for the flat nosed punch and that thickening in the flange is approximately 10% greater for the round nose

punch. It would appear that the compressive hoop stress created during forming of the flange is greater, and its influence on the cup wall realised at an earlier state in drawing, for the round nose punch than that of the flat.

5.11. Correlation of Mechanical Properties and Press Formability of Stainless Steel

Before discussing the relationships that exist between press formability and mechanical properties it is considered necessary to comment on the relationship between the initial hardness of the material prior to testing and two other properties, namely 0.5% Proof Stress and Uniform Elongation. Both of these relationships demonstrate the effect of α' martensite formation.

Two main correlations were found to exist between stretch formability and mechanical test properties. These mechanical properties were percentage uniform elongation and 0.5% proof stress. In order to understand the rôle of α' martensite formation on stretch formability these two properties are firstly related to initial sheet hardness in Fig.5.13 and 5.14. It was necessary to relate these properties to hardness for two reasons. First, hardness has already been shown to give a good correlation with magnetic response measurements (Fig.4.6) and secondly because steels D and E are non-transformable at low strains, large differences in stretch formability could not have been represented by maghetic response readings.

The graph of uniform elongation against initial hardness shows that for deformation when no transformation to martensite occurs, a linear decrease in uniform elongation is represented by a similar increase in hardness. Transformation effects occur for steel E after 40% prior cold work, after 30% for steel D and almost immediately for steel S. The formation of α' martensite can be seen to diminish the rate of decrease of uniform elongation and at the same time it increases the hardness of the material. The effect of transformation on the more unstable material S

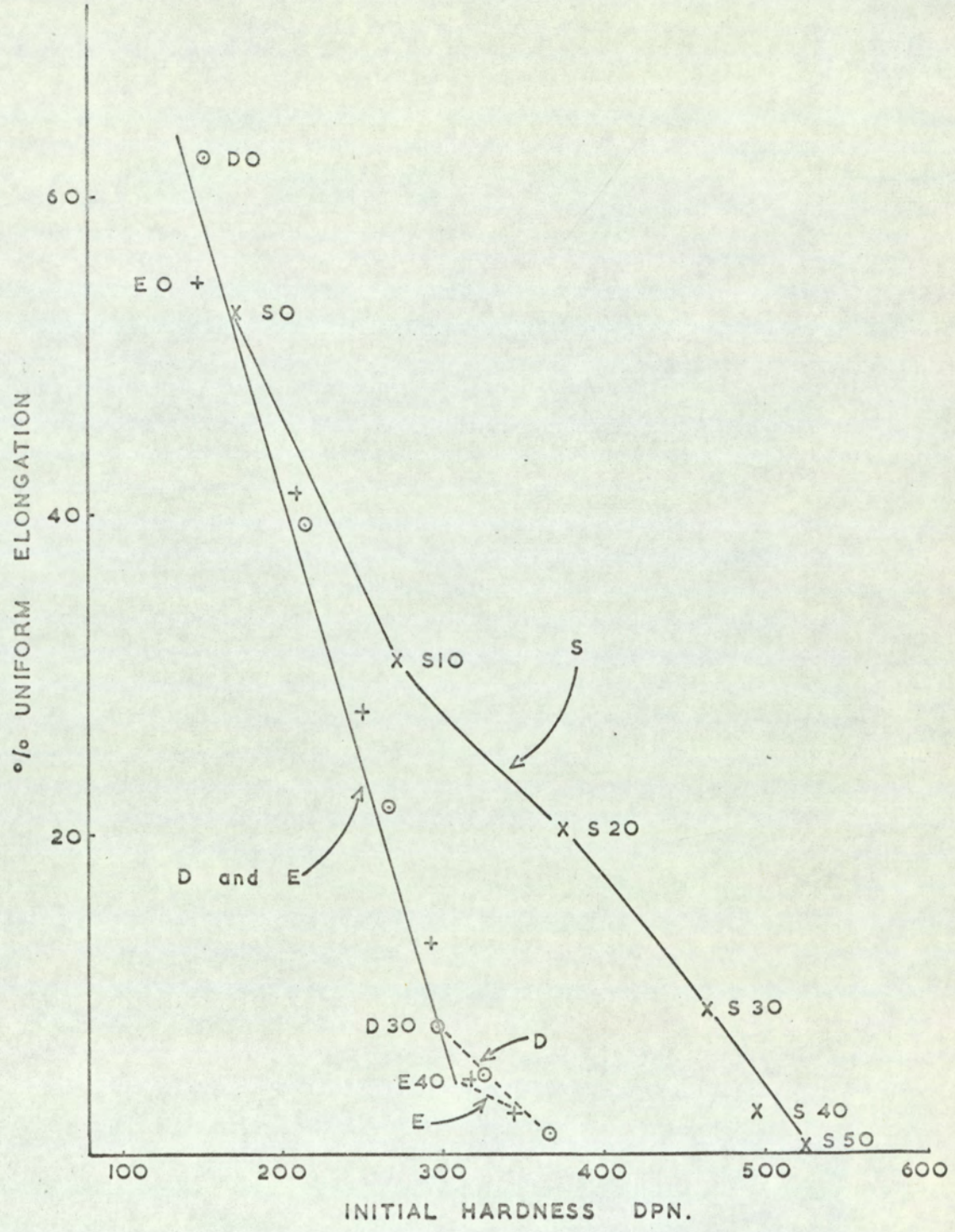

Fig. 5.13. The Relationship between Uniform Elongation and Initial Sheet Hardness.

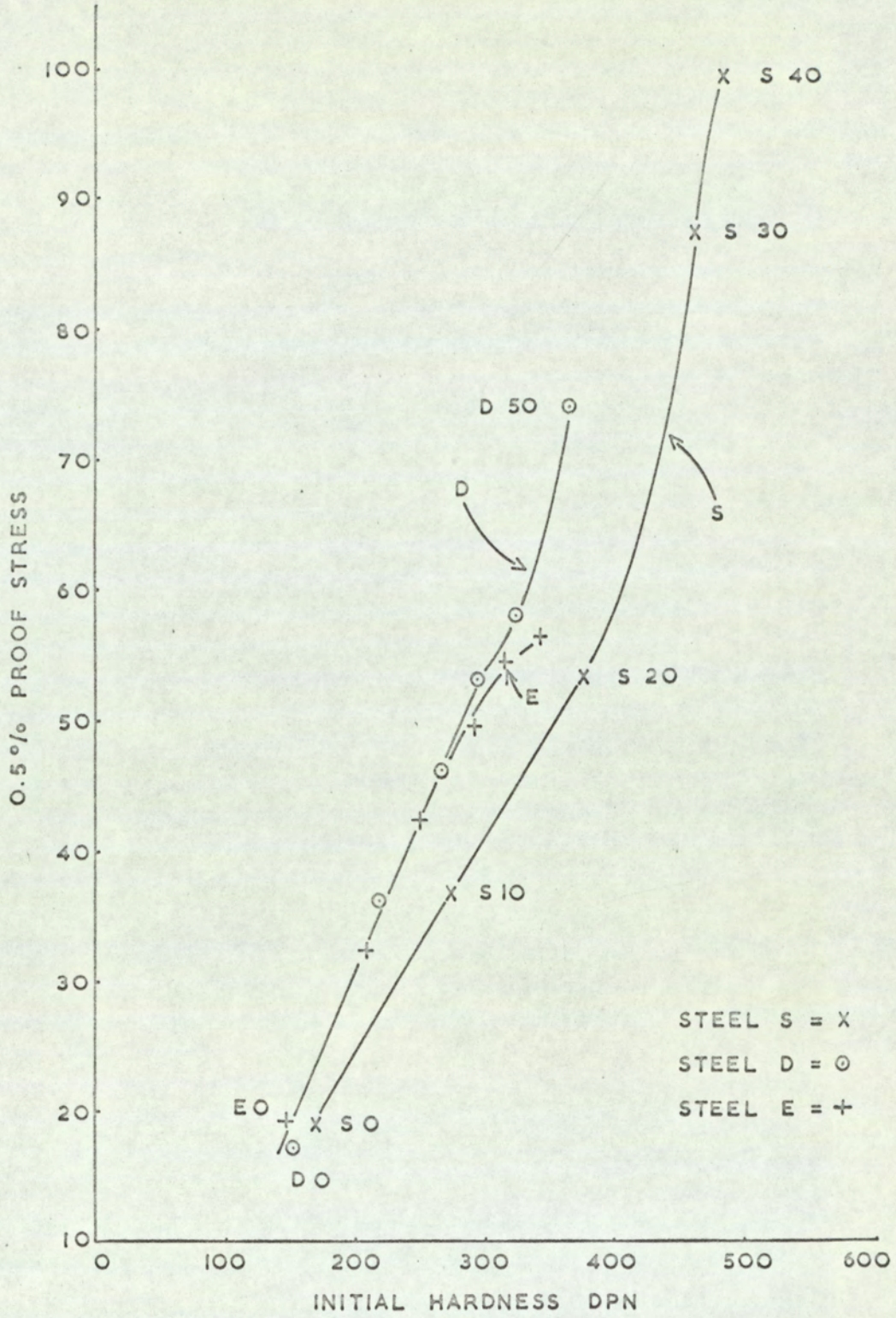

Fig. 5.14. The Relationship between 0.5% Proof Stress and Initial Sheet Hardness.

is even greater. Although overall values of uniform elongation are less for steel S, than corresponding conditions for stabler steels, the rate of decrease in elongation diminishes rapidly with increased transformation to α' martensite. It is suggested that a point is reached when the remaining austenite available for transformation in insufficient to provide the increment of α' martensite that should be formed for a given further reduction. Continued deformation therefore results in the slope of the elongation/hardness curve becoming steadily steeper.

These points are also demonstrated in Fig.5.14 in which the 0.5% proof stress values are compared with hardness. The 0.5% proof stress unlike the value of uniform elongation does not take into account the considerable amount of further plastic deformation that occurs during testing so that changes in proof stress would be expected to be apparent at higher degrees of prior deformation. This is indeed the case. The slope of the curve for steel S alters after 20% prior cold work and that for steel D after 40%. Finally it is interesting to note that the correlation between hardness and 0.5% proof stress was slightly better (+ 0.93) than between hardness and ultimate tensile strength (+ 0.79).

5.11.1. Stretch Forming

The two mechanical properties that correlated well with stretch formability, were proof stress and uniform elongation. Inevitably there was also a strong inverse relationship between these two mechanical properties (- 0.98).

The relationship between Erichsen value and uniform elongation is shown in Fig.5.15(a). Two linear relationships were obtained, one for the transformable material and one for the non-transformable steels. Biaxial stretching of stainless steels, although strongly related to uniform elongation cannot in general be directly related to this mechanical property if stretch formability is measured by the Erichsen cupping test. To investigate why two curves were obtained, stretch forming tests were also carried out using the

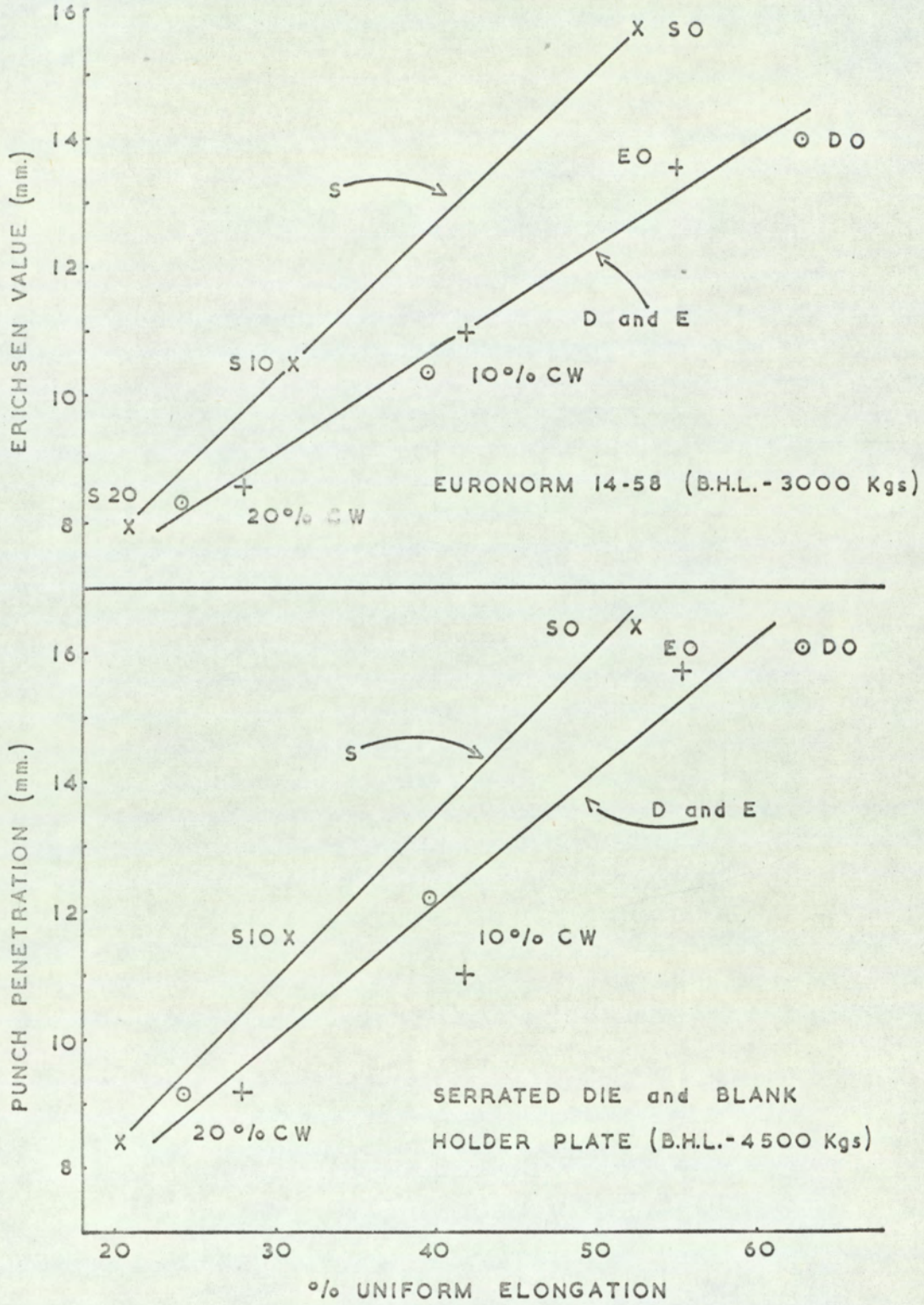

Fig. 5.15. The Relationship between the Results of Two Stretch Forming Tests and Uniform Elongation.

Erichsen punch together with a serrated die and blank holder plate. These conditions, together with the maximum possible blank holder load (4500 Kgs) were used to eliminate any drawing in of material that may have occurred in the original tests.

Drawing in of material during testing would be expected to be proportional to the maximum drawing load so that the effect would be greater for the unstable material (S). If this were true, steel S would possess relatively higher Erichsen values than steels D and E and this fact could account for the two separate curves obtained.

The results obtained using this modified test are shown in Fig.5.15(b). Although the overall formability is greater because a larger die diameter was employed, the two curves are in fact closer together, which suggests that drawing in was not completely eliminated. The degree of flow from beneath the blank holder was measured by line broadening of the serrated impressions. The average original width of a serration ring on undrawn material was 0.035 cms. Similar serration width measurements on drawn material were 0.078, 0.066 and 0.061 cms for the three steels S, D and E. Drawing in still occured and was at a maximum for the unstable material S; line broadening was found to be proportional to the drawing load. Drawing in of material must also be affected by the rigidity of the metal and would therefore be expected to be lessened by prior deformation. The two curves converge for material in such conditions. It must be concluded that complete elimination of drawing in could not be prevented and that, had it been possible, the differences between the two curves may have been removed so that stretch formability could be directly related to uniform elongation.

The relationship between proof stress and Erichsen value is given in Fig.5.16. As proof stress values increase, stretch formability is impaired. The argument relating to drawing in of material in the Erichsen test can also be applied here to explain the erroneous value of stretch formability obtained

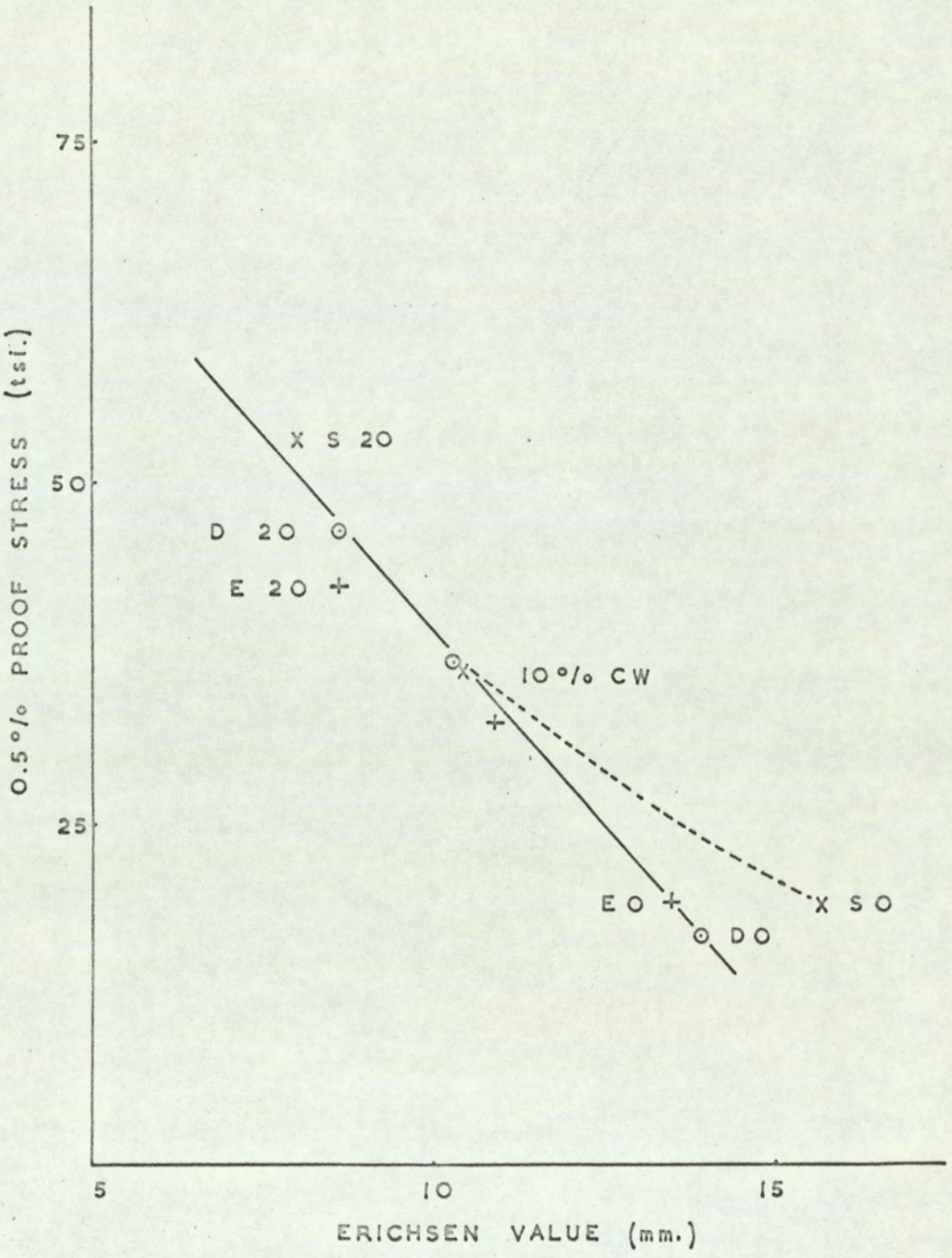

Fig. 5.16. The Dependence of Erichsen Value on the Property of 0.5% Proof Stress.

for steel S in the annealed condition. The fact that higher proof stress values were obtained for the unstable steel would indicate the necessity for higher stretch forming loads.

The effect of R value upon performance of a clamped sheet in biaxial stretching has been examined by Pearce.[39] He suggests that a high R value would not aid biaxial stretching. Butler[66] expressed the opposite view and showed that for the range in R value of 0.5 to 2.0, a slight increase was obtained in uniform elongation, and therefore biaxial stretching. The results obtained by Butler were, however, for mild steel and predicted from an assumed stress - strain relationship. The results reported here show that there was no correlation at all between $\bar{R}$ value and uniform elongation, (correlation coefficient 0.03) and an equally insignificant correlation of - .12 between $\bar{R}$ and Erichsen value. It has been shown that for the materials studied $\bar{R}$ decreased with prior working for steel S and increased for steels D and E but that in all cases stretch formability decreased almost equally for all materials. If all other factors remain constant it is considered unlikely that a variation in $\bar{R}$ value could contribute significantly to biaxial stretching. Deformation of a clamped sheet must occur by thinning and the resistance to thinning, (high $\bar{R}$ values) is not considered relevant to the extent of deformation. It is important in deep drawing operations when the stretch formed region has to be sufficiently strong in order to sustain the load required to draw in the flange of a cup.

5.11.2. Deep Drawing

Since the tested materials gave a wide range of mechanical properties and a relatively narrow range of critical blank diameters simple relationships with single mechanical properties were unlikely. However, a weak correlation, coefficient of + .83, was obtained between deep drawability and uniform elongation. The best relationship is obtained if individual compositions are examined. The results are plotted in Fig.5.17. There would appear to

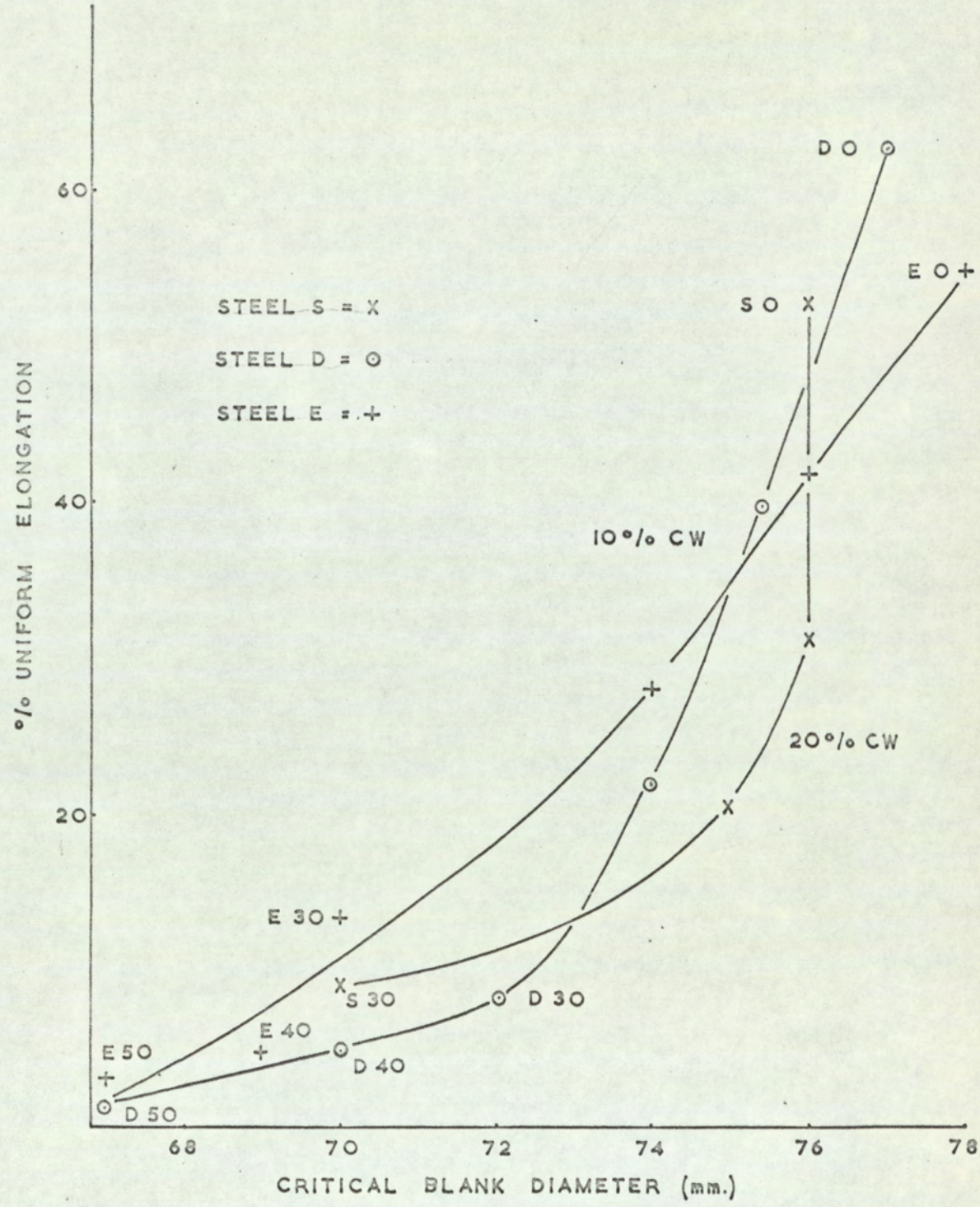

Fig. 5.17. The Relationship between Deep Drawability and the Property of Uniform Elongation.

be no correlation between uniform elongation and C.B.D. for the annealed materials but with increase in prior cold work and therefore a decrease in uniform elongation, critical blank diameter sizes decrease. The rate of decrease in C.B.D. is greatest for the most stable material. The effect of α' martensite formation in restricting a decrease in uniform elongation, particularly obvious for steel S between 0 and 10% prior cold work has already been discussed. (Section 5.8). The correlation of both stretch forming and deep drawing with performance functions as opposed to single mechanical properties will be discussed in the next section.

Before discussing performance functions, the high degree of correlation between maximum punch loads for stretch forming and deep drawing with the value of ultimate tensile strength will be mentioned. The results are shown in Fig.5.18.

The correlation coefficient for the relationship between maximum punch load in deep drawing and UTS was + 0.98. Only the load values obtained for steel S in 10 and 20% cold work deviated from the straight line. This deviation can be explained if related to the amount of α' martensite that is formed. For the non-transformable steels, the straight line relationship for the test condition used, can be expressed as maximum punch load = 150 x (UTS) and the additional load associated with transformation can be expressed by adding a factor of 50 (magnetic response) to this equation, i.e. MPL = (150 x UTS) + (50 x magnetic reading). It is not suggested that such an empirical relationship could be used other than to demonstrate the effect of α' martensite formation in metastable steels on the value of maximum punch load.

Although linear relationships were obtained between stretch forming loads and U.T.S. for individual materials in different degrees of cold work and also for different materials in similar conditions of cold work, (Fig.5.18) no general relationship was found. Maximum punch load increases with decrease in austenite stability but decreases for any given stability with prior cold work.

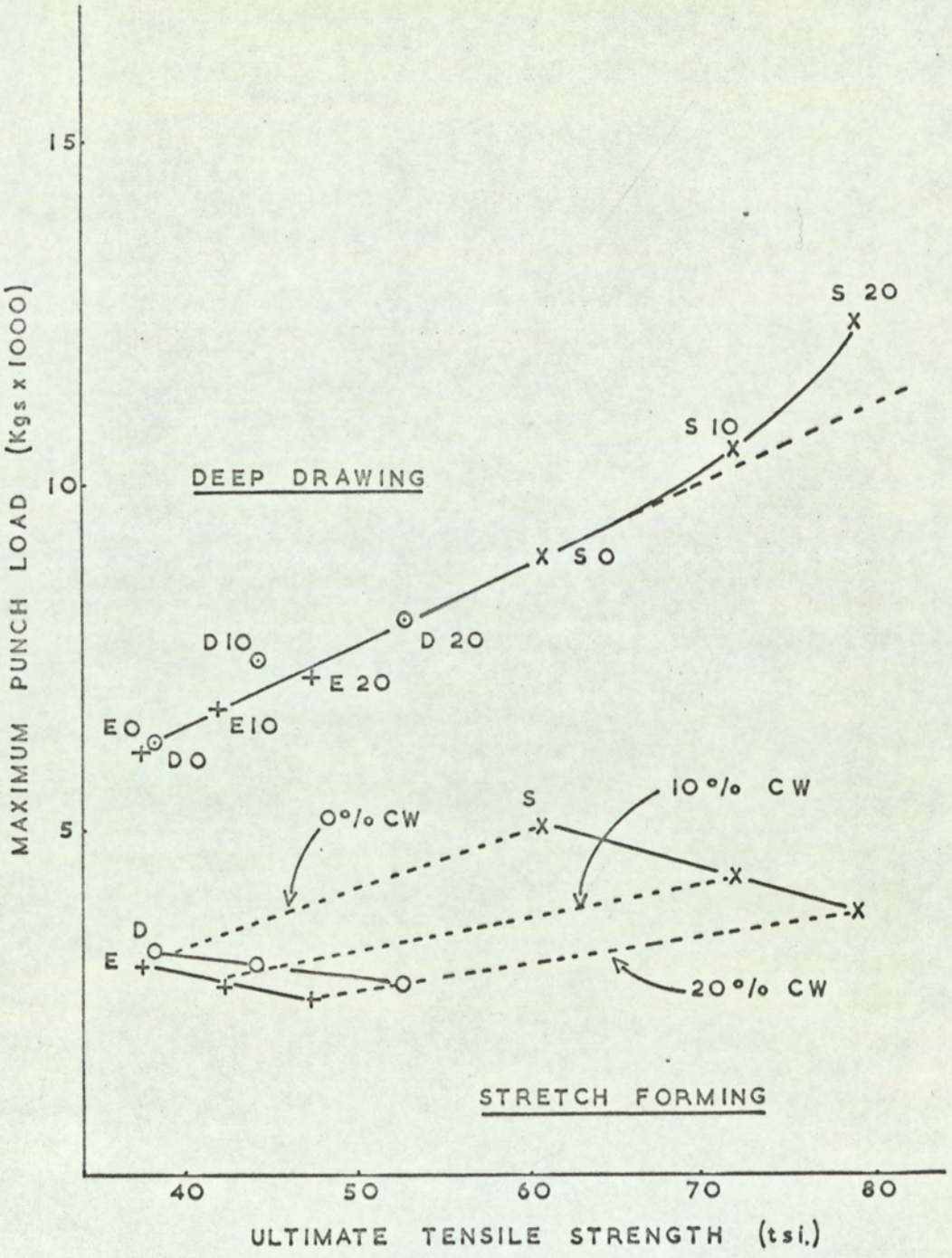

Fig. 5.18. Values of Maximum Punch Load plotted against their Corresponding Values of Ultimate Tensile Strength.

This latter trend must be associated with the degree of deformation that the material can withstand in the press.

5.12. Evaluation of Certain Performance Functions for Stretch Forming and Deep Drawing

5.12.1. Stretch Forming

Some attempts have been made to predict both deep drawing and stretch forming from a combination of mechanical properties. From a prediction point of view stretch forming has received the most attention. Butler[66] has obtained a performance function for conditions of biaxial stretching where

$$F = \frac{\text{UTS} \times \text{Uniform Elongation} \times \bar{R}}{\text{Flow Stress}}$$

This function was considered by Grimes[60] for application to aluminium and its alloys. He considered that substitution of true stress at instability, $\bar{\sigma}_m$, would improve the function where materials of considerably different ductility were being compared and it was also questioned whether values of $\bar{R}$ should be included in the numerator or denominator. For aluminium and its alloys Grimes found a better correlation with his modified function than with Butler's function. The values of this modified function for stainless steels are compared with Erichsen values in Fig.5.19. Although it has been shown that Erichsen values, particularly for the unstable material, contain some degree of drawing in, they reflect the sort of stretch formability performance that would be obtained in industry. For this and subsequent comparisons Erichsen values obtained using the Euronorm 14-58 specification will be quoted.

Again as with most parameters compared with the stretch formability of stainless steels, two curves are obtained, showing two different relationships for transformable and non-transformable steels. Maximum formability is achieved with the maximum value of this function. Analysis of this function shows that the value of uniform elongation is the dominant factor particularly for heavily cold worked materials where the ratio of $\bar{\sigma}_m/PS$

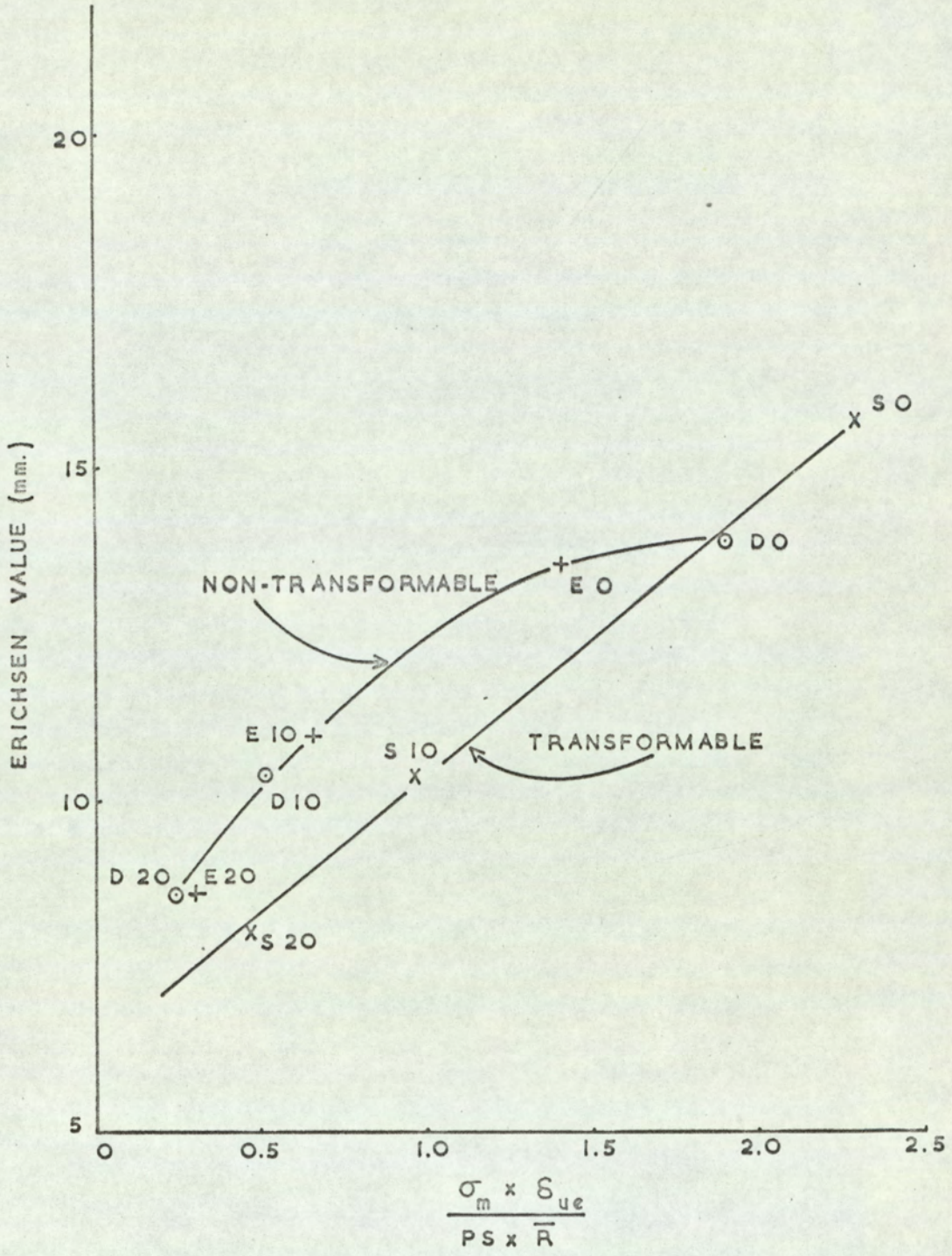

Fig. 5.19. Erichsen Values plotted against the Modified Performance Function suggested by Butler.[66]

tends towards unity. The effect of $\bar{R}$ for stainless steels is insignificant as this value varies little from unity. The relationship is not considered to be better than the simple relationships with uniform elongation.

Black and Lherbier[54] also proposed a function which is stated to have been designed for the stretch forming of stainless steels. Values of this "formability" factor ($f = \frac{\ln [\sigma_m (1 - Eu)]}{A^{Eu}}$ where σ_m is stress at instability, Eu uniform elongation and A^{Eu} is the deformation work area, are plotted against Erichsen values in Fig.5.20. Minimum values of this factor relate to maximum stretch formability and optimum properties for high formability are low stress at maximum load and a high uniform strain coupled with a high value of deformation work area. Uniform elongation again contributes significantly to this factor both directly and also in its influence on the deformation work. Good agreement is obtained particularly for the annealed material but for material in conditions of cold work the values obtained do not reflect correct Erichsen values. For example after 20% cold work steel S has a lower "formability factor" but an inferior measure of stretch formability. The relationship would be better satisfied by three curves for the individual compositions studied.

A further factor was studied which showed good agreement with stretch formability for individual compositions. This was the product of stress at maximum load and the limit of uniform elongation here expressed in terms of natural strain. The results are shown in Fig.5.21. In order to discover why this relationship existed, the properties affecting stretch formability were examined.

If the process of stretch forming is examined from the point of view of the work necessary to stretch material over a punch nose, then the work done must be a function of both force and distance moved. In stretch forming operations the equivalent values are therefore maximum punch load and punch

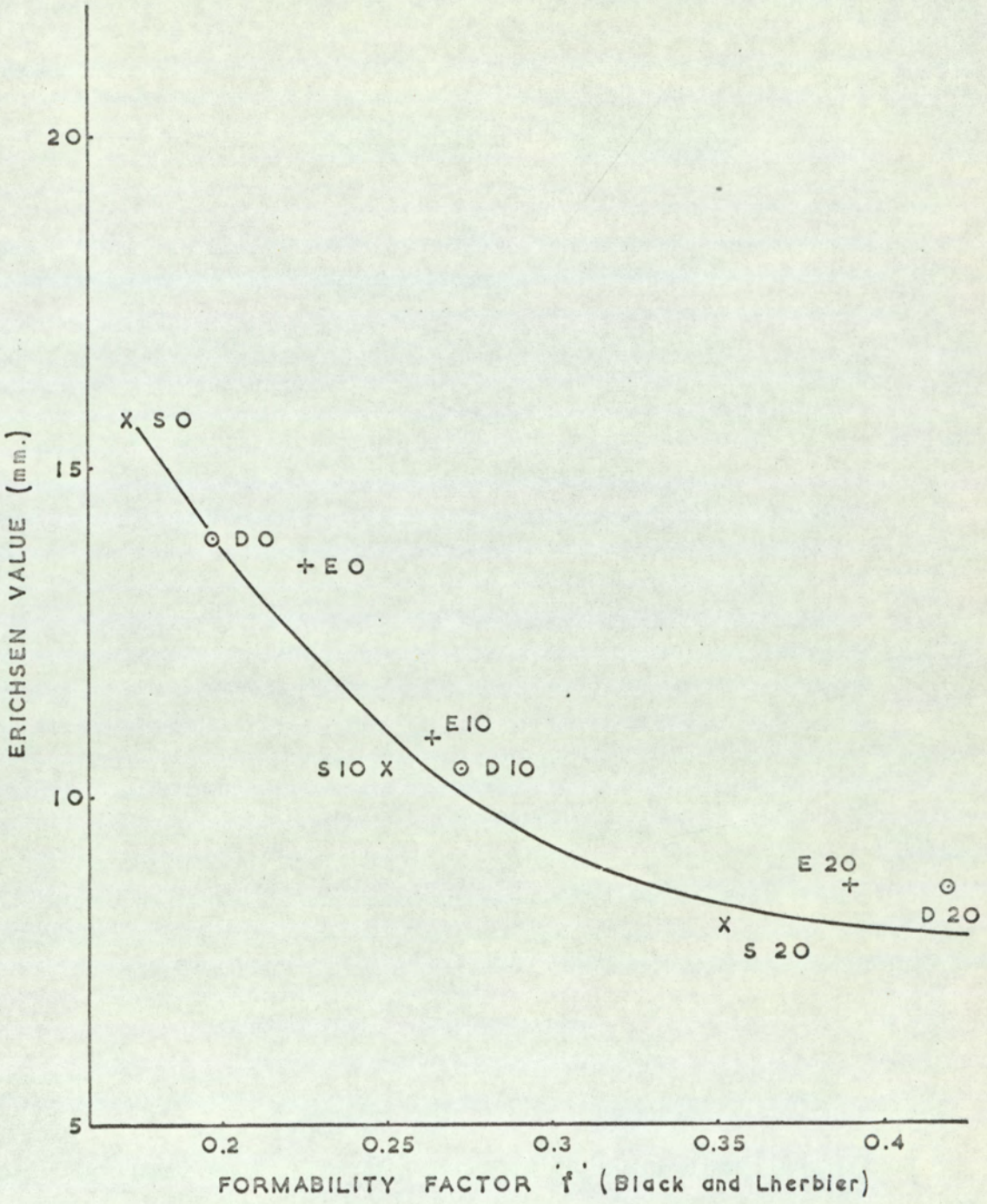

Fig. 5.20. Erichsen Values plotted against the Formability Factor proposed by Black and Lherbier.[54]

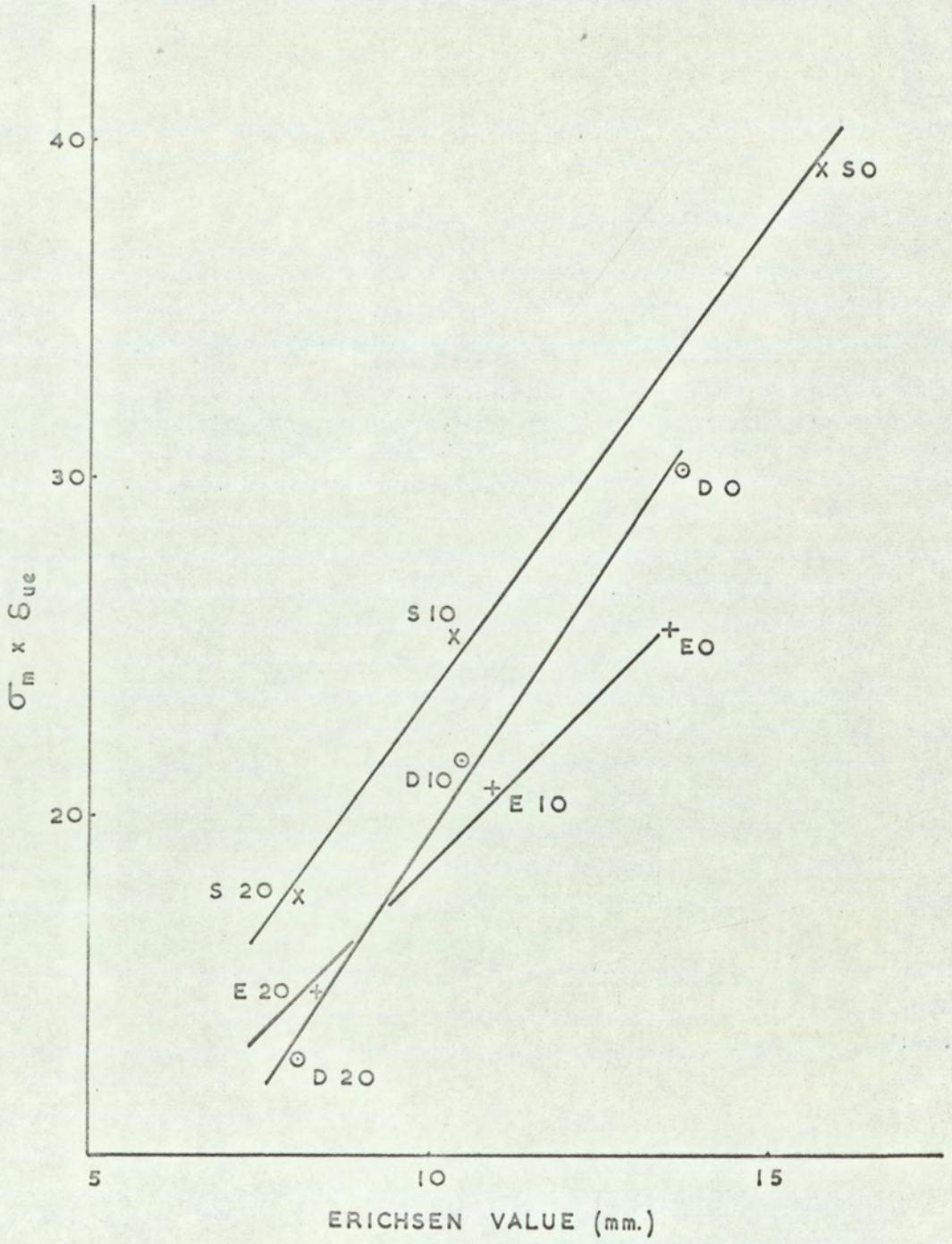

Fig. 5.21. Erichsen Values plotted against a Performance Function of Stress at Maximum Load x Strain Corresponding to the Onset of Plastic Instability.

travel. As a measure of the work done, the areas beneath the punch load/punch travel diagram were measured. The results are presented in a previous section (4.4), (Table 4.5). Therefore since WD = (MPL x Penetration)(constant) the penetration or Erichsen value should be a function of WD/(MPL)(constant). The constant is necessary to account for mainly frictional and other effects, but with lowered frictional conditions will tend towards a maximum value of 0.5. The reason for this is that the curve obtained for punch load/punch travel diagrams can roughly be represented by the shape of a right angled triangle an illustration of which is superimposed on Fig.5.22. The area of such a triangle can therefore be represented by the function $\frac{1}{2}$(b x h) where b and h respectively represent maximum punch load and punch travel in stretch forming operations. Using polythene as a lubricant in this work the value of this constant was found to be 0.44. Assuming this theory to be correct, values of work done during stretching/maximum punch load should give a straight line relationship when plotted against Erichsen value. The results obtained are shown in Fig.5.22. It was also considered that in tensile testing the product of the stress at maximum load and the limit of uniform elongation times a constant would be a measure of the work done during uniaxial tensile testing. Measurements of the area beneath the stress-strain curves were therefore made and are compared with this product in Fig.5.23. Again it can be seen that a straight line relationship resulted. The next step was therefore to compare the two deformation work values, expressed as areas for uniaxial tensile testing and biaxial stretch forming and it can be seen from examination of Fig.5.24, that for the range studied there is reasonable agreement between these two values. As a result of these conditions it is therefore suggested that performance factors for stretch formability should, to the best of their ability, assess the maximum value of deformation work and that by doing so the individual variations in different mechanical properties are minimised.

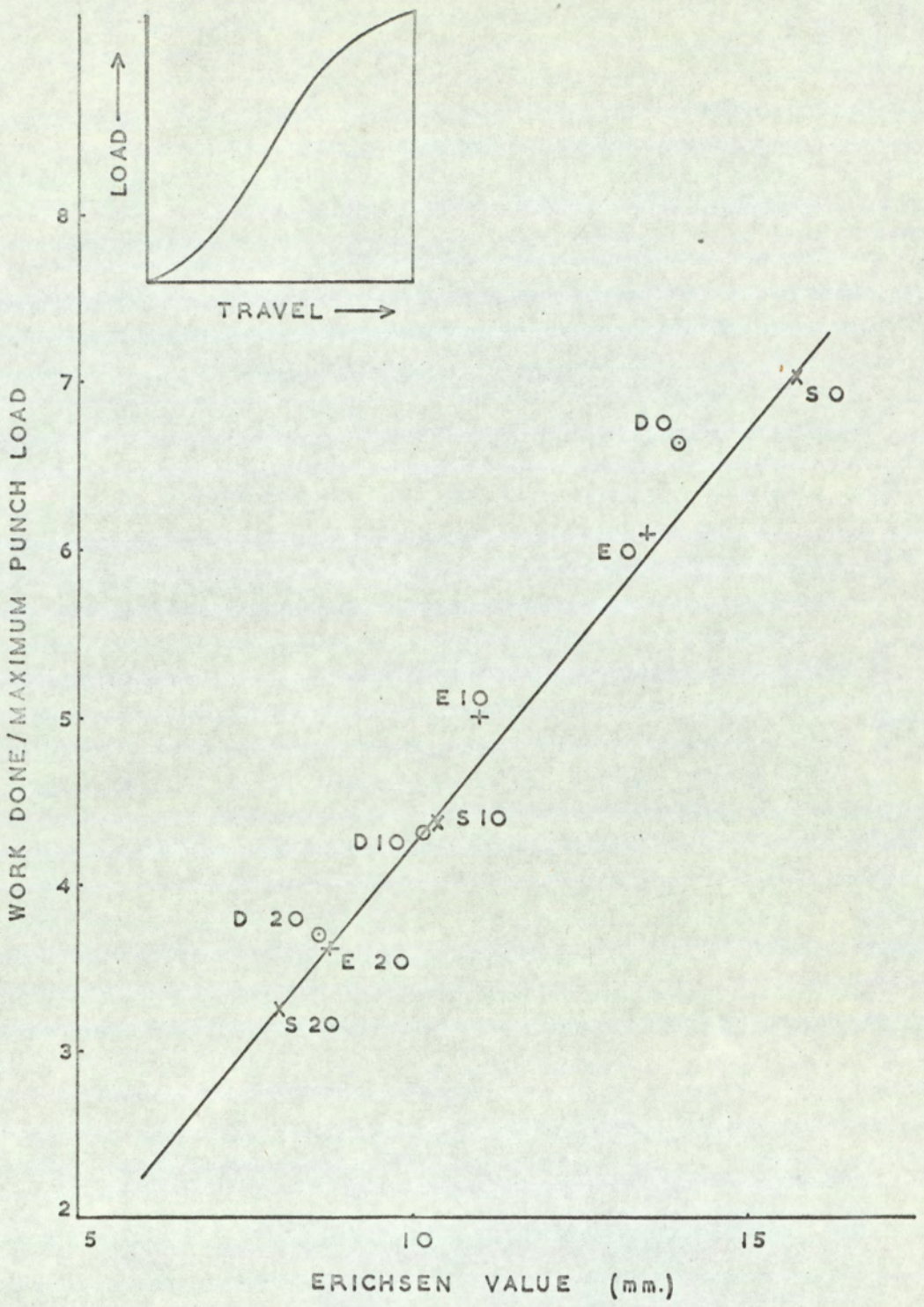

Fig. 5.22. The Relationship between Erichsen Value and Work Done/ Maximum Punch Load.

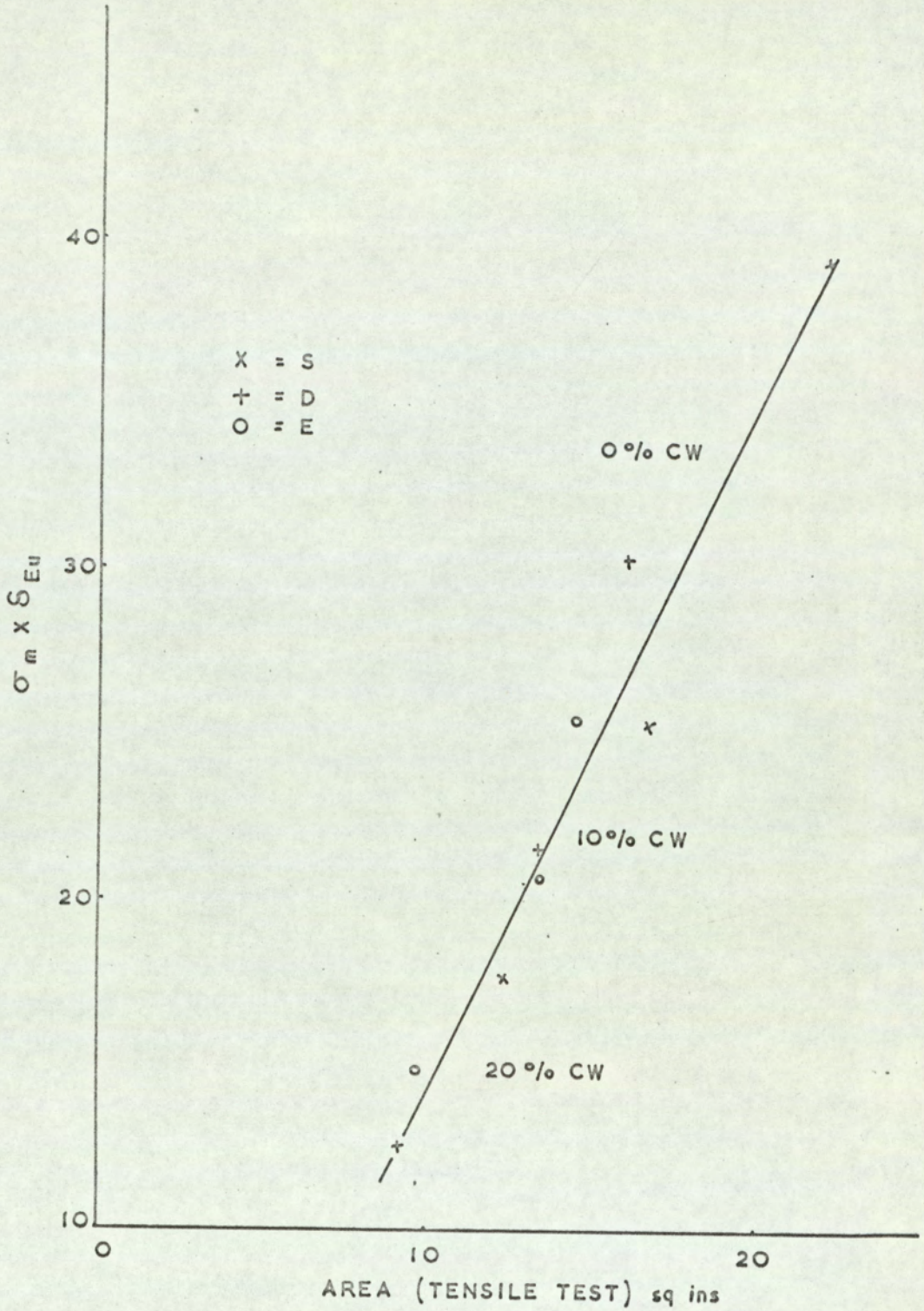

Fig. 5.23. The Relationship of the Area beneath the Load/ Extension Curve and the Product of Stress at Maximum Load and Strain at Plastic Instability.

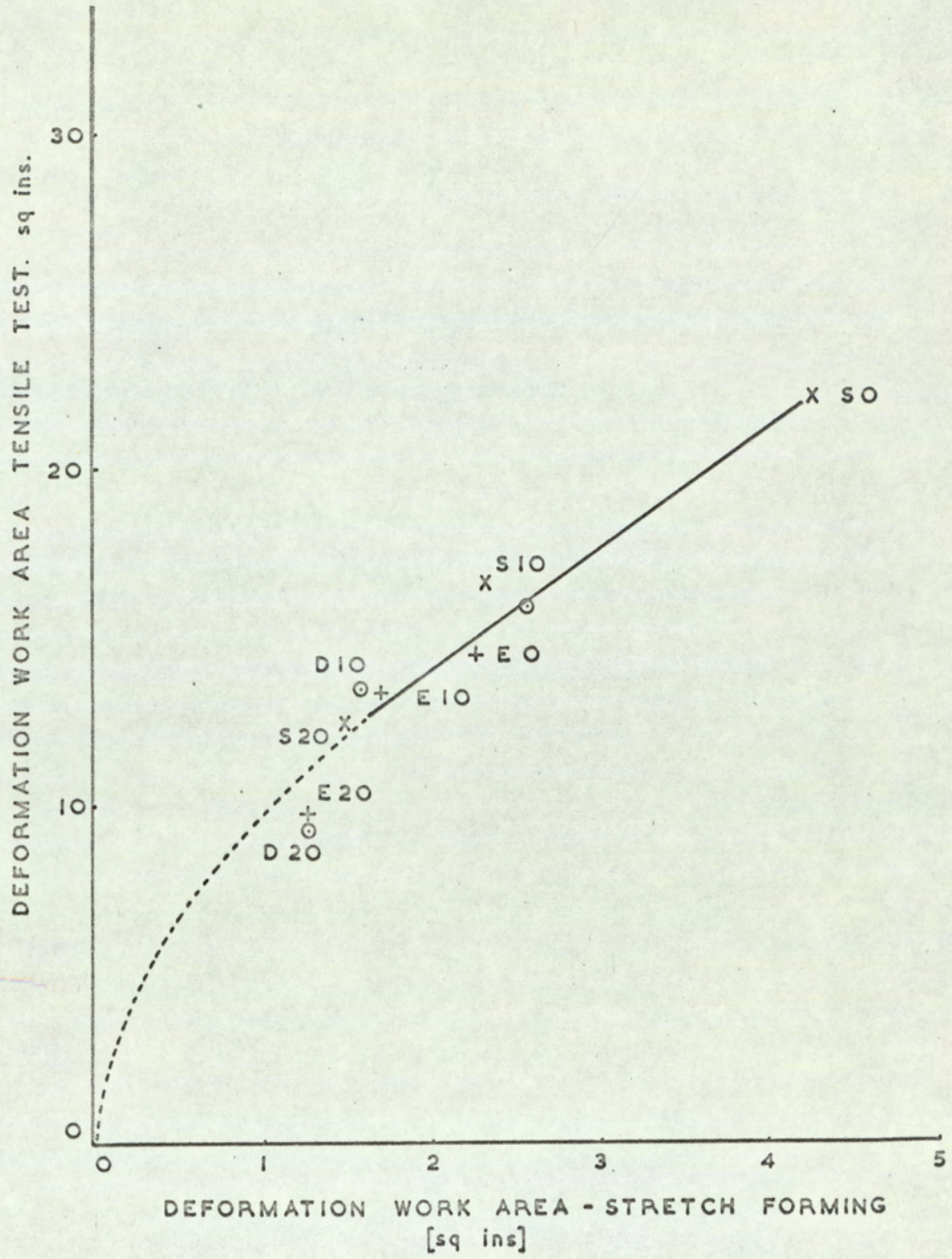

Fig. 5.24. Comparison of the Two Deformation Work Areas obtained from Tensile and Stretch Forming Tests.

5.12.2. Deep Drawing

It has previously been reported that deep drawability should depend on normal anisotropy and the expression $\ln D/d = \frac{1}{1+n}\sqrt{\frac{\bar{R}+1}{2}}$ devised by Whiteley has been mentioned. If it is assumed that this expression is also satisfied by stainless steel in the annealed condition it should be possible to estimate the value of n, a frictional parameter for drawing conditions involving polythene sheet as a lubricant. Using the values of C.B.D. obtained for the three steels in the annealed condition only, n values have been calculated and are given in Table 5.1.

TABLE 5.1.

Steel	CBD	D/d	$\bar{R}$	n	Mean value of 'n'
S	76	2.30	0.90	.140	.149
D	77	2.33	0.92	.158	
E	78	2.36	0.95	.149	

For drawing conditions involving poly thene sheet as the lubri cant it would therefore seem that the frictional parameter described by Whiteley as varying between 0.2 and 0.3, could be reduced to 0.15. Having used this formula to calculate a value of 'n', it can not therefore be used as an assessment of drawability. Obviously agreement between results predicted from Whiteley's formula and practice are good if 'n' is considered to be 0.15 but does the formula also hold good if applied to cold worked material? Since the formula does not take into account bending and unbending under tension over punch and die profiles and of work hardening, it is not surprising that it does not. The only variable, omitting friction, in the formula is that of $\bar{R}$ value and an increase in this value must be reflected in increased drawability. For the two non-transformable materials prior cold work had the effect of increasing values of $\bar{R}$ but this was also associated with a rapid decrease in drawability.

Since there was a weak relationship between drawability and uniform elongation it was therefore decided to evaluate the function $\bar{\sigma}_m \times \delta$ (at instability) to deep drawing. The factor was compared with values of mean cup height in order to assess more accurately the differences in drawability obtained with drawn cups. Although not reported here, for individual materials agreement was good. This analysis varied in two ways from the approach applied to the stretch forming operations. First, the shape of the punch load/punch travel diagram from which measurements of area was made, could not schematically be represented by a right angled triangle but more so by two such triangles. The value of the constant mentioned in the previous analysis, now under ideal conditions, becomes unity and deviates from this value with increased friction. Secondly, in comparing this factor with limiting drawability, three variables had to be taken into account, i.e. prior cold work, composition and thirdly blank diameter. It was therefore considered to be highly unlikely that a performance function derived from mechanical test data would take into account so many variables.

Finally, drawability has been assessed using the model proposed by Wilson and Butler.[42] Maximum punch loads for deep drawing a flat nosed conical cup are compared to maximum punch loads obtained for deformation of a clamped sheet using a hemispherically shaped punch. The ratio of these two load measurements is related to blank diameter in Fig.5.25. The graph shows that good agreement is obtained, with one exception, to the relationship proposed by Wilson and Butler, in that maximum drawability is obtained when Ld max = Ls max. It would appear that steel S does not completely satisfy these conditions in that the ratio of Ld/Ls max ranges from 1.0 to 1.3 for cups drawn from similar sized blanks. The ratio would normally be expected to increase when cold worked as opposed to annealed material is deformed because not only does Ld increase with prior cold work but Ls max decreases. This increase in ratio, for values greater than unity is normally associated with

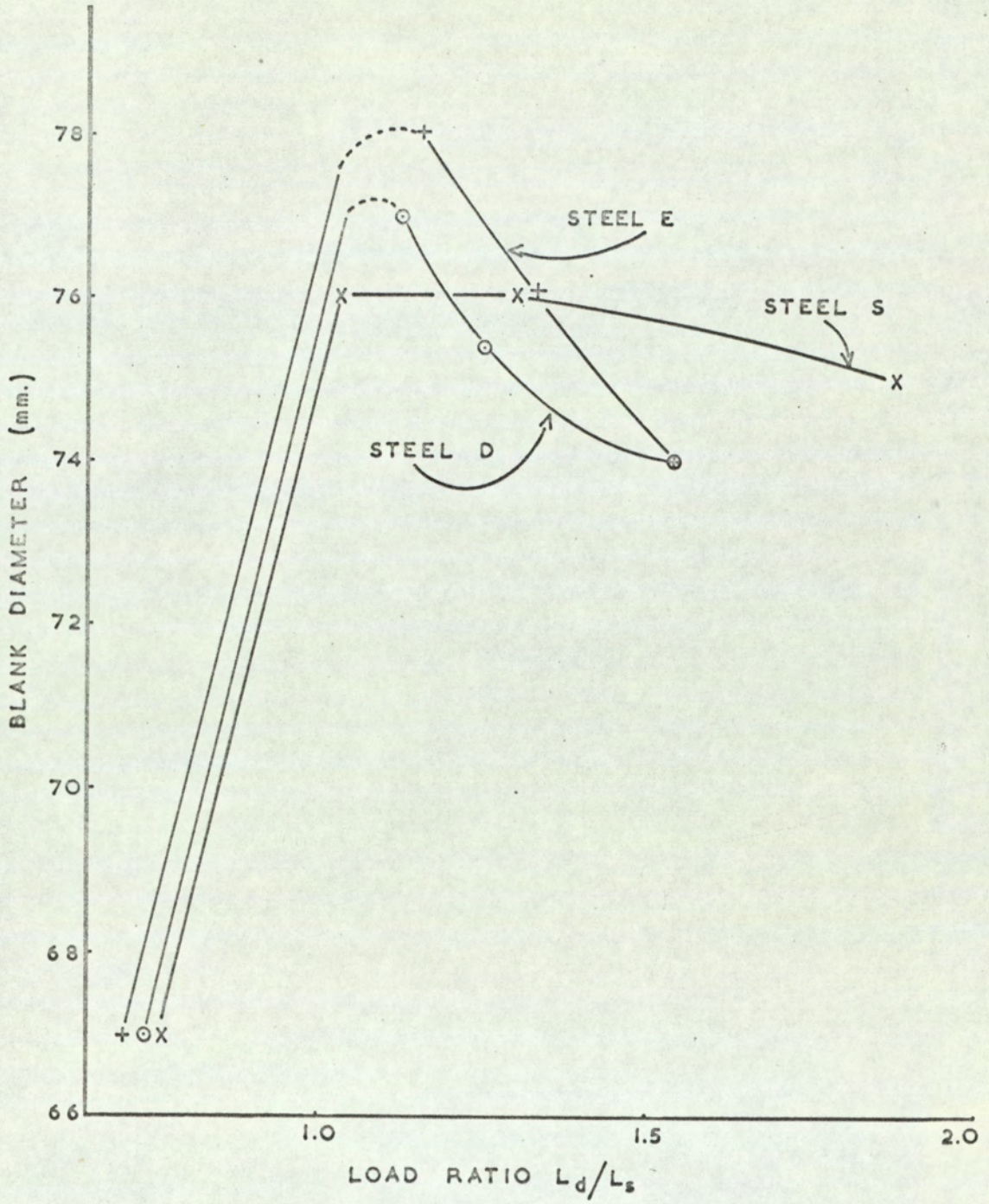

Fig. 5.25. The Relationship between the Load Ratio and Blank Diameter for Steels S,D and E in Different Degrees of Prior Cold Work.

diminished drawability. The reason suggested why this is not so for steel S is that the beneficial action of α' martensite offsets this normal decrease in CBD by reducing the effect of localised necking which is a pre-requirement for failure.

5.13. An Analysis of the True Stress-True Strain Data, obtained in Uniaxial Tension

True stress and true strain data have been calculated from the load/extension diagrams obtained from the tensile test. (Unless otherwise stated true stress and true strain will hereafter be referred to as stress and strain). Such data is conventionally plotted on a log-log basis from which a simple measure of the work hardening coefficient of the material can be obtained.

Stress-strain data for conventional non-transforming materials often obeys the Ludwik relationship ($\sigma = k\delta^n$) and when plotted on a log-log basis gives a straight line. The slope of this line is normally designated 'n', the work hardening coefficient and an extrapolation of this line to the intersection of the stress axis corresponding to $\delta = 1$ gives a measure of the strength coefficient k.

The usefulness of the Ludwik relationship has been severely questioned by Voce.,[47] who states that real stress-strain data when plotted on double logarithmic co-ordinates, gives a curve shaped like an "Italicised integration sign". Voce substitutes an exponential function, stress $S = S_\infty - (S_\infty - S_o) \exp.(-\eta/\eta_c)$ for the Ludwik equation and the increased accuracy of this equation cannot be denied. Nevertheless, even if this more complicated formula is used, the central portion of the curve is satisfied by a straight line and this part of the curve extends over the range of strain normally examined in tensile testing. It is therefore considered that for most materials the Ludwik equation would be sufficiently accurate.

Examination of the typical stress-strain curves obtained in this investigation (Fig.4.7.), shows that stainless steels neither obey the Ludwik nor the

Voce relationship. From the onset of plastic deformation to about 0.035 strain the plot is a straight line and obeys the Ludwick relationship. This relationship does not hold for the second part of the curve. It was therefore necessary to derive a function that accurately described the shape of this second part of the curve. A quadratic function was obtained:- $\log\sigma = c/e + m(\log \delta) + n.e(\log \delta)^2$. The values of the constants have already been reported (section 4.5). The slope of this second part of the curve also increases with respect to strain and an accurate measure of this slope is obtainable from a differentiation of the above equation. Values of this slope n_ε , for the steels examined here have also been calculated and are also reported in Section 4.5.

Work by Divers[30] has shown that transformable stainless steels give a stress-strain graph similar to that shown in Fig.5.26. The difference between the two strain hardening coefficients n2 and n1, which is stated as having much the same significance as the value 'n' in the Ludwik equation is said to result from the increase in strain hardening due to the formation of α' martensite The new results reported here show that the relationship between stress and strain is more complex than that assumed by Divers in that transition between the two stages is progressive and not instantaneous. It can also be seen that when α' martensite forms the slope of the curve is not constant but continues to increase as the amount of α' martensite increases.

Similar work by Barclay[33] on the mechanisms of deformation and work hardening of type 301 stainless steel, relates the point at which there is a change in the slope of the stress-strain curve to the strain level corresponding to the onset of α' martensite, and the slope of the curve to the rate of formation of this phase. It is considered, that for the steel examined by Barclay, the point of initiation and the amount of α' martensite formed would approximately coincide with this change in slope. To illustrate this point, the present work examined steels of various austenite stability and reference to Fig.4.7. clearly shows that even non-transformable steels exhibit a change in slope. In addition, the

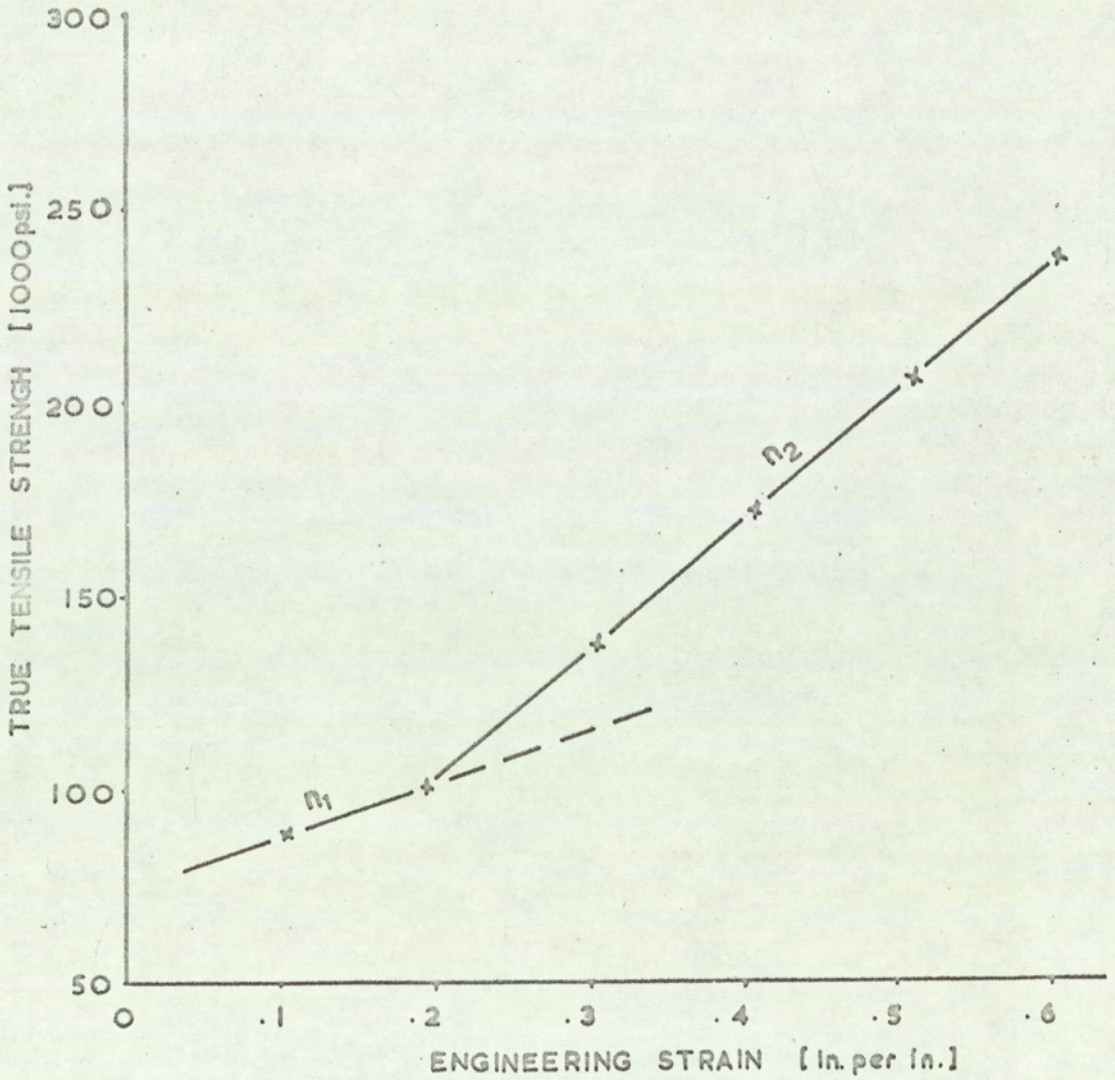

Fig 5.26. True Tensile Strength versus Engineering Strain. (Divers)

strain levels at which a change in slope was observed have been recorded and these values are compared with the strain levels at which the onset of α' martensite was detected by different means in Table 5.2 .

Table 5.2.

Steel	Austenite Stability	Minimum Strain at which a change in the Rate of Width Contraction during Tensile Testing occurred	Minimum Strain at which a Magnetic Response was Recorded	Strain corresponding to change in slope of Stress-Strain curve
S	- 5.29	0.049	.002	.045
D	- 3.34	0.14	0.14	.023
E	- 0.9	>0.34	0.34	.016

It can be seen that the change in slope of the stress-strain curve does not correspond to the strain levels at which α' martensite forms for a range of stainless steels. Indeed α' martensite forms at increasingly higher strains with increase in austenite stability whereas the strains, corresponding to a change in slope of the stress-strain curve, decrease. Furthermore, since steel E could also be represented by a curve and not a straight line, the shape of the stress-strain curve can not be wholly due to the formation of α' martensite. Nevertheless, α' martensite formation must affect the slope of this curve considerably. Values of n_δ , the slope of the stress-strain curves with respect to strain are plotted against strain for several steels in Fig.5.27.

By definition, the Ludwik equation states that the work hardening coefficient, the slope of the stress-strain curve is a constant in that it does not vary with respect to strain, e.g. mild steel. For stainless steels this is not the case. The work hardening coefficient continually increases over the range of strain experienced in the tensile test, but the rate of increase diminishes with continued strain. (Values of strain are plotted on a log scale in Fig.5.27

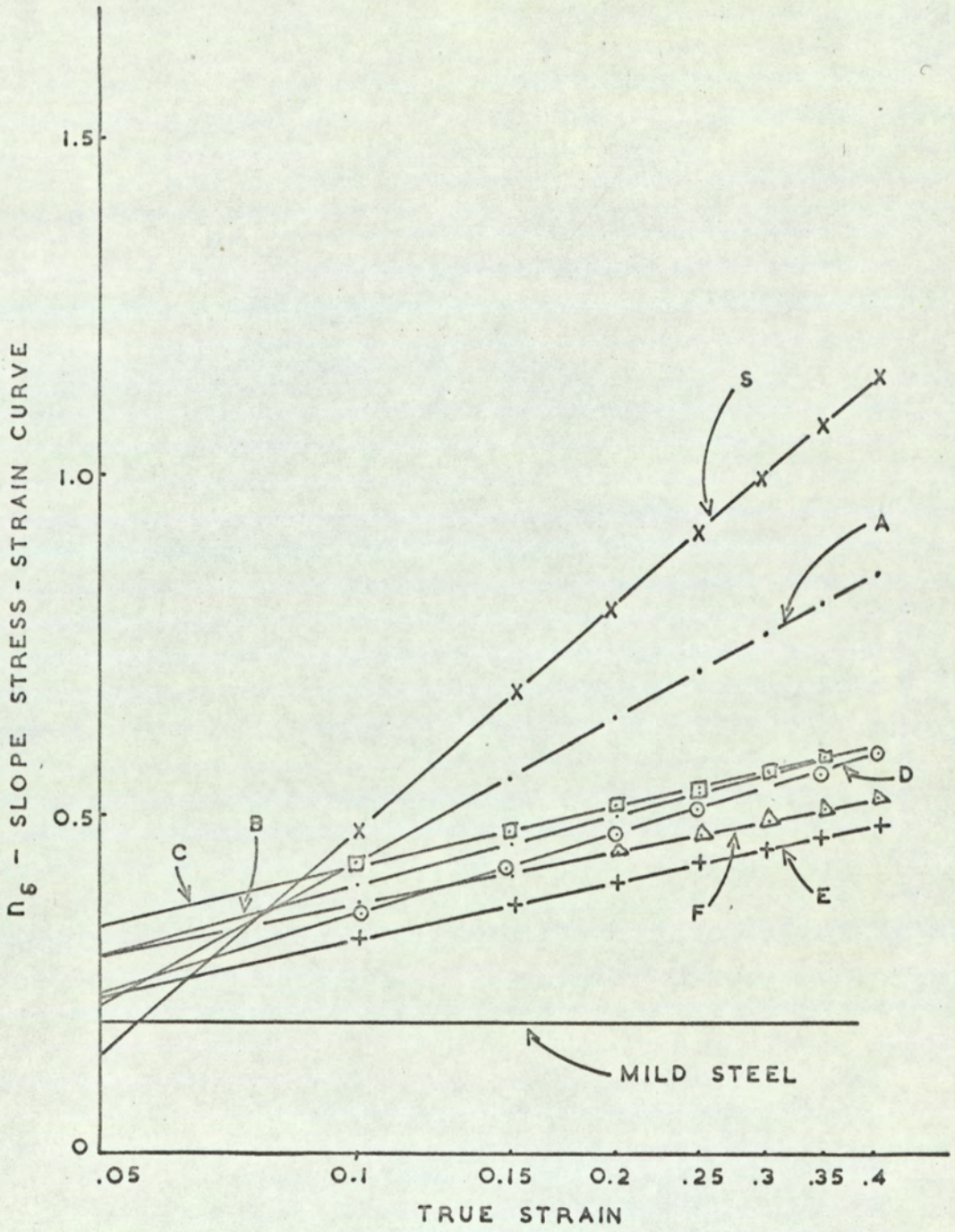

Fig. 5.27. The Effect of Austenite Stability on the Slope of the True Stress - True Strain Curve at Different Levels of Strain.

to make interpretation of equation 3, Section 4.5. easier). It can also be seen that the degree to which the steel can be strain hardened, decreases with austenite stability but even the non-transformable materials (E and F), in which no α' martensite was detected after testing, show an increase in the slope of the stress-strain curve. This further implies that, in addition to strain hardening from α' martensite which appears to be superimposed on the strain hardening component associated with deformation of the parent austenite, a third mechanism of strain hardening is operative. This is only true if deformation of the austenite alone, would be likely to obey the Ludwik equation.

It has been shown, however, that the transition between the two strain hardening portions of the stress-strain curve proposed by Divers, should be progressive. Evidence to support the fact that the change should be gradual is proposed by several workers.[18, 21, 25 and 72] They state that in austenites of low stacking fault energy (less than 25 ergs/cm^{-2}) formation of α' martensite by deformation is associated with the presence of a close packed hexagonal phase, ε martensite, and this phase is an intermediate product between face centred cubic austenite and the body centred martensite or that it is formed simultaneously with the latter. The ε phase has been considered as "an ordered arrangement of stacking faults"[23] and is formed irrespective of whether the α' martensite is induced by cooling or deformation. Guntner and Reed[22] using a difference method have shown that the amount of ε martensite first increases with the degree of deformation then decreases, while the α' martensite continually increases; which lends further evidence to the fact that this phase should be considered as a transition phase in the γ-α' transformation. In non-transformable stainless steels it is therefore suggested that considerable strain hardening results from the formation of stacking faults or "stacking fault bundles". This would account for the strain interval between the change in slope of the stress-strain curve and the

level at which α' martensite was detected.

This theory suggests that the ε martensite in paramagnetic. There is support for this from Weil[73] and Mugnier,[74] who state that since the lattice parameter (a) spacing of the stacking fault phase is equivalent to that of the parent austenite, it would be expected to be paramagnetic.

If it is assumed that significant strain hardening has resulted from the formation of ε martensite, in all the steels examined, then the amount of this phase present should be related to the total strain that the material is subjected to and not to austenite stability as is the case with α' martensite. Guntner and Reed[22] have, however, shown that the amount of ε first increases with deformation then decreases. This would be expected if the ε phase produced was utilised in the formation of α' martensite at higher strain levels and in metastable austenites.

The fact that α' martensite is not effective as a strain hardening mechanism in the stable steels is illustrated in Fig.5.28. At low values of austenite stability there is good agreement between the slope of the curves shown in Fig.5.27 and the magnetic response, indicating that for such steels strain hardening results predominantly from the formation of α' martensite. It is suggested, since the slope of the stress-strain curve increases with increase in strain, that the slope of the curves given in Fig.5.27 should be considered as a rate of strain hardening and that the difference between the initial and final strain hardening coefficients be considered as a measure of strain hardening capacity. Further reference to Fig.5.28 shows that at higher stabilities a divergence between magnetic response and work hardening occurs. At a stability of - 1.0 virtually no martensite was detected at a level of 40% prior deformation, and yet the slope of the stress-strain curve still continued to increase. The austenite stabilities examined in this graph represent austenitic and metastable stainless steels. At the low stability end of the scale used fully martensitic steels would exist.

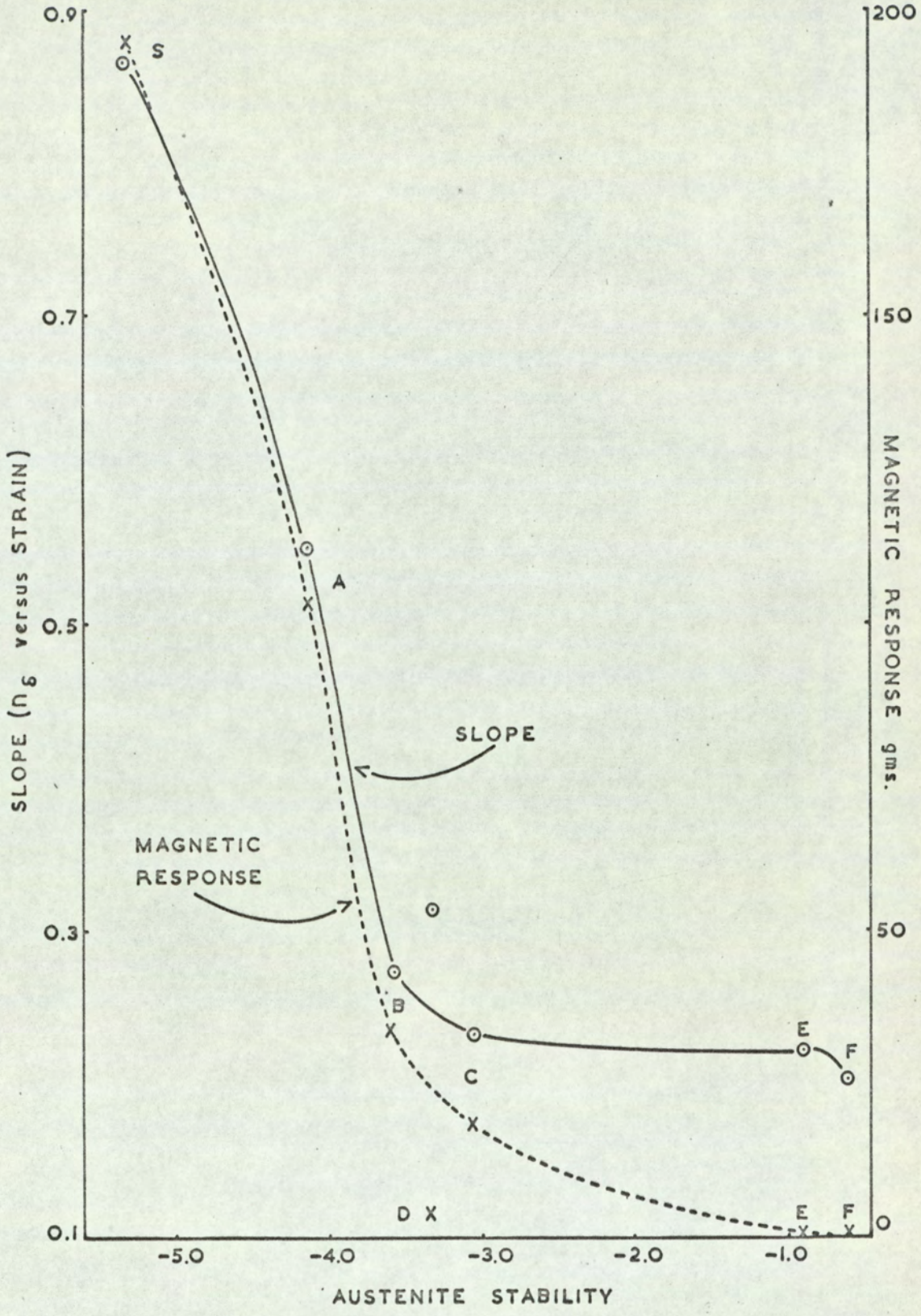

Fig. 5.28. Magnetic Response and Slope (Previous Fig.) plotted against Austenite Stability.

In Fig.5.29, a measure of work hardening is compared to the strain level at which α' martensite was first detected. In no steel did the rate of change of slope of the strain hardening curve decrease to zero which is the value required for materials exhibiting constant strain hardening coefficients. There would also appear to be two distinct rates of work hardening in stainless steels: one resultant from the formation of ε martensite and one, which occurs when significant amounts of α' martensite are produced during the straining experienced in tensile testing.

5.14. The Significance and Relationship of the Quadratic Function to Existing Stress-Strain Formulae.

The accuracy of the quadratic function $\log\sigma = {}^{c}/_{e} + m\ (\log \delta) + n_e\ (\log \delta)^2$ for all the steels examined, has been demonstrated. It will also be shown that the values of the constants given in this equation can be related to chemical composition so that it is then possible to predict stress-strain curves, and parameters derivable from such relations, for the range of stainless steels examined. The main advantage of this equation over others is that, in the form that it is most likely to be used, it is simple, i.e. in the logarithmic form.

Stress values, determined from the quadratic expression, vary in a similar manner to that given by the Ludwik equation plus the added effect related to additional work hardening mechanisms. The quadratic function has not been related to the Voce equation as it was considered that his equation, used in the form in which it would normally be employed, becomes too complicated to be practical: the quadratic being sufficiently accurate to adequately describe the stress-strain relationship for the stainless steels studied here.

Brittain[75] has shown that the value of strain hardening coefficient for materials obeying the Ludwik relationship, 'n',can be numerically related to the strain level corresponding to the point of instability in the tensile test, i.e. the limit of uniform elongation. In order to obtain a comparable value for stainless steels, values of n_δ have been calculated for values of strain

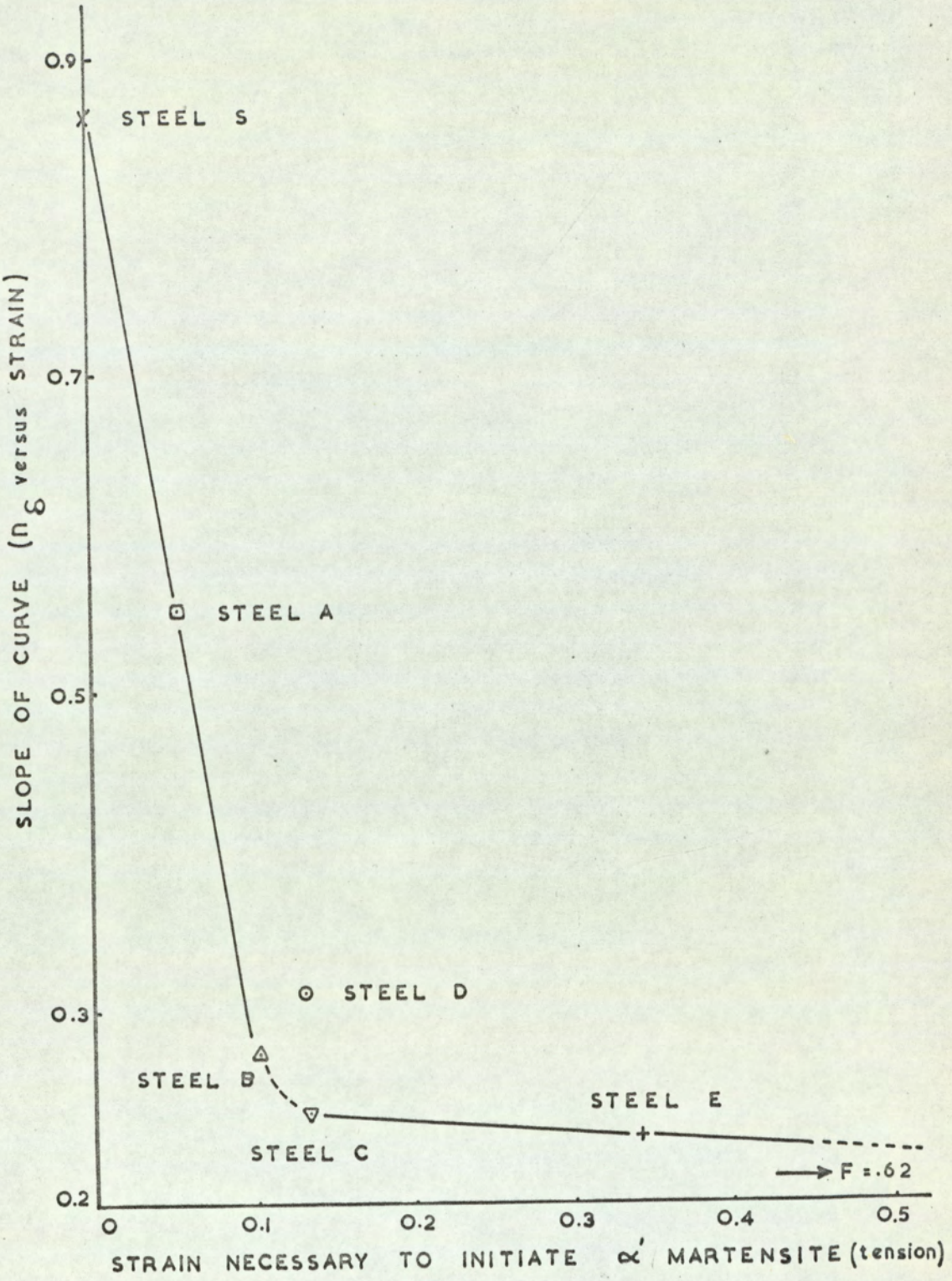

Fig. 5.29. The Relationship between Slope (Fig 5.27.) and the Strain Level necessary to Initiate α' Martensite Formation.

corresponding to the limit of uniform elongation. These values are given in Table 4.12, (Section 4.7.) If the assumption that n_δ values at instability are comparable to conventional 'n' values is valid, then there should be a similar relationship between n_δ at instability and L.D.R. as that obtained by Keeler and Backofen, for 'n' and L.D.R. Examination of Fig.5.30 shows that this is the case and that the values obtained tend toward the theoretical L.D.R. value of 2.72, for pure radial drawing conditions in which failure occurs over the punch nose. The dotted line represents the expected shape of the curve for frictional conditions. It has been shown that the slope of the stress-strain curve can be calculated from a differentiation of equation 3. (Section 4.5). The constant m in the quadratic function can therefore be considered as the slope of the stress-strain curve when the value of strain is equal to unity, i.e.

$$\text{if} \quad \frac{d(\log \sigma)}{d \log \delta} = n\delta = m + 2\, n_e (\log \delta)$$

then when $\delta = 1$ the term $2\, n.e (\log \delta) = 0$ and $n\delta = m$. In practice such strain levels are not developed in the tensile test and the slope is always less than the value of m. The degree to which this value of m is reduced is governed by the magnitude of the constant ne and the strain to which the material is subjected. The value of the term $2\, n.e(\log \delta)$ is always negative for strains less then unity and must therefore be subtracted from the value of the constant m. Both of these constants control, in a complex manner, the value of the strain hardening coefficient obtained. These constants should therefore give a straight line relationship when compared to a practical measure of work hardenability. In section 5.6 such a practical measure was obtained and is compared with the constants m and n.e. in Fig.5.31. Again good agreement is obtained.

Derivation of the strength coefficient k, in the Ludwik equation is obtained when strain is equated to unity. If a similar approach is adopted with the quadratic function then log stress becomes equal to the constant $^{c}/_{e}$

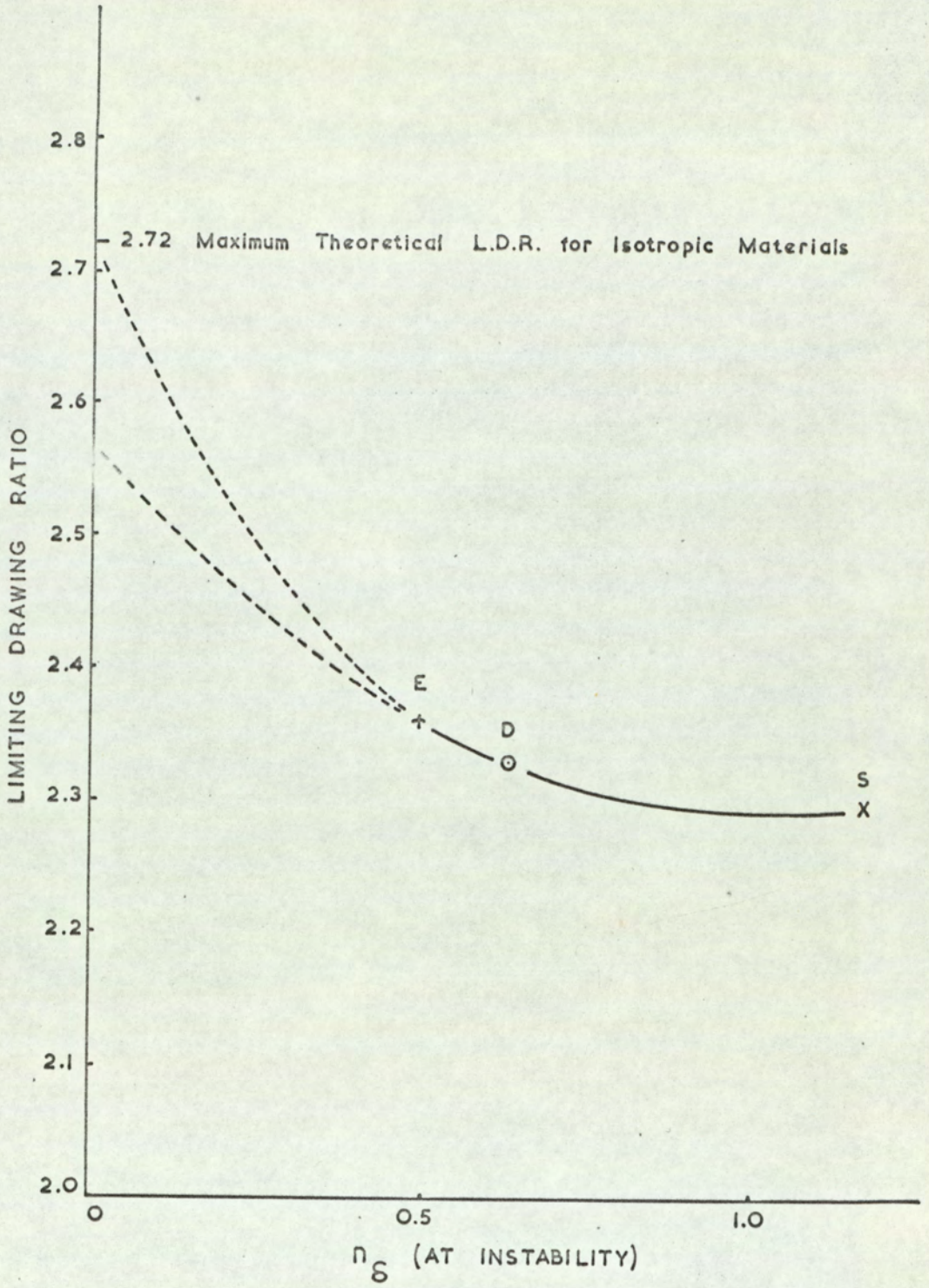

Fig. 5.30. The Slope of the True Stress - True Strain Curve at Instability plotted against Limiting Drawing Ratio.

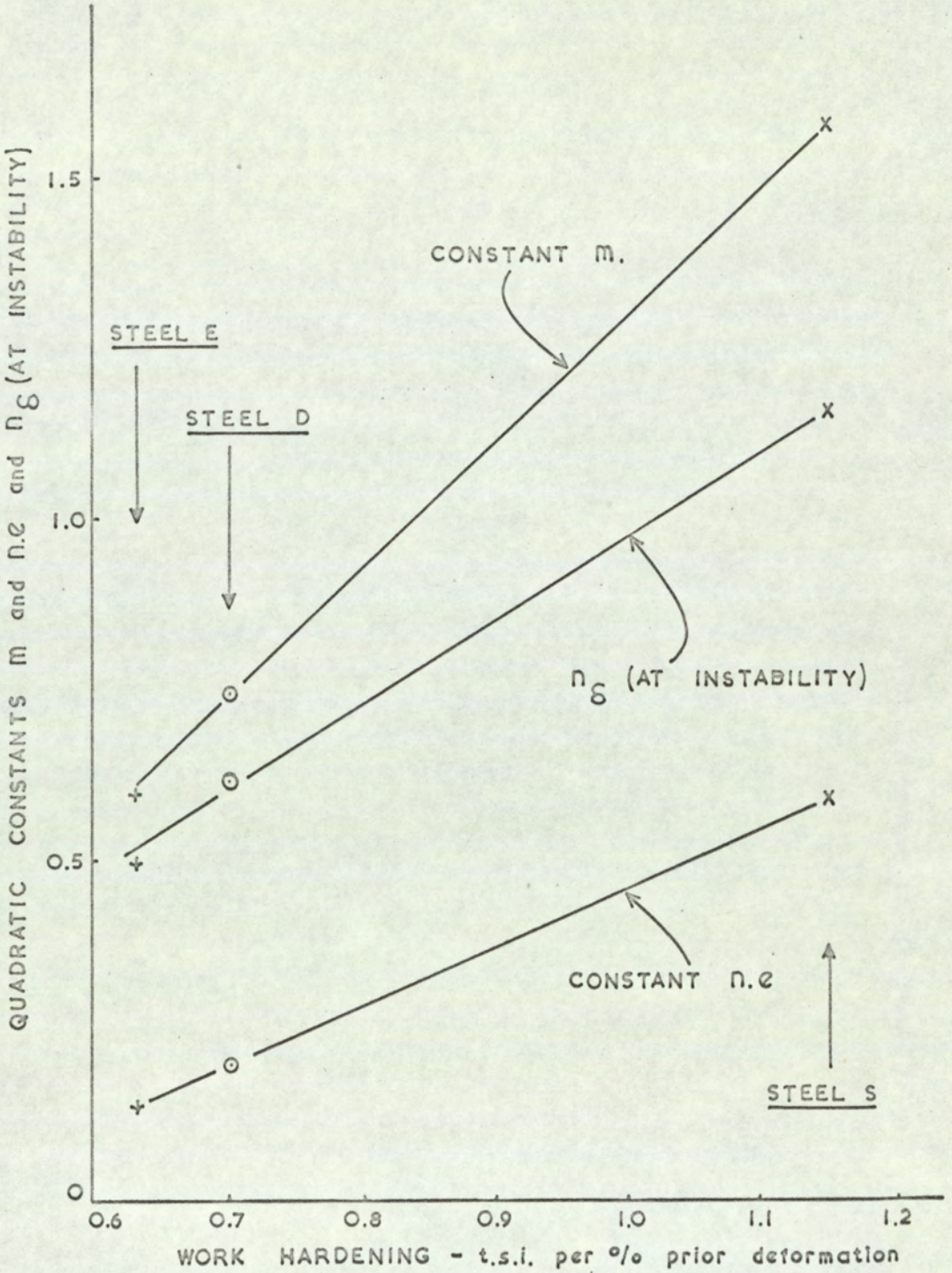

Fig. 5.31. The Relationship between the Quadratic Constants and n_δ (at instability) and a Measure of Work Hardening.

for $\delta = 1$ (i.e. $\log \delta = 0$). The constant $^{c}/_{e}$ therefore represents a level of stress, unobtainable in practice, that would be obtained if the stress-strain curve continued with increasing slope to a strain of 1.0. Although the specimen fails in tension at a strain level much below a strain of 1.0, the point of maximum strength or the stress at maximum load should correlate with this constant $^{c}/_{e}$. The results of this comparison for materials in the annealed condition are shown in Fig.5.32. Values for steels A, B, C and F have been obtained by average results from both the fully annealed and stretch straightened conditions. There is good agreement between the value of $^{c}/_{e}$ and stress at maximum load; the correlation coefficient between these two values was + 0.92.

5.15. An Analysis of the True Stress-True Strain Data obtained from Plane Strain Compression Tests

Stress-strain data have also been obtained from plane strain compression tests and the results have already been reported in Section 4.6, Fig.4.8. Prior to testing it was essential that the material condition in the test piece was similar to that used in tensile testing. The 1/8" material was therefore heat treated to give grain size and initial hardness similar to that obtained in the annealed tensile test pieces.

For isotropic materials the ratio of flow stress in compression to stress in tension should ideally be 1.154. For anisotropic materials this ratio can be calculated from the results proposed by Hosford and Backofen,[48] i.e.

$$\frac{\sigma c}{\sigma t} = \sqrt{\frac{2(\bar{R}+1)}{2\bar{R}+1}}$$

where $\bar{R}$ is a measure of normal anisotropy and σc and σt are the respective stress values in compression and tension. Values of this ratio derived from actual tension and compression tests on the three steels examined, and at different strain levels have also been reported in section 4.6. Table 4.9. From this table it can be seen that not only does the ratio increase with strain for all the materials but that the increase is greatest in the steel of lowest

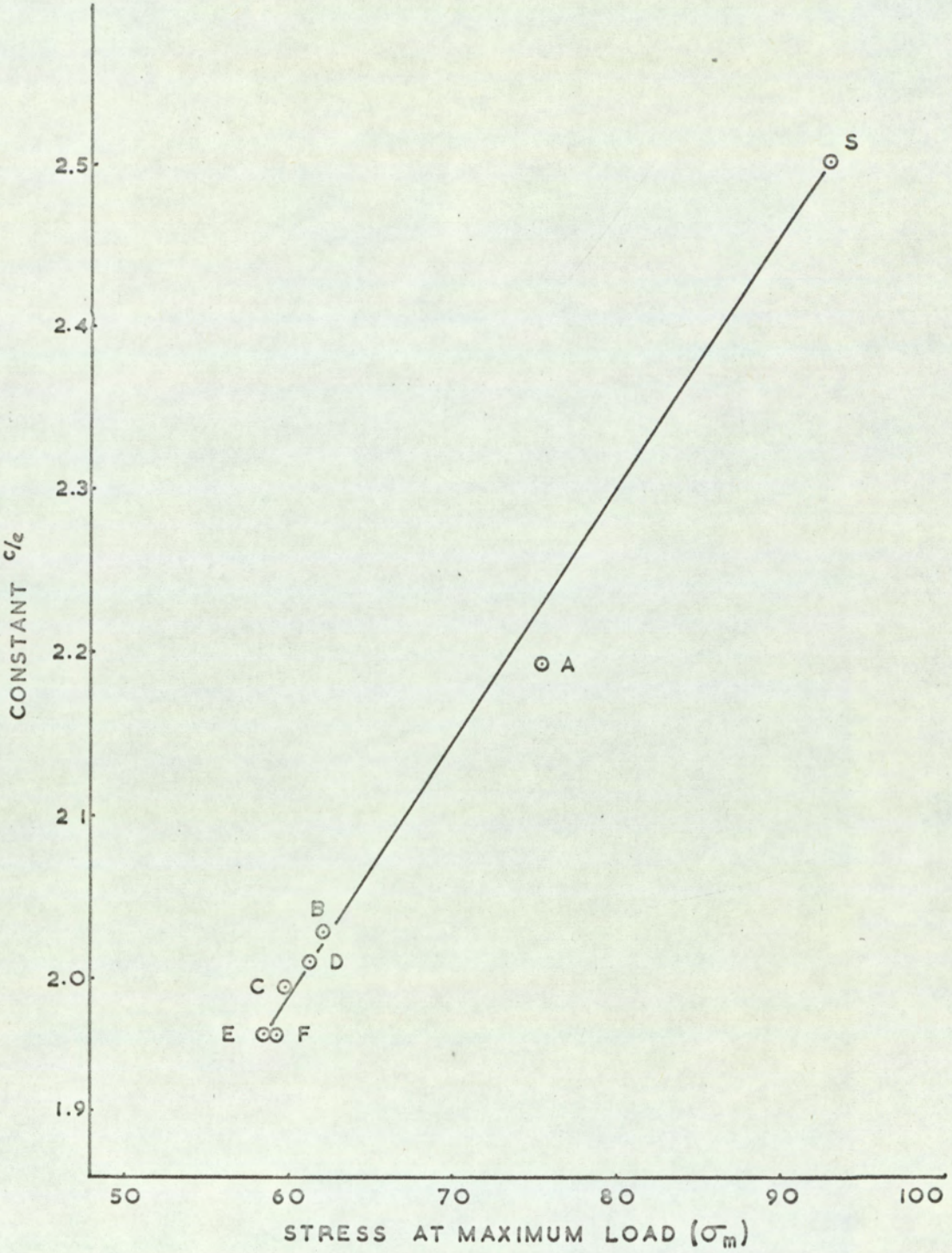

Fig. 5.32. Stress at Maximum Load plotted against the Quadratic Constant c/e.

stability (steel S). These differences are illustrated in Fig.5.33. While steels S and D both show an increase in this ratio with increase in strain, steel E shows the opposite tendency. Since the level of normal anisotropy affects this ratio it was expected that variations in this property could explain the differences between the predicted and the actual stress ratios. It has already been reported that the $\bar{R}$ value for steel S decreased with strain while for steels D and E an increase was recorded. The effect of such variations in $\bar{R}$ value on the stress ratio is however very small: the predicted ratio for steel S increases from 1.154 to 1.20 and for steels D and E to 1.14. The necessary variation in $\bar{R}$ value for steel S to account for the differences between the predicted and actual stress ratios would have to be very large and to give ratios greater than 1.4, the $\bar{R}$ value would need to be negative. The differences between the actual and predicted ratios can not therefore result simply from texture differences. The ratio for steel E decreased with strain and therefore gives an indication of one of the factors affecting this ratio. The agreement between the predicted and actual stress ratios for steel E, is better towards the end of the test and could possibly be accounted for by (a) a more homogeneous distribution of strain within the test piece, (b) improved lubrication and (c) an increase in accuracy of specimen measurement.

The differences in these ratios are obviously strongly connected to the formation of α' martensite but since it has already been shown that more of this phase was obtained for a given equivalent strain in tension than compression, it is very difficult to explain why its formation would increase the ratio. Three reasons are suggested to account for the increase in ratio:-

1. The variations in $\bar{R}$ value with strain, in pure tension, differ considerably from the mode of variation of $\bar{R}$ with strain in conditions of plane strain compression.
2. The model forwarded by Hosford and Backofen does not apply to

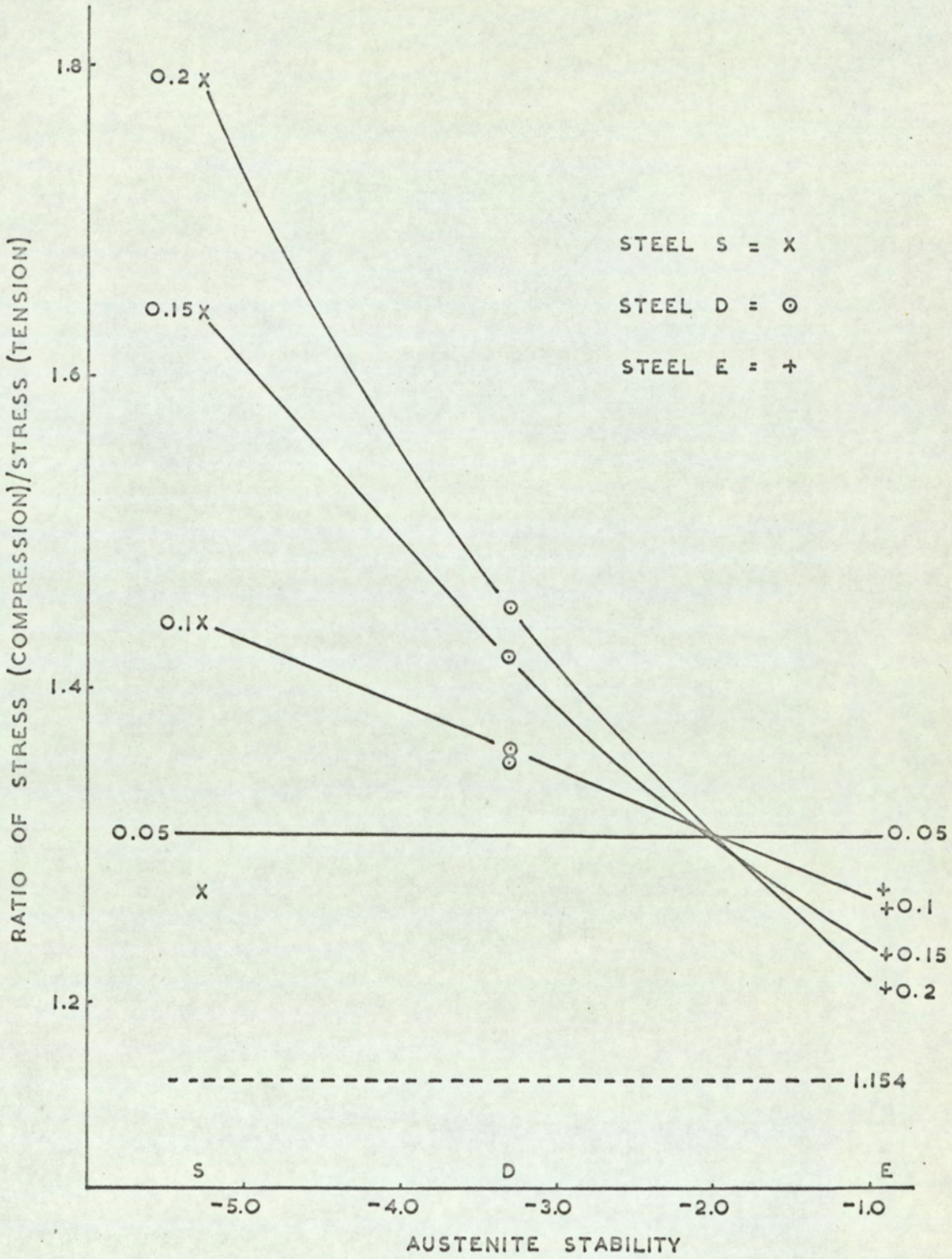

Fig. 5.33. The Effect of Austenite Stability on the Ratio of Stress in Compression/Stress in Tension.

transforming materials in which a hard second phase is produced on straining.

3. The test procedure in plane strain compression adversely affects the accuracy of stress measurements.

Plane strain compression testing is known to be inhomogeneous in its deformation at low strains. Deformation in its early stages produces areas of high strain concentrations at positions corresponding to the edges of the indenting die. The development of high local strains would encourage the formation of α' martensite in these areas, (Fig. 5.34), so that subsequent deformation would only proceed if the higher yield stress associated with this new material condition was overcome. The overall result would be an increase in the stress level of the stress-strain relationship. Such strain concentrations would also apply to non-transformable steels, but the effect would be less.

5.16. An Analysis of the True Stress-True Strain Data obtained from Hydrostatic Bulge Tests

Stress-strain data have also been obtained from hydrostatic bulge tests in which the stress system is one of biaxial tension. The results have previously been reported in Section 4.7. (Fig.4.8) along with the results from the plane strain compression tests.

For isotropic materials, the ratio of stress in biaxial tension to that in uniaxial tension should be 1.0. Hosford and Backofen also propose that this ratio can be calculated for anisotropic materials from the formula

$$\sigma_B/\sigma_t = \sqrt{\frac{\bar{R}+1}{2}}$$

where $\bar{R}$ is the degree of normal anisotropy and σ_B and σ_t are the respective stress values in biaxial and uniaxial tension.

Values of this ratio derived from actual tension and biaxial tests on the three steels examined, and at different strain levels have also been reported in Section 4.7. (Table 4.10). Again as was the case with the results from the

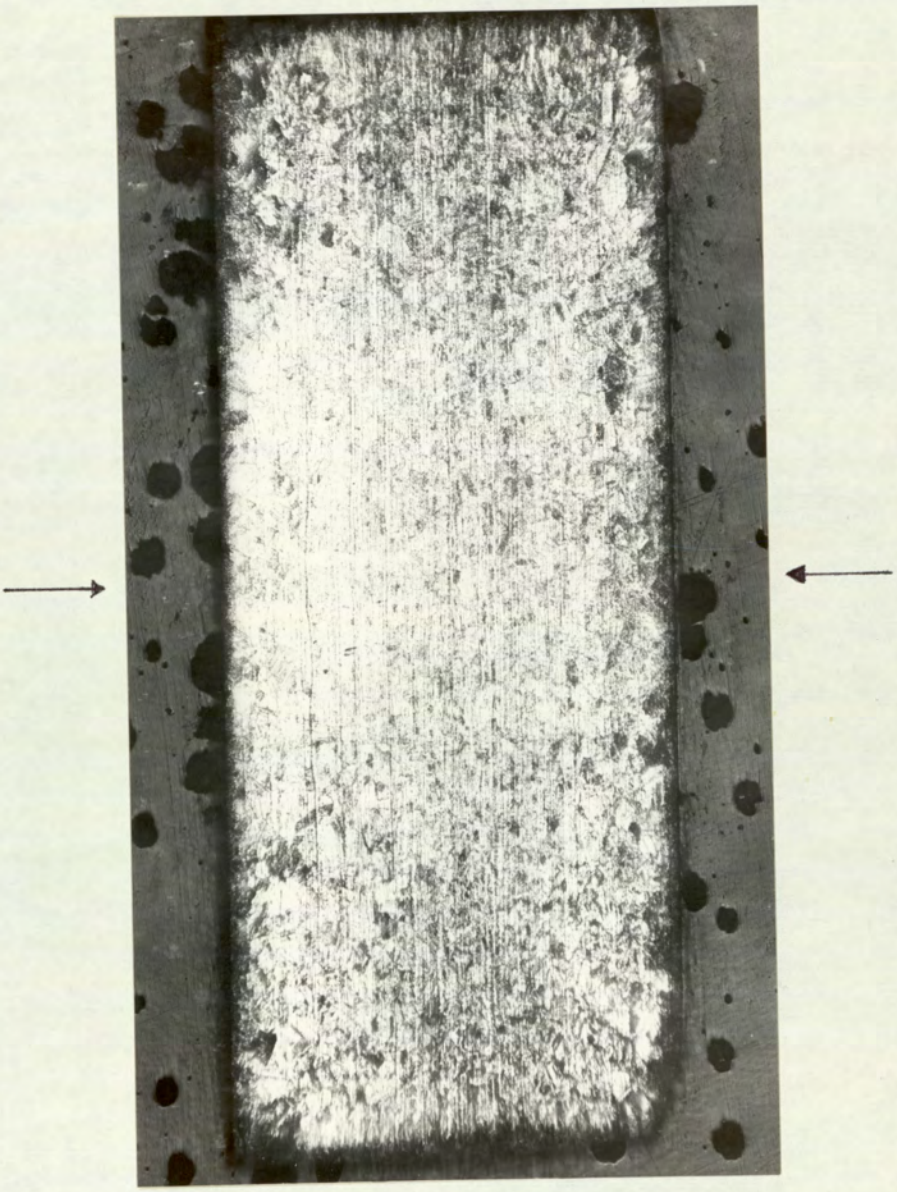

Fig. 5.34. The Development of Areas of High Local Strain obtained using the Plane Strain Compression Test. Sample Strained 10% - Longitudinal Section x 25.

plane strain compression tests the actual ratio of the two stresses appears to be dependent on α' martensite formation. Although the amount of α' martensite formed during biaxial tension was not measured, from evidence that will be discussed in a later section, it would appear that the volume formed is unlikely to exceed that formed in uniaxial tension for any given level of strain. Similarly the arguments put forward in the previous section regarding the influence of $\bar{R}$ values on the ratio of these two stresses also apply here and it is considered that they do not account for the increase in the stress ratio with strain, for the transformable steel S. Furthermore, since the material was deformed in contact with oil, hydrostatically, then it is considered that the effect of friction could be neglected. This means that for hydrostatic bulging the effect of localised transformation to α' martensite can also be eliminated.

Of the three suggestions made in the previous section to explain the increase in the stress ratioswith respect to strain, only one remains: that the theory proposed by Hosford and Backofen does not apply to transformable stainless steels. Since the magnitude of difference between the predicted and the actual stress ratios is greater for plane strain compression than biaxial tension, then it seems likely that the production of high strain concentrations in the former test, probably accounts for a large part of this difference. It is hoped that future work will help to explain the above differences more fully.

5.17. The Effect of Austenite Stability and Prior Deformation on the Analysis of the Stress-Strain Data.

In this section it is intended to examine the effect of austenite stability on the magnitude of the quadratic equation constants described in Section 4.5. for the three stress systems examined: uniaxial tension, biaxial tension and plane strain compression.

Using the computer curve fitting programme described in the experimental Section 3.7.5. the constants $^{c}/_{e}$, m and n.e. have been calculated

for all the materials, in all the conditions examined for the three tests used. The results for the annealed condition only are shown in Fig.5.35. The significance of the constants used in the quadratic equation has already been discussed. The constant $^{c}/_{e}$ has been shown to be related to the stress at maximum load and the constants m and n.e. to be related to the slope of the stress-strain curve. The curvesshown in Fig.5.35 can therefore be examined in the light of these generalities. For steel S, the compression test gave maximum values for all three constants therefore not only does this reflect the fact that higher stress values were obtained in compression but also that the rate of work hardening was greater. All three constants decreased with increase in austenite stability, the decrease being more pronounced over the range in which α' martensite was formed. For steels D and E maximum values of the constants were obtained from the biaxial test. This again implies that in such a case the slope of the stress-strain curve increased at a faster rate than in compression or uniaxial tension.

An examination of the results also revealed a discrepancy that depended on the initial condition of the annealed material. It was found that the commercial steels A, B, C and F, gave values for the constants that did not adequately fit the curves obtained on material produced by the author. Care had been taken to ensure that as far as possible, the two sets of material were, apart from composition, metallurgically similar e.g. grain size. The commercial material had, however, received a 2% stretch straightening as the last operation to provide a flat strip whilst steels S, D and E had been roller levelled. To examine this effect, tensile specimens for the steels S, A, B, C and F were annealed as the final operation to remove any residual stresses and retested. The results for the tensile test only are shown in Fig.5.36. It can be seen that only in the case of metastable austenites, steels S and A was the effect significant. The effect of only this small amount of strain reduces the value of all the

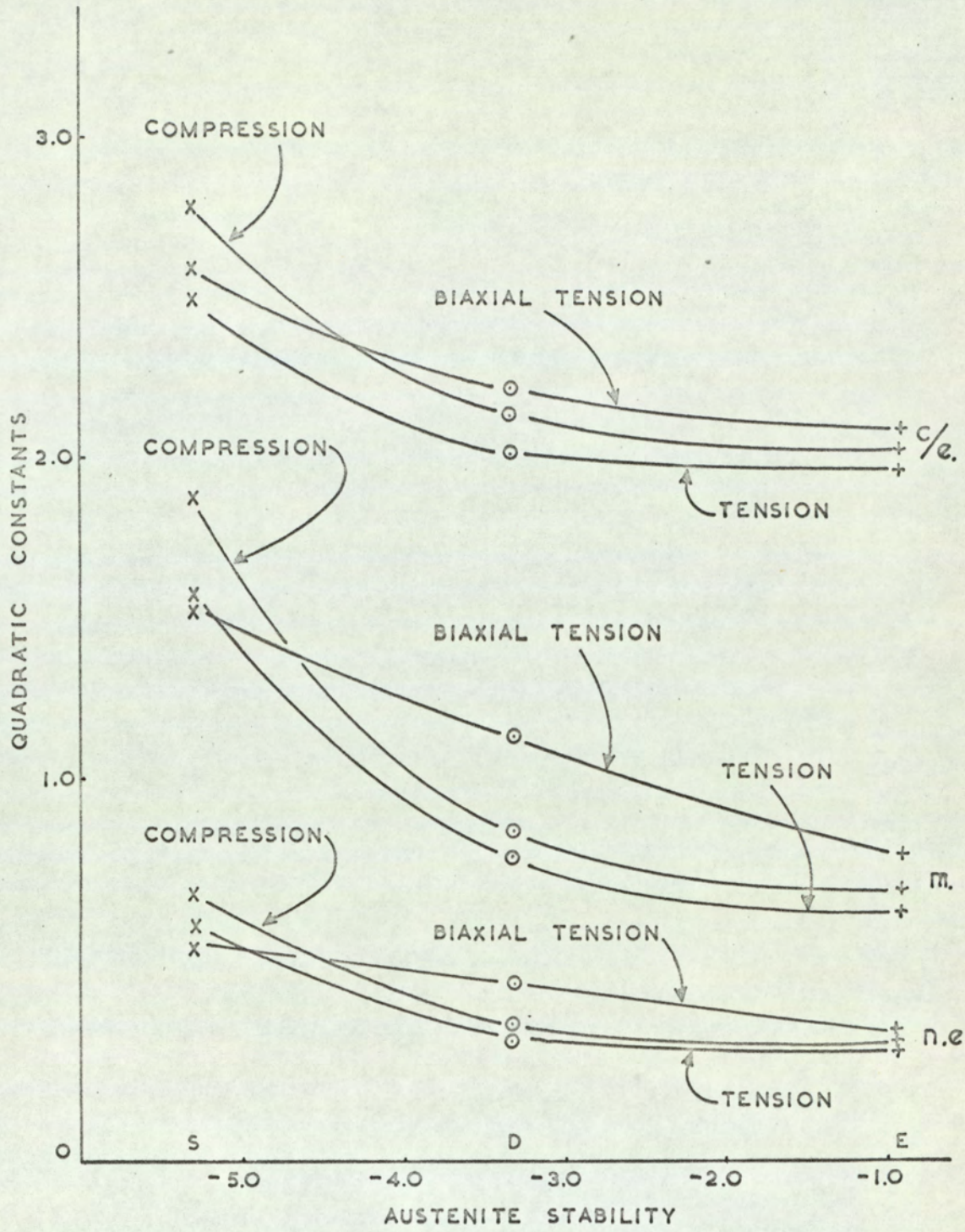

Fig. 5.35. The Effect of Austenite Stability on the Quadratic Constants c/e, m and n.e for Different Tests.

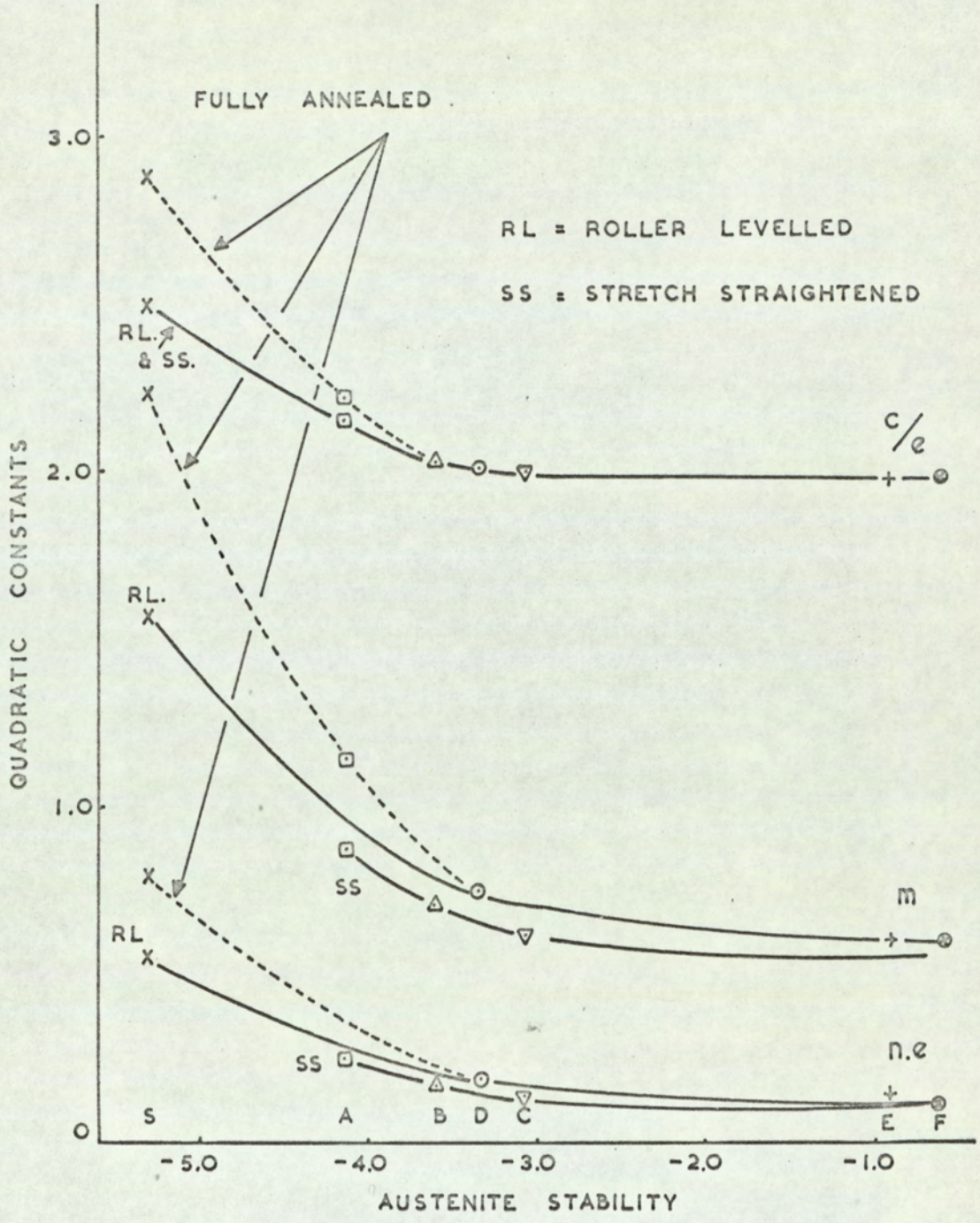

Fig. 5.36. The Effect of the Final Finishing Operation on the Quadratic Constants for Steels of Different Austenite Stability.

constants with increasing severity for a decrease in austenite stability. This suggests that the value of these constants is closely related to such properties as work hardening capacity, uniform elongation and for the metastable austenites, susceptibility to α' martensite formation. This point is further shown by examination of Table 4.7 (Section 4.5) which shows the considerable decrease in the value of these constants that accompanies prior deformation. The strong dependence of these constants on the formation of α' martensite is further reflected in Fig.5.37. This phase markedly affects the m constant which has already been shown to mainly determine the slope of the stress-strain curve. The value of the constants was almost unaffected for steels in which there is little or no transformation to α' martensite.

Using the values of the constants and the differentiated form of the quadratic function it has been shown that the slope of the stress-strain curve can be calculated at any given level of strain up to that corresponding to fracture. To illustrate the normal relationship between the slope of the stress-strain curve and the strain level at which it has been calculated, for steels S, D and E, in the annealed condition, and deformed in tension, Fig.5.38 has been drawn. The curves show that the slope of the stress-strain curves, $n\delta$, increases in all cases with the strain to which the specimen is deformed but that much higher values of $n\delta$ are achieved with the metastable steel and that ultimate values of $n\delta$ decrease with increase in austenite stability. The fact that there is a progressive increase in slope with increasing levels of strain, proves that at no stage do stainless steels give a straight line relationship between stress and strain in contrast to Diver's assumption that the stress-strain relationship for stainless steels can be represented by two straight lines. It can also be seen that the rate of increase in $n\delta$ decreases as the capacity for further deformation decreases. Since values of $n\delta$ are calculated from a log function i.e. $m + 2$ n.e.$(\log\delta)$ it was considered that this relationship could better be represented by plotting

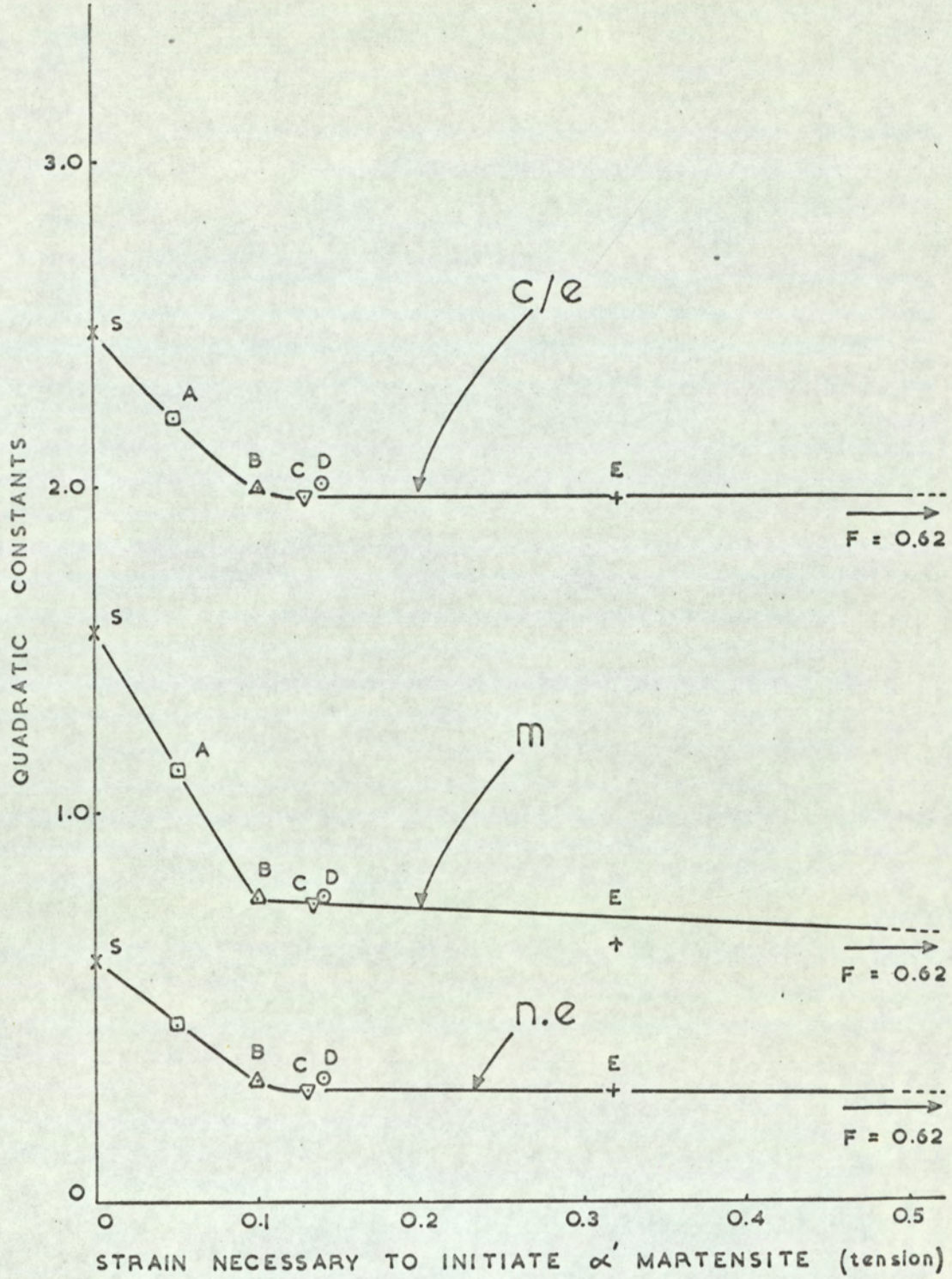

Fig. 5.37. Values of the Quadratic Constants plotted against the Strain necessary to Initiate α' Martensite Formation.

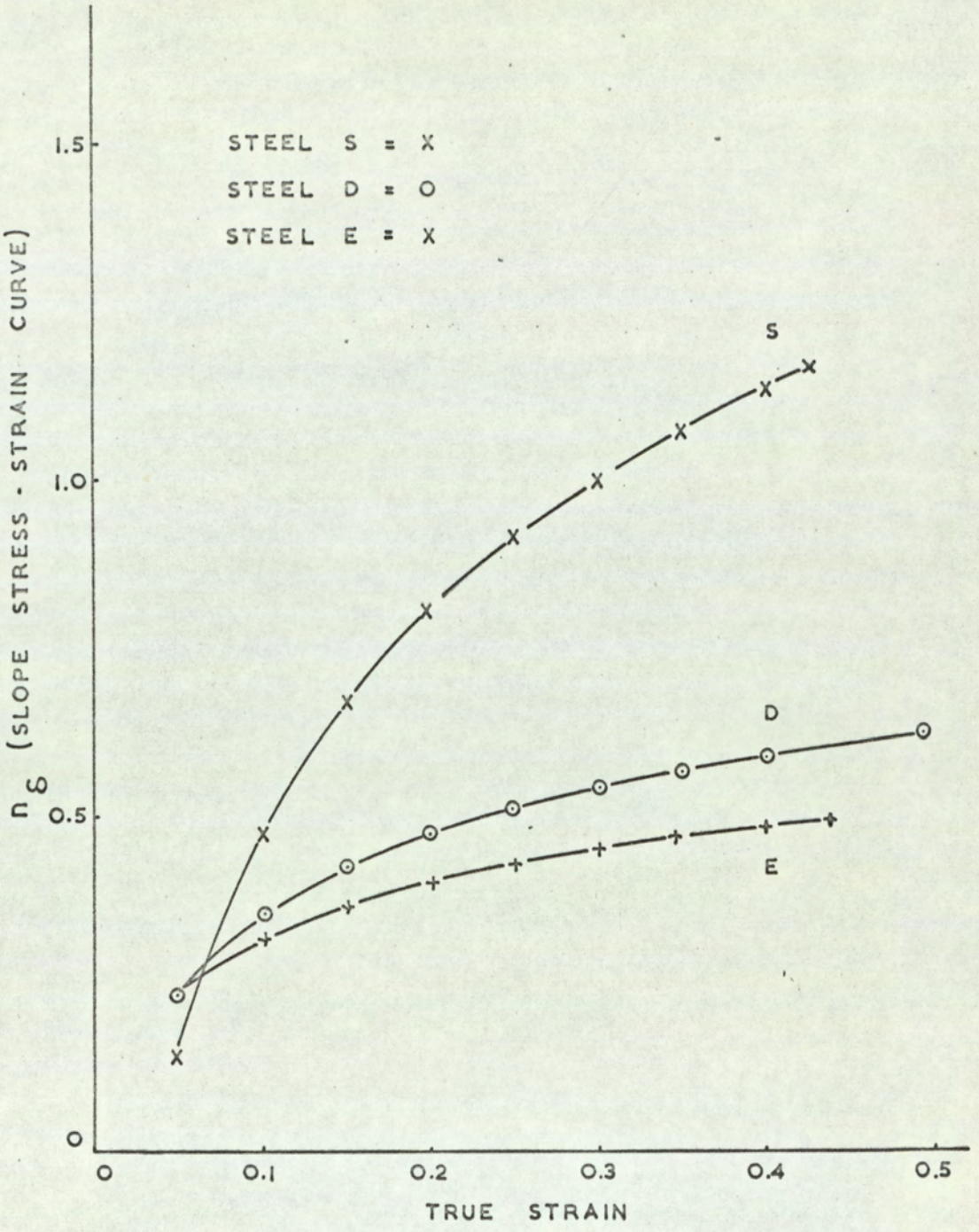

Fig. 5.38. The Variation in the Slope of the True Stress - True Strain Curve with respect to Strain.

the strain co-ordinates on a log basis. This has been done in Figs.5.39 and 5.40 in which the effect of the three stress systems examined is shown for the annealed material and in which the effect of cold work on the results from the tensile test is also considered. In these figures the maximum value of nδ refers, in all cases except plane strain compression, to the slope of the stress-strain curve at a strain level corresponding to the limit of uniform elongation, and the rate of change in nδ is measured by the slope of these curves. It has been shown that for stainless steels values of nδ at instability can be equated to the property normally designated the work hardening co-efficient and that the rate of work hardening, the slope of the stress-strain curve, varies with strain. To determine the value of work hardening capacity is a much more difficult task but since the slope of the curves shown in Figs. 5.39 and 5.40 represents the degree to which the initial value of nδ can be increased and since this value represented by the slope decreases markedly with prior deformation, it must also be strongly related to the capacity of the steel to deform. It is also considered that capacity for deformation could be equally if not better represented by nδ values at instability, a point which will be discussed in a later section. (The slope of these curves can be computed from 1.58 x n.e.) This cannot be so for materials that obey the Ludwik relationship since such work hardening coefficients remain constant with respect to strain, and their slope therefore zero.

If the nδ values that correspond to the limit of uniform elongation, are considered with respect to austenite stability for tension only, Fig.5.41, it can be seen that values of this "equivalent work hardening coefficient" increase with decreasing austenite stability. For the annealed material there is a marked increase in nδ beginning at a stability of - 3.0 which corresponds to steels in which significant amounts of α' martensite are formed. If it is assumed that a linear relationship exists between the value of nδ obtained in the annealed material, for steel S, and that obtained after 10% prior cold

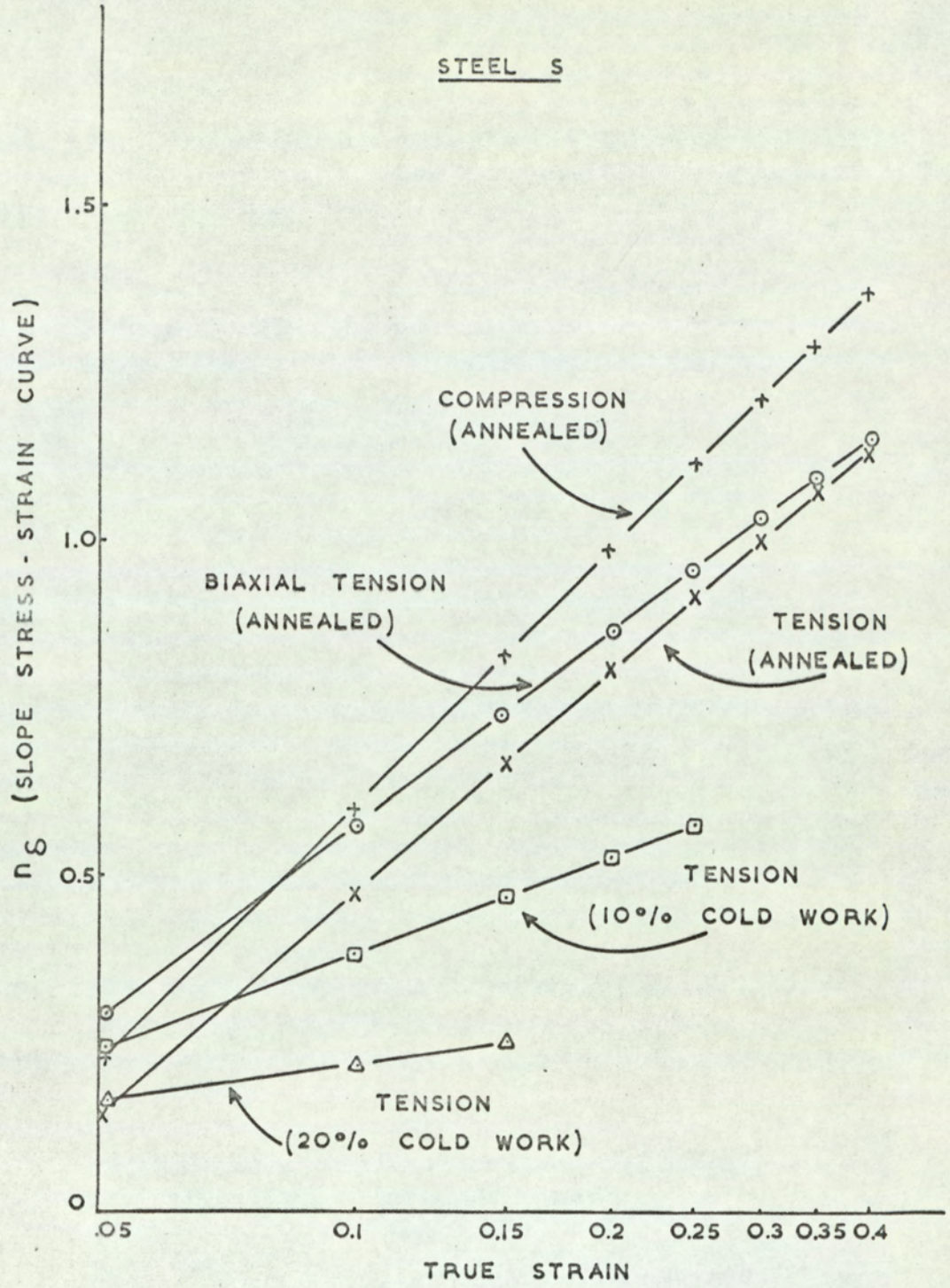

Fig. 5.39. The Variation in the Slope of the True Stress - True Strain Curve with respect to Strain - Steel S.

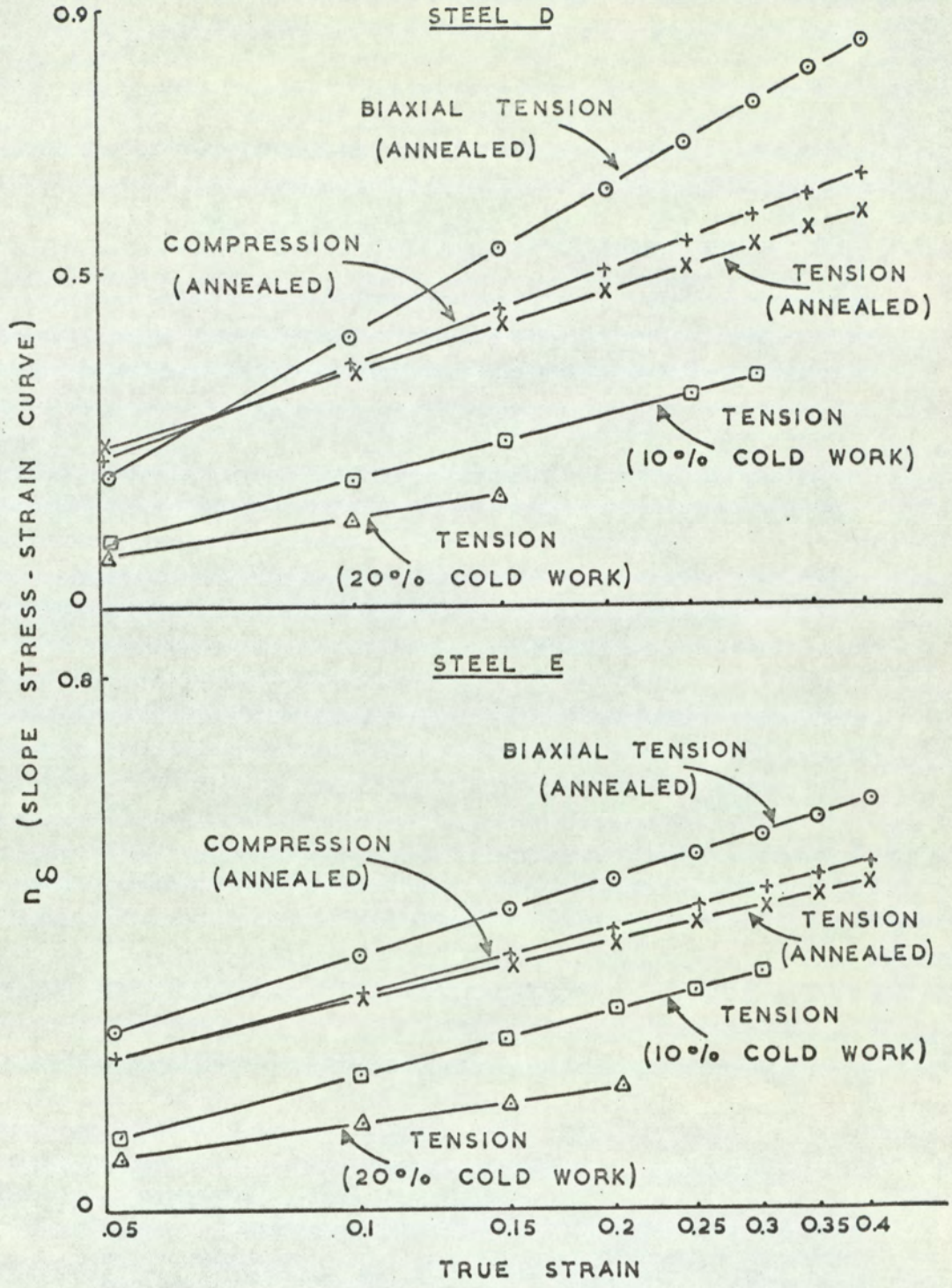

Fig. 5.40. The Variation in the Slope of the True Stress - True Strain Curve with respect to Strain - Steels D and E.

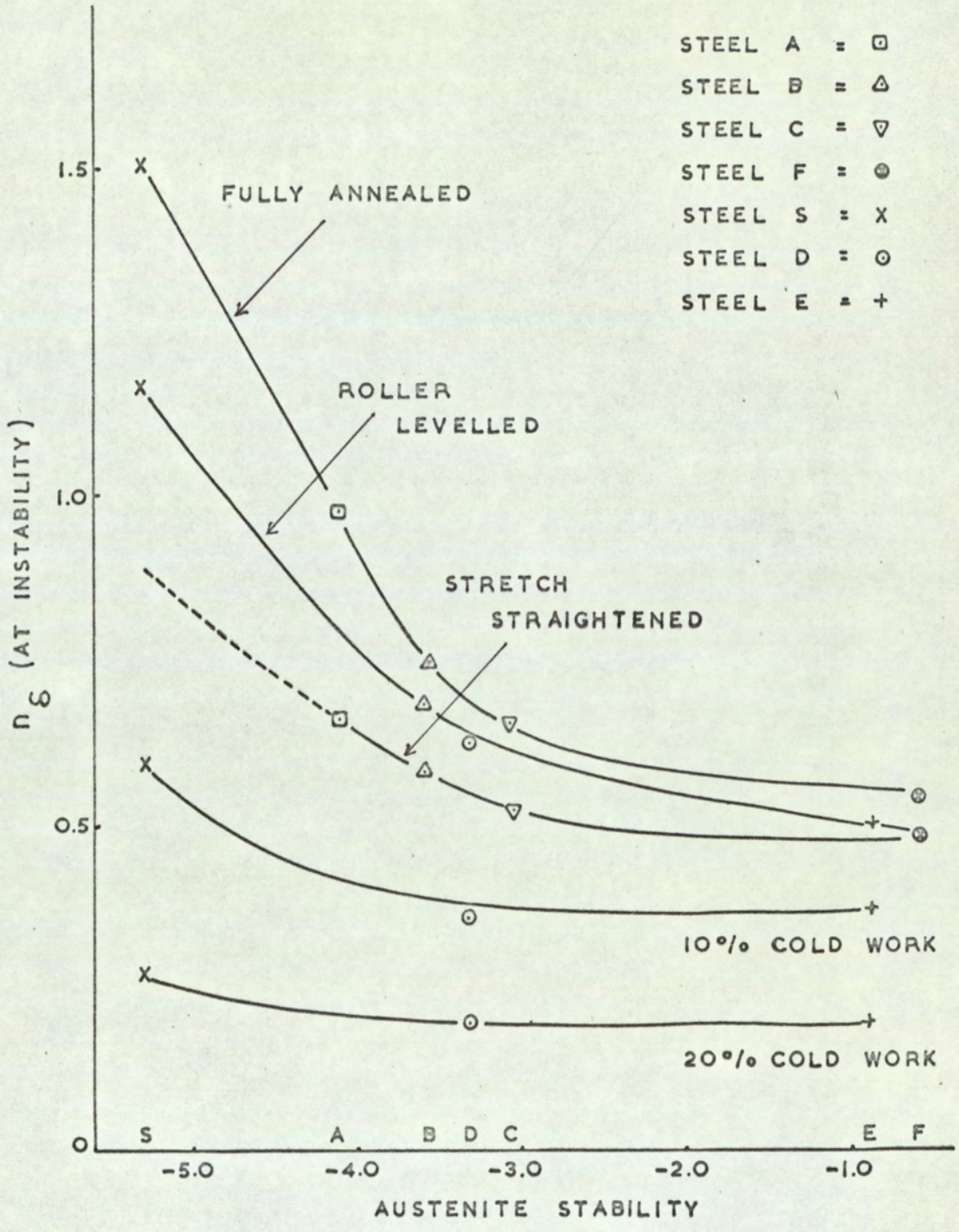

Fig. 5.41. The Relationship between n_δ (at instability) and Austenite Stability.

work, then it would appear that the roller levelled and stretch straightened material received more deformation than had been envisaged. Using values from Fig.5.41 it is considered that the roller levelled material could have had 3% prior deformation and the stretch straightened, 6%. With increased prior cold work nδ values at instability decrease considerably. It is suggested that the reason for this decrease is twofold. One, with prior deformation, the capacity for further deformation decreases, i.e. diminished values of uniform elongation and secondly for the metastable steels, the amount of austenite available for transformation to α' martensite is also reduced.

5.18. The Relationship between the Analysis of the Stress-Strain Data and the Mechanical Properties of Stainless Steels

Some of the main relationships that exist between the constants used in the quadratic function and some of the mechanical properties have already been discussed. Nevertheless, additional relationships exist, and these will now be examined.

An extremely good correlation coefficient of + 0.97 was obtained between the value of nδ at instability and the area beneath the tensile curve. Since the latter is a measure of the work hardening capacity of the material, then values of nδ at instability can also be used to describe this property. This fact can only be true if all the steels exhibit similar values of nδ at low strain levels and reference to Fig.5.27 shows that this is the case.

In addition, because there is a high degree of correlation between the area beneath the tensile curves and equivalent values of nδ at instability it is also likely that a similar correlation would exist between such areas and the constants used to calculate values of nδ. The relationship between these three sets of values and the areas beneath a tensile curve is shown in Fig.5.42. The good agreement obtained is also reflected in the correlation coefficients which were + 0.96 and + 0.92 respectively for the constants m and n.e.

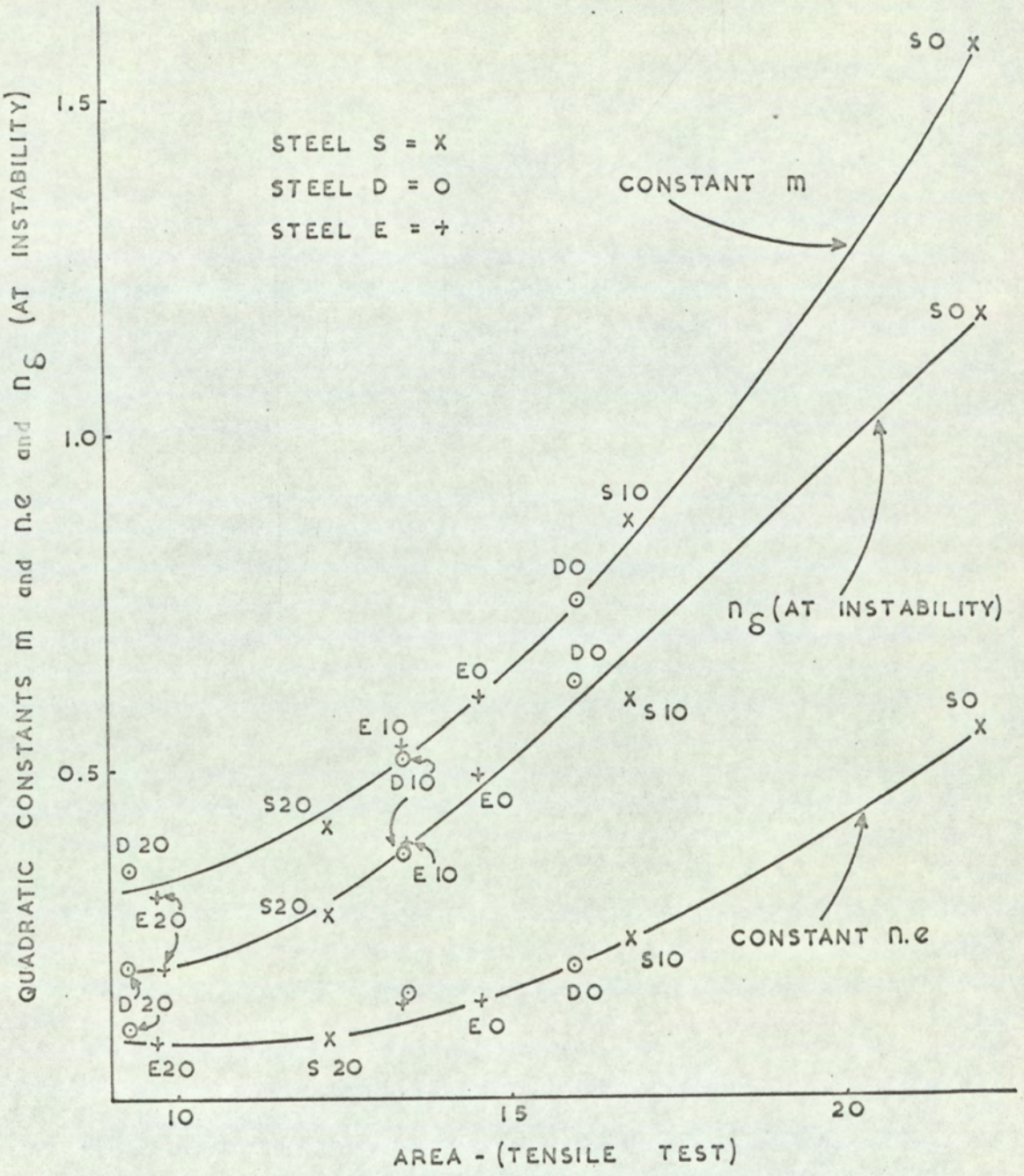

Fig. 5.42. The Relationship between the Quadratic Constants m and n.e and n_δ (at instability) and the Area beneath the Tensile Curves.

It has previously been stated that the ratio of proof stress to ultimate tensile strength has been used as a measure of pressing performance. This ratio in effect also measures the work hardening capacity of the material in that the lower this ratio the lower will be the level of stress needed to initiate deformation and the higher the strain to which the material can be deformed. It has also been shown that with increase in prior deformation all the steels examined showed an increase in this ratio. This indicates a decrease in the capacity for further deformation and thereby pressing performance, particularly stretch formability. Examination of Fig.5.43 shows that the PS/UTS ratio for the two significantly transformable steels S and A is very much lower than the other steels considered and results from the appreciably higher values of UTS obtained with these steels. Excluding the results from these two tests (steels S and A in the annealed condition), there is a good linear relationship between the PS/UTS ratio and values of $n\delta$ at instability, the correlation coefficient being - 0.89. This coefficient was the best correlation obtained between a mechanical property, excluding the area beneath the tensile curve, and the value of $n\delta$ at instability.

5.19. The Relationship between the Analysis of the Stress-Strain Data and the Press Formability of Stainless Steels

5.19.1. Stretch Forming

The analysis of the stress-strain data produced three constants and a parameter that could be derived from two of these constants ($n\delta$). Since the three constants are employed to control the shape of the stress-strain curve and because no mechanical property was found to be related to the stretch formability of all the steels examined, then it is not surprising that there was no significant correlation between any of the constants and stretch formability. Values of $n\delta$ at instability were, however, strongly related to Erichsen values and the areas beneath the punch load/punch travel diagrams for stretch forming.

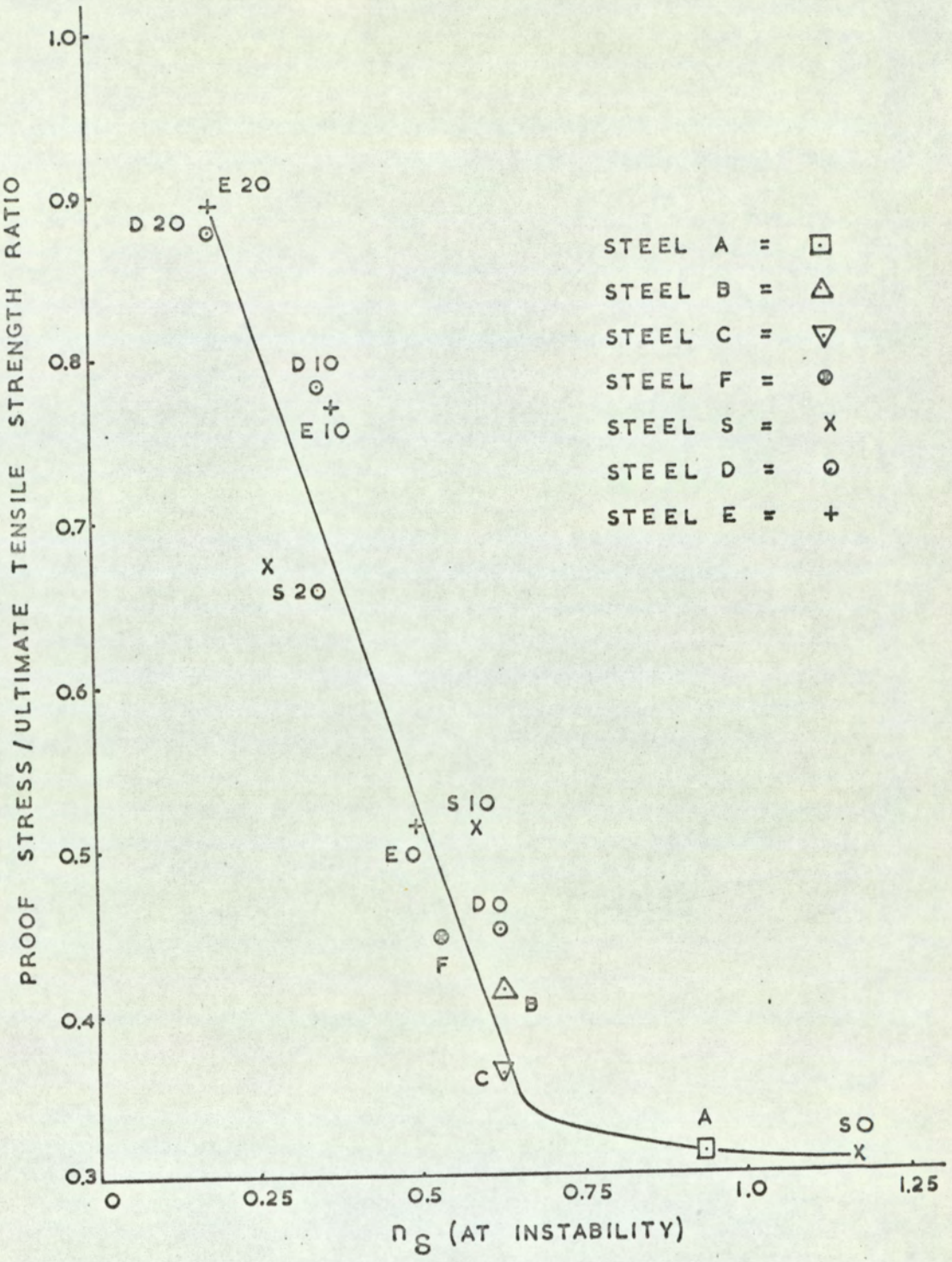

Fig. 5.43. The Relationship between the Ratio of Proof Stress/ Ultimate Tensile Strength and n_δ (at instability).

The relationship between Erichsen values and nδ at instability is illustrated in Fig.5.44. This graph gives further evidence that nδ at instability can be equated to conventional 'n' values and extends the range over which this relationship has been previously reported. The significance of previous relationships which were obtained for mild steel, aluminium, copper and 70/30 brass now becomes obvious when examined in context with materials that extend the data to much higher values of the work hardening coefficient. The curve also confirms the results of Wybo.[76] The results reported here also show the effect of increased lubrication in that Erichsen values somelto 1.5 mm greater than those obtained by Wybo have been achieved.

The second relationship obtained with the value of nδ at instability and the area beneath the stretch forming punch load/punch travel diagram is given in Fig.5.45. Although these particular results are derived from laboratory stretch forming tests it is suggested that the relationship could be used to assess relative power requirements for materials of different austenite stability.

5.19.2. Deep Drawing

The highest correlation obtained between any material property and deep drawability and for which a coefficient of + 0.90 was achieved, was between C.B.D. and a ratio of the constant m and nδ at instability. This ratio is a measure of the degree to which material can be deformed and also to which it can be hardened. Low values, of such a ratio, indicate how near the slope of the stress-strain approaches the theoretical slope that would be obtained at a strain of unity and therefore incorporates the two properties of uniform elongation and work hardenability. Low values should therefore also indicate improved formability by deep drawing. The results are presented in Fig.5.46. The relationship is obviously better than that obtained with either uniform elongation or values of nδ, the correlation

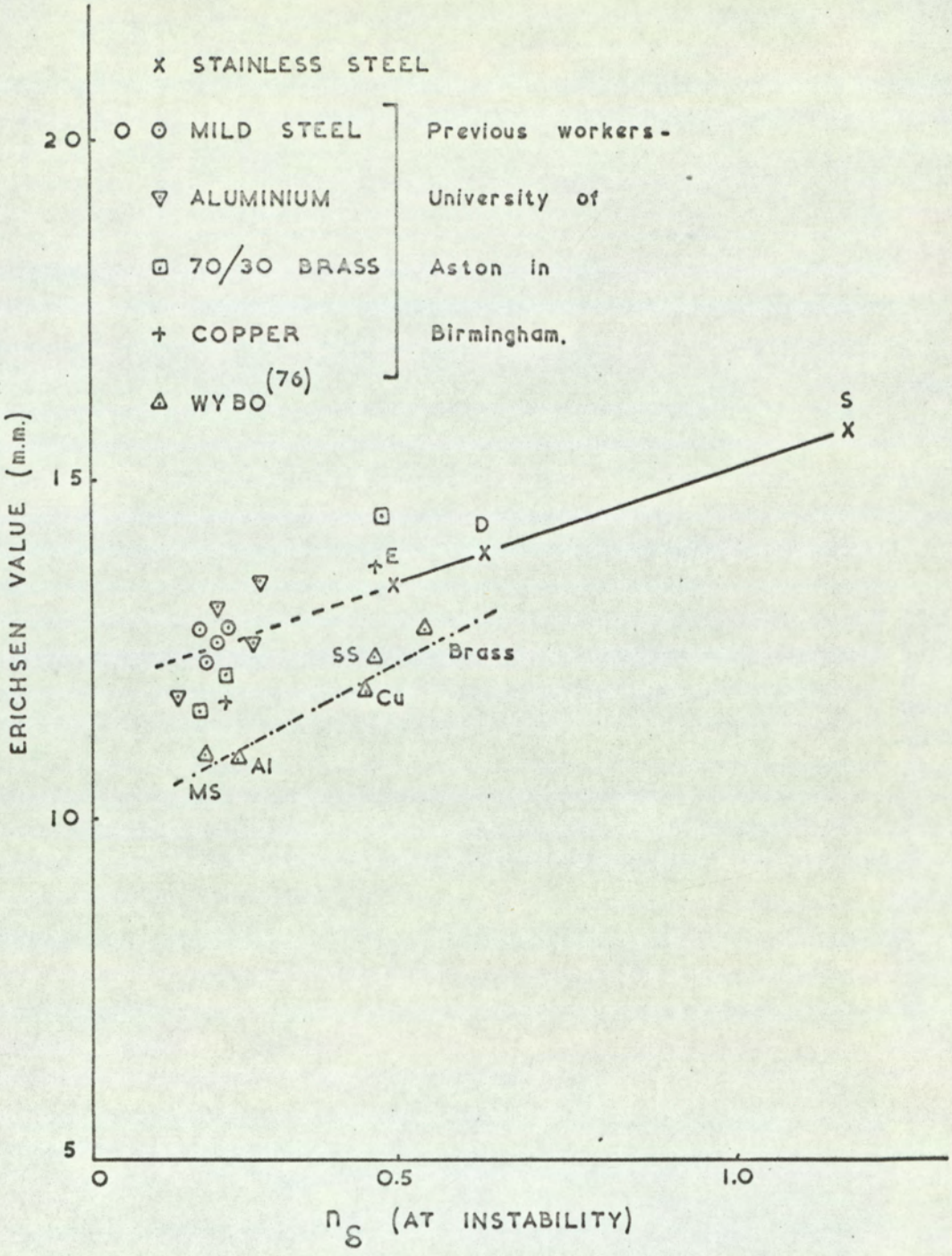

Fig. 5.44. The Relationship between Erichsen Values and n_δ (at instability) and 'n' Values for Different Materials.

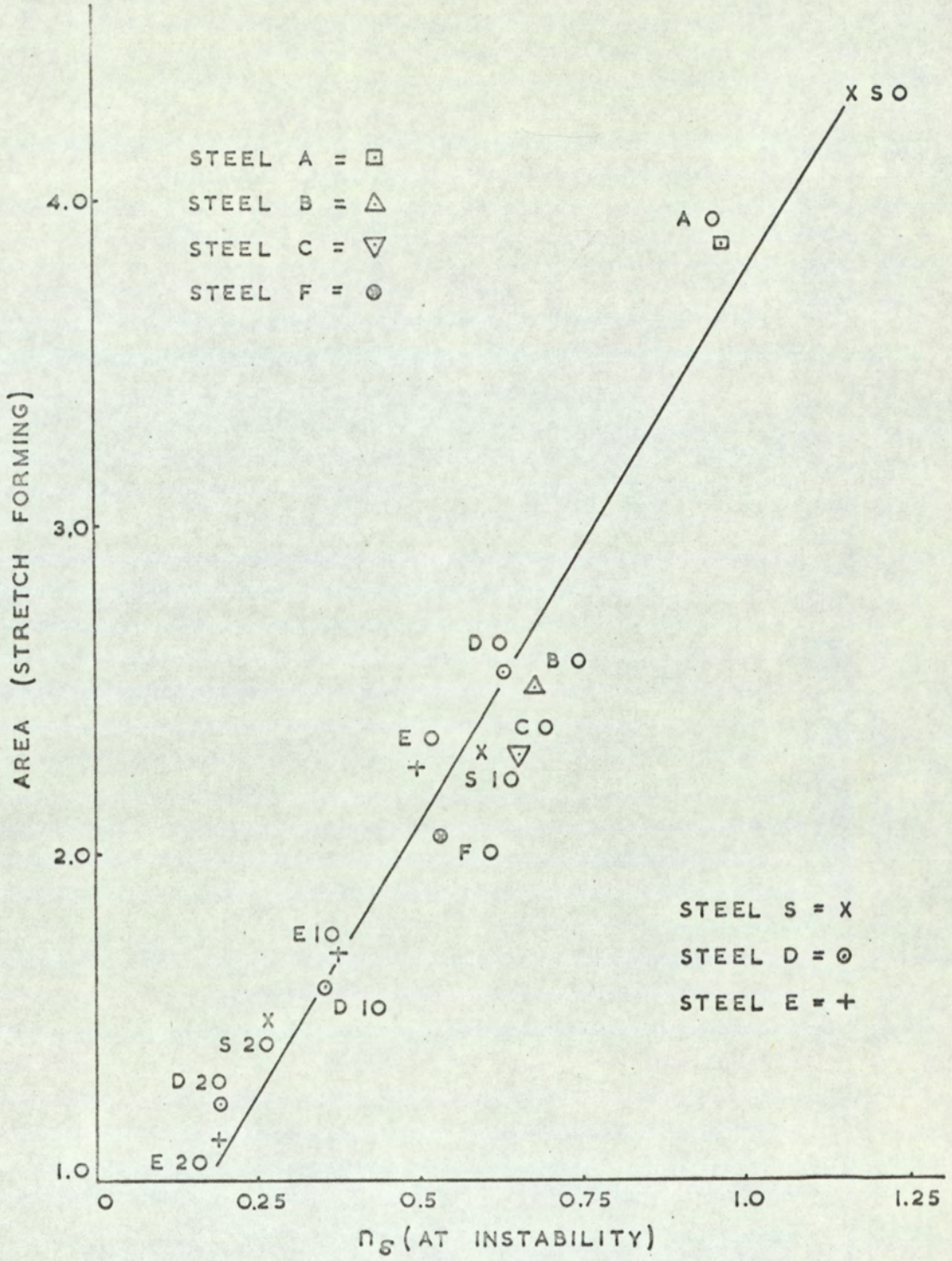

Fig. 5.45. The Relationship between Deformation Work Area (Stretch Forming) and n_δ (at instability).

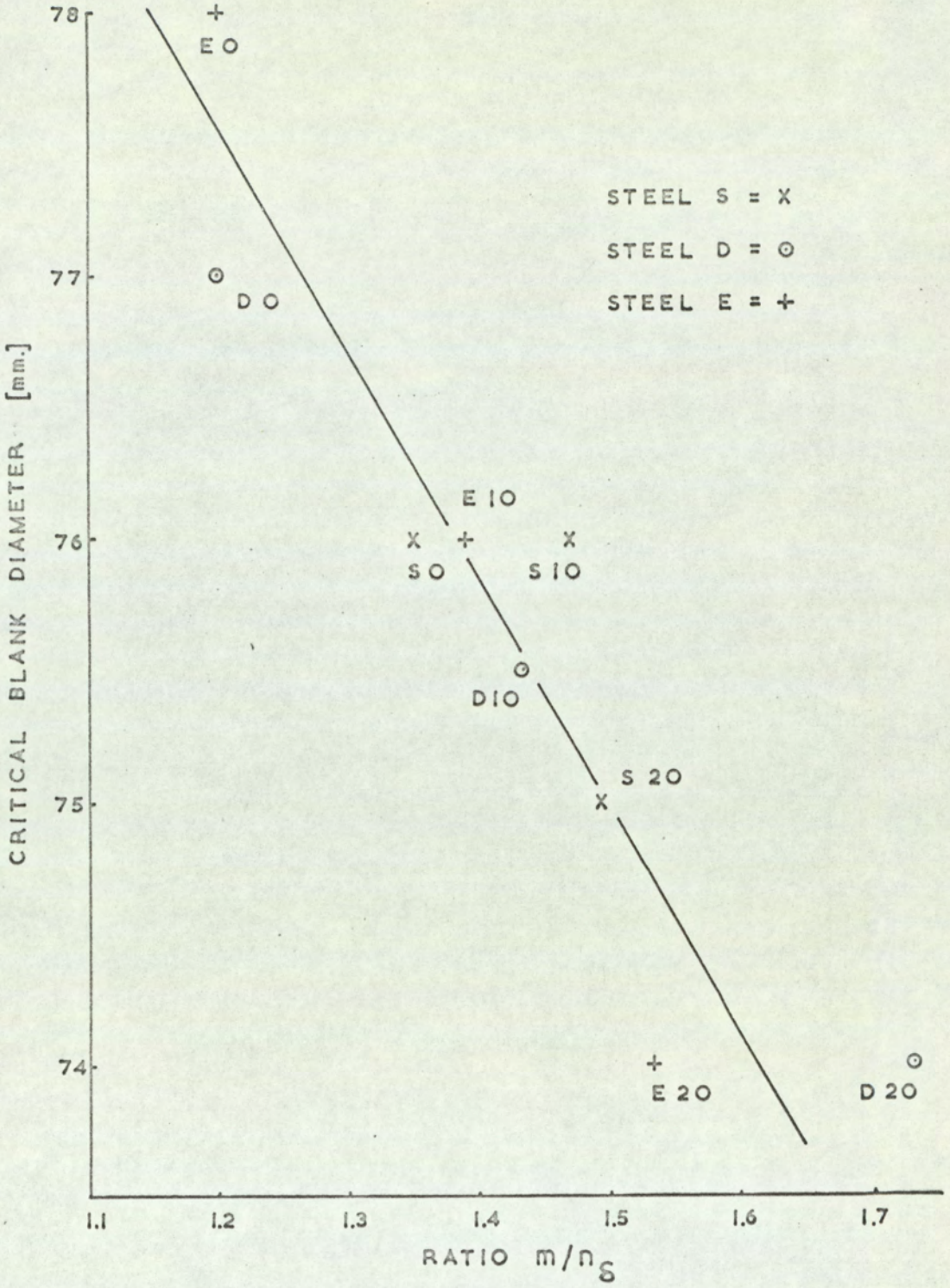

Fig. 5.46. The Relationship between Critical Blank Diameter and the Ratio of the Quadratic Constant m/n_δ (at instability).

coefficients for which were + 0.83 and + 0.48.

5.20. Information Derivable from the Analysis of the Stress-Strain Data

Throughout this investigation both the mechanical and press forming property variations have intentionally been related to austenite stability and thereby chemical composition so that the results could be more easily applied to commercial practice.

It has been shown how the constants used in the quadratic function vary with respect to austenite stability. For any given stainless steel, within the range here studied, knowledge of the chemical composition can be converted to a value of austenite stability by using the Post and Eberly formula, and from such values the constants $^{c}/_{e}$, m and n.e. can be obtained merely by reference to a relevant curve. To obtain a predicted stress-strain relationship from this data then involves substituting arbitrary values of strain in the quadratic function and calculating the equivalent value of true stress. This technique, does not, of course, enable prediction of the extent of the stress-strain curve, i.e. the strain level at which fracture occurs, to be made. Nevertheless, the strain level at fracture can be obtained from knowledge of the quadratic constant m. Since the correlation coefficient between the quadratic constant m, and n_δ at instability was extremely high, + 0.99, it was decided that such a relationship was sufficiently accurate to predict values of n_δ at instability. The relationship between these two parameters is given in Fig.5.47.

It would therefore appear possible to obtain values of the constants m and n.e. from the degree of austenite stability, and to use the value of m to obtain a value of nδ at instability. Calculation of the limit of uniform elongation, or rather the strain corresponding to this value, merely requires substituting the relevant uniform elongation in the differentiated form of the quadratic function, i.e. $\frac{d(\log \sigma)}{d \log \delta)}$ = nδ instability = m + 2 n.e (log δ instability).

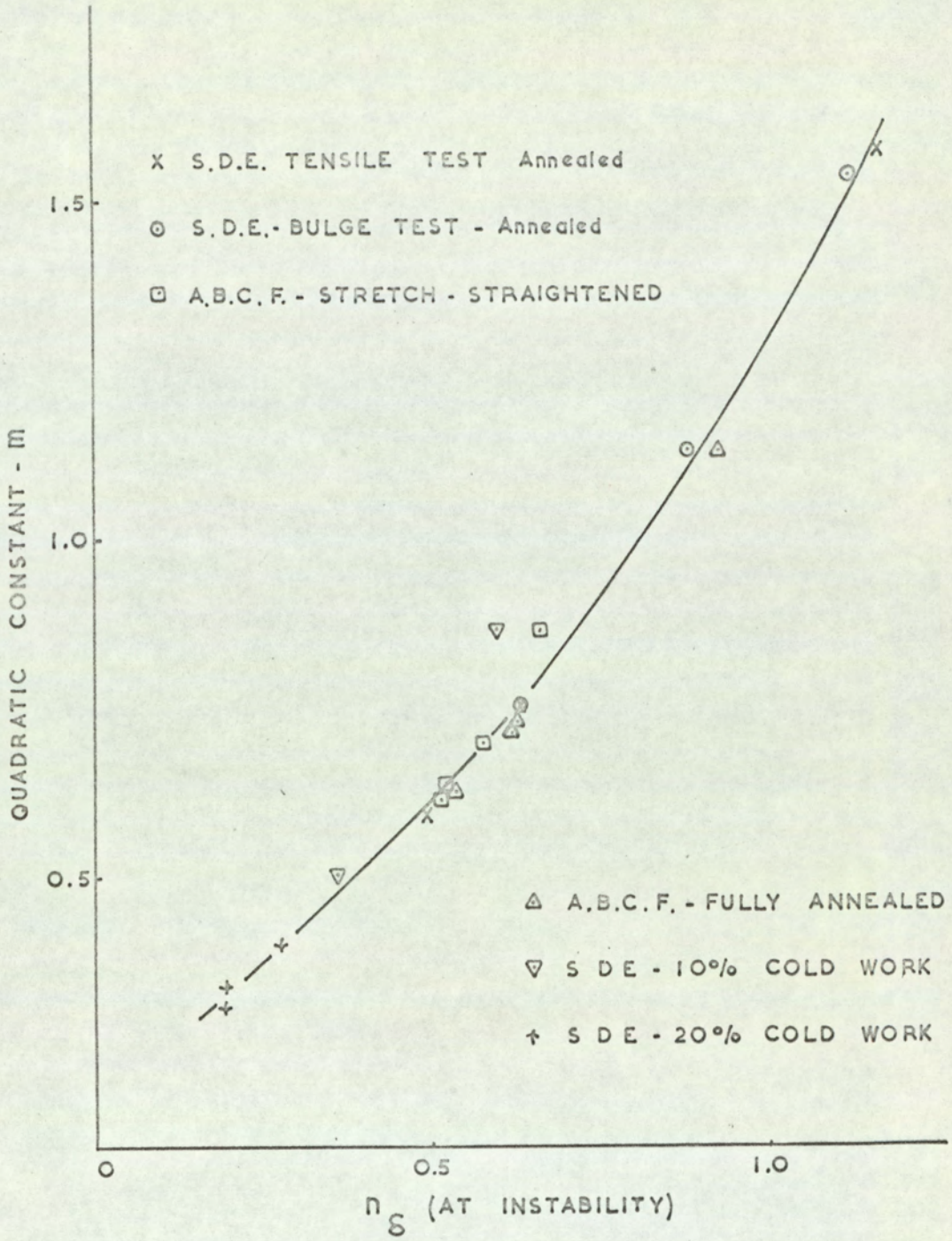

Fig. 5.47. The Relationship between the Quadratic Constant m and n_δ (at instability).

The value of $(\log \delta_{instability})$ therefore defines the limit of the stress-strain curve. In a similar manner the rate of work hardening of the material, i.e. the slope of the stress-strain curve, can be calculated, for strains less than that corresponding to the limit of uniform elongation, from the differentiation of the quadratic function.

It is further considered that the relationship between the constant c/e and the stress at maximum load, $(\bar{\sigma}_{max})$, is sufficiently accurate from which to predict this latter value and that it can be used in the formula :-

$\bar{\sigma}_{max} = UTS\ (1 + Eu)$, together with a value of uniform elongation (Eu) obtained as described, to calculate values of ultimate tensile strength.

Finally, with reference to the usefulness of the quadratic function in relation to press formability it is considered that only the relationship obtained between stretch formability and values of $n\delta$ at instability is sufficiently accurate from which to adequately predict Erichsen values, merely from knowledge of the composition of the steel.

6.0. CONCLUDING SUMMARY

Section 2.15 of this thesis established that additional information could be gained from a more critical appraisal of different deformation systems and of the effect of changes in composition and prior deformation on both the press formability and mechanical properties of stainless steel.

Optimum press forming properties were obtained for all the steels examined, from material in the annealed condition. When certain fundamental conditions such as good lubrication and the use of a liberal die entry radius are employed, stainless steels exhibit marginally superior pressing properties to that of deep drawing quality mild steel, although power requirements are higher.

The individual operations of stretch forming and deep drawing are best satisfied by different steels: the former operation being favoured by steels of low stability and deep drawing by stable materials. In stretch forming the most important single mechanical property was found to be elongation and it is possible that the correlation obtained could have been improved if drawing in of metastable material, could have been prevented. The metastable materials required a much higher drawing load than the stable steels, and resulted in material, that was originally outside the die diameter, being drawn into the die.

The effect of prior deformation on the mechanical properties of the steels has also been studied. The formation of α' martensite, both prior to and during drawing, has been shown to benefit those mechanical properties governed by strength and beneficial to deep drawing only when its presence does not radically impair ductility. In such cases the presence of α' martensite resists localised necking.

The drawing capacity has been shown not to be markedly influenced by the anisotropy ratio R. In all conditions, the steels tested were fairly isotropic except for material that transformed considerably to α' martensite. In such cases, α' martensite formation caused the value of $\bar{R}$ to decrease. The formation of this phase also produced a "mixed texture", consisting partly of a pure metal

rolling texture" and partly of a texture that resulted purely from the formation of α' martensite. The position of ears on the rim of drawn cups has been shown to be controlled by the type of texture obtained.

It was felt, after the literature had been reviewed, that insufficient information had been reported that detailed the shape of the stress-strain curves for stainless steels. For the most part, the stress-strain relationship is represented by a curve and not a straight line. The slope of the stress-strain curves has been shown to be strongly dependent on the formation of α' martensite, but that the strain level at which α' martensite is initiated does not correspond to the strain level at which the stress-strain relationship deviated from a straight line. A curve, although considerably reduced in slope was also obtained for non-transformable steels and it is suggested that the increase in slope obtained with steels of this type, results not from α' martensite formation but from the production of ε martensite, an intermediate phase in the austenite - α' martensite transformation.

The shape of this complex stress-strain curve has been analysed for the three stress systems of uniaxial tension, biaxial tension and plane strain compression and the quadratic function that was obtained related to austenite stability and composition. It is suggested that this quadratic expression more accurately represents the stress-strain relationship for stainless steels than existing stress-strain expressions. The slope of the stress-strain curve which varies with strain, can be calculated using the differentiated form of the quadratic function. The slope of the curve at the onset of plastic instability has been shown to be comparable to conventional 'n' values obtained from the Ludwik equation. It is considered that a measurement of the work hardening coefficient in this manner, is more accurate than taking an average slope of the curve.

The significance of the constants employed in the quadratic function has been reported and the results of the stress-strain analysis related to both mechanical properties and press formability.

Finally, using the derived quadratic function; it has been shown that a theoretical prediction of stress-strain data and various mechanical and press forming properties can be obtained from knowledge of the austenite stability of the steel.

7.0. CONCLUSIONS

1. The formation of α' martensite has been related to austenite stability and therefore, to composition. It was found that more of this phase resulted from deformation by uniaxial tension than by plane strain compression.
2. The formation of α' martensite has been confirmed to be beneficial to the property of uniform elongation, particularly in steels of intermediate austenite stability, i.e. for steels having Post and Eberly $\triangle$ values of approximately - 4.0.
3. Stretch formability and deep drawability, with one exception, were both impaired by prior deformation. The drawing capacity of the least stable material was not impaired by 10% prior deformation.
4. Stretch formability has been found to increase with decrease in austenite stability and can be correlated to the property of uniform elongation if drawing in of material is restricted. If the Euronorm Erichsen test is used to measure stretch formability, and it has been shown that some drawing in occurs with this test for high strength materials, then two linear relationships result: one for transformable steels and a further linear relationship for non-transformable steels.
5. In contrast to stretch formability, deep drawing behaviour increases with increase in austenite stability.
6. Prior deformation has shown that transformation to α' martensite, both prior to and during testing, markedly affects those mechanical properties governed by strength.
7. The value of $\bar{R}$ has been found not to be a significant factor in relation to the deep drawability of the steels studied. $\bar{R}$ values varied little from unity in all cases except when transformation to α' martensite was considerable. In such cases, $\bar{R}$ values decreased to approximately 0.7.

8. A performance function, ($\sigma m \times \delta_{ue}$) has been suggested to predict both stretch forming and deep drawing behaviour of stainless steels. The function is best satisfied when individual steels are considered in different conditions of prior deformation.

9. The true stress-true strain relationship for stainless steels has been found to be a curve and not a straight line when plotted on a log-log basis and the point of deviation from a straight line to that of a curve does not correspond to the strain level for the initiation of α' martensite for all the steels examined. The stable austenitic steels also gave rise to a curve that could be satisfied by the quadratic function. In such cases it is suggested that work hardening results from both the deformation of the parent matrix and from formation of ε martensite, the combined effect of which is considerably less than work hardening that is associated with α' martensite formation.

10. A quadratic function has been derived which accurately defines the stress-strain relationship for all the compositions and material conditions examined. This function is given as :-

$$\log\sigma = c/_e + m(\log \delta) + n.e(\log \delta)^2.$$

11. The quadratic function has been examined with respect to the three stress systems studied, uniaxial tension, biaxial tension and plane strain compression, the effect of prior deformation and to austenite stability. The effect of these variables has been assessed in terms of the magnitude of the constants governing the quadratic equation. The values of all the constants decreased with both prior deformation and austenite stability.

12. The analysis of the stress-strain data has been related to the mechanical properties and press formability of the steel examined. The quadratic constant $c/_e$ is strongly related to stress at maximum load in the tensile

test and the constants m and n.e., which govern the slope of the stress-strain curve, correlate strongly with a practical measure of work hardenability and the area beneath the load/extension curve in tensile testing.

13. A coefficient (nδ), the slope of the stress-strain curve measured at the point of plastic instability, is suggested as being a more accurate measure of the work hardening coefficient for stainless steels than measurement of the average slope of the curve.

14. Using the quadratic function and knowledge of the austenite stability of the steel, it has been found that stress-strain data, together with certain press forming and mechanical properties, including the limit of uniform elongation, ultimate tensile strength, stress at maximum load and Erichsen values, can be predicted.

7.1. Suggestions for further work

It is suggested that the work described in this thesis could usefully be enhanced by examination of the following three variables:-

(a) Grain size.

(b) Temperature of testing.

(c) Strain rate.

8.0. ACKNOWLEDGMENTS

The author wishes to express his gratitude for the help and encouragement given to him by his supervisor, Professor J.C. Wright, of the Department of Metallurgy, the University of Aston in Birmingham, where the research was carried out.

He would further like to thank Messrs. Brown-Firth Ltd. for useful discussions and for supplying the material described in this thesis.

9.0. REFERENCES

1. Strauss, B and Maurer, E.
   Kruppsche Monatshefte, August, 1920.

2. Jevons, J.D.
   The Metallurgy of Deep Drawing and Pressing.
   Chapman and Hall Ltd. London, 1940.

3. Keating, F.H.
   'Chromium-Nickel Austenitic Steels'. Butterworth's Scientific Publications and Imperical Chemical Industries Ltd. 1956.

4. Bain, E.C. and Griffiths, W.E.
   Trans. A.I.M.M.E. 1927, 75, 166.

5. Aborn, R.H. and Bain, E.C.
   Trans. Am. Soc. of Steel Treatment, 1930, 18, 837.

6. Mathieu, K.
   Mitt. Kaiser-Wilhelm.Inst. Eisenforsch,1942, 24, 243.

7. Cina,B.
   J.I.S.I. 1954, 177, 406.

8. Angel, T.
   J.I.S.I. 1954, 177, 165.

9. Kaufman, L. and Cohen, M.
   Progress in Metal Physics, 1958, 7, 165.

10. Patel, J.R. and Cohen, M.
    Acta Met., 1953, 1, 531.

11. Post, C.B. and Eberly, W.S.
    Trans. A.S.M. 1947, 39, 868.

12. Eichelman, G.H. and Hull, F.C.
    Trans. A.S.M. 1953, 45, 77.

13. Barclay, W.F., Green,D.S. and Jackson, J.K.
    Proc. A.S.T.M. 1964, 64, 680.

14. Bressanelli, J.P. and Moskowitz A.
Trans. A.S.M. 1966, 59, 223.

15. Dulieu, D. and Nutting, J.
Iron and Steel Inst. Special Report No.86, 1964, 140.

16. Edwards, C.A. and Carpenter, H.C.H.
J.I.S.I., 1914, 11, 138.

17. Knapp, H. and Dehlinger, U.
Acta Met, 1956, 4, 289.

18. Venables, J.A.
Phil.Mag. 1962, 7, 35.

19. Kurdjumov, G.V. and Sachs, G.
Z. Phys. 1930, 64, 325.

20. Burgers, W.G.
Physica, 1934, 1, 561.

21. Reed, R.P.
Acta Met., 1962, 10, 865.

22. Guntner, C.J. and Reed, R.P.
Trans. A.S.M. 1962, 55, 399.

23. Dash, J. and Otte, H.M.
Acta Met, 1963, 11, 1169.

24. Goldman, A.J., Robertson, W.D. and Ross, D.A.
Trans. A.I.M.E. 1964, 230, 240.

25. Lagneborg, R.
Acta Met. 1964, 12, 823.

26. Kelly, P.M.
Acta Met. 1965, 13, 635.

27. Burgers, W.G. and Klosterman, J.A.
Acta Met. 1965, 13, 568.

28. Form, G.W. and Baldwin, W.M.
Trans. A.S.M. 1956, 48, 474.

29. Powell, G.W., Marshal,E.R. and Backofen, W.A.
Trans. A.S.M. 1958, 50, 478.

30. Divers, C.K.
Metal Progress. 1964. 8, 115.

31. Binder, W.O.
Metal Progress, 1950, 201.

32. Cohen, M.
Trans. A.S.M. 1949, 41, 35.

33. Barclay, W.F.
Trans. A.S.T.M, S.T.P. 369, 1965.

34. Chung, S.Y. and Swift, H.W.
Proceedings I.M.E. 1951, 165, 199.

35. Lankford, W., Snyder, S.C., and Bauscher, J.A.
Trans. A.S.M. 1950, 42, 1197.

36. Alexander, J.M.
Met. Reviews, 1960, 5, 349.

37. Wright, J.C.
Sheet Metal Industries, 1961, 138, 649.

38. Kaftanoglu, B. and Alexander, J.M.
Jnl. Inst. Metals, 1962, 90, 457.

39. Pearce, R.
B.D.D.R.G. Colloquium, London, 11th April, 1967.

40. Keeler, S.P. and Backofen, W.A.
Trans. A.S.M., 1960, 52, 166.

41. Grimes, R, and Wright, J.C.
Sheet Metal Industries, 1967, 44, 391.

42. Wilson, D.V. and Butler, R.D.
Jnl. Inst. Metals, 1962. 90, 473.

43. Harper, D.L. and Whiteley, R.L.
I.D.D.R.G. Colloquium 1966, Liège.

44. Hill, R.
The Mathematical Theory of Plasticity, Clarendon, 1950.

45. Grumbach, M. and Pomey, G.
Sheet Metal Industries, 1966, 43, 515.

46. Hulstead, A.M., McCaughley, J.M. and Markus, H.
Product Engineering, 1954, 25, 180.

47. Voce, E.
Metallurgia, 1955, 51, 219.

48. Hosford, W.F. and Backofen, W.A.
Ninth Sagamore Ordnance Materials Research Conference, 1962, New York.

49. Whiteley, R.L.
Trans. A.S.M., 1960, 52, 154.

50. Holcomb, R.T. and Backofen, W.A.
I.D.D.R.G. Colloquium, 1964, London.

51. Lloyd, D.H.
Sheet Metal Industries, 1962, 39, 82.

52. Atkinson, M.
Sheet Metal Industries, 1967, 44, 167.

53. Ludwigson, D.C. and Brickner, K.G.
Sheet Metal Industries, 1965, 42, 245.

54. Black, H.L. and Lherbier, L.W.
Metal Progress, 1965, 87, 62.

55. Dietrich, H.
D.E.W. Technische Berichte. 6. Band, 1966, Heft. 1.

56. Avenbach, B.L. and Cohen, M.
Trans. A.I.M.E. 1948. 176, 401.

57. Cullity, B.D.
Elements of X-ray Difffaction. Addison-Wesley Publishing Co., Mass. 1956.

58. Gullberg, R,and Lagneborg, R.
Trans. A.I.M.E., 1966, 236, 1482.

59. Kay, D.H.
Techniques for Electron Microscopy. Blackwell Scientific Publications, 1965. Oxford.

60. Grimes, R.
Ph.D. Thesis. University of London. 1965.

61. Ludwik, P.
Elemente der Technologischen Mechanik. Springer Verlag, 1909. Berlin.

62. Ford, H.
Proc. Inst. M.E., 1948, 159, 121.

63. Watts, A.B. and Ford, H.
Proc. Inst. M.E., 1952, 163, 448.

64. Mellor, P.B.
J.Mech.Phys.Solids. 1956. 5, 41.

65. Johnson, W. and Mellor, P.B.
Plasticity for Mechanical Engineers.
Van Nostrand, 1962, London.

66. Butler, R.D.
B.D.D.R.G. Colloquium, 1964, London.

67. Knight, G.A.
Sheet Metal Industries, 1950. 27, 325.

68. Dillamore, I.L. and Roberts, W.T.
Acta Met. 1964. 12, 281.

69. Dixon, M.J.
Private Communication.

70. Baldwin, W.M., Howard, T.S. and Ross, A.W.
Trans. A.I.M.M.E. 1946, 166, 86.

71. Moore, G.G. and Wallace, I.F.
Jnl. Inst. Metals, 1964, 93, 33.

72. Breedis, J.F. and Robertson, W.D.
Acta Met. 1962, 10, 1077.

73. Weil, L.
Memoires Scientifiques de la Revue de Metallurgie, 1964, 61, 63.

74. Mugnier, D.
Private Communication.

75. Brittain, J.O.
Modern Applications of the Theories of Elasticity and Plasticity to Metals - Instrom Ltd. Publication, 1960.

76. Wybo, M.
I.D.D.R.G. Colloquium 1964, London.

10.0. APPENDIX

In the conclusion to the survey of the literature, Section 2.15, it was stated that an attempt would be made to assess the effect of copper and nitrogen additions on the austenite stability of stainless steels. The work now reported was partly supervised by the author which accounts for its inclusion in appendix form.

The work involved the examination of two copper bearing stainless steels, the compositions of which are given in the following table:-

Table 10.1.

STEEL	% C	%Mn	% Si	% Cr	% Ni	% Cu	% Mo	% N
Project No.1.	0.10	0.71	0.56	16.70	7.05	0.25	0.27	0.037
Project No.2.	0.62	1.61	0.56	17.02	6.56	2.13	0.15	0.067

Stress-strain data were obtained from these steels and in a similar manner to that described in the thesis, quadratic constants were calculated. The quadratic constants were then used to obtain a measure of austenite stability from Fig.5.36 of this thesis, and compared with values calculated from the Post and Eberly formula:-

$$\%\,Ni_{(theoretical)} = \frac{(\%\,Cr + 1.5\%\,Mo - 20)^2}{12} - 0.5\%\,Mn - 35\%\,C + 15$$

and the stability Δ , from the formula:-

$$\Delta = \%\,Ni_{(analysed)} - \%\,Ni_{(theoretical)}$$

The values of the quadratic constants and of austenite stability are given in Table 10.2.

TABLE 10.2.

STEEL	QUADRATIC CONSTANTS			AUSTENITE STABILITY	
	$c/_e$	m	n.e.	CONSTANTS (Fig.5.36)	POST & EBERLY
Project No.1.	2.364	1.370	0.504	- 4.50	- 4.79
Project No.2.	2.016	0.639	0.126	- 3.27	- 6.10

The differences between the two values of austenite stability must therefore be due, for Project No.1, to the addition of 0.25% Cu and in Project No.2, to the combined effect of 2.13% Cu and 0.03% N, i.e. 0.067% N minus the average nitrogen content of 0.037% for the steels examined in the thesis.

If the results from Project No.1. are examined, it is possible to isolate the effect of copper on the level of austenite stability: the nitrogen content of this steel was similar to that of steels S, D, E, A, B, C and F. The difference between the two Post and Eberly values is 0.29 and results from the presence of 0.25% copper. It would therefore seem that the addition of 1% copper is equivalent to 1% of Nickel and would be represented by a factor of - 1.0 in the Post and Eberly formula.

If this factor is applied to the results of Project No.2, then 2.13% copper must account for 2.13 parts of the 2.83 difference in the two values of austenite stability and the remaining 0.7 must have resulted from the presence of 0.03% nitrogen. If this assumption is correct then the factor for nitrogen in the Post and Eberly formula can be calculated as 23.

It is suggested that the Post and Eberly formula may be re-written as:-

$$\%\,Ni_{(theoretical)} = \frac{(\%\,Cr + 1.5\%\,Mo - 20)^2}{12} - 0.5\%\,Mn - 35\%\,C - 1.0\%\,Cu - 23\%\,N + 15.$$

Eichelman and Hull[12] have stated that nitrogen has a similar effect to that of carbon and a factor of 27 has been quoted. Dulieu and Nutting[15] have also shown that copper additions to stainless steels of this type, raise the stacking fault energy of the material and thereby increase austenite stability. They further state that copper would be expected to have a greater effect than nickel in increasing austenite stability.

The accuracies of the factors for copper and nitrogen reported here, obviously need further examination. Unfortunately, results were only obtained from two steels. This was not sufficient from which to accurately isolate the true individual effects of these two additions. It was, however, encouraging to note that the results helped to substantiate those previously reported.